Genetically engineering a new system for the expression of cytochrome P450 enzymes in insect cells using novel P450 reductases

by

Pravin Mahajan

Thesis submitted to De Montfort University, Leicester in partial fulfillment of the requirements for the degree of Doctor of Philosophy

April 2010

Abstract

Human cytochrome P450 enzymes (CYPs) are a superfamily of haem-binding monooxygenase enzymes involved in the metabolism of xenobiotics such as toxins, carcinogens and pharmaceutical drugs as well as in the biosynthesis of cholesterol, vitamins and steroids. In recent years, the area of drug metabolism in the drug discovery process has become crucial for the final clinical success of a drug candidate. Use of CYPs early in the drug discovery process can save significant amount of costs and time required in pre-clinical and clinical studies, thereby greatly facilitating the process.

The human CYP superfamily of proteins comprises more than 50 enzymes, each enzyme being able to catalyse multiple reactions. With the exception of some plants, a single NADPH cytochrome P450 reductase (CPR) of a particular eukaryotic species interacts with all CYPs of the same species. For CYP catalytic activity, CPR is absolutely essential, however at the same time CPR is detrimental for the expression of CYPs. Therefore, understanding the process by which the interaction between CYP and CPR occurs is an important biological goal.

I have cloned, expressed and studied the interactions of seven CYPs, CYP2D6, CYP3A4, CYP1A1, CYP1B1, CYP1A2, CYP2E1 and CYP2C8 in conjunction with different CPR species (the native human CPR, variants of human CPR and the yeast CPR) using the baculovirus expression system. In my studies I have found that different CPRs have different coupling efficiencies towards the individual CYP

isoforms. Use of a high-activity CPR from yeast in this study has allowed us to improve our understanding on CYP-CPR interactions. I have found that the ability of a CPR to reduce an artificial substrate like MTT is not directly proportional to its ability to reduce the physiological substrate, CYP. In other words, the strength of the reductase does not determine CYP activity but it is the ability of CPR to couple with CYP which is crucial. This study has resulted in the identification of ΔhRDM, a genetically engineered variant of human CPR, which couples with CYPs far better than the human native CPR and also offers advantage of better reaction rates for CYPs. ΔhRDM also offers an improvement in the ratio of spectrally active CYP2D6 to spectrally inactive CYP2D6. Identification of ΔhRDM has allowed us to devise an insect cell expression system that genetically provides an improvement in the levels and activities of the drug metabolising cytochrome P450 enzymes.

Acknowledgement

The preparation of this thesis would not have been a real fulfilment without the help from some truly remarkable individuals in my life, to whom I am indebted. First and foremost, I owe everlasting gratefulness to Prof. Bob Chaudhuri, my supervisor, whose continuous encouragement, guidance and support enabled me to develop an understanding of the subject. The selfless devotion of his time, ideas and funding are central to the making of my scientific path and this thesis.

I am heartily thankful to Dr. Neill Horley, my co-supervisor, for technical discussions, day-to-day experimental guidance, and sound advice. In particular he has been instrumental in the setup of the enzyme assays which have formed the core of this research project. I am also grateful to Dr. Jacob Biboy for his excellent assistance with LC-MS analysis, protein localization studies, and simply his good company. I also thank my colleagues, Glen McCann and Sachin Mahale for all the interesting conversations and for being fun to be with.

Last but not least, I would like to dedicate the thesis to my family members as a token of thanks and love: to my parents, whom I could never thank enough, who raised me with love for education and supported me in all my pursuits; and to my loving daughter, Isha and my wife, Swati for their understanding, patience and encouragement when it was most required, in the most remarkable manners. My special gratitude is also due to my brother and sisters for their loving support.

Abbreviations

BSA	Bovine Serum Albumin
bp	base pair
cDNA	Complementary deoxyribonucleic acid
CO	Carbon Monoxide
CPR	NADPH-P450 reductase
CYP	Cytochrome P450
DNA	Deoxyribonucleic acid
DMSO	Dimethyl sulfoxide
DTT	Dithiothreitol
E. coli	Escherichia coli
EDTA	Ethylene diamine tetra acetic acid
ER	Endoplasmic reticulum
G6P	Glucose-6-phosphate disodium salt hydrate
G6DPH	Glucose-6-phosphate dehydrogenase
H2DCFDA	5-(and-6)-carboxy-2´,7´-dichlorodihydrofluorescein diacetate
hRD	Human NADPH P450 reductase
IC_{50}	The half maximal inhibitory concentration
kb	kilobase
LB	Luria-Bertani (medium)
MTT	3-(4,5-Dimethylthiazol-2-yl)-2,5-diphenyltetrazolium bromide
$NADP^+$	β-Nicotinamide adenine dinucleotide phosphate
NADPH	β-Nicotinamide adenine dinucleotide phosphate (reduced form)
OD	Optical density

PBS	Phosphate buffered saline
PCR	Polymerase Chain Reaction
RFU	Relative fluorescence units
ROS	Reactive oxygen species
SDS-PAGE	Sodium dodecyl sulfate-polyacrylamide gel electrophoresis
S. cerevisiae	*Saccharomyces cerevisiae*
SDS	Sodium Dodecyl Sulfate
TAE	Tris/EDTA/Glacial acetic acid buffer
TE	Tris-HCl/EDTA
TEMED	*N*,*N*,*N'*,*N'*,-tetramethylethylenediamine
Tris-HCl	Tris(hydroxymethyl)aminomethane-HCl
U	Unit
UV	Ultraviolet
V	Volt
yRD	Yeast NADPH P450 reductase

Table of Contents

Chapter 1 Introduction

1.1 The Biotransformation Process

All living organisms are constantly exposed to xenobiotics. A xenobiotic is a chemical which is not a natural component of the human or animal organism. It is foreign to these organisms. After absorption via oral, pulmonary or cutaneous route, water soluble xenobiotics are eliminated from the body easily through body fluids like urine and faeces. But the xenobiotics that are fat-soluble could accumulate in the lipid-rich tissues which have no defence system. This could lead to toxicity. The metabolism of xenobiotics protects the body against their accumulation and eventually any toxicity. Metabolism involves conversion of xenobiotics into more polar (hydrophilic) substances and facilitates their removal from the body, a process also referred to as detoxification (Masters 1998).

The process of detoxification takes place in three phases. It is regulated by the biotransformation enzymes in Phases I, II and III. The Phase I enzymes catalyse reactions linked to oxidation, reduction or hydrolysis. These reactions release or introduce a functional group (–OH, $–NH_2$, –COOH) thus increasing the polarity of the parent compound. The most common reactions involve mono-oxygenation reactions (involving introduction of –OH groups) at unreactive carbon atoms. They are performed by cytochrome P450 (CYP) enzymes. Phase II detoxification involves conjugation with a small endogenous substance like glutathione, glucuronic acid, or

cysteine. Reactions in Phase II make the metabolite (initially formed by a Phase I reaction) even more hydrophilic and facilitate excretion via bile or urine. Phase II metabolism also decreases the pharmacological activity of the metabolite. Phase III reactions further metabolise products derived from Phase II conjugation reactions. These are catalysed by the same enzymes which are active in Phases I and/ or II (Danielson 2002).

Chemical Reactions Involved in Different Phases of Xenobiotic Metabolism:

Phase I – Oxidation, reduction and hydrolysis

Phase II – Conjugation

Phase III – Oxidation, hydrolysis and deamination

The most important enzyme system catalysing Phase I metabolic reactions is the cytochrome P450 system comprising a number of different enzymes. Cytochrome P450 is a generic term for a large number of oxidative enzymes all of which have about 500 amino acids and a single haem group. The cytochrome P450 enzymes are members of a superfamily of membrane bound haem containing monooxygenases that are responsible for metabolism of endogenous (e.g. cholesterol biosynthesis and steroidogenesis) and exogenous (xenobiotics) substrates. CYPs metabolise xenobiotic substrates which could be pharmaceutical drugs, potential carcinogens, mutagens or environmental pollutants, through the introduction of oxygen containing functionalities into substrate molecules (Danielson 2002).

CYPs are present in many human tissues that include the lung, the mucosa of the gastrointestinal tract, the brain and the kidneys. However the liver is a major organ of xenobiotic metabolism and acts as a filter for xenobiotics. In mammalian cells, CYPs are localized predominantly in the smooth endoplasmic reticulum and are different from the cytochrome proteins that function in electron transport. In contrast to CYPs, cytochrome proteins are localized in the mitochondrial membranes and act as electron carriers for aerobic energy production (Hannemann et al. 2007).

1.2 The History of Cytochrome P450

The name cytochrome P450 originated from the work done by Omura and Sato (1964). In 1964, they reported that the carbon monoxide adduct of the reduced form of a microsomal binding pigment shows a single peak at 450 nm which was readily detected in dithionite treated microsomes by difference spectrophotometry. They also reported evidence for its haemoprotein nature. Before Omura and Sato's work, the presence of a carbon monoxide binding pigment had been reported by Klingenberg and Garfinkel (1958). Since then, cytochrome P450 research has come a long way, advancing in many areas such as drug discovery and pathways related to cancer. CYPs have been characterized in many species (i.e. organisms) that include bacteria, fungi, plants, fish, and mammalian systems (Nebert and McKinnon 1994).

The fifth iron coordination site of the haem in CYPs is bound to protein through the thiolate group of a cysteine rather than through a histidine residue (Poulos et al.

1986). This structural property gives the cytochrome P450 haem its unique spectral properties and allows its detection, even in a background of other haemoproteins. Cytochromes, in a true sense, are proteins which also contain haem as the prosthetic group but carry out electron transport. Although CYPs do not strictly carry out electron transport and therefore are not true cytochromes, the name is still being used. However, the nomenclature committee of the International Union of Biochemistry and Molecular Biology (NC-IUBMB) prefers the term 'haem-thiolate' enzyme instead of 'cytochrome P450' enzyme (Graham and Peterson 1999).

1.3 Cytochrome P450 Nomenclature

The human CYP superfamily of proteins comprises more than 50 enzymes, each enzyme being able to catalyse multiple reactions. The superfamily has 18 families of cytochrome P450 genes and 43 subfamilies, out of which 57 are CYP genes and 58 pseudogenes. (http://drnelson.utmem.edu/P450lect.htm, Jan. 2007). Based on sequence similarities, a standard nomenclature has been adopted that categorizes the individual CYP into families and subfamilies.

The foundation for the P450 gene superfamily nomenclature system were laid with the first report by Nebert et al. (1987) and have been extended in subsequent updates by the same group in 1989 and 1991 and later by Nelson et al. (1993). The catalogue on the website, http://drnelson.utmem.edu/CytochromeP450.html, maintained by the P450 gene superfamily nomenclature committee is updated regularly. The

current P450 nomenclature and classification scheme was most recently reviewed in 1996 (Nelson et al. 1996). This nomenclature is genetically based and has no functional relevance. The committee recommendations for naming a P450 gene include,

The italicized root symbol *'CYP'* denotes **cy**tochrome **P**450, an Arabic number designates the P450 family, a letter indicates the subfamily when two or more subfamilies are known to exist within that family, and the Arabic numeral following the letter represents the individual gene. For example, CYP2D6 implies,

CYP	cytochrome P450
2	the P450 family
D	the subfamily
6	the individual gene

The same numbers and letters, without any spaces between them, are recommended for the corresponding gene products like mRNA, cDNA and enzyme but the product names are not italicized. For example, *CYP2D6* (italicised) represents the gene whereas CYP2D6 (non-italicised) could represent the corresponding mRNA, cDNA or protein.

A P450 protein sequence from one gene family usually is defined as having ≤40% amino acid identity to a P450 protein from any other family. This means

that the P450 protein sequences within a given gene family are >40% identical. Mammalian sequences within the same subfamily are always >55% identical.

Table 1.1 highlights some of the important human CYPs with respect to their expression and xenobiotic metabolism. The information compiled in this Table is gathered from Omiecinski et al. (1999).

Table 1.1. The CYP isoforms that stem from different subfamilies.

Family	Subfamily	Isoforms
CYP1	CYP1A	CYP1A1 and CYP1A2
	CYP1B	CYP1B1
CYP2	CYP2A	CYP2A6 and CYP2A7
	CYP2B	CYP2B6
	CYP2C	CYP2C8, CYP2C9, CYP2C18, and CYP2C19
	CYP2D	CYP2D6
	CYP2E	CYP2E1
CYP3	CYP3A	CYP3A4, CYP3A5 and CYP3A7

1.4 Role of CYPs in Human Diseases and Drug Discovery

Hepatic cytochrome P450s are the most widely studied of the P450 enzymes. As briefly mentioned earlier, CYPs are involved in oxidative metabolism of many xeno- and endobiotics. Most CYPs metabolise multiple substrates participating in the catalysis of specific reactions linked to substrate metabolism. This accounts for their

key role in metabolising an extremely large number of endogenous and exogenous molecules.

CYPs play important roles in endogenous biochemical pathways linked to steroid hormone biosynthesis, metabolism of polyunsaturated fatty acids (such as arachidonic acid and prostaglandins) and activation of vitamin A and D_3 to biologically active hormones. They also participate in the activation and detoxification of a variety of different types of chemicals, some of which possess medicinal properties and others which are known to contaminate or pollute the environment (Estabrook 2003).

Mutations in *CYP* genes that correlate with deficiencies in enzyme activities are responsible for several human diseases (Watanabe 1998). CYPs can also show great inter-individual variability mainly due to environmental factors (e.g. CYP2E being induced in individuals who drink ethanol and CYP1A being induced in individuals who are exposed to aromatic hydrocarbons), genetic factors (that could result in specific CYP enzyme deficiencies) and patho-physiological factors (CYP2E being induced in diabetics).

Moreover, induction of CYP1 family (e.g. which is induced by polycyclic hydrocarbons found in cigarette smoke and charred food) is a risk factor in several cancers such as lung and colon cancers because these enzymes can convert pro-carcinogens to carcinogens. Mutations in the *CYP1B1* gene (leading to defects in

CYP1B1 activity) are linked to congenital glaucoma possibly because of the enzyme's major role in steroidogenesis. A metabolite formed from acetaminophen (Paracetamol) by CYP2E1 can cause severe toxic effects in humans. People who are alcoholic are at high risk to Paracetamol toxicity because they possess alcohol-induced highlevels of CYP2E1. CYP2C8 is selectively responsible for inactivation of the anti-cancer drug paclitaxel (Taxol) through oxidation to 6α-hydroxypaclitaxel. Specific alleles of CYP2C8 are known to have a great influence on the pharmacokinetics of paclitaxel (Nakajima et al. 2005). CYP2C19 is known to metabolise a proton pump inhibitor, omeprazole, which is used to treat peptic ulcer. Omeprazole has been used as a CYP2C19 marker to assess gene-dose effect and its intra-subject variability (Yin et al. 2004).

Some drug molecules can activate or inhibit the CYPs and this can lead to adverse effects of drugs on the human body. For example if ketoconazole (an antifungal compound), a CYP3A4 inhibitor, is administered together with Triazolam (sedative to treat insomnia) which is metabolised by CYP3A4, it will result in an overdose of Triazolam. This is an example of drug-drug interactions which often can cause major problems in the clinic. New drug candidates with poor metabolism profile or which cause drug-drug interactions do not survive the drug development process which is a very expensive process often leading to expenditures of $1 billion or more. Therefore, choosing drugs that do not interact with CYPs is very important at an early stage of drug development. In recent years, the area of drug metabolism has become crucial to the drug discovery process. Use of drug metabolising enzymes early in the drug discovery process can save significant amount of costs and time required in pre-

clinical and clinical studies, thereby greatly facilitating the process. That is the reason why introduction of drug metabolism screens as early as possible in the drug discovery process is gaining appeal. Drug metabolism studies have become as important as primary screening in the drug discovery process.

A relatively small subset of CYPs (CYP1A2, CYP2D6, CYP2C9, CYP2C19, CYP3A4 and CYP2E1) appears to be responsible for the metabolism of most drugs and associated drug-drug interactions (Spatzenegger and Jaeger 1995). It appears that these enzymes have a high affinity towards chemical structures commonly found in pharmaceutical drugs. CYP2D6 is known to metabolise a quarter of all known pharmaceutical entities (Werck and Feyereisen 2000). This subset of enzymes is also considered to be highly important in drug metabolism studies because of their presence in the human liver – the main organ involved in metabolism. For example, CYP3A4 is the most abundant CYP at ~30% of the total CYPs present in the human liver, the others existing in lower yet substantial amounts as indicated in Figure 1.1 (Gonzalez 1992; Beaune 1993).

Figure 1.1 shows relative percentage of CYPs in human liver samples. The information compiled in this chart is gathered from Shimada et al. (1994).

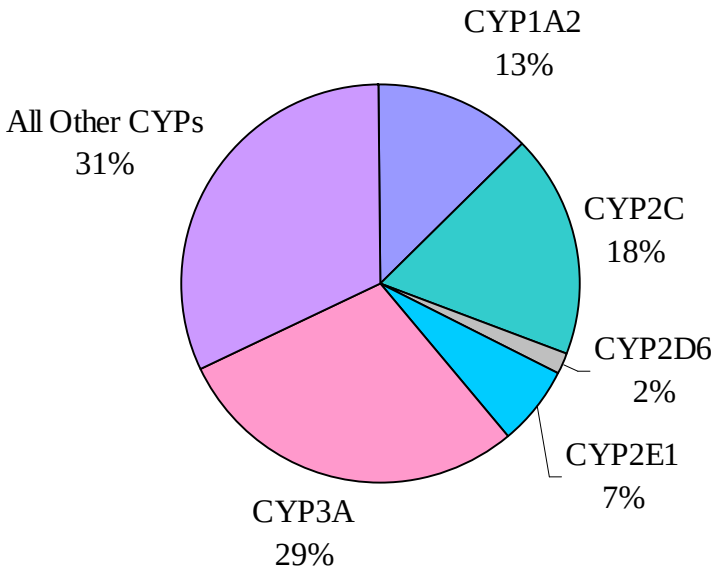

Figure 1.1. Relative percentage of CYPs present in the human liver.

Table 1.2 lists substrates, inducers and inhibitors of the important CYPs mentioned above. The information compiled in this table is gathered from Rendic and DiCarlo (1997) and Parkinson (1996).

Table 1.2. Pharmaceutical substrates for different CYPs.

CYP	Xenobiotics Metabolised	Xenobiotics Activated	Inducers	Inhibitors
CYP1A2	Caffeine; 7-ethoxy-resorufin; 7-methoxy- resorufin; imipramine; phenacetin; theophylline; tacrine R-warfarin	Acetaminophen (paracetamol); aflatoxin B1; 2-aminoacetyl fluorine;	Omeprazol; cruciferous vegetables; cigarette smoking	Enoxacin; fluvoxamine ; isosafrole; apigenin
CYP2C9	Chloramphenicol; diclofenac; ibuprofen; flurbiprofen; hexabarbital; naproxen; omeprazole; phenytoin; retinoids		Rifampin	Warfarin; tolbutamide; sulfaphenazoe
CYP2C19	Diazepam; hexobarbital; mephobarbital; omeprazole; propanolol; phenytoin		Rifampin	Omeprazole; mephenytoin (competitive)
CYP2D6	Bufarolol; dextromethorp-han;			Quinidine; quinine;

	desipramine; ethylmorphine; imipramine; metoprolol;			paroxetine; fluoxetine; norfluoxetine
CYP2E1	Acetaminophen; acrylonitrile; dapsone; enflurane; ethanol; halothane; isoflurane; p-nitrophenol	Acetaminophen acrylonitrile; benzene; chloroform; nitrosamine; styrene; vinylbromide	Alcohol; acetone; pyrazole; isoniazid; obesity	Disulfiram; diethyldithio - carbamate; 4-methyl-pyrazole
CYP3A4	Alfentanil; antipyrine; chloropromazine;clarithro mycin; cyclosporine-A; dapsone; dexamethasone; erythromycin	Acetaminophen aflatoxin B1;	Phenobarbital ;dexa- methasone; rifampin; phenytoin; carbamazepie	Triacetyl- oleandomycin; clarithromycin erythromycin; gestodene; ketoconazole; clotrimazole ; naringenin

1.5 Mechanism of Action of CYPs

Though different CYPs are able to react with a number of chemically different substrates, the basic mechanism of substrate oxygenation is the same for all CYPs. The

CYP reaction is governed by the thermodynamic parameters of the oxygenation process described below (White 1980),

RH (substrate) + O_2 + NADPH + H^+ → ROH (product) + H_2O + $NADP^+$

Substrate oxygenation by CYPs is a multi-step process as described below (Groves 1995).

In the first step, the substrate binds to CYP to form a CYP-substrate complex.

In the second step, the CYP-substrate complex is reduced by another endoplasmic reticulum anchored enzyme known as NADPH-cytochrome P450 reductase (CPR) (French et al 1980; Blanck 1984). CPR reduces ferric cytochrome P450 to ferrous cytochrome P450 by an electron derived from NADPH.

In the third step, dioxygen binds to the ferrous haem iron of CYP and forms the ternary CYP-dioxygen-substrate complex.

In the fourth step, a second electron is introduced into the ternary CYP-dioxygen-substrate complex by CPR or cytochrome b5.

The fifth step includes splitting of the O-O bond with formation of reactive iron-oxo intermediate and a water molecule.

In the sixth step, transfer of oxygen molecule takes place from the reactive iron-oxo intermediate to the substrate bound next to the haem.

Finally, in the seventh step, product dissociation completes the cycle. Thus the introduction of oxygen molecule in a substrate makes the substrate more water-soluble and this process helps in excretion of the substrate from the body (human or animal).

Under physiological conditions, electron transfer steps are believed to be rate limiting. The consensus catalytic cycle for oxygen activation and transfer by cytochrome P450 is shown in Figure 1.2, adapted from John Groves, Models and Mechanism of Cytochrome P450 Action (Groves 1995).

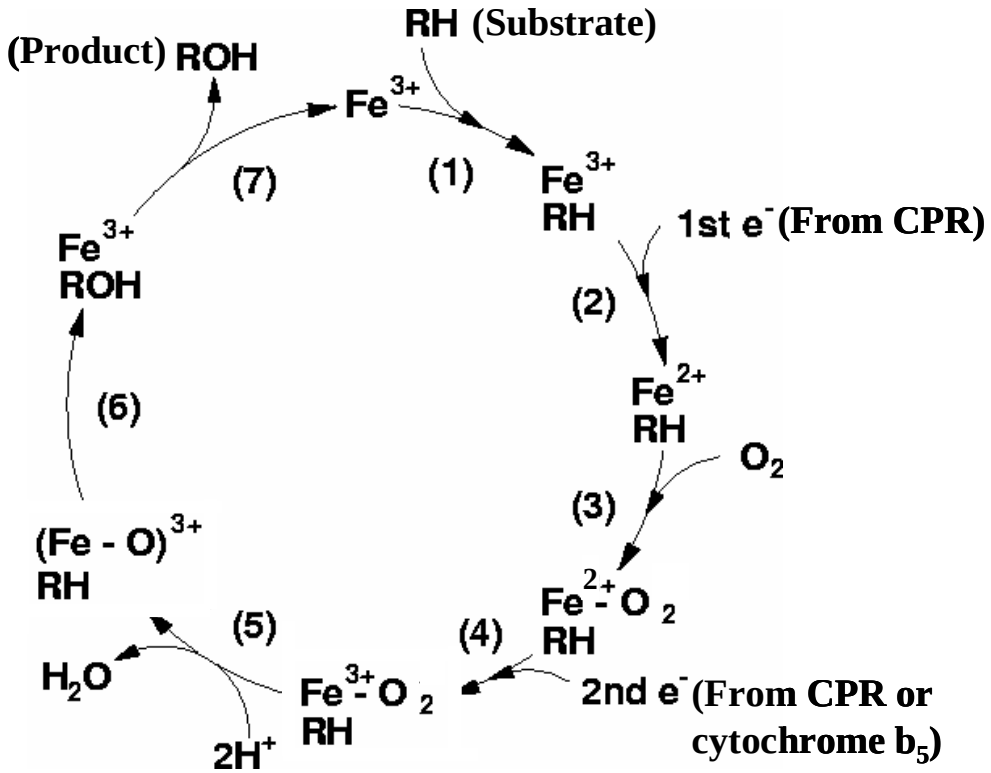

Figure 1.2. The consensus catalytic cycle for oxygen activation and transfer by cytochrome P450.

1.6 Role of NADPH-Cytochrome P450 Reductase (CPR) in CYP Reaction

CPR is responsible for the transfer of electrons from NADPH to CYPs and also to cytochrome b_5. Cytochrome b_5 is another membrane bound protein, which enhances the activity of some but not all CYPs. Similar to the CYPs, CPR is also membrane bound and most abundant in the liver. The amino-terminal hydrophobic region of the CPR anchors the protein in the membrane. Unlike the CYPs which belong to a superfamily of genes, CPR is encoded by a single gene in most mammalian species (Simmons 1985; Sutter and Loper 1989; Yamano et al 1989; Shephard 1989). This single enzyme interacts with all the CYPs. CPR levels are not modulated by inducers of the cytochrome P450 system.

As described earlier in Section 1.5, "Mechanism of Action of CYPs", CYPs cannot metabolise the substrates on their own, they require molecular oxygen and an electron donor protein for their catalytic activity. The first step of the catalytic cycle after formation of the CYP-substrate complex is transfer of the first electron. NADPH-cytochrome P450 reductase (CPR) acts as the electron transfer protein.

In 1950, Horecker (Horecker 1950) reported CPR in liver tissues. He also reported that the enzyme used NADPH as a source of reducing equivalents and contained flavin adenine dinucleotide (FAD) as a prosthetic group. After another 12 years, the enzyme was found to be located in the microsomal fraction which essentially

consist of the endoplasmic reticular membranes (Phillips and Langdon 1962; Wiliams and Kamin 1962). Direct evidence for the involvement of the reductase in microsomal hydroxylation reactions was shown by reconstitution of laurate ω-hydroxylase activity from a preparation of cytochrome P450, NADPH-cytochrome c reductase and phosphatidylcholine (Lu and Coon 1968; Lu et al. 1969). Subsequently, the CPR was reported to contain one molecule of FAD and one molecule of FMN for each molecule of enzyme (Iyanagi and Mason 1973; Yasukochi and Masters 1976). Kinetic analysis of reduction of CPR established that NADPH donates electron to FAD, FAD donates electron to FMN and finally FMN transfers electron to cytochrome P450. CPR is an electron donor protein not only for CYPs but also for several other oxygenase enzymes such as squalene monooxygenase and haem oxygenase.

Many scientists (Iyanagi et al. 1978; Vermilion et al. 1981) have suggested that the mammalian CPR cycles between the 1- and 3-electron containing subforms during steady state, as shown in Figure 1.3. According to this mechanism, two electrons are added by NADPH to the air-stable semiquinone of the reductase resulting in a 3-electron reductase. The two flavin molecules rearrange electrons to yield $FMNH_2$ and then an electron is transferred to CYP. The 2-electron reductase again undergoes inter-flavin rearrangement and yields $FMNH_2$, transfers another electron to CYP which is ready to accept the second electron from NADPH.

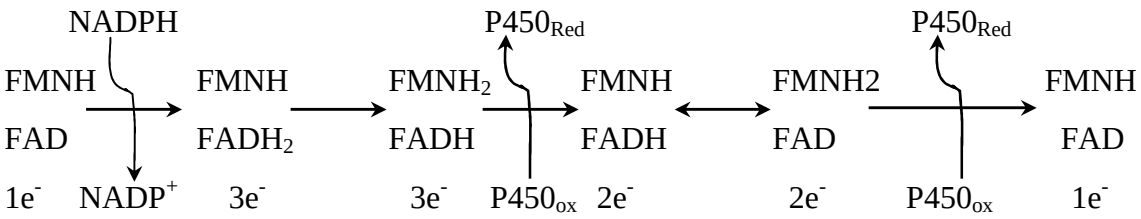

Figure 1.3. The mammalian CPR cycles between the 1- and 3-electron containing subforms during steady state

It is important to note that the catalytic activity of a particular CYP in a specific tissue, sub-cellular fraction, or recombinant expression system is determined not only by the abundance of the CYP, but also by the amount of its electron transport partner CPR (Crespi & Miller 1999).

1.7 Role of Cytochrome b_5 in CYP Reactions

In 1971, Hildebrandt and Estabrook (Hildebrandt and Estabrook 1971) showed evidence for the involvement of cytochrome b_5 in hepatic CYP reactions. It is a 17-kDa haemprotein which is also associated with microsomes. Surprisingly, it enhances the activity of some CYP reactions *in vitro*, but not all. In early days of research on cytochrome b_5 this perplexing aspect was a subject of much debate. Reports from some investigators suggested that it is not necessary at all for CYP reactions but others have shown that it is absolutely essential for particular CYP reactions with specific substrates (Porter 2002). Cytochrome b_5 is reduced by an NADPH-dependent flavoprotein,

NADPH- b_5 reductase (Strittmatter 1967; Takesue and Omura 1970). However, it is confirmed that cytochrome b_5 is also reduced by CPR (Enoch and Strittmatter 1979; Noshiro et al. 1979). The evidence today indicates that cytochrome b_5 enhances the activities of many CYP reactions (Vergeres and Waskell 1995)[40]. It has been reported that, in the presence of NADPH, recombinant co-expression of b_5 reductase, b_5 and CYP3A4 catalyses testosterone and nifidepine oxidation at greater rates than that obtained with CPR and CYP3A4 (Yamazaki 2002). Similar augmentation in reaction rates, mediated by b_5, has been reported for other CYPs such as CYP2A6, CYP2B6, CYP2C8, CYP2C9, CYP2C19, and CYP2E1 (Mokashi et al. 2003; Schenkman and Jansson 2003; Shimada et al. 2005).

Cytochrome b_5 also acts as an electron donor protein for fatty acid desaturase (Holloway and Katz 1975), reduction of haemoglobin (Mauk and Mauk 1982) and synthesis of methionine (Chen and Banerjee 1988). Figure 1.4 shows the mechanism of action of cytochrome b_5 (Porter 2002).

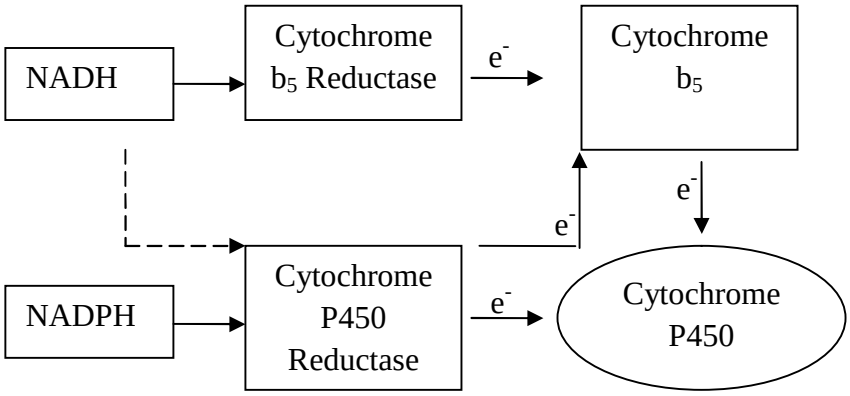

Figure 1.4. The mechanism of action of cytochrome b_5

1.8 Experimental Systems for CYP mediated drug metabolism

1.8.1 Human liver tissues

Despite considerable sequence similarity in CYPs across species, even small differences can cause significant changes in catalytic activity. For example, the 6- and 8-hydroxylation of warfarin is catalysed by rat CYP1A1 but not by the corresponding enzyme in mice, despite 93% identity in their protein sequences (Kaminsky et al. 1984). S-mephenytoin is 4-hydroxylated by only human CYP2C19 but this reaction is also specifically mediated by the rat CYP3A (Shimada and Guengerich 1985; Shimada et al. 1986). Therefore, drug metabolism studies with human liver tissues, containing active CYP enzymes are considered to be crucial for drug discovery. However, this in turn raises wider issues of availability and ethics (Bardsley 1994).

1.8.2 Human liver microsomes

Although the preparation of microsomes (essentially the endoplasmic reticular membranes) from human liver tissues is not too difficult, microsomal samples on their own are unable to gauge accurately the degree of inhibition of individual CYPs (present in the human liver) by specific chemical compounds. Moreover, microsomes (non-living entities) do not allow assessment of the levels of CYPs that could be induced by a particular chemical.

1.8.3 Hepatocytes

In contrast to microsomes, hepatocytes are usually used mainly to study induction of CYPs. Hepatocytes are specialised liver cells which contain 70-80% of the cytoplasmic mass of the liver. However, primary hepatocytes isolated from the liver have very limited life span when grown *in-vitro*.

1.8.4 Heterologous cDNA-Expression Systems for CYPs

Several heterologous expression systems like bacteria (*Escherichia coli*), yeast (*Saccharomyces cerevisiae*), insect cells and mammalian cells have been used successfully to express CYPs (Gonzalez and Korzekwa 1995). These systems can be used for expression of CYP alone or together with its redox partners, CPR and/or b_5.

As CYPs require their redox partners, expression of CYP alone in any expression system does not give optimum catalytic activity. A CYP can be expressed, purified and later mixed with its redox partners or, alternatively, these redox partners can be co-expressed with a CYP.

Unfortunately, high level co-expression of a CYP and CPR in heterologous systems poses some problems to host cells. These are related to the activity of CYP enzymes that are expressed and their content. Since CYP-CPR complexes are associated with the endoplasmic reticulum, a vital organelle of eukaryotic cells, their high level expression cause an increased stress on the cell. Co-expression of CPR with a specific CYP definitely increases the catalytic activity of the CYP enzyme but also dramatically reduces the yield of spectrally active CYP enzyme (Pritchard et al. 1998; Dong and Porter 1996; Chen et al. 1997) which is shown quite emphatically in the recombinant baculovirus-insect cell system. Although the CYP apoprotein levels remain unchanged during co-expression of a CYP and a CPR, the amounts of spectrally active CYP decrease remarkably (Chen et al. 1997; Gonzalez et al. 1991; Tamura et al. 1992).

1.8.4.1 Bacterial Expression System

E. coli has been used for expressing high levels of several CYPs (Gonzalez and Korzekwa, 1995). The culture media requirements for this expression system are inexpensive compared to insect and mammalian expression systems. CYPs expressed

in bacterium have provided valuable information regarding structure-function relationships. The N-terminal hydrophobic region of mammalian CYPs (Haugen 1997) is responsible for the insertion of the protein into membrane structures. Truncation or modification of this hydrophobic region results in change of location of the expressed enzyme to the cytosol. In order to produce catalytically active CYP and to facilitate purification, N-terminal modifications of the CYP proteins have been performed (Iwata et al. 1998; Barnes et al. 1991). Another approach for bacterial expression is insertion of the outer membrane protein A (*omp*A) targeting sequence which directs the CYP protein, devoid of the N-terminal hydrophobic region, to the periplasmic space of the bacteria, where it is then removed by proteolytic cleavage (Pritchard et al. 1998). OmpA is a major protein in the *E. coli* outer membrane. Construction of plasmids that allow expression of catalytically active CYP-CPR fusion proteins (where the CPR lacks the N-terminal membrane anchor) has provided some advantages such as convenience in purification and avoiding the need for reconstitution.

The ability of the bacterium to produce large quantities of an active CYP enzyme may offer applications of this system in industrial scale biocatalysis and biosynthesis of metabolites. However, the major drawback of the prokaryotic bacterial system is that bacterial cells do not contain the endoplasmic reticulum, an intracellular compartment to which human and mammalian CYPs are naturally associated. Endoplasmic reticular membrane association is essential for human CYP activity – human CYPs shorn off the ER membranes are totally inactive. In order to express CYPs in bacteria, *CYP* genes must undergo drastic alterations at the genetic level.

1.8.4.2 Yeast Expression System

Like bacterial expression systems, a yeast expression system is inexpensive in terms of culture media requirements and faster doubling time of the cells. Unlike bacteria, yeast provides a eukaryotic intracellular environment and therefore mammalian CYPs can be expressed and obtained in their native form, anchored to yeast's endoplasmic reticulum. In order to achieve higher catalytic activity, a CYP and CPR can be co-expressed in yeast. Both CPR and b_5 have been successfully co-expressed with CYPs by stable co-transfection in yeast (Peyronneau et al. 1992). Studies in our laboratories at De Montfort University (unpublished data) have shown that high level expression of CYPs with higher catalytic activities can be obtained in *Saccharomyces cerevisiae*. The strategies used at De Montfort University allow one to co-express a human CYP, human CPR and where necessary b_5.

1.8.4.3 Mammalian Expression System

Several mammalian host cells have been used for expression of CYPs. Human lymphoblast cells (Crespi et al. 1990), human hepatic HepG2 cells (Aoyama et al. 1990; Dai et al. 1993), Chinese hamster ovary cells (Ding et al. 1997), NIH 3T3 cells (Battula et al. 1987) and V79 cells (Doehmer et al. 1988) have been successfully used for expression of CYPs. Use of hepatic cell lines provides appropriate electron transport ability and a host environment in which the CYPs are naturally predominant. There is some level of natural expression of CYP, CPR and b_5 in some hepatic host cells but that

may be rate limiting and not enough for catalysis. There is an upper limit on the expression levels of human CYPs that can be achieved in mammalian expression systems. However the CYP mammalian expression system, if conveniently available, could be highly relevant for cytotoxicity studies, malignant transformation and mutagenesis studies (Crespi & Miller 1999).

1.8.4.4 Baculovirus Expression System

Baculoviruses are double stranded DNA viruses which infect insects but are not pathogenic to mammals. Baculovirus mediated expression of recombinant cDNA proteins in insect cells is a valuable tool for expressing proteins. The recombinant virus harbouring a cDNA infects insect cells *in-vitro*, uses the host cells' machinery for multiplication and the protein expression is driven by viral promoters. The baculovirus-insect cell expression system allows high level expression of recombinant proteins targeted to the correct cellular compartment (Summers and Smith 1987). It also provides, like the yeast system, correct folding of recombinant protein, disulfide bond formation, oligomerization and some of the important post-translational modifications.

The baculovirus-insect cell expression system has gained widespread popularity. Several recombinant cytoplasmic, secreted and membrane-bound proteins have been successfully expressed using this system. The recombinant viruses use viral polyhedrin or p10 gene promoters to drive the expression of proteins (Luckow 1991). The traditional method of generating recombinant baculoviruses is labour- and time-

consuming. However, significant progress has been made over the past decade on methods in recombinant baculovirus generation and insect cells. The time and effort involved in developing recombinant viruses have been reduced by the use of commercially available systems. Often multiple baculovirus promoters allow one to simultaneously express two or more proteins via a single recombinant virus (Weyer and Possee 1991).

The size of the baculovirus genome is very large (134 kbps) (Ayres 1994), and therefore no unique restriction site is available for direct subcloning of a gene of interest into the genome. In view of that, homologous recombination appears to be a convenient method for generating a recombinant virus. One approach to achieve this is to co-transfect insect cells with a shuttle plasmid (in which the gene of interest is subcloned) and the linearized viral genomic DNA. Thus the foreign gene, encoded by a shuttle plasmid, is introduced into a nonessential region of the viral genome via homologous recombination. The linearised viral DNA is commercially available from both BD Pharmingen (BaculoGold, Baculovirus Expression Vector System) and Clontech (BacPAK6).

Another approach to generate a recombinant baculovirus is newer and developed by researchers at Monsanto. It is based on site-specific transposition of an expression cassette from a donor plasmid into a baculovirus shuttle vector (bacmid) which is propagated in *E. coli* (Luckow et al. 1993). The system is marketed by Invitrogen (Bac-to-Bac Baculovirus Expression System). In order to carry a gene of interest on an

expression cassette, a number of donor plasmids are available for use with this system. These include pFastBac1 with the polyhedrin promoter (Anderson et al. 1996), N-terminal 6xHis tag on pFastBacHT together with the polyhedrin promoter (Polayes et al. 1996) and pFastbacDual which contain both the polyhedrin and p10 promoters for simultaneous expression of two different proteins (Harris and Polayes 1997).

In order to generate recombinant bacmid DNA, the Bac-to-Bac Expression System takes advantage of the site specific transposition properties of the Tn7 transposon. In the first part of the process, a gene of interest is cloned, for example, in the pFastBac donor plasmid under the control of viral promoter, polyhedrin (PH) or p10. The promoters are derived from *Autographa californica* multiple nuclear polyhedrosis virus (AcMNPV). The expression cassette is flanked by the left and right arms of Tn7 transposon. The expression cassette also contains a gentamycin resistance gene and an SV40 polyadenylation transcription stop signal to form a mini Tn7 transposon.

In the second part of the process the recombinant bacmid is generated. To achieve this, a DH10Bac *E. coli* strain is used which contains a bacmid with the mini-*att*Tn7 target site (i.e. a specific site present in the chromosomes of many bacteria) and a helper plasmid. The helper plasmid provides the transposase protein required for the process of transposition and it also contains a tetracycline resistance gene. The pFastBac donor plasmid transformation into the DH10Bac cells results in transposition

between the mini-Tn7 element on the pFastBac donor plasmid and the mini-*att*Tn7 target site on the bacmid to generate the recombinant bacmid.

The bacmid in DH10Bac cells also contains a low copy number mini-F replicon, kanamycin resistance marker and a segment of DNA encoding the LacZα peptide (from a pUC-based cloning vector) into which the attachment site for the bacterial transposon, Tn7 (mini-*att*Tn7) has been inserted. The reading frame of the LacZα peptide is not disrupted by this insertion. However the LacZ gene is deleted from the chromosome of DH10Bac cells. The LacZ gene present on bacmid complements for the deletion and produces blue (Lac^+) colonies when induced with IPTG in the presence of chromogenic substrates like Bluo-gal or X-gal. Homologous recombination disrupts the DNA encoding LacZα peptide on bacmid and the DH10Bac cells harbouring recombinant bacmid develop white colour (Lac^-) (Bac-to-Bac Baculovirus Expression System, Invitrogen, Version D, 2004).

High molecular weight recombinant bacmids from white colonies are then isolated, checked for veracity using PCR and used for transfection into insect cells to generate recombinant baculovirus. The resulting baculoviruses can be used for expression of proteins in insect cells. Figure 1.5 shows the schematic representation of the recombinant baculovirus generation.

The host cells of insect origin are Sf9, Sf21 and *Trichoplusia ni* cells (BTI-TN-5B1-4). The later one has been developed by Boyce Thompson Institute and commercially available as High Five from Invitrogen Corp. These cells grow as adherent cultures as well as in suspension. Since the cells also grow in suspension, large scale biorectors can be used for expression of the recombinant proteins.

Both the CYP and the CPR can be expressed at high levels in insect cells using the baculovirus expression system (Lee et al. 1995). Amongst different recombinant expression systems, it appears to offer the best combination of high CYP content and high catalytic activity per unit CYP enzyme (Crespi and Miller 1999).

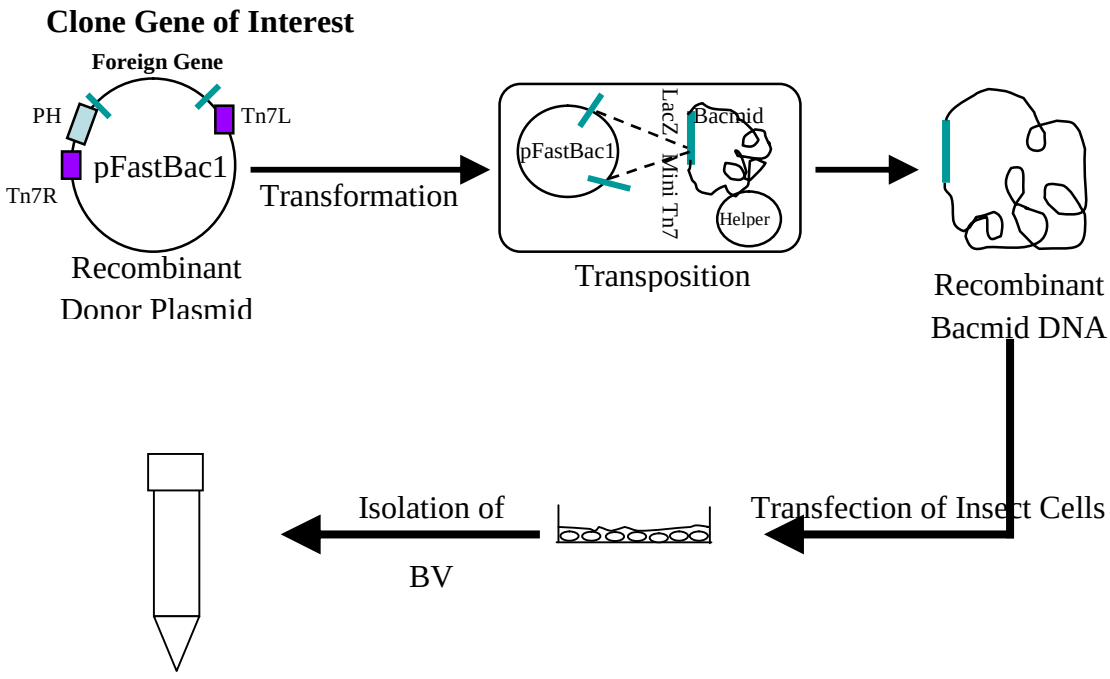

Figure 1.5. Schematic representation of recombinant baculovirus generation (Adapted from Bac-to-Bac Baculovirus Expression System, Invitrogen, Version D, 2004).

1.9 Objectives of the Research

The main aim of the investigation was to devise an insect cell expression system that would allow improvement of the levels and activities of the drug metabolising cytochrome P450 enzyme (CYPs). With this aim in mind, I embarked on research that would allow me to answer the following questions:

(1) Is a genetically engineered variant of the human NADPH cytochrome P450 reductase (CPR) less toxic than the native CPR?

(2) Does the genetically engineered CPR variant couple better with CYPs than the native CPR? and

(3) How does the heterologous yeast CPR, which is so highly active and which in theory should provide super active CYP enzymes, function when co-expressed with human CYP genes in insect cells?

It was decided that the four CYPs, CYP3A4, CYP2E1, CYP2D6 and CYP1A2, which are more prominently expressed in human liver tissues and therefore widely used for drug metabolism studies, would form the basis of my investigations.

The CYPs cannot metabolise substrates on their own, they require CPR for their catalytic activity. The catalytic activity of a particular CYP is determined not only by the abundance of the CYP, but also by the amount of CPR (Crespi and Miller 1999). Although CPR is essential for CYP activity, paradoxically the mere presence of CPR

contributes to a dramatic decrease in the levels of active CYP. It can be speculated that this is possibly the result of production of hydroxyl radicals which are involved in an uncoupled CYP reaction cycle. The process of transferring electrons from NADPH via the CPR/CYP complex to oxygen to form reactive oxygen species (ROS) is termed uncoupling. Some CYPs, such as CYP2E1, have shown a high degree of uncoupling which results in damage to cellular components, including CYP2E1 itself (Wang et al. 1996). It appears that coupling of the electron transport partner (CPR) to CYPs is a crucial factor towards high activity of CYP holoenzymes but also an extremely important element that causes low levels of CYP holoproteins.

There is a pressing need for solving this paradox in view of the widespread biotechnological applications of recombinant CYP enzymes. It has been reported that use of radical scavengers (i.e. anti-oxidants) such as dimethyl sulfoxide (DMSO), which is capable of trapping free radicals, increases the CYP holoenzyme content (Narimatsu et al. 2005). But this purported to be only a crude attempt in trying to increase levels of CYP holoenzyme through chemical modulations of the enzymes after their production. My research hoped to address this paradox through defined genetic means, namely through

(1) Designing a genetically engineered variant of the human CPR which could be less toxic and yet could couple better with CYPs than the native enzyme allowing us to improve upon both CYP levels and activity in an insect cell expression system, and

(2) Using a high-activity CPR from a heterologous organism to enable us to monitor the ability of this particular CPR to couple with a human CYP and compare results obtained with the native human CPR permitting us to understand better the phenomenon of CYP activation by a CPR.

We had earlier engineered and cloned a variant of the human CPR (hRD) (Figure 2.1 Gene Alignment and Protein Alignment) for our yeast expression studies and surprisingly observed that it was active (see below). I wanted to explore if this mutant enzyme was less toxic than the native enzyme in the insect cell expression system.

The native CPR contains binding sites for the essential cofactors FMN and FAD at its NH_2-terminus. The first 165 bps at the 5'-end of the hRD gene code for a 55-amino acid domain that permit anchoring to microsomal membranes. Within this DNA sequence lies a 72 bps region which code for a 24-amino acid negatively charged domain. The FMN binding site spans a sequence that includes the membrane anchor whereas the region to which FAD binds is positioned beyond this domain. The complete hRD membrane anchor is essential for coupling to CYPs. The lack of the NH_2-terminal 24-amino acid charged region present in hRD prevents association of the resultant molecule, ΔhRD, to microsomal membranes. However, the ΔhRDM protein which also lacks the NH_2-terminal 24-amino acids of CPR but contains an extra 12-amino acid sequence (referred to as the c-myc tag) added to ΔhRD's COOH-terminus

has the inexplicable ability to adhere once again to microsomal membranes like the native CPR.

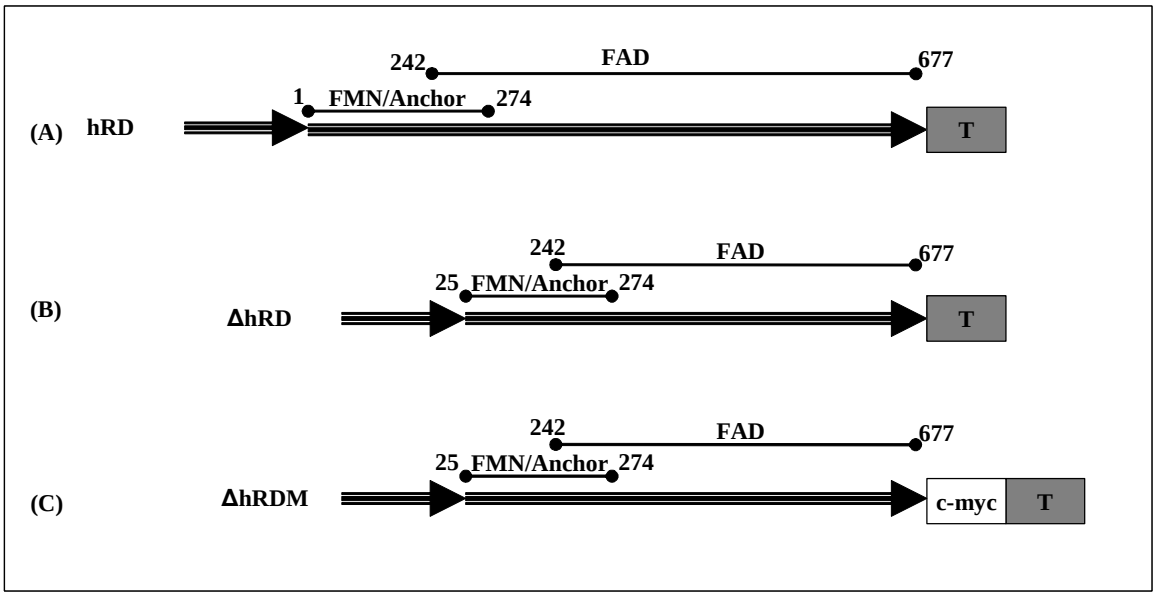

Figure 1.6. The genetically engineered variant of human CPR, ΔhRDM.

Gene Alignment of *hRD* and *ΔhRDM*. Comparison of the coding strand of full length human P450 reductase gene (hRD) with its genetically engineered variant ΔhRDM.

```
                  10         20         30         40         50         60
hRD      GGATCCATGGGAGACTCCCACGTGGACACCAGCTCCACCGTGTCCGAGGCGGTGGCCGAA

ΔhRDM    ------------------------------------------------------------

                   70         80         90        100        110        120
hRD       GAAGTATCTCTTTTCAGCATGACGGACATGATTCTGTTTTCGCTCATCGTGGGTCTCCTA
                                :::::::::::::::::::::::::::::::::::::::
ΔhRDM     -----------------ATGACGGACATGATTCTGTTTTCGCTCATCGTGGGTCTCCTA
                                       10         20         30         40
```

```
                130       140       150       160       170       180
hRD     ACCTACTGGTTCCTCTTCAGAAAGAAAAAAGAAGAAGTCCCCGAGTTCACCAAAATTCAG
        ::::::::::::::::::::::::::::::::::::::::::::::::::::::::::::
ΔhRDM   ACCTACTGGTTCCTCTTCAGAAAGAAAAAAGAAGAAGTCCCCGAGTTCACCAAAATTCAG
              50        60        70        80        90       100

                 190       200       210       220       230       240
hRD     ACATTGACCTCCTCTGTCAGAGAGAGCAGCTTTGTGGAAAAGATGAAGAAAACGGGGAGG
        ::::::::::::::::::::::::::::::::::::::::::::::::::::::::::::
ΔhRDM   ACATTGACCTCCTCTGTCAGAGAGAGCAGCTTTGTGGAAAAGATGAAGAAAACGGGGAGG
             110       120       130       140       150       160

               250       260       270       280       290       300
hRD     AACATCATCGTGTTCTACGGCTCCCAGACGGGGACTGCAGAGGAGTTTGCCAACCGCCTG
        ::::::::::::::::::::::::::::::::::::::::::::::::::::::::::::
ΔhRDM   AACATCATCGTGTTCTACGGCTCCCAGACGGGGACTGCAGAGGAGTTTGCCAACCGCCTG
             170       180       190       200       210       220

                 310       320       330       340       350       360
hRD     TCCAAGGACGCCCACCGCTACGGGATGCGAGGCATGTCAGCGGACCCTGAGGAGTATGAC
        ::::::::::::::::::::::::::::::::::::::::::::::::::::::::::::
ΔhRDM   TCCAAGGACGCCCACCGCTACGGGATGCGAGGCATGTCAGCGGACCCTGAGGAGTATGAC
             230       240       250       260       270       280

                 370       380       390       400       410       420
hRD     CTGGCCGACCTGAGCAGCCTGCCAGAGATCGACAACGCCCTGGTGGTTTTCTGCATGGCC
        ::::::::::::::::::::::::::::::::::::::::::::::::::::::::::::
ΔhRDM   CTGGCCGACCTGAGCAGCCTGCCAGAGATCGACAACGCCCTGGTGGTTTTCTGCATGGCC
             290       300       310       320       330       340
```

```
                 430       440       450       460       470       480
hRD      ACCTACGGTGAGGGAGACCCCACCGACAATGCCCAGGACTTCTACGACTGGCTGCAGGAG
         ::::::::::::::::::::::::::::::::::::::::::::::::::::::::::::
ΔhRDM    ACCTACGGTGAGGGAGACCCCACCGACAATGCCCAGGACTTCTACGACTGGCTGCAGGAG
               350       360       370       380       390       400
                 490       500       510       520       530       540
hRD      ACAGACGTGGATCTCTCTGGGGTCAAGTTCGCGGTGTTTGGTCTTGGGAACAAGACCTAC
         ::::::::::::::::::::::::::::::::::::::::::::::::::::::::::::
ΔhRDM    ACAGACGTGGATCTCTCTGGGGTCAAGTTCGCGGTGTTTGGTCTTGGGAACAAGACCTAC
               410       420       430       440       450       460
                 550       560       570       580       590       600
hRD      GAGCACTTCAATGCCATGGGCAAGTACGTGGACAAGCGGCTGGAGCAGCTCGGCGCCCAG
         ::::::::::::::::::::::::::::::::::::::::::::::::::::::::::::
ΔhRDM    GAGCACTTCAATGCCATGGGCAAGTACGTGGACAAGCGGCTGGAGCAGCTCGGCGCCCAG
               470       480       490       500       510       520
                 610       620       630       640       650       660
hRD      CGCATCTTTGAGCTGGGGTTGGGCGACGACGATGGGAACTTGGAGGAGGACTTCATCACC
         ::::::::::::::::::::::::::::::::::::::::::::::::::::::::::::
ΔhRDM    CGCATCTTTGAGCTGGGGTTGGGCGACGACGATGGGAACTTGGAGGAGGACTTCATCACC
               530       540       550       560       570       580
                 670       680       690       700       710       720
hRD      TGGCGAGAGCAGTTCTGGCCGGCCGTGTGTGAACACTTTGGGGTGGAAGCCACTGGCGAG
         ::::::::::::::::::::::::::::::::::::::::::::::::::::::::::::
ΔhRDM    TGGCGAGAGCAGTTCTGGCCGGCCGTGTGTGAACACTTTGGGGTGGAAGCCACTGGCGAG
               590       600       610       620       630       640
```

```
                730       740       750       760       770       780
hRD     GAGTCCAGCATTCGCCAGTACGAGCTTGTGGTCCACACCGACATAGATGCGGCCAAGGTG
        ::::::::::::::::::::::::::::::::::::::::::::::::::::::::::::
ΔhRDM   GAGTCCAGCATTCGCCAGTACGAGCTTGTGGTCCACACCGACATAGATGCGGCCAAGGTG
             650       660       670       680       690       700
                790       800       810       820       830       840
hRD     TACATGGGGGAGATGGGCCGGCTGAAGAGCTACGAGAACCAGAAGCCCCCCTTTGATGCC
        ::::::::::::::::::::::::::::::::::::::::::::::::::::::::::::
ΔhRDM   TACATGGGGGAGATGGGCCGGCTGAAGAGCTACGAGAACCAGAAGCCCCCCTTTGATGCC
             710       720       730       740       750       760
                850       860       870       880       890       900
hRD     AAGAATCCGTTCCTGGCTGCAGTCACCACCAACCGGAAGCTGAACCAGGGAACCGAGCGC
        ::::::::::::::::::::::::::::::::::::::::::::::::::::::::::::
ΔhRDM   AAGAATCCGTTCCTGGCTGCAGTCACCACCAACCGGAAGCTGAACCAGGGAACCGAGCGC
             770       780       790       800       810       820
                910       920       930       940       950       960
hRD     CACCTCATGCACCTGGAATTGGACATCTCGGACTCCAAAATCAGGTATGAATCTGGGGAC
        ::::::::::::::::::::::::::::::::::::::::::::::::::::::::::::
ΔhRDM   CACCTCATGCACCTGGAATTGGACATCTCGGACTCCAAAATCAGGTATGAATCTGGGGAC
             830       840       850       860       870       880
                970       980       990      1000      1010      1020
hRD     CACGTGGCTGTGTACCCAGCCAACGACTCTGCTCTCGTCAACCAGCTGGGCAAAATCCTG
        ::::::::::::::::::::::::::::::::::::::::::::::::::::::::::::
ΔhRDM   CACGTGGCTGTGTACCCAGCCAACGACTCTGCTCTCGTCAACCAGCTGGGCAAAATCCTG
             890       900       910       920       930       940
```

```
                1030      1040      1050      1060      1070      1080
hRD     GGTGCCGACCTGGACGTCGTCATGTCCCTGAACAACCTGGATGAGGAGTCCAACAAGAAG
        ::::::::::::::::::::::::::::::::::::::::::::::::::::::::::::
ΔhRDM   GGTGCCGACCTGGACGTCGTCATGTCCCTGAACAACCTGGATGAGGAGTCCAACAAGAAG
             950       960       970       980       990      1000
                1090      1100      1110      1120      1130      1140
hRD     CACCCATTCCCGTGCCCTACGTCCTACCGCACGGCCCTCACCTACTACCTGGACATCACC
        ::::::::::::::::::::::::::::::::::::::::::::::::::::::::::::
ΔhRDM   CACCCATTCCCGTGCCCTACGTCCTACCGCACGGCCCTCACCTACTACCTGGACATCACC
            1010      1020      1030      1040      1050      1060
                1150      1160      1170      1180      1190      1200
hRD     AACCCGCCGCGTACCAACGTGCTGTACGAGCTGGCGCAGTACGCCTCGGAGCCCTCGGAG
        ::::::::::::::::::::::::::::::::::::::::::::::::::::::::::::
ΔhRDM   AACCCGCCGCGTACCAACGTGCTGTACGAGCTGGCGCAGTACGCCTCGGAGCCCTCGGAG
            1070      1080      1090      1100      1110      1120
                1210      1220      1230      1240      1250      1260
hRD     CAGGAGCTGCTGCGCAAGCTGGCCTCCTCCTCCGGCGAGGGCAAGGAGCTGTACCTGAGC
        ::::::::::::::::: ::::::::::::::::::::::::::::::::::::::::::
ΔhRDM   CAGGAGCTGCTGCGCAAGATGGCCTCCTCCTCCGGCGAGGGCAAGGAGCTGTACCTGAGC
            1130      1140      1150      1160      1170      1180
                1270      1280      1290      1300      1310      1320
hRD     TGGGTGGTGGAGGCCCGGAGGCACATCCTGGCCATCCTGCAGGACTGCCCGTCCCTGCGG
        ::::::::::::::::::::::::::::::::::::::::::::::::::::::::::::
ΔhRDM   TGGGTGGTGGAGGCCCGGAGGCACATCCTGGCCATCCTGCAGGACTGCCCGTCCCTGCGG
            1190      1200      1210      1220      1230      1240
```

```
                1330      1340      1350      1360      1370      1380
hRD     CCCCCCATCGACCACCTGTGTGAGCTGCTGCCGCGCCTGCAGGCCCGCTACTACTCCATC
        ::::::::::::::::::::::::::::::::::::::::::::::::::::::::::::
ΔhRDM   CCCCCCATCGACCACCTGTGTGAGCTGCTGCCGCGCCTGCAGGCCCGCTACTACTCCATC
            1250      1260      1270      1280      1290      1300
                1390      1400      1410      1420      1430      1440
hRD     GCCTCATCCTCCAAGGTCCACCCCAACTCTGTGCACATCTGTGCGGTGGTTGTGGAGTAC
        ::::::::::::::::::::::::::::::::::::::::::::::::::::::::::::
ΔhRDM   GCCTCATCCTCCAAGGTCCACCCCAACTCTGTGCACATCTGTGCGGTGGTTGTGGAGTAC
            1310      1320      1330      1340      1350      1360
                1450      1460      1470      1480      1490      1500
hRD     GAGACCAAGGCCGGCCGCATCAACAAGGGCGTGGCCACCAACTGGCTGCGGGCCAAGGAG
        ::::::::::::::::::::::::::::::::::::::::::::::::::::::::::::
ΔhRDM   GAGACCAAGGCCGGCCGCATCAACAAGGGCGTGGCCACCAACTGGCTGCGGGCCAAGGAG
            1370      1380      1390      1400      1410      1420
                1510      1520      1530      1540      1550      1560
hRD     CCTGCCGGGGAGAACGGCGGCCGTGCGCTGGTGCCCATGTTCGTGCGCAAGTCCCAGTTA
        :::: ::::::::::::::::::::::::::::::::::::::::::::::::::::::::
ΔhRDM   CCTGTCGGGGAGAACGGCGGCCGTGCGCTGGTGCCCATGTTCGTGCGCAAGTCCCAGTTA
            1430      1440      1450      1460      1470      1480
                1570      1580      1590      1600      1610      1620
hRD     CGCCTGCCCTTCAAGGCCACCACGCCTGTCATCATGGTGGGCCCCGGCACCGGGGTGGCA
        :::::::::::::::::::::::::::::::::::::::::::::::::::: :::::
ΔhRDM   CGCCTGCCCTTCAAGGCCACCACGCCTGTCATCATGGTGGGCCCCGGCACCGGG-TGGCA
           1490      1500      1510      1520      1530       1540
```

```
                1630      1640      1650      1660      1670
hRD     CCCTT-CATAGGCTTCATCCAGGAGCGGGCCTGGCTGCGACAGCAGGGCAAGGAGGTGGG
        ::::: ::::::::::::::::::::::::::::::::::::::::::::::::::::::
ΔhRDM   CCCTTTCATAGGCTTCATCCAGGAGCGGGCCTGGCTGCGACAGCAGGGCAAGGAGGTGGG
            1550      1560      1570      1580      1590      1600
        1680      1690      1700      1710      1720      1730
hRD     GGAGACGCTGCTGTACTACGGCTGCCGCCGCTCAGATGAGGACTACCTGTACCGGGAGGA
        :::::::::::::::::::::::::::::::: ::::::::::::::::::::::::::
ΔhRDM   GGAGACGCTGCTGTACTACGGCTGCCGCCGCTCGGATGAGGACTACCTGTACCGGGAGGA
            1610      1620      1630      1640      1650      1660
        1740      1750      1760      1770      1780      1790
hRD     GCTGGCGCAGTTCCACAGGGACGGTGCGCTCACCCAGCTCAACGTGGCCTTCTCCCGGGA
        ::::::::::::::::::::::::::::::::::::::::::::::::::::::::::::
ΔhRDM   GCTGGCGCAGTTCCACAGGGACGGTGCGCTCACCCAGCTCAACGTGGCCTTCTCCCGGGA
            1670      1680      1690      1700      1710      1720
        1800      1810      1820      1830      1840      1850
hRD     GCAGTCCCACAAGGTCTACGTCCAGCACCTGCTAAAGCAAGACCGAGAGCACCTGTGGAA
        ::::::::::::::::::::::::::::::::::::::::::::::::::::::::::::
ΔhRDM   GCAGTCCCACAAGGTCTACGTCCAGCACCTGCTAAAGCAAGACCGAGAGCACCTGTGGAA
            1730      1740      1750      1760      1770      1780
        1860      1870      1880      1890      1900      1910
hRD     GTTGATCGAAGGCGGTGCCCACATCTACGTCTGTGGGGATGCACGGAACATGGCCAGGGA
        ::::::::::::::::::::::::::::::::::::::::::::::::::::::::::::
ΔhRDM   GTTGATCGAAGGCGGTGCCCACATCTACGTCTGTGGGGATGCACGGAACATGGCCAGGGA
            1790      1800      1810      1820      1830      1840
```

```
        1920      1930      1940      1950      1960      1970
hRD     TGTGCAGAACACCTTCTACGACATCGTGGCTGAGCTCGGGGCCATGGAGCACGCGCAGGC
        ::::::::::::::::::::::::::::::::::::::::::::::::::::::::::::
ΔhRDM   TGTGCAGAACACCTTCTACGACATCGTGGCTGAGCTCGGGGCCATGGAGCACGCGCAGGC
            1850      1860      1870      1880      1890      1900
        1980      1990      2000      2010      2020      2030
hRD     GGTGGACTACATCAAGAAACTGATGACCAAGGGCCGCTACTCCCTGGACGTGTGGAGCT-
        ::::::::::::::::::::::::::::::::::::::::::::::::::::::::::::
ΔhRDM   GGTGGACTACATCAAGAAACTGATGACCAAGGGCCGCTACTCCCTGGACGTGTGGAGCTC
            1910      1920      1930      1940      1950      1960
        2040
hRD     -AG---------------------------------------------

ΔhRDM   TAGTGAACAAAAGTTGATCTCTGAAGAAGACTTGAACGGTTCTAGGTTATAA
            1970      1980      1990      2000      2010
```

Protein Alignment of hRD and ΔhRDM. Comparison of the full length human P450 reductase (hRD) and genetically engineered variant ΔhRDM protein sequences.

```
                    10         20         30         40         50         60
                     *          *          *          *          *          *
hRD.PRT      MGDSHVDTSSTVSEAVAEEVSLFSMTDMILFSLIVGLLTYWFLFRKKKEEVPEFTKIQTL
ΔhRDM.PRT    ------------------------MTDMILFSLIVGLLTYWFLFRKKKEEVPEFTKIQTL

                    70         80         90        100        110        120
                     *          *          *          *          *          *
hRD.PRT      TSSVRESSFVEKMKKTGRNIIVFYGSQTGTAEEFANRLSKDAHRYGMRGMSADPEEYDLA
ΔhRDM.PRT    TSSVRESSFVEKMKKTGRNIIVFYGSQTGTAEEFANRLSKDAHRYGMRGMSADPEEYDLA

                   130        140        150        160        170        180
                     *          *          *          *          *          *
hRD.PRT      DLSSLPEIDNALVVFCMATYGEGDPTDNAQDFYDWLQETDVDLSGVKFAVFGLGNKTYEH
ΔhRDM.PRT    DLSSLPEIDNALVVFCMATYGEGDPTDNAQDFYDWLQETDVDLSGVKFAVFGLGNKTYEH

                   190        200        210        220        230        240
                     *          *          *          *          *          *
hRD.PRT      FNAMGKYVDKRLEQLGAQRIFELGLGDDDGNLEEDFITWREQFWPAVCEHFGVEATGEES
ΔhRDM.PRT    FNAMGKYVDKRLEQLGAQRIFELGLGDDDGNLEEDFITWREQFWPAVCEHFGVEATGEES

                   250        260        270        280        290        300
                     *          *          *          *          *          *
hRD.PRT      SIRQYELVVHTDIDAAKVYMGEMGRLKSYENQKPPFDAKNPFLAAVTTNRKLNQGTERHL
ΔhRDM.PRT    SIRQYELVVHTDIDAAKVYMGEMGRLKSYENQKPPFDAKNPFLAAVTTNRKLNQGTERHL

                   310        320        330        340        350        360
                     *          *          *          *          *          *
hRD.PRT      MHLELDISDSKIRYESGDHVAVYPANDSALVNQLGKILGADLDVVMSLNNLDEESNKKHP
ΔhRDM.PRT    MHLELDISDSKIRYESGDHVAVYPANDSALVNQLGKILGADLDVVMSLNNLDEESNKKHP

                   370        380        390        400        410        420
                     *          *          *          *          *          *
hRD.PRT      FPCPTSYRTALTYYLDITNPPRTNVLYELAQYASEPSEQELLRKLASSSGEGKELYLSWV
ΔhRDM.PRT    FPCPTSYRTALTYYLDITNPPRTNVLYELAQYASEPSEQELLRKLASSSGEGKELYLSWV

                   430        440        450        460        470        480
                     *          *          *          *          *          *
hRD.PRT      VEARRHILAILQDCPSLRPPIDHLCELLPRLQARYYSIASSSKVHPNSVHICAVVVEYET
ΔhRDM.PRT    VEARRHILAILQDCPSLRPPIDHLCELLPRLQARYYSIASSSKVHPNSVHICAVVVEYET

                   490        500        510        520        530        540
                     *          *          *          *          *          *
hRD.PRT      KAGRINKGVATNWLRAKEPAGENGGRALVPMFVRKSQLRLPFKATTPVIMVGPGTGVAPF
ΔhRDM.PRT    KAGRINKGVATNWLRAKEPAGENGGRALVPMFVRKSQLRLPFKATTPVIMVGPGTGVAPF

                   550        560        570        580        590        600
                     *          *          *          *          *          *
hRD.PRT      IGFIQERAWLRQQGKEVGETLLYYGCRRSDEDYLYREELAQFHRDGALTQLNVAFSREQS
ΔhRDM.PRT    IGFIQERAWLRQQGKEVGETLLYYGCRRSDEDYLYREELAQFHRDGALTQLNVAFSREQS

                   610        620        630        640        650        660
                     *          *          *          *          *          *
hRD.PRT      HKVYVQHLLKQDREHLWKLIEGGAHIYVCGDARNMARDVQNTFYDIVAELGAMEHAQAVD
ΔhRDM.PRT    HKVYVQHLLKQDREHLWKLIEGGAHIYVCGDARNMARDVQNTFYDIVAELGAMEHAQAVD

                   670
                     *
hRD.PRT      YIKKLMTKGRYSLDVWS------------
ΔhRDM.PRT    YIKKLMTKGRYSLDVWSSSEQKLISEEDL
```

We surmised that it is likely that by deleting an N-terminal domain and introducing an unusual peptide fragment at the C-terminus, we may have grossly altered the membrane-binding topology of the engineered molecule, ΔhRDM. From earlier studies in baker's yeast, we already knew that ΔhRDM was active and membrane-bound. Hence we thought we could now study the consequence of using this CPR variant in the context of different human CYPs in insect cells and compare these studies vis-à-vis the native CPR. We chose to use four CYPs for our studies. Two of them, CYP3A4 and CYP2E1 require, besides CPR, the additional electron transport partner b_5 for expression of activity. The other two CYPS used are CYP2D6 and CYP1A2 which are able to manifest activity, in the absence of b_5, together with only CPR.

We also wished to explore the activity of these four human CYPs in the presence of the heterologous yeast CPR (yRD) via co-expression in insect cells. The *yRD* gene has never been studied in insect cells. We conjectured that the yRD enzyme, which has extremely high activity, expressed in the context of human CYPs in insect cells may well provide a better understanding of a CPR's ability to contribute to the activity and the levels of different human CYPs.

In addition to the four CYPs enumerated above (CYP2D6, CYP1A2, CYP3A4 and CYP2E1), I have extended my studies and have cloned and expressed CYP1A1, CYP1B1, CYP2C8 in conjunction with different CPR species (human CPR, variants of human CPR and yeast CPR) and b_5 (where necessary) in order to create functionally

active enzymes from insect cells. It was envisaged that all protein expression from insect cells would be mediated by baculoviruses which specifically infect these cells.

With these experiments in mind, we hoped that my results would ultimately provide a deeper insight into how CPR interactions with CYPs influence the latter's activity and correspondingly the levels of synthesis. We were aiming, of course, to find a set of experimental conditions that probably would be less destructive to CYPs and also yield higher CYP activity. If successful, the findings could have major applications in drug metabolism research.

The results that I obtained are presented in the eight chapters of the thesis, as follows.

In this first chapter, consisting of an Introduction, the literature has been reviewed focussing on the biotransformation process, history of cytochrome P450, cytochrome P450 nomenclature, role of CYPs in human diseases and drug discovery, mechanism of action of CYPs, role of NADPH- cytochrome P450 reductase in CYP reaction, role of cytochrome b5 in CYP reactions, along with various experimental systems that have been employed to measure CYP mediated drug metabolism. They include human liver tissues, human liver microsomes, hepatocytes, and different expression systems, namely, bacterial, yeast, mammalian and baculoviral. At the end of the introduction, objectives of the proposed research have been highlighted.

In the second chapter, Materials and Methods elaborate the source of reagents, chemicals, cells and instruments used for my research. Together with this, a detailed account of procedures employed for various experimental designs have been provided.

In the third chapter, results of isolation, expression and catalytic activities of human NADPH- cytochrome P450 reductase, variants of human NADPH- cytochrome P450 reductase (ΔhRD and ΔhRDM) and yeast NADPH- cytochrome P450 reductase are described. The chapter details the cloning and expression of the genes in the baculovirus expression system. The catalytic activities of all the NADPH- cytochrome P450 reductases are compared. The results of CYP2D6 which was used as a model enzyme to study its interactions with various reductases are presented. The results described in the chapter comprise of isolation, optimisation of protein expression, identification and biochemical characteristics of proteins after co-expression with the different reductases in the baculovirus expression system. The chapter also presents evidence for oxidative damage of CYP2D6 caused by the reductases.

In the fourth chapter, results obtained with CYP3A4 expressed in conjunction with different CPR species (human CPR, variants of human CPR and yeast CPR) and b5 are detailed.

In the fifth chapter, results encompassing CYP1A2, CYP3A4, CYP2E1, CYP1A1, CYP1B1 and CYP2C8 expressed in conjunction with different CPR species (human CPR, variants of human CPR and yeast CPR) and b5 where necessary are detailed. The

chapter compares the interactions of the individual reductases with individual CYPs and provides evidences for poor or stronger interactions. The methodologies used for improvement of CYP expression levels and CYP catalytic activities are also presented.

In the sixth chapter, CYP inhibition by isoform specific inhibitors is presented. CYP inhibition assays have been validated for various CYPs whose activities are supported by different reductase species. The experimental evidence is detailed to show that inhibition potential of the inhibitors remain unchanged irrespective of reductase species that is co-expressed to support the CYP activity.

In the seventh chapter, the results obtained with the four reductase species and their interactions with the seven CYPs are compared and discussed as part of the argument for destructive nature of the NADPH-cytochrome P450 reductase. The improvement in CYP-CPR interaction is discussed. Conclusions and unifying summary of the study are presented.

In the eighth chapter, all the references are provided.

Chapter 2 Materials and Methods

2.1 Chemicals and Reagents

General reagents and biochemicals were purchased from Sigma-Aldrich (Gillingham, UK), Fisher Scientific (Loughborough, UK) and Melford Laboratories Ltd. (Suffolk, UK).

Sf9 insect cells, Grace's insect cell medium, Express Five SFM, fetal bovine serum, Cellfectin®, primers, pFastBac-1 cloning vector, DH-5α and DH10Bac *E. coli* cells, 4% agarose gel for plaque assays, fluorogenic substrates for CYP assays, H_2DCFDA, Dihydrorhodamine-123 were all purchased from Invitrogen Ltd. (Paisley,UK).

Molecular biology reagents like Vent DNA polymerase, dNTP mix, restriction endonucleases and T4 DNA Ligase were purchased from New England Biolabs (Hitchin, UK).

All electrophoresis and protein blotting reagents and equipments were obtained from Bio-Rad laboratories (Hemel Hempstead, UK).

Mouse monoclonal antibody to CYP2D6 (Catalogue Number A246), mouse polyclonal antibody to CYP3A4 (Catalogue Number 458258), goat polyclonal antibody to CYP1A1 (Cataloue Number 458124) and goat polyclonal antibody to CYP2E1 (Catalogue Number 458216) were purchased from Gentest. Rabbit polyclonal antibody to NADPH CYP450 human reductase (Catalogue Number ab13513-50) was purchased from Abcam. Mouse monoclonal antibody to the *c*-myc epitope (9E10) (Catalogue Number SC-40) and the secondary antibody, anti-mouse IgG-HRP conjugate (Catalogue Number SC-2302), were purchased from Santa Cruz Biotechnology. The secondary antibody, goat anti-rabbit HRP conjugate (Catalogue Number 1858415) was purchased from PIERCE.

2.2 Molecular Biology Methods

To study the protein functions and interactions, the baculovirus expression system was used to express the proteins. In order to express the enzymes in a heterologous system a range of molecular biology techniques like the polymerase chain reaction, agarose gel electrophoresis, purification of DNA, gene cloning, transformations of competent cells, etc were used.

2.2.1 Quantitation of DNA

DNA concentration was determined by measuring absorbance of the sample at 260 nm. If the sample is free from protein and RNA, DNA concentration can be measured accurately by determining the amount of UV light absorbed by the bases

present in the DNA sample. For double-stranded DNA quantification, the following conversion factor was used:

1 OD at 260 nm = 50 mg DNA/ml.

The absorbance, measured at 280 nm, indicates the presence of protein in the sample. The ratio between the readings between 260 and 280 nm provides an estimate of the purity of the sample, a value in the range of 1.7 to 1.8 is acceptable.

A 5 µl sample was diluted in 1 ml of molecular biology grade water in a quartz cuvette and the absorbance was measured at 260 and 280 nm in the spectrophotometer after blanking with molecular biology grade water.

2.2.2 Polymerase Chain Reaction (PCR)

The polymerase chain reaction (PCR) is a technique that amplifies a target DNA sequence *in vitro* rather than in living cells. PCR was developed in the early 1980s by Dr. Kerry Mullis (Mullis et al. 1986). However, the technique has been greatly improved since then. PCR can make virtually unlimited copies of a target DNA sequence even if it is initially present in extremely small amounts in a mixture of many different DNA sequences.

In order to perform the reaction, sequence of the DNA of interest must be known. Based on the DNA sequence, short deoxyoligonucleotides, called primers, can

be chemically synthesised. The primers are precisely complementary to the 3' end of each strand of the target DNA sequence. The reaction mixture contains the DNA to be amplified, the primers, all four deoxynucleotides (dATP, dCTP, dGTP, dTTP) and a DNA polymerase that is not deactivated by the high temperature needed to separate the DNA strands.

The technique uses an automated thermal cycler which provides a fast heating and cooling of the reaction mixture. The reaction mixture is first heated to separate the DNA strands. If the primers find their complementary sequence in the DNA, they bind to them. DNA polymerase begins the synthesis of the target DNA molecule from the 5' to 3' direction using the four deoxynucleotides. The synthesis continues until each newly synthesized strand reaches the site recognized by the other primer. This first cycle of the PCR generates two identical DNA molecules which are again doubled in the next cycle. After 30 cycles a single DNA molecule is amplified into more than a billion copies.

The genes of interest were amplified using high-fidelity Vent DNA polymerase under the following PCR conditions: A 50 µl reaction mixture contained 1X Thermopol Reaction Buffer (20 mM Tris-HCL, 10 mM $(NH_4)_2$ SO_4, 10 mM KCl, 2 mM $MgSO_4$, 0.1% Triton X-100, pH8.8 at 25°C), 0.8 mM dNTP mix, 20 ng forward primer, 20 ng reverse primer, 20 ng template DNA (which often was a cDNA library) and 2.5 units of Vent DNA polymerase. The final reaction volume was adjusted to 50 µl using molecular biology grade water. A negative control was set up using the same mixture

as above but lacking the template DNA. The reaction mixture in PCR tubes was overlaid with 30 µl mineral oil to prevent the contents of the reaction mixture from evaporation. The PCR was performed in a Biometra T3 Thermocycler, the reaction was started with the initial denaturation at 95ºC for 3 min, followed by a cycle of 95ºC denaturation for 45 sec, annealing for 90 sec at the calculated melting temperature for the two PCR primers, and finally chain extension was repeated 29 times at 72ºC for 3 min. A final chain extension was performed at 72ºC for 10 min. Products obtained from the PCR were then analyzed by agarose gel electrophoresis using standard restriction enzyme(s) digested DNA as markers.

Primer melting temperature (Tm) was calculated according to the following formula: $Tm = 61.8ºC + [\sum(G+C) \times 41ºC - 675] / \sum(A+T+G+C)$

2.2.3 Cloning of genes in basic plasmids

For initial cloning of a gene from a cDNA library or a parent plasmid, two basic plasmids were used, either pBluescript II KS+ (Stratagene, UK, Cat. N^{o}. 212207) or pSP73 (Promega, UK, Cat. N^{o}. P2221). The pBluescript II KS+ has an extensive polylinker with 21 unique restriction enzyme recognition sites which can be used for cloning most genes of interest. Similarly, pSP73 has a wide range of unique restriction sites, but different from pBluescript II KS+, for cloning a gene of interest. Both the plasmid vectors contain a 'bacterial origin of replication' that allows extra-chomosomal DNA replication. The plasmids also carry the β-lactamase gene which on expression

hydrolyses and inactivates ampicillin. Hence, on ampicillin containing LB agar plates only those cells grow which harbour the plasmid bearing the ampicillin resistant β-lactamase gene. These are known as transformants.

The plasmid map and list of features for the pBluescript II KS+ and pSP73 are shown in Figures 2.1 and 2.2 respectively.

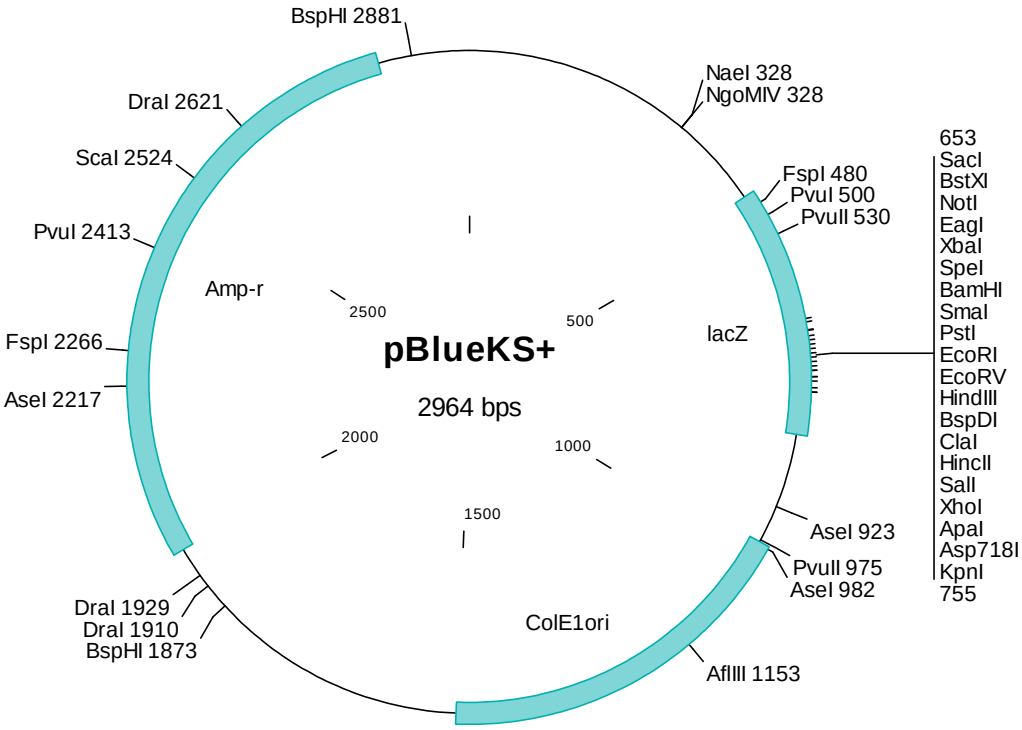

Figure 2.1. Map and abbreviated multiple cloning site region of the plasmid, pBluescript II KS+.

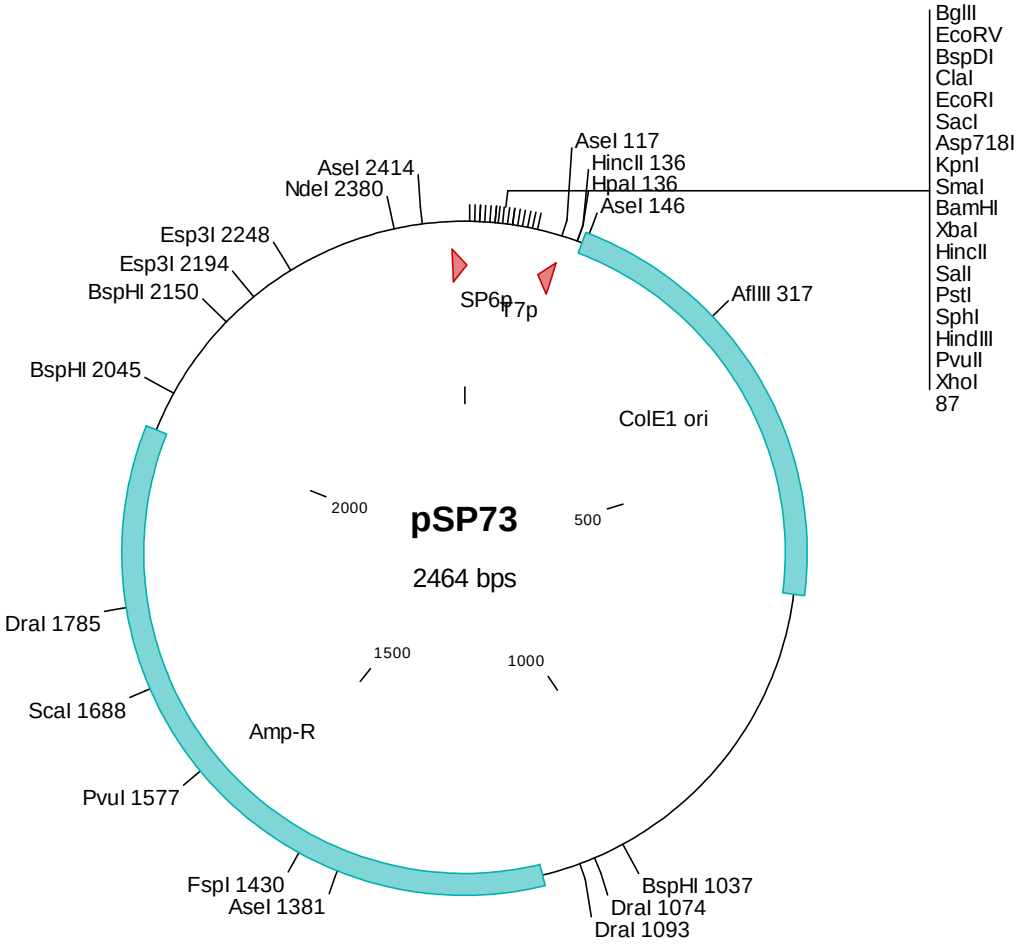

Figure 2.2. Map and abbreviated multiple cloning site region of the plasmid, pSP73.

For directional cloning, vector and insert DNA were first digested using a set of two compatible restriction enzymes. The digested DNA was fractionated via agarose gel electrophoresis. DNA was then extracted from the agarose gel. Purified and vector DNA were ligated and the ligation mixture was transformed in DH5α competent cells and plasmids were isolated.

2.2.4 Restriction enzyme digestion of DNA

Restriction enzymes recognize specific sequences in the DNA molecule and cleave wherever the particular sequence occurs in the DNA. Restriction enzyme digestion is either performed for analysis of the DNA or for further treatment such as ligation and cloning.

A restriction enzyme digestion was usually performed using 10 units of a restriction enzyme and 1 µg of purified DNA in a final volume of 30 µl of the appropriate 1X buffer followed by incubation for 2 h at the recommended temperature (usually 37ºC). The reaction was then terminated by adding 3 µl of 10X loading buffer (containing 50% glycerol, 0.2mM EDTA, pH 8.0, 0.25 % xylene cyanol and 0.25% bromophenol blue in molecular biology grade water). After restriction enzyme digestion, agarose gel electrophoresis was performed to separate the DNA fragments by size and to visualize the fragments.

2.2.5 Agarose gel electrophoresis

Agarose gel electrophoresis separates DNA fragments according to their size. An electric current is used to move the DNA molecules across an agarose gel from the negative to the positive end.

Agarose gel electrophoresis was performed to analyze and purify products from PCR and restriction enzyme digestion of DNA. Agarose was added to TAE buffer (40 mM Tris-acetate and 1 mM EDTA) at a concentration of 1% (w/v) and was dissolved by boiling in a microwave oven. Agarose solution was allowed to cool to about 60°C and ethidium bromide (10 mg/ml stock) was added to it to give a final concentration of 0.2 µg/ml. The gel was poured into the casting tray with a well-forming comb. The gel was allowed to solidify for about 30 min. The solidified gel was then placed in an electrophoresis tank that contained enough TAE buffer to submerge the gel. Along with the samples, 1 kb DNA ladder was loaded on to the gel so as to analyse the approximate size of the DNA fragments. The samples were run at 100 V for 45 min. The DNA bands were then visualised on a UV trans-illuminator and the photograph were captured to document the results.

2.2.6 DNA purification from agarose gel

In order to purify the PCR products and restriction enzyme digested DNA from agarose gel, QIAquick gel extraction kit (from Qiagen, UK) was used. QIAquick column has a silica membrane to which DNA with size ranging from 70 bp to 10 kb can bind in high salt buffer. The column is then washed to remove primers, nucleotides, enzymes, mineral oil, salts, agarose and other impurities from DNA samples. After removing the impurities, the DNA bound on silica membrane is eluted with low-salt buffer or water.

PCR products or restriction enzyme digested DNA samples were separated on 1% agarose gel as described above. After analyzing the samples on a UV-trans-illuminator, the gel slice containing the DNA band of interest was excised with a clean scalpel. The DNA extraction from agarose gel slice was then performed according to manufacturer's recommendations. The gel slice was weighed in a microfuge tube, three volumes of QG buffer were added and the tube was incubated at 50°C with intermittent mixing until the gel slice was dissolved. One gel volume of 100% isopropanaol was then added to the tube and mixed. The sample in the tube was added to the column, centrifuged at 13,000 rpm for 1 min and the flow-though was discarded. The column was washed once with 0.5 ml of buffer QC followed by 0.75 ml of buffer PE after centrifugation at 13,000 rpm for 1 min. After the washing steps, QIAquick column was centrifuged for one more minute at 13,000 rpm to remove residual ethanol from previous wash with buffer PE. DNA was eluted from the column by loading 50 µl TE buffer (10 mM Tris-HCL, 1 mM EDTA, pH 8.0) and by centrifuging the column at 13,000 rpm for 1 min. The eluted DNA was stored at

–20°C until used for further manipulations.

2.2.7 Ligation of DNA and construction of recombinant DNA molecules

Recombinant DNA is DNA from two or more sources incorporated together to make a single recombinant molecule. The gene of interest is incorporated into plasmid that is used as a vector. In order to make the recombinant DNA molecule, both the gene of interest and plasmid DNA are treated with restriction enzymes followed by ligation

using T4 DNA ligase. T4 DNA ligase catalyzes the joining of two DNA molecules at the 5'-phosphate and the 3'- hydroxyl groups of adjacent nucleotides. The molar ratio of vector DNA to insert DNA is very critical when performing a ligation reaction. The insert concentration is usually adjusted to a two to four fold molar excess over plasmid DNA.

The ligation reaction was performed in a total volume of 20 µl in a microfuge tube. The reaction mixture contained 1 µl of plasmid DNA, 4 µl of insert DNA, 2 µl of 10X T4 DNA ligase reaction buffer (500 mM Tris-HCL, 100 mM $MgCl_2$, 10 mM ATP, 100 mM dithiotheitol, pH 7.5 at 25°C) and the final volume was adjusted to 20 µl with molecular biology grade water. The reaction mixture was incubated overnight at 4°C followed by transformation of competent cells.

2.2.8 Preparation of competent *E.coli* DH5α cells

Competent cells are bacterial cells that are chemically treated to allow incorporation of foreign DNA (Hanahan 1983). DH5α is a popular strain of *E. coli* for cloning experiments and has the following chomosomal genotype,

F^-, φ80d*lacZ*ΔM15, Δ(*lacZYA-argF*)U169, *deoR*, *recA*1, *endA*1, *hdR*17(rk^-, mk^+), *phoA*, *supE*44, λ^-, *thi*-1, *gyrA*96, *relA*1

The *endA1* mutation in the strain causes inactivation of the intracellular endonuclease which is responsible for plasmid DNA degradation in most miniprep methods. The *recA* mutation eliminates the possibilities of homologous recombination. Moreover, as this strain does not carry *lacI*^{q}, it allows selection of recombinant DNA with X-gal when subcloning a recombinant plasmid.

DH5α cells were streaked out from a glycerol stock on to LB agar plates. The plates were incubated overnight at 37°C. Then a single colony was picked up and inoculated in 5 ml of LB broth. The culture was grown overnight in a 37°C shaking incubator set at 220 rpm. The overnight culture was diluted 1:100 in LB broth which was supplemented with 1 mM glucose. The culture was grown in 37°C shaking incubator to an OD_{600} of 0.5 -0.6. The cells were spun at 3,500 rpm for 20 min at 4°C. The cell pellet was gently resuspended in 20 ml of ice-cold 100 mM $MgCl_2$ and incubated on ice for 20 min. The cells were spun at 3,500 rpm for 20 min at 4°C. The cell pellet was gently resuspended in 20 ml of ice-cold 100 mM $CaCl_2$ and incubated on ice for 20 min. The cells were spun down again and gently resuspended in 6 ml of sterile, ice-cold 100 mM $CaCl_2$ and 13.3% glycerol. The cells were quickly dispensed in 100 µl aliquots and stored at –80°C.

2.2.9 Transformation of competent cells

After ligation of an insert and vector DNA, the next step is to introduce the resulting recombinant DNA into competent cells. The process of introducing foreign DNA into bacterial cells is called transformation.

A 50 µl aliquot of *E. coli* DH5α competent cells was thawed on ice and 7.5 µl of ligation reaction mixture was added directly to the thawed competent cells. The cells were incubated on ice for 30 min followed by heat-shock at 42°C for 45 sec. After the short heat-shock, the cells were placed back on ice immediately for 2 min and 900 µl of pre-warmed LB medium was added to the cells. The cells were incubated in 37°C shaking incubator set at 220 rpm for 1 h. After the incubation 50 to 100 µl of the cells were plated on LB agar plates containing 100 µg/ml ampicillin. The plates were then incubated overnight at 37°C. As the vector DNA contained β-lactamase, the ampicillin-resistant gene, only the transformed cells could survive and grow on ampicillin containing LB agar plates. The recombinant DNA was isolated from several transformants and screened by means of restriction digestion analysis for identification of transformants bearing the correct size DNA fragments.

2.2.10 Isolation and identification of recombinant plasmid DNA

Transformation is followed by identification of correct constructs using restriction digestion analysis; however before restriction digestion analysis DNA is isolated from transformants.

Recombinant plasmid DNA was purified using miniprep DNA preparation as follows:

Six colonies of transformants from the LB agar plates were picked with a disposable loop and inoculated into 2 ml of LB broth containing 100 µg/ml ampicillin. The cultures were grown overnight in a 37°C shaking incubator set at 220 rpm. 1.5 ml of the overnight culture from each transformant was transferred to a microfuge tube and centrifuged at 8000 rpm for 3 min. The pelleted cells were resuspended in 150 µl buffer P1 (50 mM glucose, 25 mM Tris-HCl pH 8.0, 10 mM EDTA, 100 µg/ml RNAse A) by pipetting up and down. After incubating for 5 min at room temperature, 150 µl buffer P2 (200 mM NaOH, 1% SDS) was added, mixed by inverting the tube 4-6 times and again incubated at room temperature for 5 min. 150 µl of buffer P3 (3M potassium acetate, pH 5.5) was then added and mixed by inverting the tube 4-6 times followed by incubation on ice for 5 min. The tube was centrifuged at 13,000 rpm for 25 min. The supernatant was transferred to a fresh microfuge tube and 0.7 volume of isopropanol was added to the supernatant. The tube was then centrifuged at 13,000 rpm for 4 min. The supernatant was carefully decanted and 500 µl of 70% ethanol was added to the tube to wash the DNA pellet. The tube was inverted 4-6 times followed by

centrifugation at 13,000 rpm for 15 min. Ethanol was poured off, the DNA pellet was air-dried and the DNA was reconstituted in TE buffer (10 mM Tris-HCl, 1 mM EDTA, pH 8.0). The purified DNA was then used for restriction digestion analysis for identification of correct recombinants. The restriction digestion analysis was performed using different sets of restriction enzymes as described before (see Section 2.2.4).

2.2.11 Purification of Plasmid DNA using QIAGEN mini prep column

After identifying the correct recombinant plasmids, one of the recombinant plasmids was purified using a mini prep column. The QIAprep spin miniprep kit, commercially available from QIAGEN was used which is based on alkaline lysis of bacterial cells followed by adsorption of DNA onto a silica column in the presence of high salt. The column is then washed with a buffer to remove impurities followed by elution of DNA in elution buffer or molecular biology grade water.

The culture from a correct transformant, grown in the previous step, was used as pre-culture to inoculate 10 ml of LB broth containing 100 µg/ml ampicillin. The cultures were grown overnight in 37°C shaking incubator set at 220 rpm. 6 ml of the overnight culture from each transformant was transferred to six microfuge tubes, 1 ml in each and centrifuged at 8000 rpm for 3 min. The pelleted cells in each tube were resuspended in 150 µl buffer P1 (50 mM glucose, 25 mM Tris-HCl pH 8.0, 10 mM EDTA, 100 µg/ml RNAse A) by pipetting up and down. After incubating for 5 min at room temperature, to each tube 150 µl buffer P2 (200 mM NaOH, 1% SDS) was added,

mixed by inverting the tube 4-6 times and again incubated at room temperature for 5 min. 200 µl of buffer P3 (3M potassium acetate, pH 5.5) was then added and mixed by inverting the tubes 4-6 times followed by incubation on ice for 5 min. The tubes were centrifuged at 13,000 rpm for 10 min. The supernatant was applied to the QIAprep mini columns by pipetting, centrifuged at 13,000 rpm for 1 min and flow though was discarded. The columns were then washed by adding 0.75 ml of PE buffer and then by centrifuging at 13,000 rpm for 1 min. The flow through was discarded and the columns were centrifuged for an additional 1 min to remove residual wash buffer. The columns were placed in clean microfuge tubes. To elute DNA, 50 µl of buffer EB (10 mM Tris-HCl, pH 8.5) was added to the centre of the columns, incubated for 1 min and then centrifuged at 13,000 rpm for 1 min.

2.2.12 Automated fluorescent sequencing

High copy number plasmids containing genes of interest were purified using QIAGEN plasmid Midi preparation kits before sequencing. The plasmids were diluted to a concentration of 10 ng/µl and sent to PNACL DNA sequencing service, Protein and Nucleic Acid Characterisation Laboratory, Leicester University or DNA sequencing service of Yorkshire Bioscience Ltd. Sequencing was performed using the T7 or SP6 universal primers or primers designed on the basis of the position of the insert.

The sequencing method was based on the one developed by Frederick Sanger (commonly called the Sanger or dideoxychain-termination method) (Sanger, 1997)

which utilises a mixture of deoxynucleotide triphosphates (dNTPs) and dideoxynucleotide triphosphates (ddNTPs). The ddNTPs differ from dNTPs by having a hydrogen atom attached to the 3' carbon instead of an –OH group and as such these molecules terminate DNA chain elongation because they cannot form a phosphodiester bond with the next deoxynucleotide. Four reactions consisting of the DNA template, primers, DNA polymerase, and the four dNTPs are set up, with each reaction also containing a different ddNTP. Polymerisation takes place until a ddNTP is incorporated, resulting in the synthesis of DNA sequences with varying length in each tube. These are then sorted according to size by gel electrophoresis and the sequence read from the bottom of the gel to the top to give the 5' to 3' DNA sequence. The DNA sequencing results were then compared with sequences published in current NCBI databases.

2.2.13 Cloning of the genes in donor plasmid, pFastBac1

The genes cloned into cloning vectors (pBluescript KS+ and pSP73) were isolated by means of restriction digestion and further sub-cloned into the donor plasmid, pFastBac1. A donor plasmid allows transposition of the sub-cloned gene along with the expression cassette onto the baculovirus shuttle vector (bacmid). Insect cells are then transfected with the recombinant bacmid DNA to generate a recombinant baculovirus. Thus the protein can be expressed as part of the baculoviral genome. pFastBac1 contains *Autographa californica* multiple nuclear polyhedrosis virus (AcMNPV) ployhedrin (P_H) promoter for protein expression in insect cells. The expression cassette

is flanked by the left and right arms of Tn7 and also contains a gentamicin resistance gene and an SV40 polyadenylation signal to form a mini Tn7 cassette.

The pFastBac1 vector has a multiple cloning site for cloning a gene of interest. The vector contains the 'origin of replication' for plasmid DNA replication that occurs independent of chomosomal DNA replication of bacteria. It also contains the ampicillin-resistance gene which helps in the identification of plasmid-bearing transformants on ampicillin containing LB agar plates. The circular map and list of features for the pFastBac1 are shown in Figure 2.3.

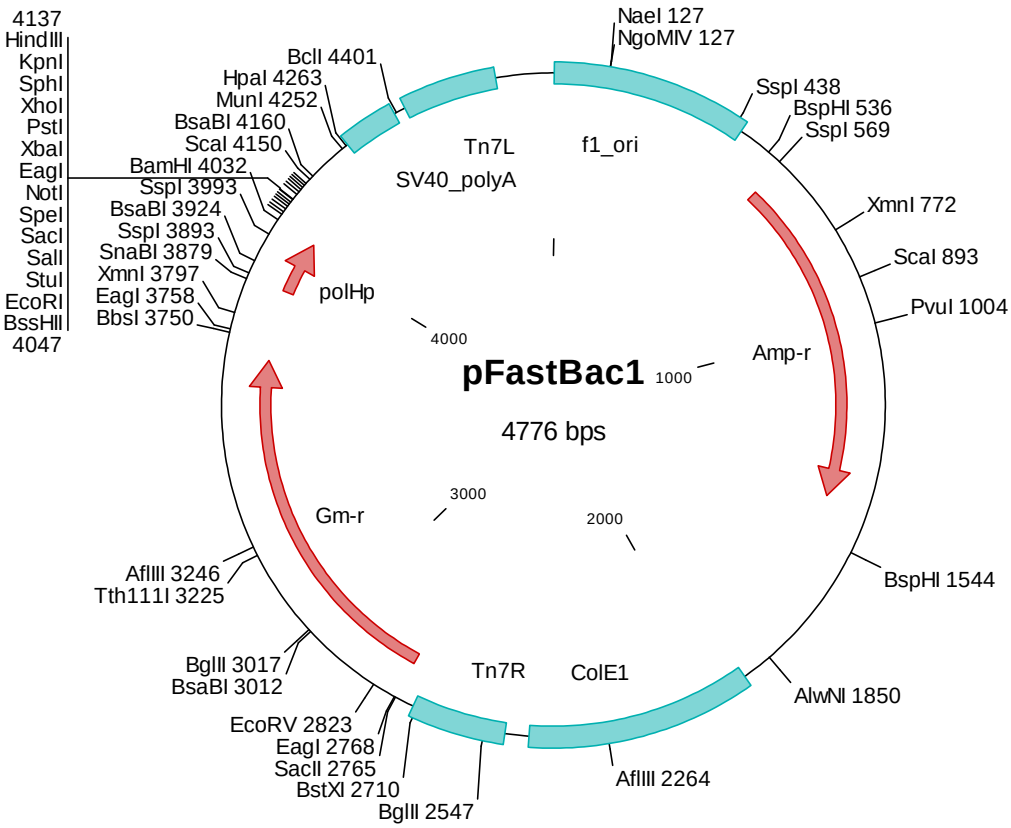

Figure 2.3. Map and abbreviated multiple cloning site region of the plasmid, pFastBac1.

For directional cloning, pFastBac1 and insert DNA from cloning vectors were cut using a set of two restriction enzymes followed by agarose gel electrophoresis, DNA extraction from the agarose gel, ligation, transformation in DH5α competent cells and plasmid isolation as described above.

2.2.14 Generation of recombinant bacmid by transforming DH10Bac *E.coli*

An *E.coli* host strain, DH10Bac, contains a baculovirus shuttle vector (bacmid) and a helper plasmid, and allows generation of a recombinant bacmid following transposition of the pFastBac expression construct.

E. coli DH10Bac competent cells were prepared exactly as described before for the preparation of competent cells from *E. coli* strain, DH5α.

The transformation was performed according to manufacturer's recommendations. A vial containing 100 µl of the DH10Bac competent cells was thawed on ice for 10 min and distributed in 25 µl aliquots in sterile microfuge tubes which had been kept on ice. For each transformation, 1 ng of pFastBac1 construct in 5 µl of sterile water was added to the 25 µl aliquot of competent cells and mixed gently. Cells were incubated on ice for 30 min followed by heat-shock at 42°C for 45 secs. The tubes were immediately transferred on ice for 2 min and 900 µl of LB broth, at room temperature, was added. The tubes were incubated at 37°C shaking at 225 rpm for 4 h.

Then the cells were diluted 10-fold (10^{-1}, 10^{-2}, 10^{-3}) with LB broth and 100 µl from each dilution was plated on LB agar plates containing 50µg/ml kanamycin, 7 µg/ml gentamicin, 10 µg/ml tetracycline, 100 µg/ml Bluo-gal and 40 µg/ml IPTG. The plates were incubated at 37°C for 48 h.

Transposition of the mini-Tn7 into the mini-*att*Tn7 attachment site on the bacmid disrupts the expression of the LacZα peptide. Therefore, colonies containing the recombinant bacmid are white in a background of blue colonies that harbour the unaltered bacmid.

After 48 h of incubation, six white colonies were picked and re-streaked on fresh LB agar plates containing 50µg/ml kanamycin, 7 µg/ml gentamicin, 10 µg/ml tetracycline, 100 µg/ml Bluo-gal and 40 µg/ml IPTG. The plates were incubated overnight at 37°C. After confirming a white phenotype of re-streaked colonies, a loop-full of culture was inoculated into 2 ml of LB broth containing 50µg/ml kanamycin, 7 µg/ml gentamicin, 10 µg/ml tetracycline and grown overnight at 37°C with shaking at 225 rpm. The bacmid was then isolated as described below.

2.2.15 Isolation of recombinant bacmid DNA

Six colonies of transformants from the LB agar plates were picked with a disposable loop and inoculated into 2 ml of LB broth containing 50µg/ml kanamycin, 7 µg/ml gentamicin and 10 µg/ml tetracycline. The cultures were grown overnight in

37°C shaking incubator set at 220 rpm. 1.5 ml of the overnight culture from each transformant was transferred to a microfuge tube and centrifuged at 8,000 rpm for 3 min. The pelleted cells were resuspended in 150 µl buffer P1 (50 mM glucose, 25 mM Tris-HCl pH 8.0, 10 mM EDTA, 100 µg/ml RNAse A) by pipetting up and down. After incubating for 5 min at room temperature, 150 µl buffer P2 (200 mM NaOH, 1% SDS) was added, mixed by inverting the tube 4-6 times and again incubated at room temperature for 5 min. 150 µl of buffer P3 (3M potassium acetate, pH 5.5) was then added and mixed by inverting the tube 4-6 times followed by incubation on ice for 5 min. The tube was centrifuged at 13,000 rpm for 25 min. The supernatant was transferred to a fresh microfuge tube and 0.7 volume of isopropanol was added to the supernatant. The tube was then centrifuged at 13,000 rpm for 4 min. The supernatant was carefully decanted and 500 µl of 70% ethanol was added to the tube to wash the DNA pellet. The tube was inverted 4-6 times followed by centrifugation at 13,000 rpm for 15 min. Ethanol was poured off, the DNA pellet was air-dried and the DNA was reconstituted in TE buffer (10 mM Tris-HCl, 1 mM EDTA, pH 8.0). The purified DNA was then used for confirming the transposition of the gene of interest on the bacmid DNA.

2.2.16 PCR analysis of recombinant bacmid DNA

Recombinant bacmid DNA is over 135 kb in size. Restriction analysis of this large DNA is difficult and so the transposition of the gene of interest on the bacmid DNA was verified by PCR analysis. The PCR was performed on all six bacmids (isolated in the previous step) by using the pUC/M13 forward primer (5'-

CCCAGTCACGACGTTGTAAAACG-3') and the reverse primer (5'-AGCGGATAACAATTTCACACAGG-3') or a combination of either M13 forward or reverse primer together with a gene specific primer. The PCR was set up as follows:

A 50 µl reaction mixture contained 1X Taq DNA polymerase Buffer (75 mM Tris-HCL, 20 mM $(NH_4)_2$ SO_4, 1.5 mM $MgCl_2$, 0.1% Triton X-100, pH8.8 at 25°C), 0.8 mM dNTP mix, 20 ng M13 forward primer, 20 ng M13 reverse primer, 20 ng bacmid DNA and 2.5 units of Taq DNA polymerase (purchased from Cancer Research, UK). The final reaction volume was adjusted to 50 µl using molecular biology grade water. A negative control was set up using the same mixture as above except template bacmid DNA was replaced by water. The reaction mixture in PCR tubes was overlaid with 30 µl of mineral oil to prevent the reaction from evaporation. The PCR was performed in Biometra T3 Thermocycler. The reaction was started with the initial denaturation at 95ºC for 3 min, followed by a cycle of 95ºC denaturation for 45 sec, annealing at 50°C for 90 sec, chain extension at 72ºC for 3 min which was repeated 29 times. A final chain extension was performed at 72ºC for 10 min. PCR products were then analyzed by agarose gel electrophoresis along with standard DNA markers.

pUC/M13 forward and reverse primers hybridize to sites flanking the mini-*att*Tn7 site within the *lacZ*α-complementation region. If transposition took place and pUC/M13 forward and reverse primers were used, PCR product of '2300 bp + insert size' would be observed on the agarose gel. Alternatively, a smaller fragment would be observed using either a pUC/M13 forward or a reverse primer together with a gene

specific primer. After the presence of gene of interest on bacmid DNA was verified, recombinant baculoviruses were generated in Sf9 insect cells as described below (Section number: 2.3.7).

2.3 Cell Biology Methods

2.3.1 Insect cell culture

The use of insect cell culture for heterologous protein expression is gaining popularity for basic research as well as for commercial applications. Insect cell expression systems produce relatively large quantities of post-translationally modified heterologous proteins.

All cell culture techniques were performed under aseptic conditions using class-II biological safety cabinet. Two insect cells lines were used viz, Sf9 and Tni and they were routinely maintained in Grace's insect cell culture medium supplemented with 10% FBS and Express Five serum free medium respectively. The Grace's medium was supplemented with 10% FBS and Express five medium was supplemented with 10 mM L-glutamine. To both the media, penicillin-streptomycin-neomycin antibiotic mixture was added at the final concentration of 50 µg/ml penicillin, 50 µg/ml streptomycin and 100 µg/ml neomycin. A new culture was started from a cryopreserved vial after every one and a half months and the cells were always maintained in mid-log phase.

2.3.2 Sf9 Insect Cell Culture

Sf9 cells are derived from the pupal ovarian tissue of the fall army worm, *Spodoptera frugiperda*. Sf9 cells grow in monolayer as well as in suspension culture. The small regular size of Sf9 makes it an ideal cell line for plaque formation (i.e. the plaques formed after infection with the baculovirus of an insect cell line). The cell line is suitable for generating high titre baculovirus stocks. Sf9 cells were cultured in Grace's insect cell culture medium supplemented with L-glutamine, yeastolate and lactalbumin and 10% FBS. The cells were maintained in spinner flasks with continuous stirring at 90 RPM in a 27^0C humidified incubator. Suspension cultures were passaged before they reached a density of 3×10^6 cells/ml and diluted back to 0.5 to 1.0×10^6 cells/ml. Cell count and viability were determined using the trypan blue exclusion method.

2.3.3 T.ni insect cell culture

The T.ni insect cell line, derived from ovarian cells of the cabbage looper, *Trichoplusia ni,* is capable of expressing significantly higher levels of recombinant proteins compared to other insect cell lines like Sf9 and Sf21. This cell line can grow in a monolayer as well as in suspension culture. T.ni cells also offer faster doubling time. The cells were cultured in Express Five SFM serum free medium (Invitrogen, Catalogue number- 10486), supplemented with 10 mM L-Glutamine (Invitrogen, Catalogue Number-10486) and 1X Antibiotic: Penicillin-Streptomycin-Neomycin (Invitrogen, Catalogue Number-15640-055) prior to use. Express Five SFM contains surfactant,

Pluronic F-68 to minimize damage to cells caused by the shearing force of stirring. The cells were maintained in spinner flasks with continuous stirring at 95 rpm in a humidified 27ºC incubator. Suspension cultures were passaged before they reached a density of 3×10^6 cells/ml and diluted back to 0.5 to 1.0×10^6 cells/ml. Cell count and viability was determined using trypan blue exclusion method.

2.3.4 Setting up a Monolayer culture

A cryovial of insect cells, previously cryo-preserved in liquid nitrogen, was removed and thawed rapidly in 37°C water-bath. The cells were transferred to 25 cm^2 tissue culture grade flask (T25) already containing room-temperature insect cell medium. Viability of the cells was checked using the trypan blue exclusion method under phase contrast microscope as described below (section: 2.3.5). The cells were allowed to attach to the substratum of the flask for 30 min at 27°C humidified incubator. After 30 min medium was replaced with fresh insect cell medium, this step is necessary to remove DMSO used during cryopreservation of cells. The T25 flask was returned to the incubator until the cells reached about 80% confluency. For subculturing, the cells were detached from T25 by repetitively streaming the medium over the monolayer. The cells were then transferred to 75 cm^2 tissue culture grade flask (T75) to which 20 ml of fresh room-temperature Grace's medium was added. The flask was returned to 27°C humidified incubator, cells were routinely monitored under phase contrast microscope for viability, morphology and confluency. When the flask was 80% confluent, the cells were again sub-cultured in a 1:3 ratio by detaching them from the T75 flask and equally distributing the detached cells into three fresh T75 flasks containing 20 ml of fresh

Grace's medium. The flasks were returned to the incubator until the cells reached 80% confluency. The cells were then detached from all the flasks and suspension culture was initiated by seeding these cells in 500 ml spinner flask.

2.3.5 Cell counting and trypan blue exclusion viability assay using haemocytometer

The haemocytometer (Figure 2.4) is a specially designed glass slide with a 0.1 mm^3 chamber and a counting grid. It is commonly used in cell culture to determine cell density of cells in suspension. Estimation of the number of dead cells in a cell suspension is required before they can be used for cell-based assays or protein expression studies. Trypan blue dye exclusion viability test in conjunction with haemocytometer estimates are commonly used for this purpose. Viable cells exclude trypan blue dye whereas non-viable cells stain due to damage in their cell membrane.

The haemocytometer and the glass cover-slip were thoroughly cleaned with 70% ethanol and the cover-slip was placed over the grooves and counting area. A 50 µl of cell suspension was mixed with trypan blue solution (0.4% in PBS) in 1:1 ratio. Using a pipette, the cell suspension was loaded to the edge of the haemocytometer and the suspension was allowed to spread evenly by capillary action without under-filling or overfilling the area within the chamber. The haemocytometer was placed under the microscope and the 10X objective focus was adjusted on grid lines in the chamber. Unstained (viable) and blue (dead) cells were counted in all four 16-square grid areas and the average was calculated from the cells counted in four 16-square areas.

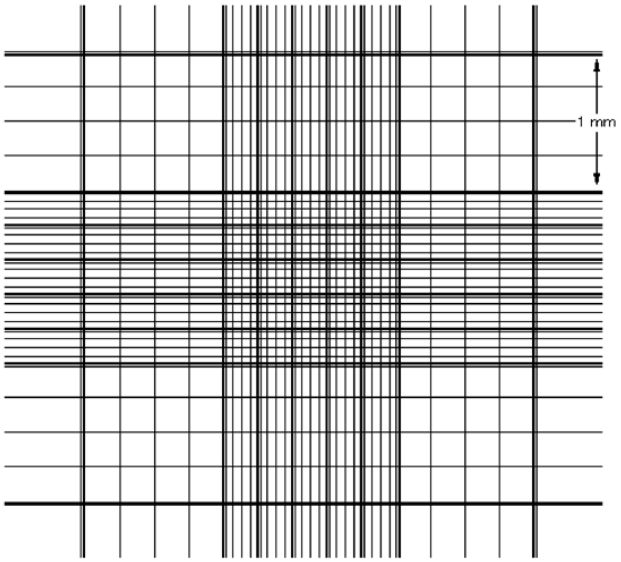

Figure 2.4. Appearance of haemocytometer grid visualised under the microscope.

Each 16-square area is 1 mm^2 and the depth of the chamber after placing the cover-slip is 0.1 mm, therefore the volume taken up by this area is 0.1 mm x 1.0 mm^2= 0.1 mm^3, that is 10^{-4} ml. Therefore,

Cell density (cells/ml) = number of viable cells counted ⁄ 10^{-4} ml

or

Cell density (cells ⁄ ml) = number of viable cells counted X 10^4 ⁄ ml

The concentration of the total number of viable cells was determined by viable cell concentration multiplied by the dilution factor, 2. (1:1 of cell suspension and trypan blue). The percentage cell viability was calculated using the following equation:

% cell viability = [total viable cells (unstained) ⁄ total cells (stained + unstained)] X 100

2.3.6 Initiating suspension culture

The cells were detached and removed from the T75 flasks. They were seeded in a sterile 250 ml spinner flask at a density of 1X 10^6 cells/ ml. The spinner flask was placed on a stirrer set with constant stirring of 90 rpm in a 27ºC humidified incubator. When the cells reached a density of 3X 10^6 cells/ ml, cells were diluted to a density of 1X 10^6 cells/ml by adding fresh medium. Once in every two weeks, the cells were centrifuged at 1,000 rpm for 10 min and resuspended in complete fresh medium to minimize cell debris and metabolic by-product accumulation.

2.3.7 Generation of recombinant baculovirus

After isolation (see Section 2.2.15) and confirmation (see Section 2.2.16) of the recombinant bacmid DNA, Sf9 cells were transfected to generate recombinant baculovirus. All baculoviruses were generated in Sf9 cells.

For generation of baculoviruses, Sf9 cells were transfected with recombinant bacmids in 6-well tissue culture grade plates. The Sf9 cells in log phase were adjusted to a cell density of 4.5X 10^5 cells/ml in Grace's medium supplemented with 10% FBS and 2 ml of this cell suspension was seeded into each well of the 6-well plates. The cells were allowed to attach to the plates over a period of 2 h. Whilst cells were attaching, 1 µg of purified bacmid DNA was diluted in 200 µl un-supplemented Grace's medium already containing 6 µl of the transfection reagent, Cellfectin. Bacmid DNA – Cellfectin complexes were allowed to form over 45 min at room temperature. During

this incubation, cells were washed once in the plate with un-supplemented Grace's medium. The bacmid DNA-Cellfectin complexes were diluted to 1 ml with un-supplemented Grace's medium and this mixture was added to the cell monolayer in the 6-well plate. Cells were incubated in a 27ºC humidified incubator for 5 h and DNA-Cellfectin complexes were then placed in 2 ml of complete Grace's medium supplemented with 10% FBS. Cells were incubated in a 27ºC incubator for 72 h. When signs of viral infection were observed under the microscope, primary baculovirus stocks were isolated by separating the supernatant containing baculoviruses from cell pellet by centrifugation at 800X g for 10 min. The clarified baculovirus stocks were transferred into fresh sterile tubes and stored at 4°C, protected from light.

2.3.8 Amplification of baculoviruses

The baculoviruses were amplified in Sf9 cells by infecting the cells with primary baculovirus stocks. Sf9 cells were adjusted to a cell density of 1X 10^6 cells/ml in Grace's medium supplemented with 10% FBS and 2 ml of this cell suspension was seeded in each well of the 6-well plate. The cells were allowed to attach for 1 h and then 40 µl of the primary baculovirus stock was added per well. The infected cells were incubated at 27ºC in a humidified incubator for 96 h. After 96 h, signs of late infection like detachment of cells, increased cell diameter and granular appearance of cells were observed and the amplified stock of baculoviruses was isolated as a suspension by centrifugation at 800X g for 10 min. The supernatant was transferred to a fresh sterile tube covered with aluminium foil to avoid exposure to light. The amplified stock was stored at +4ºC, protected from light. For long term storage an aliquot was stored at –

80ºC which could be used for re-amplification at a later date, if required.

2.3.9 Viral plaque assay

The viral plaque assay was performed to plaque purify the baculoviruses or to titrate baculovirus stocks. Sf9 cells, grown in Grace's medium supplemented with 10% FBS, were seeded in 6-well tissue culture grade plates at a density of 1×10^6 cells/well in 2 ml volume and were allowed to attach for 1 h. Baculovirus stocks were serially diluted in Grace's medium to achieve 10^{-1} to 10^{-8} dilutions. The medium was removed from the plates and replaced with 1 ml of baculovirus dilutions from 10^{-3} to 10^{-8} duplicate. Cells were incubated with virus for 1 h; after 1 h, the virus was removed from the plates and replaced with 2 ml plaquing medium. To prepare plaquing medium, 4% low melting point agarose was melted and kept at 40ºC. The melted agarose was diluted in 2X Grace's medium and sterile distilled water to achieve a final agarose concentrations of 1% and 1X Grace's medium. Plates were incubated at 27ºC for 7-10 days until plaques were visible with the naked eye or under low-power magnification of the microscope. The plaques were stained for 1 h with 0.5 ml of 1 mg/ml neutral red prepared in cell culture grade sterile distilled water. The excess stain was gently removed with pipette. Plaques were counted and viral titre was determined using the following formula:

Titer (pfu/ml) = number of plaques × dilution factor X (1 / ml of inoculum per well)

2.3.10 Plaque purification of baculoviruses

The viral plaque assay was performed as described above. The plaques were picked with a pipette tip before staining with neutral red and inoculated in 500 µl of Grace's medium in a microfuge tube. The tube was vortexed to homogenize the agarose. The plaque-purified baculovirus suspension was then used for amplification of the baculovirus as described before (see Section 2.3.8).

2.3.11 Optimization of protein expression conditions

Optimal expression conditions are dependent on many factors such as nature of the gene of interest, multiplicity of infection (MOI), the number of hours of infection (i.e. the time course) and the cell line. Therefore, determining the optimal expression conditions of each of these factors is vital for the expression of an active recombinant protein of interest.

2.3.11.1 Multiplicity of infection (MOI) of baculoviruses and time course of recombinant protein expression

MOI is defined as ratio of infectious virus particles to cells. Inoculum required to achieve a particular MOI is calculated based on titre of a viral stock and the number of cells as follows:

Inoculum required (ml) = [MOI (pfu/cell) X number of cells]/ [titre of viral stock (pfu/ml)]

For determining optimal MOI, Sf9 cells were seeded in T75 flask at a density of 12 X 10^6 cells in 20 ml of Grace's medium supplemented with 10% FBS and were allowed to attach for 1 h. The cells were then infected with baculoviruses using a range of MOI from 0.03 to 3 0 (0.03, 0.1, 0.3, 1.0 and 3.0). The cells were harvested at 48, 63 and 72 h post-infection by centrifugation at 800X g for 15 min at 4°C. The microsomes were isolated (see Section 2.4.1), assayed for protein concentration (see Section 2.4.2) and CYP concentrations were determined spectrophotometrically (see Section 2.4.3). Afterwards, specific activities of the expressed reductase were measured (see Section 2.4.7) followed by determination of individual CYP activities (see Section 2.4.9). A particular MOI and time of harvest that resulted in both optimal protein production and enzyme activity were selected for further protein expression.

2.3.11.2 Choice of cell line for expression of recombinant proteins from baculoviruses

To determine which of the cell lines, Sf9 or T.ni., was optimal for expression further experiments were performed. Based on the results obtained from the above MOI and time-course optimisation experiment, both Sf9 and Tni cells were infected with a particular MOI and harvested at a single time point. Microsomes were prepared, were assayed for protein concentration (Section 2.4.2), CYP concentrations were spectrophotometrically analysed (Section 2.4.3), CYP assays were performed (Section 2.4.10) and reductase activities were determined (Section 2.4.7). The T.ni cell line was

chosen for large scale protein production in spinner flasks and was based on parallel studies performed with Sf9 and T.ni.

2.3.12 Recombinant protein expression in T75 flasks

For protein expression, the cells were seeded in T75 flasks at a density of 12 X 10^6 cells/T75 flask in 20 ml of medium and allowed to attach to the plates for 1 h. The cells were infected with virus at the indicated multiplicity of infection and incubated in a humidified 27ºC incubator. 24 h post-infection, haemin (2 µg/ml) and δ-amino levulinic acid (100µM) were added to the cells to compensate for low endogenous levels of haeme in insect cells. Cells were harvested at the indicated time point by scraping with a cell rake and were washed twice with ice cold PBS. The microsomes were then prepared as described below.

2.3.13 Recombinant protein expression in spinner flasks

For protein expression in spinner flasks, the cells were seeded at a density of 1.5 × 10^6 cells/ml in a volume of medium that was half that of the spinner flask capacity. The cells were infected with recombinant baculovirus at indicated multiplicity of infection (MOI) and incubated in a humidified 27ºC incubator. The cells were stirred continuously on a stirrer set at 95 rpm. 24 h post-infection, haemin (2 µg/ml) and δ-amino levulinic acid (100µM) were added to the cells to compensate for low

endogenous levels of haeme in insect cells. Cells were harvested at indicated time points by pouring the cells into centrifuge bottles and centrifuging them at 800X g for 25 min. The cell pellets were washed twice with ice cold PBS. The microsomes were then prepared as described below.

2.4 Biochemical Methods

2.4.1 Preparation of Microsomes

The harvested cells were resuspended in five volumes of ice cold 100 mM potassium phosphate buffer, pH 7.4, 20% (v/v) glycerol, 1mM DTT, 1mM EDTA, and 1mM AEBSF (a protease inhibitor). Cells were lysed by sonication: amplitude 30%, pulse-1 with 6 bursts of 6 sec duration. Cellular debris was removed by centrifugation at 9,000 rpm at 4ºC for 30 min. and microsomes were pelleted by centrifugation at 45,000 rpm for 70 min at 4ºC in a Beckman Coulter Optima L100 XP ultracentrifuge using the Ti70.1 rotor. Microsome pellets were resuspended in 100 mM potassium phosphate buffer, pH 7.4, 20% (v/v) glycerol, 1mM EDTA and homogenized using a Glass-Teflon homogenizer to make a uniform microsome suspension. The microsomes were aliquoted and frozen at –80ºC until further use. All steps of the procedure were carried out at 4ºC.

2.4.2 Protein estimation by Bradford assay

Protein concentrations in cell lysates were determined via a modified Bradford analysis (Bradford 1976) using a kit available from Bio-Rad. The Bradford assay is a method for determining protein concentrations in solutions and involves the binding of the dye, Coomassie brilliant blue G-250, to proteins. The protein-dye complex is spectrophotometrically detected at 595 nm.

The standard curve was prepared using a range of concentrations of bovine serum albumin (40, 20, 15, 10, 7.5, 5, 2.5 and 1 µg/ml in PBS). Test samples were diluted 40X in PBS. The total reaction volume was 200 µl which contained 1X Bradford reagent, indicated concentration of BSA or 40X diluted test sample and PBS. The assay for standard, as well as sample, was performed in triplicate in 96-well flat bottomed microtitre plates. Wells containing only PBS were used as blanks. Absorbance was measured at 595 nm using a spectrophotometer (Bio-Tek, Synergy HT). Standard curve of BSA was plotted and protein concentrations in test samples were measured using the equation from the standard curve. A representative standard curve is shown in Figure 2.5.

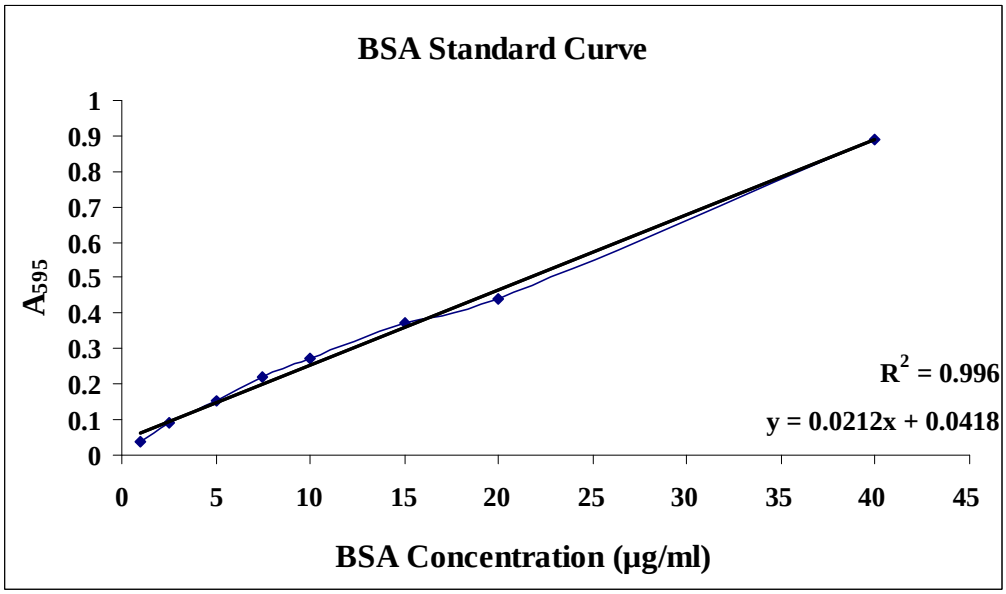

Figure 2.5. A representative protein standard curve for calculations of protein concentrations in cell lysates.

2.4.3 Reduced CO difference spectra for calculation of cytochome P450 enzyme concentrations in microsomes

The carbon monoxide (CO) binding assay (Omura and Sato 1964) is a method for quantifying the amounts of CYP holoproteins (i.e. active proteins) in microsome preparations. The CO-binding assay gave the enzyme family its name. The reduced haeme moiety of CYP binds to carbon monoxide and exhibits maximum absorbance at 450 nm. The method detects only the active haeme-bound CYP holoprotein.

Into two cuvettes (one ml capacity), 800 µl of 100 mM phosphate buffer, pH7.4, containing 20% glycerol were added. The microsomal fractions were diluted to a

protein concentration of about 1 mg/ml and were added to one of these cuvettes (referred to as the sample cuvette). A few grains (3-5 mg) of sodium dithionite powder from the tip of a small spatula were added to both the sample and the reference cuvette and the contents were gently mixed by inverting the cuvettes. The sample cuvette and the reference cuvette were placed in the respective sample and reference holders of a dual beam spectrophotometer (Shimadzu UV-2401PC). A baseline was recorded for the sample verses the reference cuvette. CO was then slowly bubbled through the sample cuvette for approximately 30 sec in a chemical extraction hood. The difference spectrum was recorded between 400 and 500 nm and the CYP holoprotein content was quantified by measuring the change in absorption between wavelengths 450 nm and 490 nm using the extinction coefficient of 91 $mM^{-1}cm^{-1}$. The CYP content was measured using the following formula:

CYP content (nmole/ml) = $[(A_{450nm} - A_{490\ nm})$ X dilution factor X 1000]/ 91

Specific CYP content (nmole/ mg protein) = CYP content/ total protein in the reaction

2.4.4 Sodium dodecyl sulphate polyacrylamide gel electrophoresis (SDS-PAGE)

SDS-PAGE electrophoresis separates or resolves proteins according to their electrophoretic mobility which is a function of size and charge. Proteins are exposed to SDS before and during electrophoresis which binds and denatures proteins giving them uniform negative charge along the length of the polypeptide. The similar charge to mass ratio on all polypeptide chains results in protein mass being the sole determinant of the migration rate of proteins in SDS-PAGE. A tracking dye like bromophenol blue

is added to the protein solution to allow tracking of the protein through the gel (Schägger and von Jagow 1987).

The mini-Protean 3 system from Bio-Rad which includes a casting stand, glass plates with permanently bonded gel spacers and the mini tank was used for protein gel electrophoresis. The polyacrylamide gels were prepared by mixing 10% of acrylamide/bis-acrylamide solution, 375 mM Tris-HCl pH 8.8, 0.1% SDS, 0.066% N,N,N',N'-Tetramethylethylenediamine (TEMED) and 0.05% ammonium persulfate (APS) in distilled water. The mixture was poured in the assembled gel cassette, up to the level of about 1 cm below the comb teeth and overlayed with 0.5 ml of water-saturated butanol. The resolving gel was allowed to polymerise for 1 h followed by washing of the gel surface with distilled water to remove butanol. The stacking gel was prepared by mixing 4% acrylamide/bis-acrylamide (from a 30% stock solution), 125 mM Tris-HCl pH 6.8, 0.1% SDS, 0.066% TEMED and 0.05% ammonium persulfate in distilled water. The multi-teeth comb was inserted in the gel cassette and the stacking gel mixture was slowly poured up to the top of the cassette taking care not to introduce the bubbles. The stacking gel was allowed to polymerise for 45 min. The comb was gently removed and the wells were rinsed with the running buffer (25 mM Tris-HCl pH 8.6, 192 mM glycine and 0.1 SDS). The gel cassettes were clamped on the clamping frame of the electrode assembly to form the inner chamber. The inner chamber was placed in the mini tank and filled with about 125 ml of running buffer. The lower chamber of the mini tank was filled with about 200 ml of running buffer before use.

The protein samples were prepared by mixing with the protein loading buffer (50 mM Tris-HCl pH 6.8, 12.5 mM EDTA, 2% SDS, 10% gylcerol, 1% β-mercaptoethanol and 0.02% Bromophenol blue) and boiling for 5 min. The samples were allowed to cool on ice and then loaded into the wells with a pipette. A 7.5 µl of pre-stained protein molecular weight marker was also loaded into the first well. The lid was placed on the mini tank, the correct orientation was made by matching the black and red colour on the lid and electrode assembly. The electrical leads were inserted into a power supply with the proper polarity and power was applied at constant 125 volts for 1 h. The gels from the gel cassettes were removed and washed with distilled water followed by visualization of protein bands with Coomassie staining or Western blotting as described below (see Sections 2.4.5 and 2.4.6).

2.4.5 Coomassie staining of Sodium dodecyl sulphate polyacrylamide gels

Coomassie blue staining is based on the binding of the dye Comassie brilliant blue to virtually all proteins. After separating the proteins on SDS-PAGE, the gel is stained by soaking in the dye solution followed by de-staining step (see below) in which the unbound dye diffuses out of the gel.

For Coomassie staining, microsomal samples (25 µg/lane) were separated on 10% sodium dodecyl sulfate-polyacrylamide gel (SDS-PAGE) at a constant 125 volts for about 1h. The gel was fixed in fixing solution (50% methanol and 10% glacial acetic acid in water) for 2 h with gentle agitation. The gel was stained in staining

solution (0.1% Coomassie Brilliant Blue G-250, 50% methanol and 10% glacial acetic acid) for 30 min with gentle agitation. De-staining of the gel was performed in de-staining solution (40% methanol and 10% glacial acetic acid in water) until background of the gel was fully de-stained. The image of stained protein bands on the gel was captured on Gel Doc™ workstation (Bio-Rad).

2.4.6 Western Blotting for Immunodetection of Proteins

SDS-PAGE coupled with Western blotting is commonly used to determine the presence and abundance of a target protein. After separating the proteins on SDS-PAGE, they are transferred to a polyvinylidene fluoride (PVDF) or nitrocellulose membranes by applying electric current. The electric current forces the protein molecules to migrate out of the gel onto the membrane. After transferring the proteins onto the membrane, a target protein can be subsequently identified through its reaction with an antigen-specific antibody.

For Western blot analysis, the microsomal samples (1.5µg/lane) were separated on 10% SDS-PAGE. The gel was washed twice with distilled water and was equilibrated in cathode buffer (25 mM Tris, 40 mM 6-aminohexanoic acid and 20% methanol). Three 3 mm Whatman papers, cut to double the size of the gel, and three cut to the size of the gel were pre-soaked in the cathode buffer. A piece of Immobilon-P PVDF membrane (Millipore) was cut to the size of the gel and rinsed in methanol for 1 min before equilibrating it in anode buffer II (25 mM Tris, 20% methanol, pH 10.4).

Three more 3 mm Whatman papers, cut to the size of the gel were pre-soaked in anode buffer II and three Whatman papers, cut to double the size of the gel were soaked in Anode buffer I (300 mM Tris, 20% methanol, pH 10.4). The transfer sandwich was assembled in the following order,

1. Three 3 mm Whatman papers cut to double the size of the gel and pre-soaked in cathode buffer were placed onto cathode (–ve) plate of the semi-dry transfer unit.
2. Three 3 mm Whatman papers, cut to the size of the gel and pre-soaked in cathode buffer were placed on the previous layer of the Whatman papers.
3. The gel equilibrated in cathode buffer was placed on top.
4. A piece of Immobilon-P membrane, cut to the size of the gel and equilibrated in anode buffer II was placed on the gel; all the air bubbles trapped in the layers were removed by rolling a pipette over the membrane.
5. Three 3 mm Whatman papers, cut to the size of the gel and pre-soaked in the Anode buffer II, were placed on the membrane.
6. Three more 3 mm Whatman papers, cut to double the size of the gel and pre-soaked in anode buffer I, were placed on top.
7. Anode (+ve) plate of the semi-dry transfer unit was placed on top and secured in position.

The electrical leads were inserted into a power supply with the proper polarity and power was applied at 0.8 mA per 1 cm^2 of gel for 1 h. When the transfer was complete, the membrane was removed with a pair of forceps and rinsed in sterile distilled water.

The unoccupied membrane binding sites on the blot were blocked by incubating the membrane with blocking solution (5% non-fat dry milk in PBS) overnight at 4°C. The primary antibody was diluted to the indicated concentration in freshly prepared blocking solution (1% non-fat dry milk in PBS). The membrane was incubated in the primary antibody solution for 1 h at room temperature with gentle agitation. The membrane was washed three times for 5 min each with PBS containing 0.05% Tween-20. The membrane was subsequently incubated with secondary antibody diluted at indicated concentrations in freshly prepared blocking solution (1% non-fat dry milk in PBS). The membrane was incubated in the HRP-conjugated secondary antibody solution for 1 h at room temperature with gentle agitation. The membrane was washed five times for 5 min each with PBS containing 0.05% Tween-20. Finally the blot was washed with sterile distilled water. Equal quantities of Luminol reagent solution A and solution B (Santa Cruz Biotechnology, Catalogue number: sc-2048) were mixed by inversion, the water was poured off from the blot and the mixed Luminol reagent solution was added to the membrane with protein side facing up for 2 min at room temperature. The excess Luminol reagent was poured off and the membrane was lifted with a pair of forceps to drain excess reagent. The membrane was tightly covered, protein side facing up, with a single layer of plastic wrap. The chemiluminescence was detected with the Gel Doc™ system (Bio-Rad) with multiple exposures of 15 seconds, up to a period of 10 min.

2.4.7 Measurement of Enzymatic Activity of NADPH cytochome P450 Reductase (CPR)

Physiologically, CPR is an electron donor protein for CYPs. However, quantitative measurement of the reduction of CYP by CPR is relatively difficult to assay. Therefore, non-physiological substrates like 3-(4,5-dimethylthiazol-2-yl)-2,5-diphenyltetrazolium bromide (MTT) or cytochome c, which act as artificial electron acceptors are widely used for determining CPR activity (Yim et al. 2005). The reduction of these substrates mirrors the reduction of CYP. Both MTT and cytochome C were used for assaying the CPR activity as described below.

2.4.7.1 Reductase assay using cytochrome c as a substrate

Stock solutions for cytochrome *c* reductase assay

0.6 M Potassium Phosphate (KPO4), pH 7.4 (Kpi buffer)

19.8 ml of buffer A and 80.2 ml of buffer B was made up to 167 ml with sterile water and adjusted to pH 7.4 (using 0.5 M HCl and 0.5 M NaOH).

Buffer A = 136.1 g KH_2PO_4/L (1 M) (potassium dihydrogen phosphate) from Sigma-Aldrich Cat No P2222, MW 136.09.

Buffer B = 174.2 g K_2HPO_4/L (1 M) (dipotassium hydrogen phosphate) from Sigma-Aldrich Cat No P5655, MW 174.18.

Buffer A and buffer B were autoclaved before use.

Solution A: 10 ml stock in deionised water contained 200 mg $NADP^+$, a final concentration of 26.13 mM (Sigma-Aldrich Cat N^o N0505, MW 765.4); 200 mg D-glucose-6-phosphate disodium salt hydrate, a final concentration of 65.77 mM (Sigma-Aldrich Cat N^o F7250, MW 304.1); 1 M $MgCl_2$, a final concentration of 65.42 mM (Sigma-Aldrich Cat N^o M1028). The solution was stored in aliquots at

–20°C.

Solution B: 6.25 ml stock in 5 mM sodium citrate contained 250U glucose-6-phosphate dehydrogenase (Sigma-Aldrich Cat N^o G6378) in a 6.25 ml solution of 5 mM trisbasic sodium citrate (Sigma-Aldrich Cat N^o S46410). The resultant solution was stored in aliquots at –20°C.

0.4 mM cytochrome *c* contained 50 mg cytochrome *c* (from bovine heart; Sigma-Aldrich Cat N^o C3131, MW 12 327) in 10 ml of deionised water. The solution was stored in aliquots at –20ºC.

The principle behind the reductase assay is that the oxidized ferric form of cytochrome *c* has a characteristic absorption spectrum, as does the reduced (ferrous form). The reduced ferrous form has a characteristic absorption band at 550 nm, a band

that is absent in the oxidized form. Therefore, the enzyme activity can be conveniently assayed by measuring the increase in absorbance at 550 nm as a function of time.

The assay was carried out in a 1 ml cuvette. 860 µl of Kpi buffer was added into a cuvette together with 100 µg of microsomes (~20 µl), 10 µl of solution B and 100 µl of 0.4 mM cytochrome *c*. The contents were mixed gently. 10 µl of solution A was quickly added to the cuvette, and all contents were mixed by inverting a few times. The addition of all reagents gave a reaction mixture which contained 40 micromoles of cytochrome *c*, 100 µg of microsomal proteins and an NADPH generating system (1.3 mM NADP+, 3.3 mM glucose-6-phosphate, 3.3 mM $MgCl_2$ and 0.4U/ml glucose-6-phosphate dehydrogenase). The increase in absorbance at 550 nm was measured for about 10 min. An extinction coefficient of 19.6 mM^{-1} cm^{-1} was used to calculate the moles of cytochrome *c* reduced per minute per mg of protein (Fukushima et al. 1984).

2.4.7.2 Reductase assay using MTT as a substrate

Stock solutions for MTT reductase assay

10 mM potassium phosphate buffer, pH 7.4

It was prepared by mixing 8 ml of 1 M K_2HPO_4 and 2 ml of 1 M KH_2PO_4, the volume being adjusted to 1 litre with deionised water.

10 mM MTT

It was prepared by dissolving 41.4 mg of MTT (Sigma-Aldrich Cat N^{o} M2128) was dissolved into 10 ml of 10 mM potassium phosphate buffer pH 7.4 to give 10 mM MTT.

100 mM potassium phosphate buffer, pH 7.6

86.6 ml of 1 M K_2HPO_4 and 13.4 ml of 1 M KH_2PO_4 were mixed and the volume was adjusted to 1 litre with deionised water.

Solution A: 131 µl of 1M magnesium chloride solution (Sigma-Aldrich Cat N^{o} M1028) was diluted to 1 ml in deionised water to achieve final concentration of 66 mM. To this solution, the following reagents were added and dissolved: 43.5 mg of $NADP^{+}$ at a final concentration of 50 mM (Sigma-Aldrich Cat N^{o} N0505, MW 765.4), 172 mg of D-glucose-6-phosphate disodium salt hydrate at a final concentration of 500 mM (Sigma-Aldrich Cat N^{o} F7250, MW 304.1). The solution was stored in aliquots at

–20°C.

Solution B: 17U glucose-6-phosphate dehydrogenase (Sigma-Aldrich Cat N^{o} G6378) was dissolved in 340 µl of 5 mM trisbasic sodium citrate (14.7 mg/ml; Sigma-Aldrich Cat N^{o} S46410). The solution was stored in aliquots at –20°C.

MTT, a tetrazolium salt, is reduced by various reductases to a blue formazan product which shows maximum absorption at 610 nm. Therefore, NADPH-cytochome P450 reductase activity can be measured by the reduction of MTT (Yim, 2005).

The assay was carried out in a 1 ml cuvette. 950 µl of 100 mM potassium phosphate buffer, pH 7.6, was added to a cuvette together with 100 µg of microsomes, 10 µl of solution B and 10 µl of 10 mM MTT. Then 10 µl of solution A was quickly added to the cuvette and the contents were mixed by inverting a few times. The resulting reaction mixture contained 100 µM MTT (Sigma Cat N^o M5655), 100 µg microsomal protein in 100 mM potassium phosphate buffer, pH 7.4, and the NADPH generating system (final concentrations of 0.5 mM $NADP^+$, 5 mM glucose 6-phosphate, 1.3 mM $MgCl_2$ and 0.5 unit of glucose 6-phosphate dehydrogenase/ ml). The increase in absorbance at 610 nm was measured for about 10 min. An extinction coefficient of 11.3 mM^{-1} cm^{-1} was used to calculate the moles of MTT reduced per min per mg of protein as follows:

ΔA_{610} / min/ 11.3 X 0.1 mg/ ml= µmole MTT reduced/ min/ mg protein.

2.4.9 CYP assays

Stock solutions for the CYP assays

Solution A: 200 mg $NADP^+$ (Sigma-Aldrich Cat N^o N0505, MW 765.4), 200 mg D-glucose-6-phosphate disodium salt hydrate (Sigma-Aldrich Cat N^o F7250, MW 304.1), 1M $MgCl_2$ solution (Sigma-Aldrich Cat N^o M1028) were used to make a 10 ml solution in deionised water which gave final concentrations of 26.13 mM, 65.77 mM, and 65.42 mM of the three constituents. The solution was stored in aliquots at –20°C.

Solution B: 250 U glucose-6-phosphate dehydrogenase (Sigma-Aldrich Cat N^o G6378) was dissolved in 6.25 ml solution of 5 mM trisbasic sodium citrate (Sigma-Aldrich Cat N^o S46410) and stored in aliquots at –20°C.

Solution C: Solution C was freshly prepared just before the assay by mixing 1.5 ml of 0.5 M KPO_4 pH 7.4, 1.5 ml of solution A and 0.3 ml of solution B. The final volume was made up to 15 ml with deionised water.

0.5 M Potassium Phosphate (KPO4) buffer pH 7.4 (Kpi buffer)

19.8 ml of buffer A and 80.2 ml of buffer B (see below) were mixed and the final volume was made up to 200 ml with deionised water and pH was adjusted to 7.4 (using 0.5 M HCl and 0.5 M NaOH).

Buffer A = 136.1 g KH_2PO_4/L (1 M), autoclaved.

Buffer B = 174.2 g K_2HPO_4/L (1 M), autoclaved.

0.1 M Potassium Phosphate (KPO_4) buffer pH 7.4

1.98 ml of buffer A and 8.02 ml of buffer B were mixed and the final volume was made up to 100 ml with deionised water and the pH was adjusted (using 0.5 M HCl and 0.5 M NaOH).

Buffer A = 136.1 g KH_2PO_4/L (1 M), autoclaved.

Buffer B = 174.2 g K_2HPO_4/L (1 M), autoclaved.

50 mM tribasic Sodium Citrate

147 mg of tribasic sodium citrate (Sigma-Aldrich Cat N^o S4641) was dissolved in deionised water and the final volume was made up to 10 ml.

Assay procedures

The substrates for enzymes assays used in this study are CYP isozyme-specific fluorogenic substrates which upon oxidative cleavage yield fluorescence at specific excitation-emission wavelength. The substrates are light sensitive. Therefore, all assays were set up in the laboratory with yellow lights switched on.

The reactions were preformed in black 96-well plates with clear flat bottom (Fisher Cat N^{o} FB86083). The assay plate and the solutions were pre-warmed at 37ºC before initiation of the assay. The plate layout, reaction temperature (37°C), reaction time (20 to 40 min), fluorescence sensitivity, the wavelength parameters and other kinetic assay parameters (i.e. excitation-emission wavelengths) were set as is indicated in the following chapters. Each reaction was performed in triplicate. Each 100 µl reaction contained a specific concentration of Kpi buffer (as indicated in respective chapters), solution C, CYP isozyme and an isozyme-specific fluorogenic substrate. Blank values were measured in reactions where CYP isozyme was not added. The known concentrations of metabolites were used to plot standard curves. The fluorescence was measured in terms of relative fluorescence unit (RFU) in kinetic reactions over a period of 20 to 40 min. Finally, the CYP activities were calculated as product formed/ min/ pmole of CYP or product formed/min/ ml.

2.4.10 Measurement of reactive oxygen species

2.4.10.1 H_2DCFDA Assay

2',7'-dichlorodihydrofluorescein diacetate (H_2DCFDA) is a cell-permeable indicator for reactive oxygen species that is non-fluorescent until the acetate groups are removed by intracellular esterases and oxidation occurs within the cell. The reactive oxygen species measurement (ROS) assay (Bondza-Kibangou et al. 2004) was performed using the fluorescent dye H_2DCFDA with some modifications as follows.

Sf9 cells were seeded at a density of 20,000 cells/ well in a 96-well tissue culture grade black plate. Cells were allowed to attach for 2 h at 27ºC in a humidified incubator. Sf9 cells were then infected with a range of MOIs (0.2 to 4.0 pfu/ ml) of different CPR species, as indicated, for 72 h when the medium was removed from the plate and 100 µl of 10 µM H_2DCFDA, diluted in PBS was added to each well. The plate was incubated in a 27ºC humidified incubator for 30 min. The oxidation of intracellular non-fluorescent 2',7'-dichlorodihydrofluorescein (H_2DCF) to highly fluorescent 2′,7′-dichlorofluorescein (DCF) was measured on a fluorometer (Bio-Tek Synegy HT) using an excitation 485/20 nm and emission 528/20 nm filter set. Blank values indicating the fluorescence of the dye in PBS were subtracted from all samples. Percentage induction over control was calculated in baculovirus infected cells.

2.4.10.2 Dihydrorhodamine-123 Assay

ROS was also measured by using dihydrorhodamine-123 dye. Briefly, Sf9 cells were seeded at a density of 20,000 cells/well in a 96-well tissue culture grade black plate. Cells were allowed to attach for 2 h at 27ºC in a humidified incubator. Sf9 cells were then infected with a range of MOIs (0.2 to 4.0 pfu/ ml) of different CPR species, as indicated, for 72 h. At 72 h, the dihydrorhodamine-123 dye assay was performed.

Medium was removed from the plate and 100 µl of 10 µM dihydrorhodamine-123, diluted in PBS, was added to each well. The plate was incubated in a 27ºC humidified incubator for 60 min. The oxidation of dihydrorhodamine-123 to highly

fluorescent rhodamine was measured on a fluorometer at an excitation wavelength of 500 nm and emission wavelength of 536 nm. Blank values, indicating the fluorescence of the dye, in PBS were subtracted from all samples. Percentage induction over control was calculated in baculovirus infected cells.

2.4.11 CYP Inhibition assay

IC_{50} Determinations

The assay method was adapted from Gentest CYP inhibition protocols (BD Biosciences, www.bd.com). The CYP inhibition assays were performed in a 96-well microtitre plates (Figure 2.6). The assays were performed for IC_{50} determination in duplicate rows of 12 wells. A test compound was added to the wells in column 1 and serially diluted to the wells in column 8. Wells 9 and 10, which were used as control wells, contained no test compound or positive controls (therefore no inhibition – full signal is detected). The wells in columns 11 and 12 were used as blanks (STOP solution was added prior to the addition of the enzyme/ substrate mix to the NADPH regenerating system in columns 11 and 12) – the only signal present in these wells was background noise). The assays were conducted in a final volume of 0.2 ml per well.

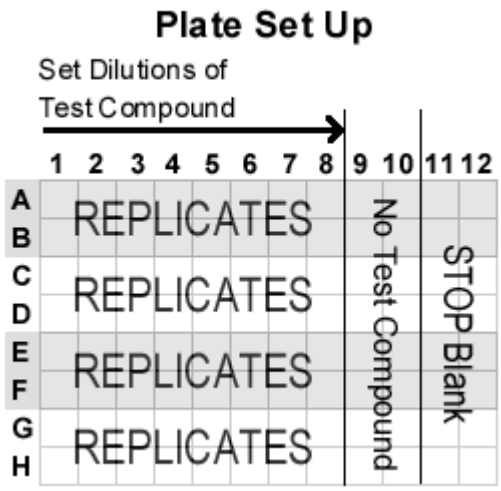

Figure 2.6. Typical plate set up for a high through-put assay.

Columns 1-8 are serial dilutions (3-fold) of the test compound or positive control.

Columns 9 and 10 contain no test compound.

Columns 11 and 12 are blank controls (STOP solution added prior to initiation of the reaction).

Rows A/B, C/D, E/F and G/H are replicates.

The detailed methodology of inhibition assays, using CYP isoform-specific inhibitors, is described in the fifth chapter.

Chapter 3 Cloning, expression, catalytic activities of CPR species and CYP2D6 when expressed alone and together

3.1 Introduction

Human cytochrome P450 enzymes (CYPs) are a superfamily of haem-binding monooxygenase enzymes involved in the metabolism of xenobiotics such as toxins, carcinogens and drugs as well as in the biosynthesis of cholesterol, vitamins and steroids (Wolf et al 1986; Shou et al. 2001). Biotransformation of these xenobiotics and endobiotics by CYPs requires molecular oxygen and supply of reducing equivalents from its redox partner NADPH cytochrome P450 reductase (CPR). CPR is responsible for the transfer of electrons from NADPH to CYPs and is essential for CYP activity. Similar to the CYPs, human CPR is also endoplasmic reticular (ER) membrane (microsome) bound and most abundant in the liver. However unlike the CYP superfamily of genes, CPR is encoded by a single gene (Simmons, 1985; Shephard et al. 1989). This single enzyme couples with all the known human CYPs to make them active.

The CPR contains FMN, FAD and NADPH binding domains and electrons are transferred from NADPH to FAD to FMN and finally to CYP. The interaction between CYP and CPR occurs on the surface of the endoplasmic reticulum. Electrostatic (Shen and Kasper 1995), hydrophobic and van der Waals forces (Voznesensky and Schenkman 1994) have been implicated as determinants of this interaction. However

the mode of CYP-CPR interaction and the formation of a productive monooxygenase complex are still not clearly understood (Deeni et al. 2001). Both CYP and CPR have NH_2 (N)-terminus hydrophobic domains which anchor on the microsomes and are important for correct spatial orientation of the redox centres for effective electron transfer.

The catalytic activity of a particular CYP in a specific tissue, sub-cellular fraction, or recombinant expression systems is determined not only by the abundance of the CYP, but also by the amount of its electron transport partner CPR (Crespi and Miller, 1999). However when a CYP is co-expressed with the CPR, there are some problems posed by high level heterologous expression of the CYP-CPR complex to host cells as well as to the activity and content of CYP enzymes. As CYPs are associated with the endoplasmic reticulum, high level expression causes an increased stress on the cell (Szczesna-skorupa et al. 2004). Co-expression of CPR with CYP increases the catalytic activity of the CYP enzyme but unfortunately reduces the yield of spectrally active CYP enzyme (Pritchard et al., 1998; Chen et al., 1997). Although the CYP apoprotein levels remain unchanged during co-expression of CYP and CPR, the amounts of spectrally active CYP holoprotein decreases remarkably (Tamura et al., 1992), which is possibly the result of an uncoupled CYP reaction cycle. Some CYPs, such as CYP2E1, have shown a high degree of uncoupling which results in damage to cellular components, including CYP itself (Wang et al. 1996).

In order to investigate the interactions of CPR with CYPs and to find out whether we could improve upon both CYP levels and activity in an insect cell expression system, we studied human native (wild-type) CPR, two of its genetically engineered variants and the yeast CPR (yRD) in the context of various human CYPs. In order to do so, we have cloned full-length human native CPR (hRD) gene together with its two engineered variants (Figure 3.2).

The N-terminus of the wild-type human hRD protein contains the binding sites for the essential cofactors FMN and FAD. However, the first 55-amino acids of the hRD protein (165 bp of the *hRD* gene) constitute a domain that allows anchoring to microsomal membranes. Within this sequence lies a 24-amino acid negatively charged domain. The FMN binding site spans a sequence that includes the membrane anchor whereas the region to which FAD binds is positioned beyond this domain. It has been suggested that the complete hRD membrane anchor (the 55-amino acid domain) may be essential for coupling to CYPs (Bonina et al. 2005). In this chapter we show that deletion of a 24-amino acid N-terminal charged region present in the hRD's membrane anchoring domain prevents association of the resultant molecule, ΔhRD, to microsomal membranes. However, the ΔhRDM protein which also lacks the N-terminal 24-amino acids of CPR but contains an extra 17-amino acid sequence (SSEQKLISEEDLNGSRL) linked to ΔhRD's COOH (C)-terminus has the ability to adhere once again to microsomal membranes like the native CPR. This C-terminal 17-amino acid sequence includes a 12-amino acid motif (EQKLISEEDLN) which is often referred to as the *c*-

myc tag and belongs to an exposed epitope in the oncogenic protein *c*-myc (Evan et al. 1985).

Comparison of the wild type hRD and ΔhRDM protein sequences is shown below in Figure 3.1.

```
                    10        20        30        40        50
                     *         *         *         *         *
hRD          MGDSHVDTSSTVSEAVAEEVSLFSMTDMILFSLIVGLLTYWFLFRKKKEE
ΔhRDM        ------------------------MTDMILFSLIVGLLTYWFLFRKKKEE
                    60        70        80        90       100
                     *         *         *         *         *
hRD          VPEFTKIQTLTSSVRESSFVEKMKKTGRNIIVFYGSQTGTAEEFANRLSK
ΔhRDM        VPEFTKIQTLTSSVRESSFVEKMKKTGRNIIVFYGSQTGTAEEFANRLSK
                   110       120       130       140       150
                     *         *         *         *         *
hRD          DAHRYGMRGMSADPEEYDLADLSSLPEIDNALVVFCMATYGEGDPTDNAQ
ΔhRDM        DAHRYGMRGMSADPEEYDLADLSSLPEIDNALVVFCMATYGEGDPTDNAQ
                   160       170       180       190       200
                     *         *         *         *         *
hRD          DFYDWLQETDVDLSGVKFAVFGLGNKTYEHFNAMGKYVDKRLEQLGAQRI
ΔhRDM        DFYDWLQETDVDLSGVKFAVFGLGNKTYEHFNAMGKYVDKRLEQLGAQRI
                   210       220       230       240       250
                     *         *         *         *         *
hRD          FELGLGDDDGNLEEDFITWREQFWPAVCEHFGVEATGEESSIRQYELVVH
ΔhRDM        FELGLGDDDGNLEEDFITWREQFWPAVCEHFGVEATGEESSIRQYELVVH
```

```
                    260        270        280        290        300
                     *          *          *          *          *
hRD          TDIDAAKVYMGEMGRLKSYENQKPPFDAKNPFLAAVTTNRKLNQGTERHL
ΔhRDM        TDIDAAKVYMGEMGRLKSYENQKPPFDAKNPFLAAVTTNRKLNQGTERHL
                    310        320        330        340        350
                     *          *          *          *          *
hRD          MHLELDISDSKIRYESGDHVAVYPANDSALVNQLGKILGADLDVVMSLNN
ΔhRDM        MHLELDISDSKIRYESGDHVAVYPANDSALVNQLGKILGADLDVVMSLNN
                    360        370        380        390        400
                     *          *          *          *          *
hRD          LDEESNKKHPFPCPTSYRTALTYYLDITNPPRTNVLYELAQYASEPSEQE
ΔhRDM        LDEESNKKHPFPCPTSYRTALTYYLDITNPPRTNVLYELAQYASEPSEQE
                    410        420        430        440        450
                     *          *          *          *          *
hRD          LLRKLASSSGEGKELYLSWVVEARRHILAILQDCPSLRPPIDHLCELLPR
ΔhRDM        LLRKLASSSGEGKELYLSWVVEARRHILAILQDCPSLRPPIDHLCELLPR
                    460        470        480        490        500
                     *          *          *          *          *
hRD          LQARYYSIASSSKVHPNSVHICAVVVEYETKAGRINKGVATNWLRAKEPA
ΔhRDM        LQARYYSIASSSKVHPNSVHICAVVVEYETKAGRINKGVATNWLRAKEPV
                    510        520        530        540        550
                     *          *          *          *          *
hRD          GENGGRALVPMFVRKSQLRLPFKATTPVIMVGPGTGVAPFIGFIQERAWL
ΔhRDM        GENGGRALVPMFVRKSQLRLPFKATTPVIMVGPGTGVAPFIGFIQERAWL
                    560        570        580        590        600
                     *          *          *          *          *
hRD          RQQGKEVGETLLYYGCRRSDEDYLYREELAQFHRDGALTQLNVAFSREQS
ΔhRDM        RQQGKEVGETLLYYGCRRSDEDYLYREELAQFHRDGALTQLNVAFSREQS
```

```
                          610        620        630        640        650
                           *          *          *          *          *
hRD                HKVYVQHLLKQDREHLWKLIEGGAHIYVCGDARNMARDVQNTFYDIVAEL
ΔhRDM              HKVYVQHLLKQDREHLWKLIEGGAHIYVCGDARNMARDVQNTFYDIVAEL
                          660        670
                           *          *
hRD                GAMEHAQAVDYIKKLMTKGRYSLDVWS----------------
ΔhRDM              GAMEHAQAVDYIKKLMTKGRYSLDVWSSSEQKLISEEDLNGSRL
```

Figure 3.1. Comparison of the two protein sequences, wild-type hRD and the mutant ΔhRDM.

We have cloned and expressed human wild-type CPR (hRD) and its two variants (Figure 3.2) in insect cells in order to study their interactions with human CYPs.

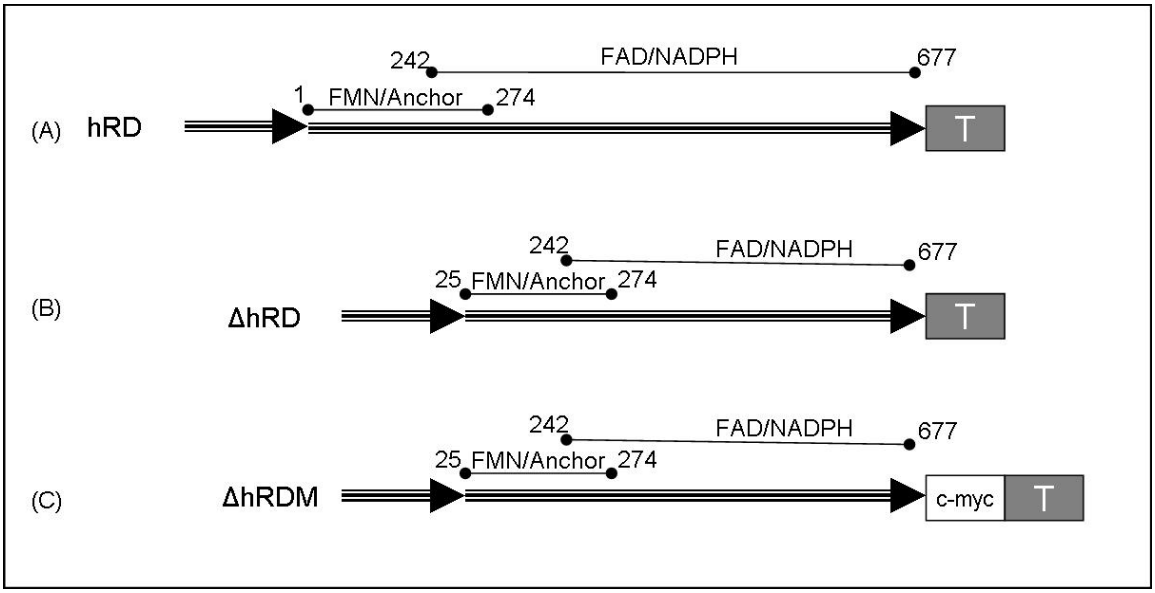

Figure 3.2. Human wild-type (i.e. native) hRD and its two engineered variants.

The yeast CPR (yRD) has been studied extensively in conjunction with human CYPs in our yeast expression systems. In fact, human CPR functions extremely poorly in yeast (unpublished results from our lab) and has rarely been used in the published literature for expression of human CYPs in yeast. However, although yeast CPR has been successfully used for heterologous expression of human CYPs in yeast, it has never been used for expression studies in any other eukaryotic cell system. Therefore, we considered that we should explore the possible interactions of yeast CPR with human CYPs in microsomes (ER membranes) derived from insect cells. Hence, we decided to clone and express yeast CPR (yRD) for co-expression with human CYPs in insect cells.

At the outset, we envisaged that it would be important to confirm initially the validity of the insect cell-based baculovirus system by studying the expression of a prototypic CYP so that the results obtained could be used later as a generic system for expression of all CYPs. In this chapter, we have studied CYP2D6 in conjunction with different CPR species with the aim of producing functionally active CYP2D6 enzymes. CYP2D6 was chosen as a model to study CPR-CYP interactions because it is a very important isozyme in terms of drug metabolism studies. It is known to metabolise a quarter of all marketed pharmaceutical entities (Werck-Reichhart and Feyereisen, 2000).

Hence we embarked on comparing in some detail the known coupling of hRD and CYP2D6 in insect cells with the possible interactions with CYP2D6 in insect cells of two novel genetically engineered variants of hRD (which may or may not possess CPR activities) and the very highly active yeast CPR (yRD) which has never been studied in any other organism besides yeast. The aim was to find out whether we could improve upon levels of recombinant CYP2D6 produced and its activity using an insect cell expression system.

In the following sections of this chapter, a comparative analysis of CYP2D6 activities obtained after coupling with hRD, ΔhRD, ΔhRDM and yRD is presented. Results suggesting the probable localisation of the two novel human CPRs, ΔhRD and ΔhRDM, are also included.

3.2 Gene Cloning in Basic Vectors

Cytochrome P450 2D6 (*CYP2D6*) and human full length human NADPH-cytochrome P450 reductase (*hRD*) genes were isolated from a human liver cDNA library obtained from BD-Clontech. Human delta-N24-NADPH-cytochrome P450 reductase with a stop codon at its 3'-end (*ΔhRD-stop*) and human delta-N24-NADPH-cytochrome P450 reductase without a stop codon (*ΔhRD-w/ostop*) were also isolated from the same human liver cDNA library. The yeast NADPH-cytochrome P450 reductase (*yRD*) gene was isolated from a *S. cerevisiae* genomic library (which was available in the lab). All four genes had previously been cloned in basic vectors

(pBlueScript KS+ or pSP73) for expression in yeast cells (unpublished results from our lab). The *CYP2D6* gene was re-cloned for insertion of a Kozak consensus translation initiation sequence (GCCACC) for expression in insect cells.

The genes were amplified via PCR using the primers mentioned below. The process of amplification has been described in 'Materials and Methods' (Section Number 2.2.2). The PCR products were run on an agarose gel containing ethidium bromide. DNA fragments of expected size were isolated and purified using Qiagen gel extraction kit according to the manufacturer's protocol. The purified DNA fragments were digested with the indicated restriction enzymes and after digestion run again on an agarose gel containing ethidium bromide. The digested DNA fragments were purified using Qiagen gel extraction kit. *CYP2D6*, *hRD*, *ΔhRD-stop*, *ΔhRD-w/ostop* and *ΔhRDM* genes were then directionally ligated using T4 DNA ligase into linearised pBluescript KS+ (already digested with appropriate restriction enzymes). The *yRD* gene was directionally ligated into pSP73 (*Bgl*II-*Xba*I digested and purified) using T4 DNA ligase. The ligation mixture was used to transform *E .coli* DH5α competent cells, and colonies containing the correct recombinant constructs were identified with restriction analysis. Plasmids were extracted from positive clones. The experimental methods employed are detailed in 'Materials and Methods' (Section Number 2.2.11). The gene sequences were confirmed by DNA sequencing and their alignment with reference sequences in the NCBI database.

3.2.1 Cloning of the *CYP2D6* gene in pBluescript KS+

CYP2D6 was isolated with forward primer (5'-ATGGATCC**GC CACC**ATGGGG CTAGAAGCAC TGGTGCCCCT GGCCGTG-3', the *BamH*I site and the Kozak sequence are underlined and bold letters respectively), and reverse primer (5'-ATGTCGACCT AGCGGGGCAC AGCACAAAGC-3', the *Sal*I site underlined). The CYP2D6 gene was then cloned into a pBluescriptKS+ vector at the *BamHI*, *Sal*I sites to obtain the plasmid, pBluKS+/Bam-Sal/CYP2D6 (Figure 3.3).

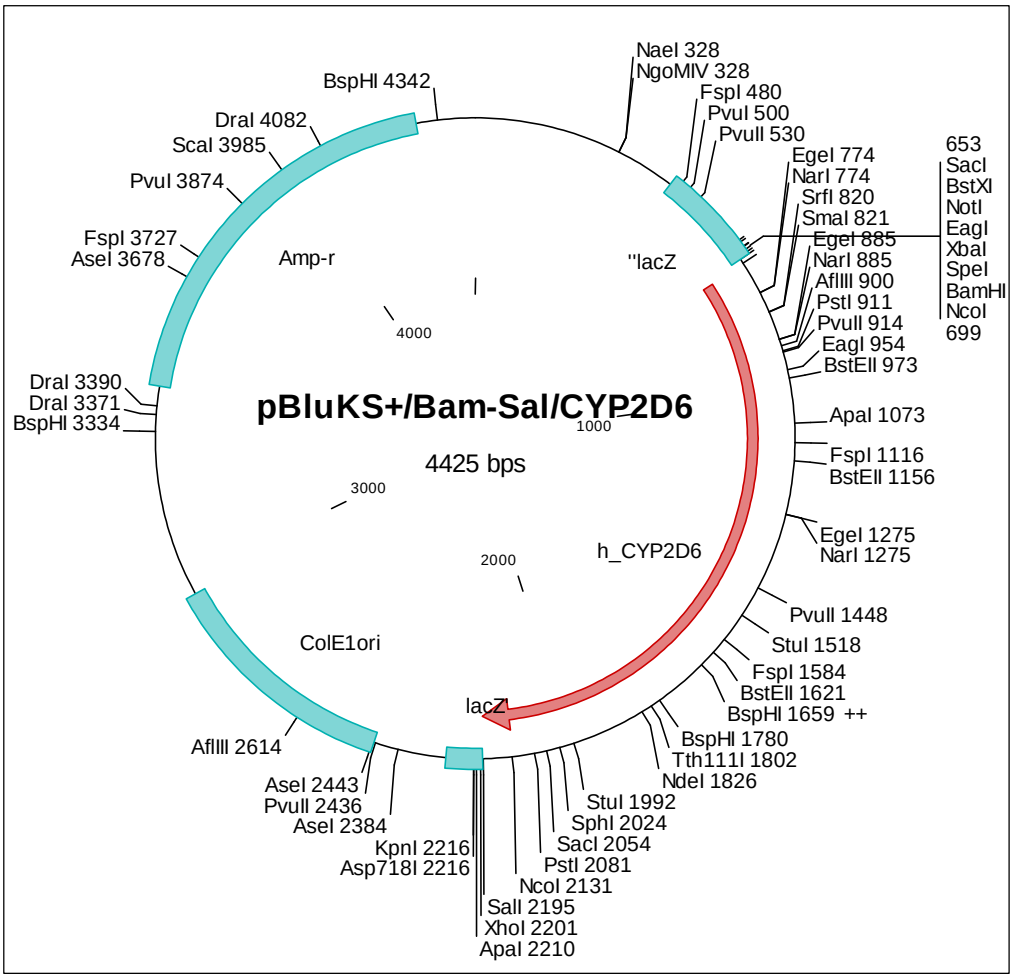

Figure 3.3. The plasmid map of pBluKS+/Bam-Sal/CYP2D6.

3.2.2 Cloning of the *hRD* gene in pBluescript KS+

The *hRD* gene was isolated with the forward primer (5'- CGCGGATCCA TGGGAGACTC CCACGTGGAC ACCAGCTCCA CCG -3', the *BamH*I site is underlined) and the reverse primer (5'- CTAGTCTAGA CTAGCTCCAC ACGTCCAGGG AGTAGCGGCC C -3', the *Xba*I site is underlined). The hRD gene was then cloned into a pBluescriptKS+ vector at the *BamH*I, *Xba*I sites to construct the plasmid, pBluKS+/Bam-Xba/hRD (Figure 3.4).

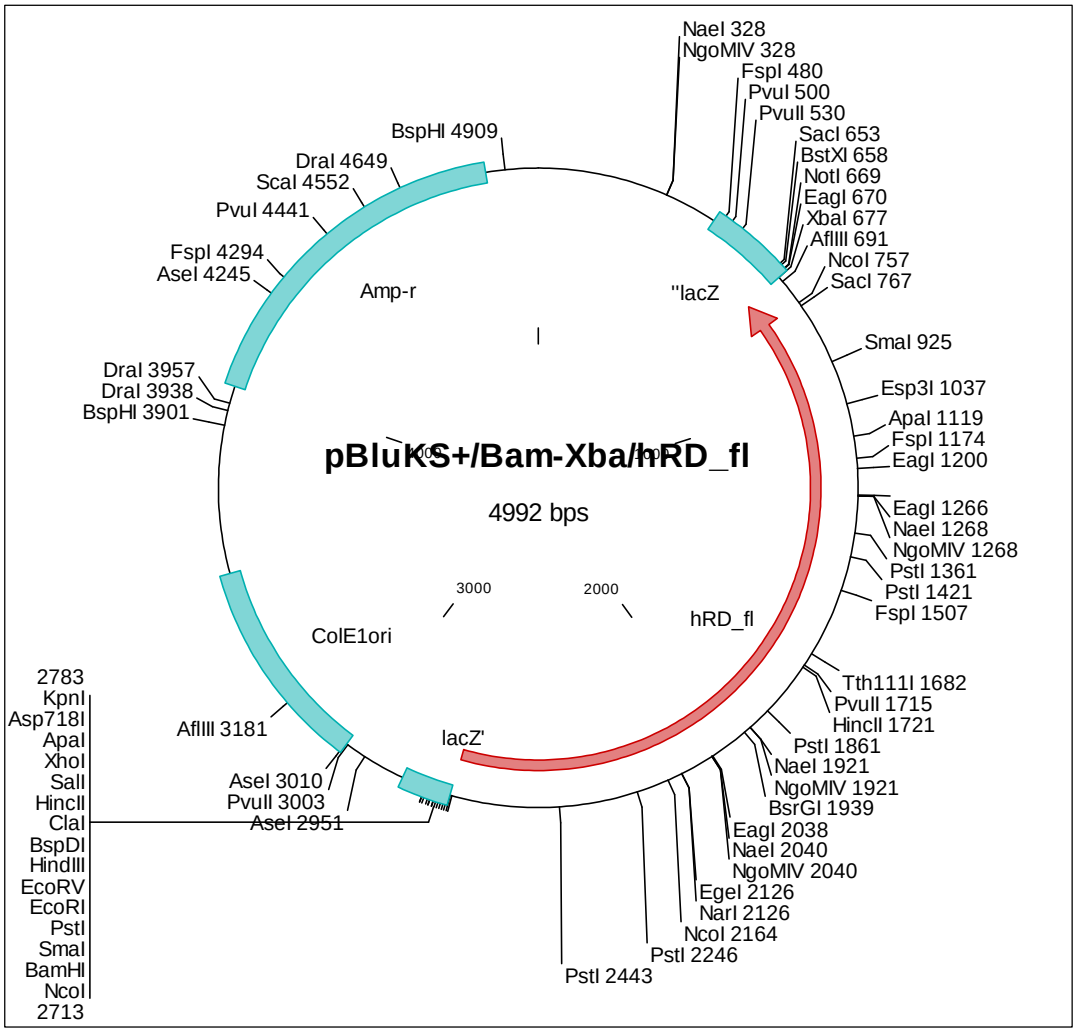

Figure 3.4. The plasmid map of pBluKS+/Bam-Xba/hRD.

3.2.3 Cloning of the *ΔhRD* gene with a stop codon at its 5'-end in pBluescript KS+

The *ΔhRD* gene with a stop codon at its 5'-end (i.e. *ΔhRD-stop*) was isolated with the forward primer (5'-CGCGGATCCA TGACGGACAT GATTCTGTTT TCGC-3', the *BamH*I site is underlined) and the reverse primer (5'- CTAGTCTAGA CTAGCTCCAC ACGTCCAGGG AGTAGCGGCC C -3', the *Xba*I site is underlined). The *ΔhRD-stop* gene was then cloned into the basic pBluescriptKS+ vector at the *BamHI, XbaI* sites to construct the plasmid, pBluKS+/Bam-Xba/ΔhRD-stop (Figure 3.5).

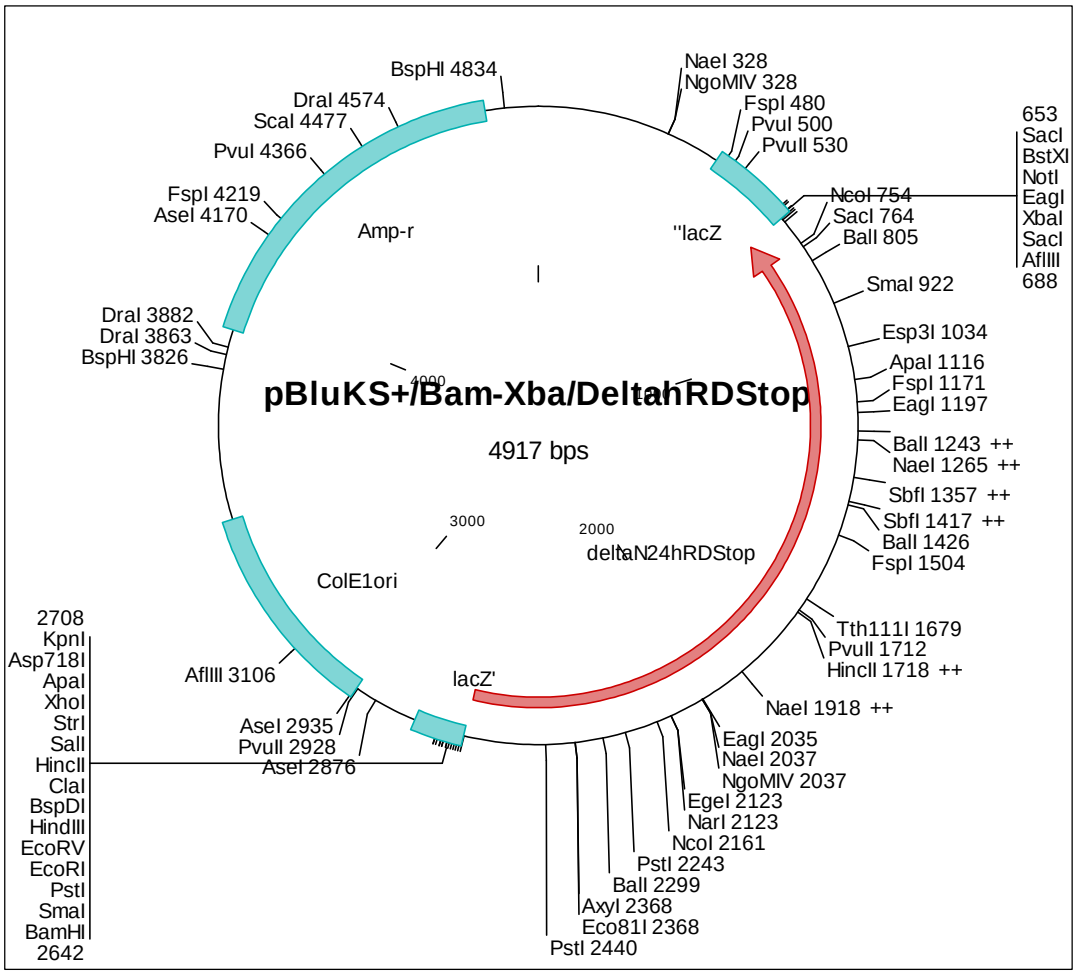

Figure 3.5. The plasmid map of pBluKS+/Bam-Xba/ΔhRD-stop.

3.2.4 Cloning of the *ΔhRD* gene without a stop codon at its 5'-end in pBluescript KS+

The *ΔhRD-w/ostop* gene was isolated with the forward primer (5'-CGCGGATCCA TGACGGACAT GATTCTGTTT TCGC-3', the *BamH*I site is underlined) and the reverse primer (5'- CTAGTCTAGA GCTCCAC ACGTCCAGGG AGTAGCGGCC C -3', the *Xba*I site is underlined). The *ΔhRD-w/ostop* gene was then cloned into a pBluescriptKS+ vector at the *BamH*I, *Xba*I sites to construct the plasmid, pBluKS+/ΔhRD-w/ostop.

3.2.5 Cloning of the *ΔhRDM* gene in pBluescript KS+

The plasmid pSYIGal1MS, which contains the yeast *GAL1* promoter (*GAL1p*) and encodes the *c*-myc tag linked to the transcription terminator from the yeast *SUC2* gene (*SUC2t*), was previously constructed in our laboratory. The plasmid pSYIGal1MS was constructed utilizing the pRS305 vector (ATCC 77140). The yeast *GAL1p* gene was first cloned into the pBluescriptKS+ plasmid at the *EcoR*I-*BamH*I sites. The resultant plasmid was named pBluscriptKS/Gal1. The *c*-myc tagged *SUC2t* was introduced into this plasmid at the *Xba*I, *Sac*I sites to generate the plasmid pBGal1MS. The fragment containing the *GAL1p—c-myc-SUC2t* fusion was isolated from the plasmid pBGal1MS using the *NgoM*IV and *Hin*dIII restriction enzymes and the isolated fragment was cloned into pRS305 at the *NgoM*IV-*Hin*dIII sites to create the plasmid pSYIGal1MS. This plasmid was utilized for sub-cloning of *ΔhRD w/ostop* as a *BamH*I-*Xba*I gene fragment, isolated from pBluKS+/ΔhRD w/ostop. The new plasmid was named pSYI/ΔhRDM. The ΔhRDM (ΔhRDw/ostop-c.myc) fragment was isolated from

pSYI/ΔhRDM with the forward primer (5'-CGCGGATCCA TGACGGACAT GATTCTGTTT TCGC-3', the *BamH*I site is underlined) and the reverse primer for *c-myc* (5'- CCGTCTAGAT CAACCGTTCA AGTCTTCTTC AGAGATCAAC -3', the *Xba*I site is underlined). The *ΔhRDM* gene was then cloned into pBluescriptKS+ at the *BamH*I, *Xba*I sites to construct the plasmid, pBluKS+/Bam-Xba/ΔhRDM (Figure 3.6).

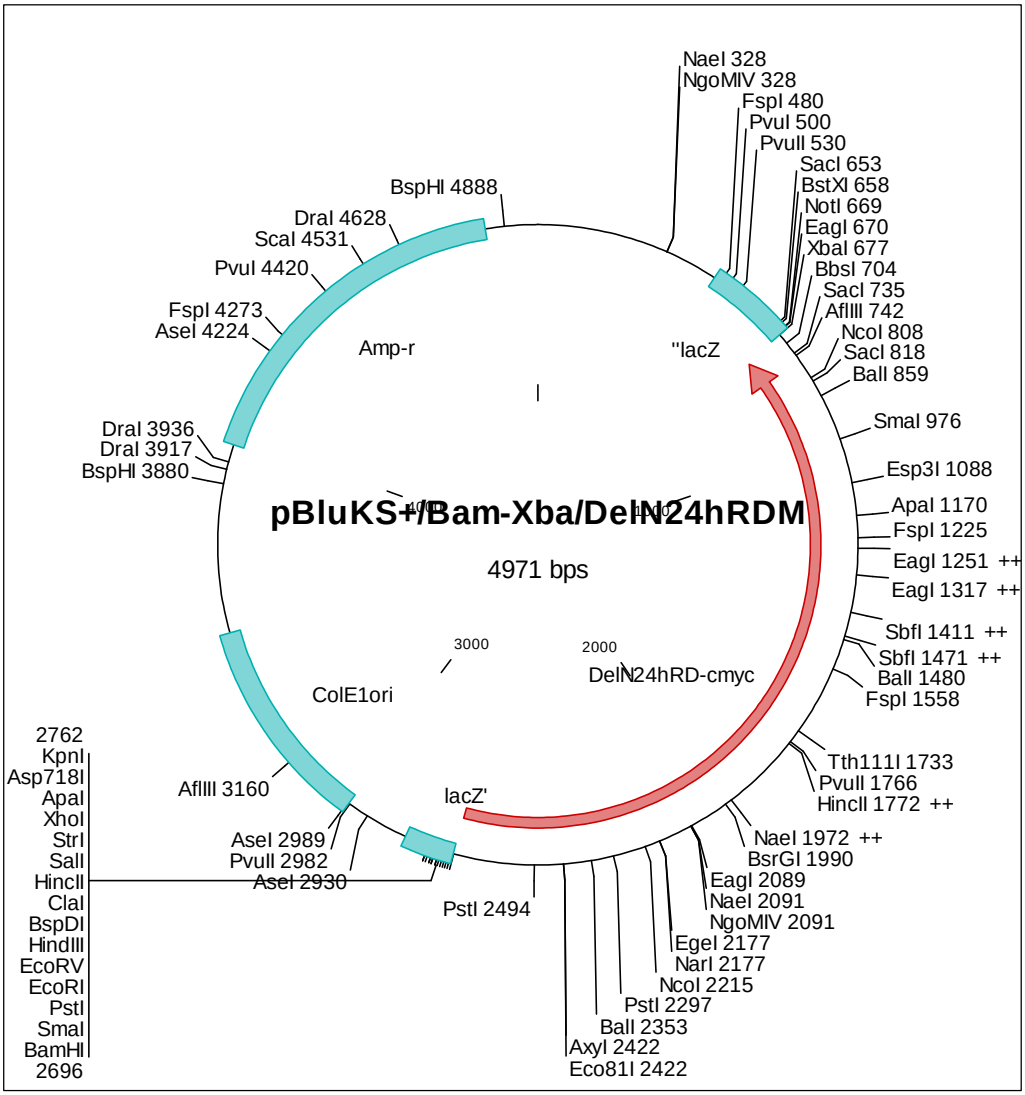

Figure 3.6. The plasmid map of pBluKS+/Bam-Xba/ΔhRDM.

3.2.6 Cloning of the *yRD* gene in pSP73

The *yRD* gene was isolated from a *S. cerevisiae* genomic library with the forward primer (5'-GGAATTC AGATCT ATG CCG TTT GGA ATA GAC AAC AC-3', the *Bgl*II site is underlined) and the reverse primer (5'-CTAG TCTAGA TTA CCA GAC ATC TTC TTG GTA TC-3', the *Xba*I site is underlined). The *yRD* gene was then cloned into the pSP73 basic vector at the *Bgl*II, *Xba*I sites to construct the plasmid, pSP73/BglII-XbaI/yRD (Figure 3.7). The experimental methods employed are detailed in 'Materials and Methods'.

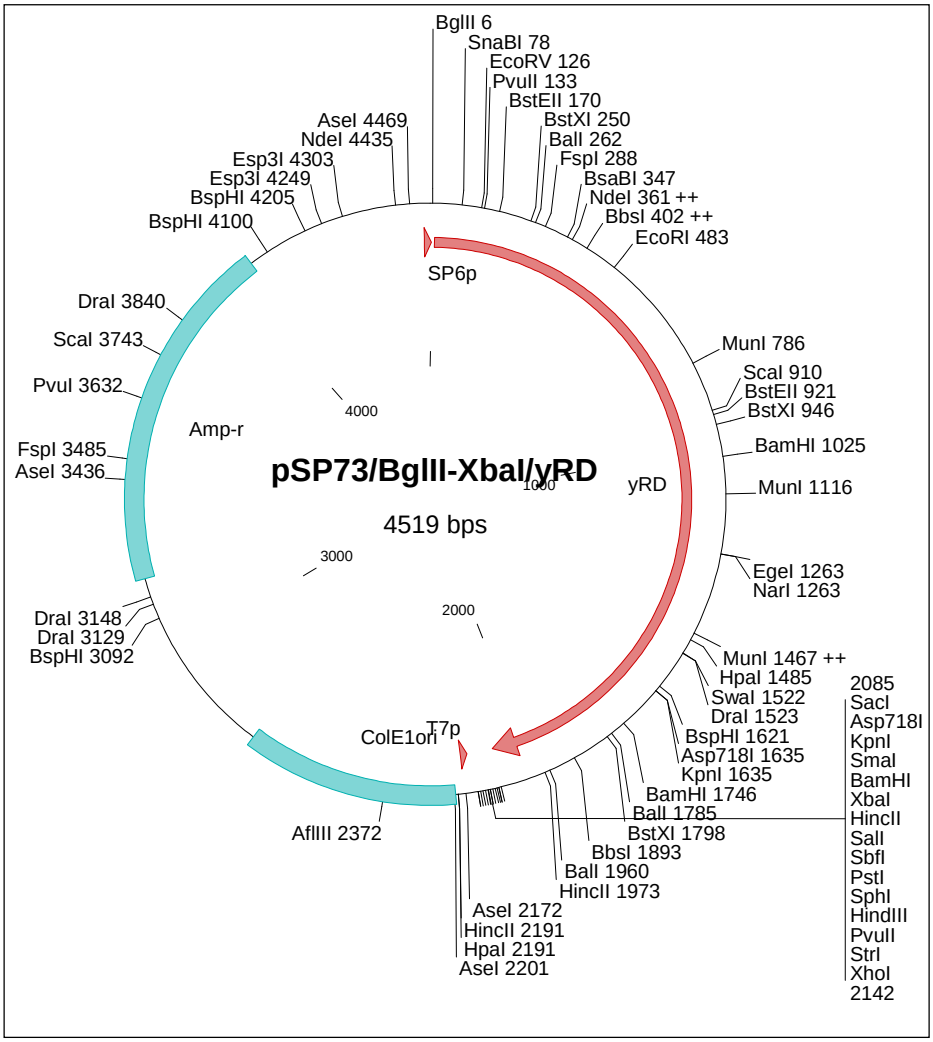

Figure 3.7. The plasmid map of pSP73/BglII-XbaI/yRD.

3.3 Sub-cloning of genes in a transfer vector for construction of bacmids

The genes were isolated from the basic vectors by means of restriction enzyme digestions as follows:

- To isolate the *CYP2D6* gene, the pBluKS+/Bam-Sal/CYP2D6 plasmid was digested with *BamH*I, *Sal*I.
- To isolate the *hRD* gene, the pBluKS+/Bam-Xba/hRD plasmid was digested with *BamH*I, *Xba*I.
- To isolate the *ΔhRD-stop* gene, the pBluKS+/Bam-Xba/ΔhRD-stop plasmid was digested with *BamH*I, *Xba*I.
- To isolate the *ΔhRDM* gene, the pBluKS+/Bam-Xba/ΔhRDM plasmid was digested with *BamH*I, *Xba*I.
- To isolate the *yRD* gene, the pSP73/BglII-XbaI/yRD plasmid was digested with *Bgl*II, *Xba*I.

The isolated genes were then sub-cloned into the transfer vector, pFastBac1, under the control of the polyhedrin promoter (polHp) as follows. The pFastBac1 vector was digested with

- *BamH*I, *Sal*I for cloning of *CYP2D6* gene,
- *BamH*I, *Xba*I for cloning of *hRD*, *ΔhRD-stop*, *ΔhRDM* and *yRD* genes.

The digested fragments of all genes and the linearised pFastBac1 vectors were run on agarose gels and purified. The digested gene fragments were directionally ligated into linearised pFastBac1 using T4 DNA ligase. The ligation mixture was then used to

transform DH5α *E. coli* competent cells, and colonies containing the correct recombinant constructs were identified via restriction enzyme analyses. Plasmids were extracted from positive clones and named as follows:

- pFastBac1/Bam-Sal/CYP2D6 (Figure 3.8),
- pFastBac1/Bam-Xba/hRD (Figure 3.9),
- pFastBac1/Bam-Xba/ΔhRD-stop (Figure 3.10),
- pFastBac1/Bam-Xba/ΔhRDM (Figure 3.11) and
- pFastBac1/yRD (Figure 3.12).

The experimental methods employed are detailed in 'Materials and Methods', Chapter 2.

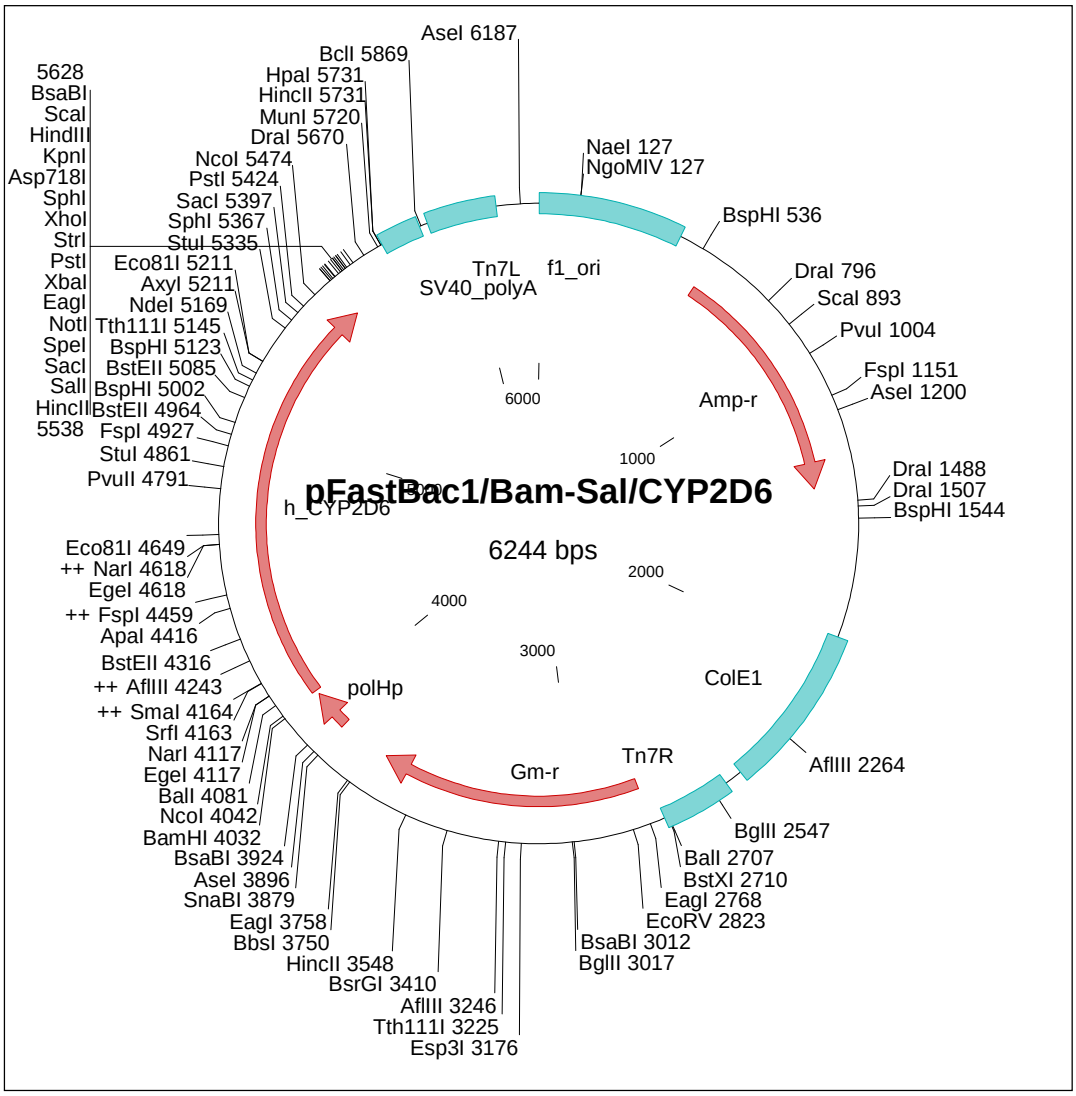

Figure 3.8. The plasmid map of pFastBac1/Bam-Sal/CYP2D6.

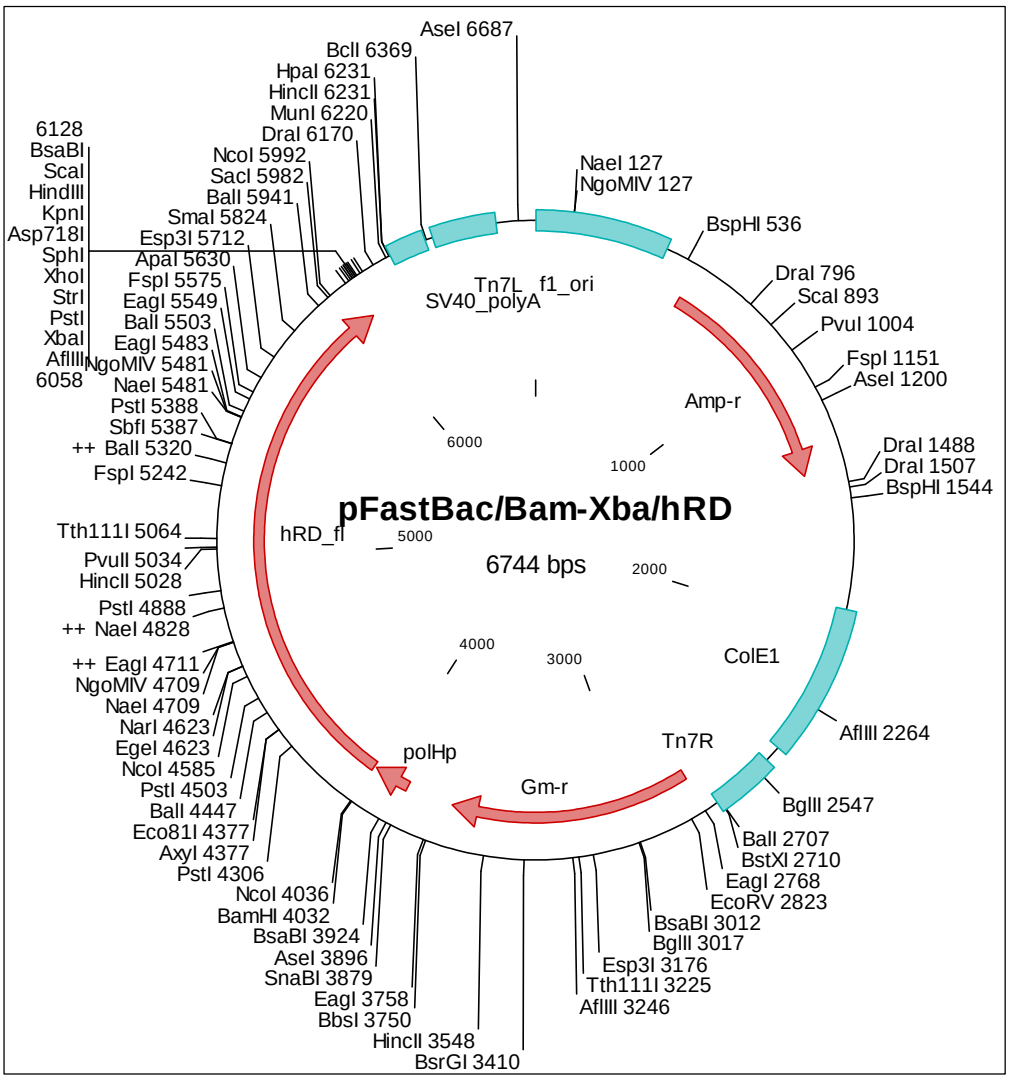

Figure 3.9. The plasmid map of pFastBac1/Bam-Xba/hRD.

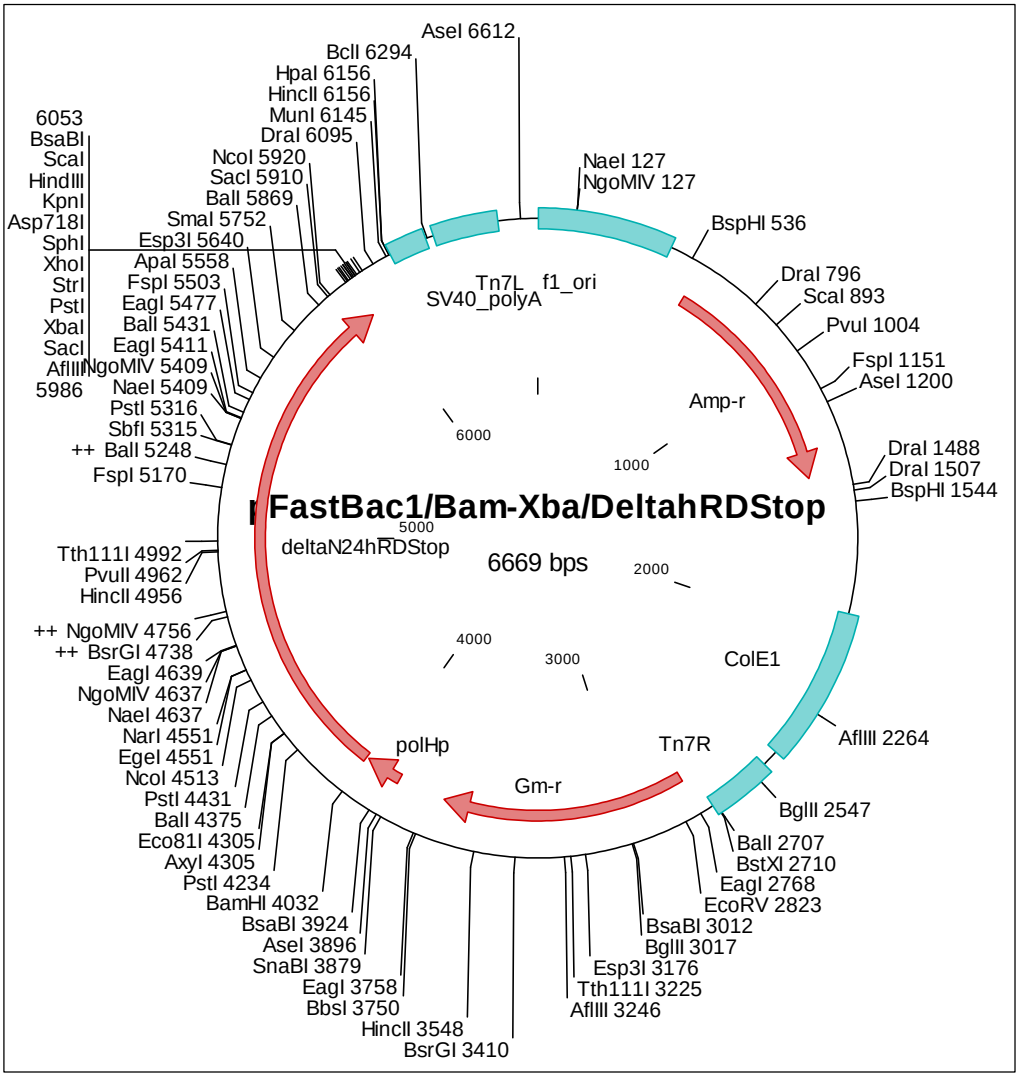

Figure 3.10. The plasmid map of pFastBac1/Bam-Xba/ΔhRD-stop.

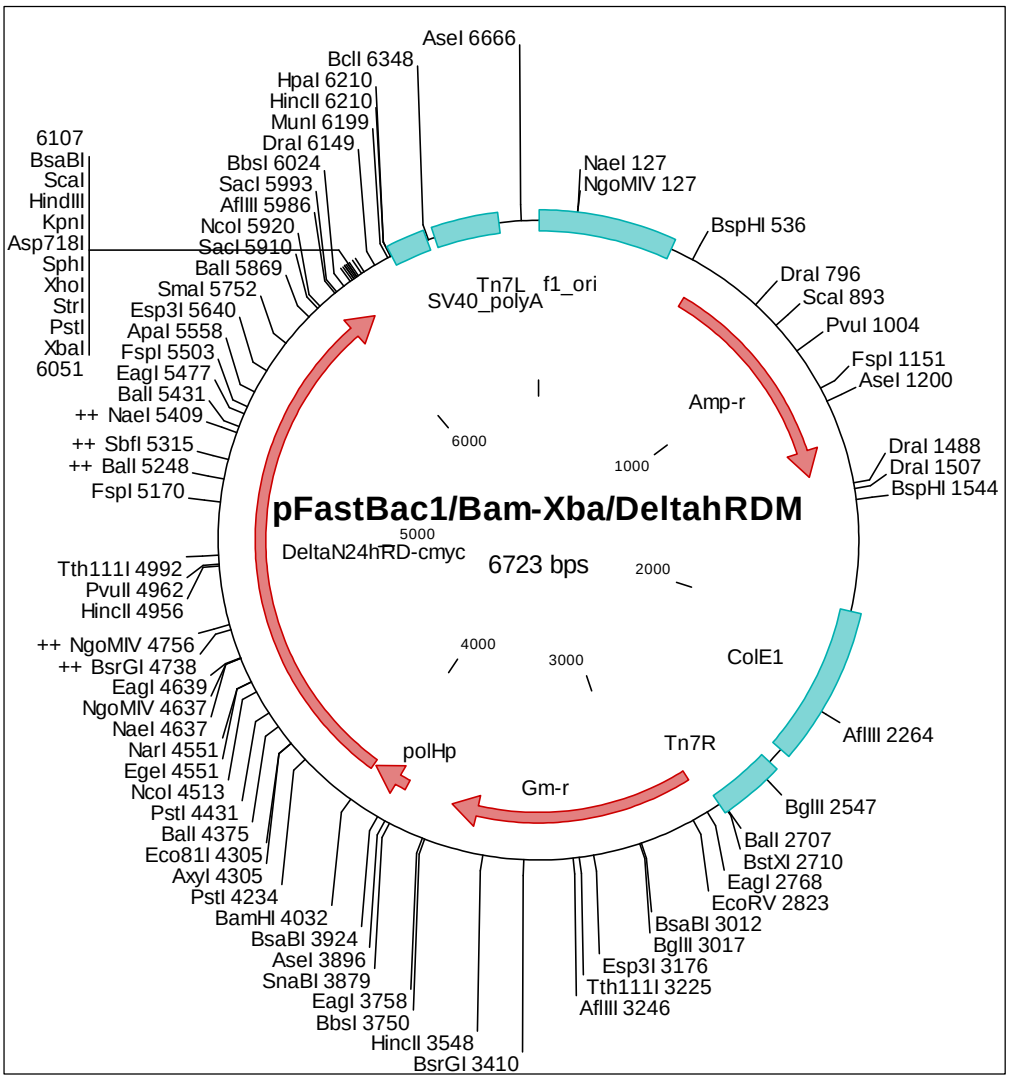

Figure 3.11. The plasmid map of pFastBac1/Bam-Xba/ΔhRDM.

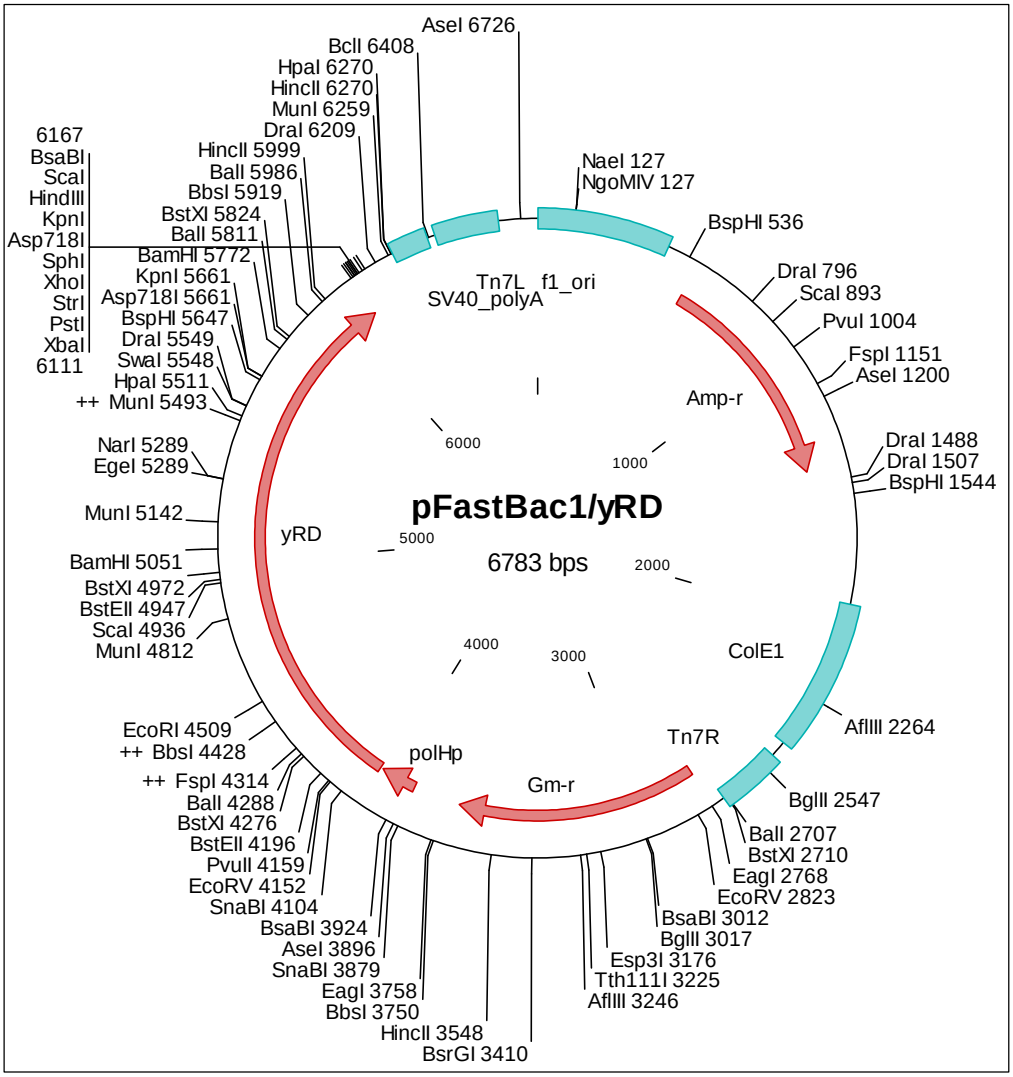

Figure 3.12. The plasmid map of pFastBac1/yRD – a *Bgl*II-*Xba*I fragment of the *yRD* gene was cloned in pFastBac1 digested with *BamH*I, *Xba*I.

3.4 Generation of bacmid constructs and baculoviruses

The recombinant donor vectors- pFastBac1/Bam-Sal/CYP2D6, pFastBac1/ Bam-Xba/hRD, pFastBac1/Bam-Xba/ΔhRD-stop, pFastBac1/Bam-Xba/ΔhRDM and pFastBac1/yRD were used for transformation of *E. coli* DH10Bac competent cells as described in Chapter 2 (‘Materials and Methods’). The propagation of recombinant

bacmid in DH10Bac cells was identified by the white colour of colonies in the presence of the chromogenic substrate-Bluo-gal and the inducer IPTG. The white colonies were streaked out for a second time on Bluo-gal containing plates and after confirming the phenotype of white colonies, recombinant bacmids were isolated and their veracities were confirmed by PCR (Figure 3.13). PCR was performed using the M13 forward primer (5'GTTTTCCCAGTCACGAC 3') and gene specific reverse primers. The experimental methods employed are detailed in 'Materials and Methods'.

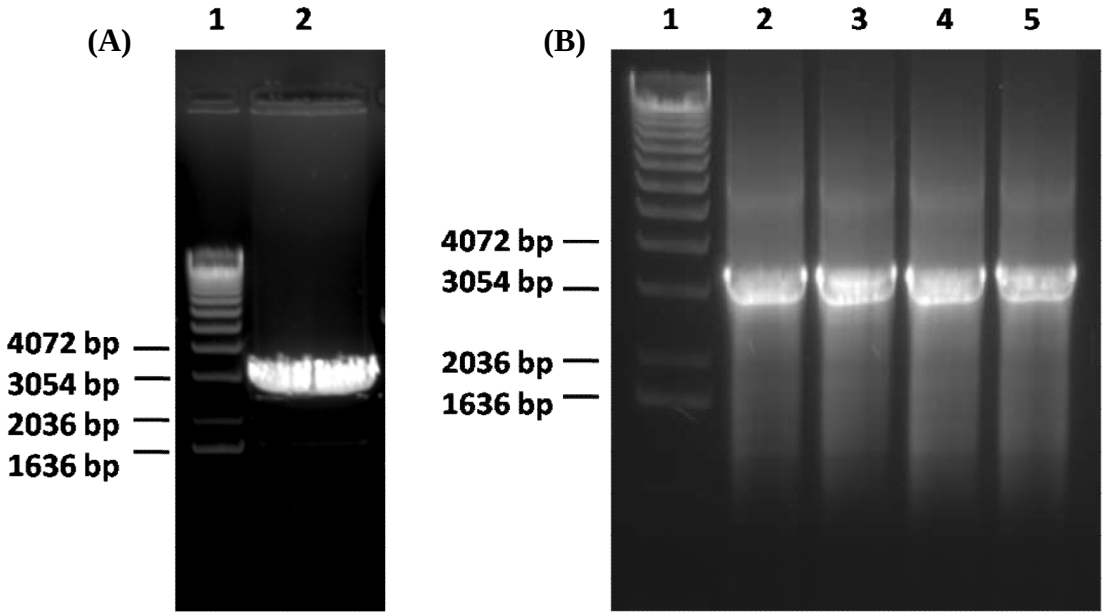

Figure 3.13. Confirmation of recombinant bacmid formation by PCR. The recombinant bacmids were confirmed as described in 'Materials and Methods' by PCR using M13 forward primer and gene specific reverse primers. (A) Lane 1, 1 Kb DNA ladder; Lane 2, confirmation of CYP2D6 gene transposition on the bacmid, expected size is about 3200 bp. (B) Lane 1, 1 Kb DNA ladder; Lane 2, confirmation of yRD gene transposition on the bacmid, expected size is about 3700 bp; Lane 3, confirmation

of hRD gene transposition on the bacmid, expected size is about 3700 bp; Lane 4, confirmation of ΔhRD gene transposition on the bacmid, expected size is about 3700 bp; Lane 5, confirmation of ΔhRDM gene transposition on the bacmid, expected size is about 3700 bp.

For generation of baculoviruses, the transfection of Sf9 cells with recombinant bacmids was performed in 6-well plates and the initial baculovirus stocks were amplified. The baculoviruses were titrated using plaque assays (Figure 3.14) as described in Materials and Methods (Section Number 2.3.9).

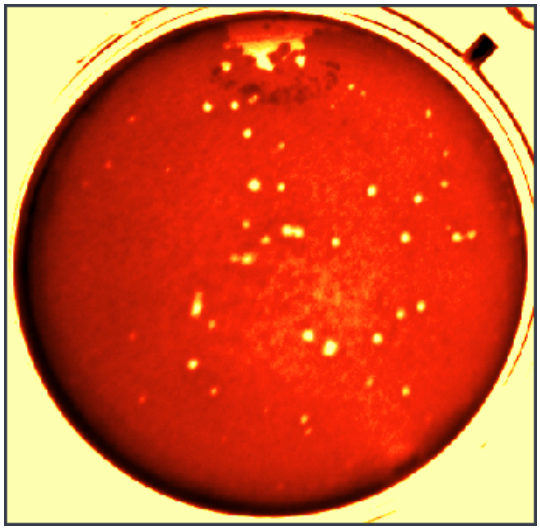

Figure 3.14. Viral plaque assay for determining baculovirus titres. The plaque assays were performed as described in 'Materials and Methods' (Section Number 2.3.9) using baculovirus stock dilutions from 10^{-3} to 10^{-8}. The plaques were stained with neutral red and viral titres were determined.

3.5 Expression of hRD, ΔhRD, ΔhRDM and yRD in insect cells

Following amplification and titration of recombinant baculoviruses, Sf9 cells were infected with **b**aculo**v**iruses that encode the different species of CPRs (i.e. BV-CPRs). Hereafter, the specific recombinant baculoviruses would be referred to as BV-hRD, BV-ΔhRD, BV-ΔhRDM and BV-yRD. All baculoviruses were used at an MOI of 1 for infection of Sf9 cells. The microsomes prepared after 63 h of infection with BV-CPRs were subjected to sodium dodecyl sulfate-polyacrylamide gel (SDS-PAGE) electrophoresis as described in 'Materials and Methods' (Section Number 2.4.4). Twenty-five μg of microsomal protein samples were separated on SDS-PAGE and protein bands were visualized by staining with Coomassie blue staining (Figure 3.15) as described in 'Materials and Methods' (Section Number 2.4.25). Coomassie blue staining detected the hRD, ΔhRDM and yRD proteins, but the ΔhRD protein band was not observed on the gel which could mean that either that the protein is not expressed or that ΔhRD does not anchor to microsomal membranes. From experiments in yeast, it was shown that indeed the ΔhRD protein is cytosolic (unpublished observations). However, it is quite clear from the gel that the addition of a 17-amino acid sequence, which includes the classical *c-myc* tag, to the C-terminal end of ΔhRD allows ΔhRDM to be anchored to the microsomal membranes. The image of stained protein bands on the gel was captured on Gel Doc™ (Bio-Rad). The experimental methods employed are described in 'Materials and Methods'.

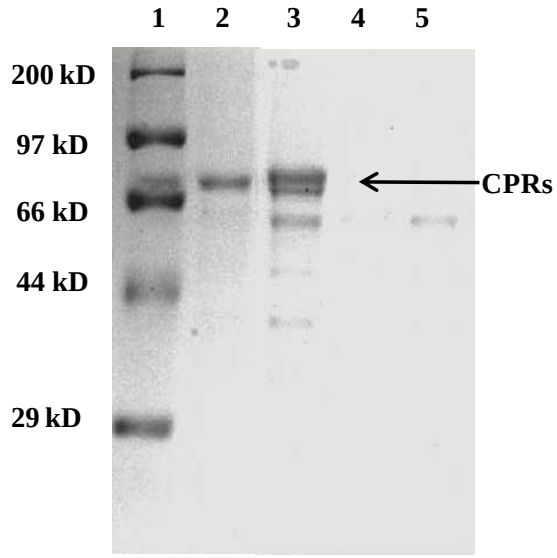

Figure 3.15 (A). Analysis of human CPRs expressed from insect cells on Coomassie-stained SDS-PAGE. 25 µg of microsomal proteins were loaded per lane on 10% SDS-PAGE. Gels were stained with Coomassie blue G-250. Lane 1, protein marker; Lane 2, ΔhRDM (expected MW, 76.257 kD); Lane 3, hRD (expected MW, 76.637 kD); Lane 4, ΔhRD (expected MW, 74.370 kD); Lane 5, negative control (proteins from cells infected with baculovirus encoding no foreign gene).

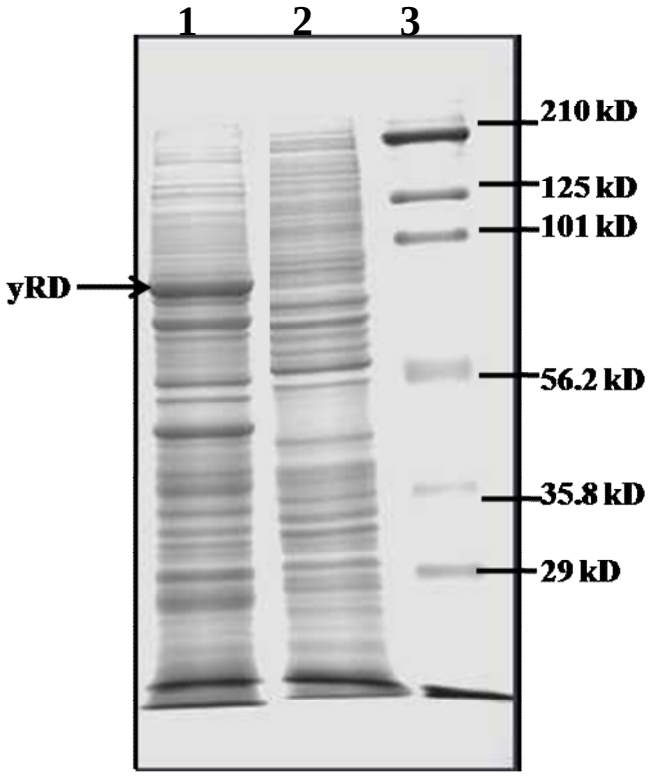

Figure 3.15 (B). Analysis of yRD protein expressed from insect cells on Coomassie-stained SDS-PAGE. 25 µg of microsomal proteins were loaded per lane on 10% SDS-PAGE. Gels were stained with Coomassie blue G-250. Lane 1, yRD (expected MW, 80.388 kD); Lane 2, negative control (proteins from cells infected with baculovirus encoding no foreign gene). Lane 3, protein marker

All the microsomal protein samples except yRD were further subjected to immunoblotting (antibodies to yRD are not commercially available). For Western blot analysis, microsomal samples (1.5µg/lane) were separated on 10% SDS-PAGE. The proteins were electro-transferred to Immobilon-P-membranes (Millipore) by the semi-dry transfer method. The membranes were blocked with 5% non-fat dry milk in PBS.

The blots were probed with 1:2000 dilution of mouse monoclonal antibody to CYP2D6 (BD-Gentest, Catalogue No A246), rabbit polyclonal antibody to human NADPH CYP450 reductase (Abcam, Catalogue No ab13513-50), and mouse monoclonal antibody to the *c*-myc epitope (9E10) (Santa Cruz Biotechnology, Catalogue No SC-40). The immune complexes were detected and visualized with 1:10,000 dilutions of secondary antibodies, anti-mouse IgG-HRP conjugate and goat anti-rabbit HRP conjugate. Bound horseradish peroxidase was detected by chemiluminescence with the luminol chemiluminescent substrate. Chemiluminescence was detected with Gel Doc™ (Bio-Rad). The complete experimental methods employed have been described in 'Materials and Methods'.

Immunoblotting for CPRs detected hRD and ΔhRDM but did not detect ΔhRD (Figure 3.16 A). Immunoblotting confirmed the findings of Coomassie staining which had shown that ΔhRD was also not present in the microsomes. In the Western blot performed with the *c*-myc antibody only ΔhRDM was detected since it is the only CPR species that contains the *c*-myc tag (Figure 3.16 B).

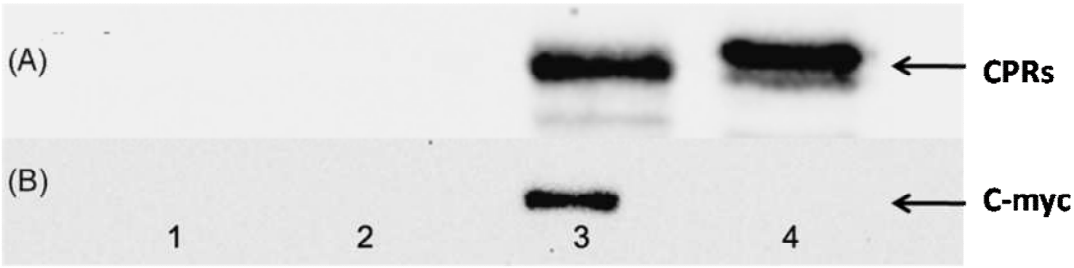

Figure 3.16. Western blot analyses of different CPR species expressed in insect cells. 1.5 μg of microsomal proteins were loaded per lane on 10% SDS-PAGE and immuno-

blotting was performed as described in 'Materials and Methods' (Section Number 2.4.6) by using antibodies to human CPR (A) and c-myc tag (B). Lane 1, Negative control; Lane 2, ΔhRD; Lane 3, ΔhRDM; Lane 4, hRD.

3.6 Localisation of ΔhRDM by confocal laser microscopy

In order to confirm the initial observation that ΔhRDM associates with microsomal (i.e. endoplasmic reticular, ER) membranes, its intracellular localisation was studied using confocal microscopy. Insect cells were infected either with BV-ΔhRDM alone or co-infected with BV-ΔhRDM and BV-CYP2D6. 24 h after infection, cells were prepared for confocal microscopy as described before (Atkins 1999) but with no lysozyme treatment. The cells were fixed using methanol and acetone treatment. Subsequently the cells were incubated with

(1) 1:200 dilution of a rabbit polyclonal IgG antibody to the *c*-myc epitope (9E10) which is conjugated to Alexafluor 647 (Santa Cruz sc789AF647) and

(2) 1:200 dilution of a monoclonal antibody (Santa Cruz sc-57963) to protein disulphide isomerase (PDI1) which is an ubiquitous ER membrane protein. A 1:1000 dilution of goat anti mouse IgG secondary antibody against PDI1 protein, conjugated to FITC (Santa Cruz sc2010) was used to demonstrate localisation of the house-keeping protein, PDI1, to the ER.

Confocal microscopy was performed on a Leica DMIRE2 microscope (Leica TCS SP2) with a 63X plan-apochromat objective (1.2 water). To detect Alexaflour and FITC fluorochromes Ar/HeN2 lasers were used at 488 and 543 nm respectively. No signal from one flourochrome could be detected on the other filter set under standard imaging

conditions (no cross-talk). Conditions were also standardized for the pinhole size, for gain and offset (contrast and brightness) and these were used for image capture. Each image was an average of 12 scans. For direct comparisons, image capture and background subtractions were done uniformly on all images. The confocal microscopic images of ΔhRDM, which co-localises with PDI1, to the microsomal (i.e. ER) membranes are portrayed in Figure 3.17.

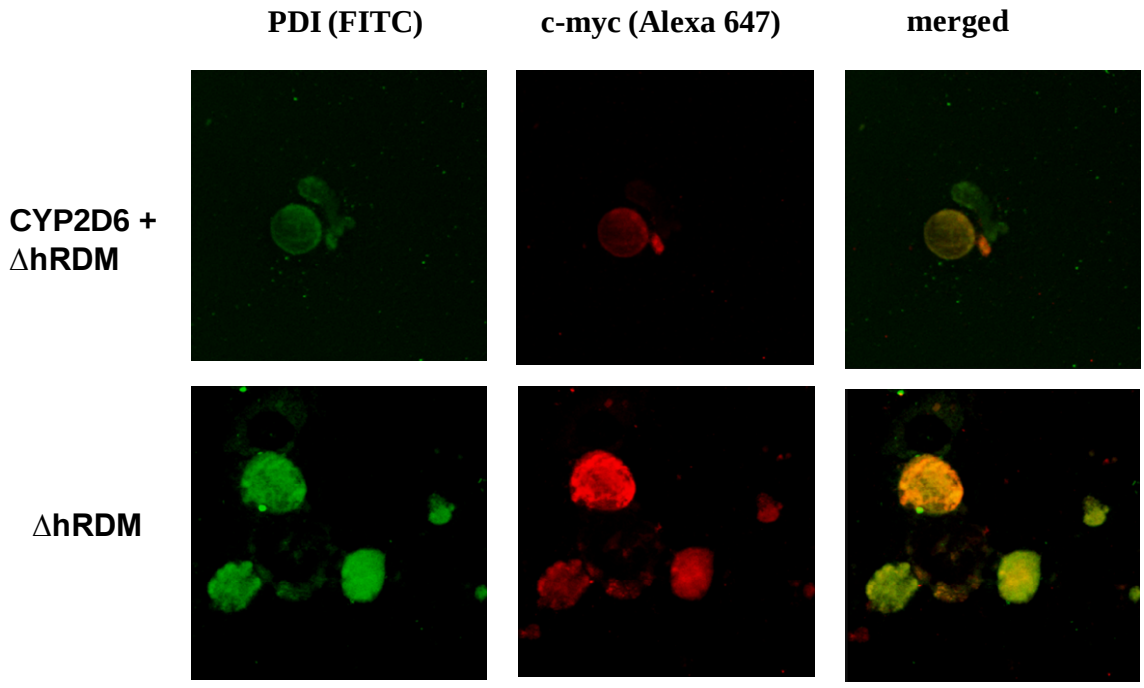

Figure 3.17. Confocal microscopy images confirming localization of ΔhRDM in recombinant baculovirus infected Sf9 cells. The cells were treated with primary antibodies for protein disulphide isomerase (PDI), an ER membrane protein, and *c*-myc antibody tagged with the fluorochrome, Alexafluor 647. The primary antibody to the PDI1 protein was counter-stained with a secondary antibody that is conjugated to the fluorochrome, FITC.

3.7 Reductase activities of hRD, ΔhRD and ΔhRDM in insect cell microsomes

CPR is an electron donor protein for CYP but the direct reduction of CYP is relatively difficult to assay. Therefore substrates like MTT or cytochrome *c*, which act as artificial electron acceptors, are widely used for determining CPR activity. The reduction of these substrates mirrors the reduction of CYPs.

In order to find out the reductase activities in microsomal samples, reductase assays were performed. Sf9 cells were infected with BV-hRD, BV-ΔhRD, BV-ΔhRDM and BV-yRD at an MOI of 1. The microsomes prepared after 63 h of infection with BV-CPRs were assayed for reductase activities using MTT as described in 'Materials and Methods' (Section Number 2.4.7). Reductase activity of yRD was highest among all the CPRs. ΔhRD reductase activity was equal to the cell control which was expected as the ΔhRD product does not anchor to (at least not present in) the microsomal membranes as revealed by Coomassie staining and Western blotting (see Section 3.5). The reductase activity of wild-type, native hRD was higher than ΔhRDM (Table 3.1).

Table 3.1. CPR activities as exhibited by different CPR species. Sf9 cells were infected with CPR baculoviruses and microsomes were prepared at 63 h. Reductase activity was measured by using MTT as described in 'Materials and Methods' (Section Number 2.4.7). The moles of MTT reduced per minute per mg of protein were calculated. Data are presented as mean values ± STDEV.

CPR Species	Reductase activity (nmole MTT reduced/min/mg protein)
Control	10.6 ± 2.1
ΔhRD	15.5 ± 1.7
ΔhRDM	1550.4 ± 187.2
hRD	2325.7 ± 154.7
yRD	2643.7 ± 251.2

3.8 CYP2D6 expression in insect cells

Following amplification and titration of CYP2D6 recombinant baculovirus (hereafter referred as BV-2D6), Sf9 cells were infected with BV-2D6 at an MOI of 1. Haemin and δ-amino laevulinic acid were added 24 h post-infection to compensate for low levels of haem in insect cells. The microsomes prepared after 63 h of infection with BV-2D6 were subjected to sodium dodecyl sulfate-polyacrylamide gel (SDS-PAGE)

electrophoresis. Twenty-five μg of the microsomal protein sample was separated on SDS-PAGE and the protein band was visualised by staining with Coomassie blue dye (Figure 3.18). Coomassie blue staining detected the expressed CYP2D6 protein. The image of the stained protein band on the gel was captured on Gel Doc™ (Bio-Rad). The detailed experimental method employed is provided in 'Materials and Methods'.

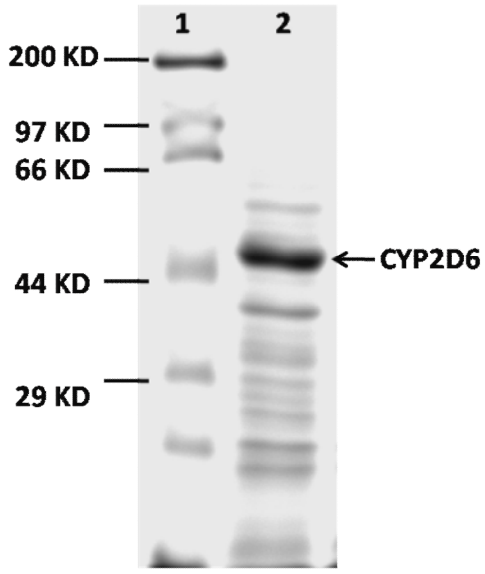

Figure 3.18. Coomassie staining of SDS-PAGE for CYP2D6 expressed in Sf9 cells. 25 μg of microsomal protein was separated on 10% SDS-PAGE. Gel was stained with Coomassie G-250 as described in 'Materials and Methods' (Section Number 2.4.5). Lane 1, Protein Marker; Lane 2, CYP2D6 expressed in Sf9 cells.

3.9 Optimization of CYP2D6 expression

In order to find out an optimum MOI for producing spectrally active CYP2D6, Sf9 cells were infected with BV-2D6 using a range of MOIs (from 1 x 10^{-1} pfu/cell to 4

pfu/cell). The microsomes were prepared after 63 h of infection and were subjected to CO-binding assay. The carbon monoxide (CO) binding assay is a method for quantifying the amount of CYP holoprotein in a microsomal preparation. The CO-assay gives the P450 enzyme family its name. The reduced haem moiety of CYP binds to carbon monoxide and exhibits maximum absorbance at 450 nm. The method detects the active haem-bound CYP holoprotein.

After determining protein concentrations using a modified Bradford method (Bio-Rad kit; Bradford 1976), CYP content in the microsomes was measured using a dual wavelength spectrophotometer as described in 'Materials and Methods' (Section Number 2.4.3). The spectral analysis was typical of P450 proteins. It was observed that infection with the lowest MOI of 0.1 pfu/cell resulted in a major peak at 450 nm and a very small peak at 420 nm (Figure 3.19). The peak at 420 nm is an indication of spectrally inactive CYP. Our results clearly indicate that using higher MOIs of BV-2D6 result in a gradual increase in the formation of inactive CYP2D6.

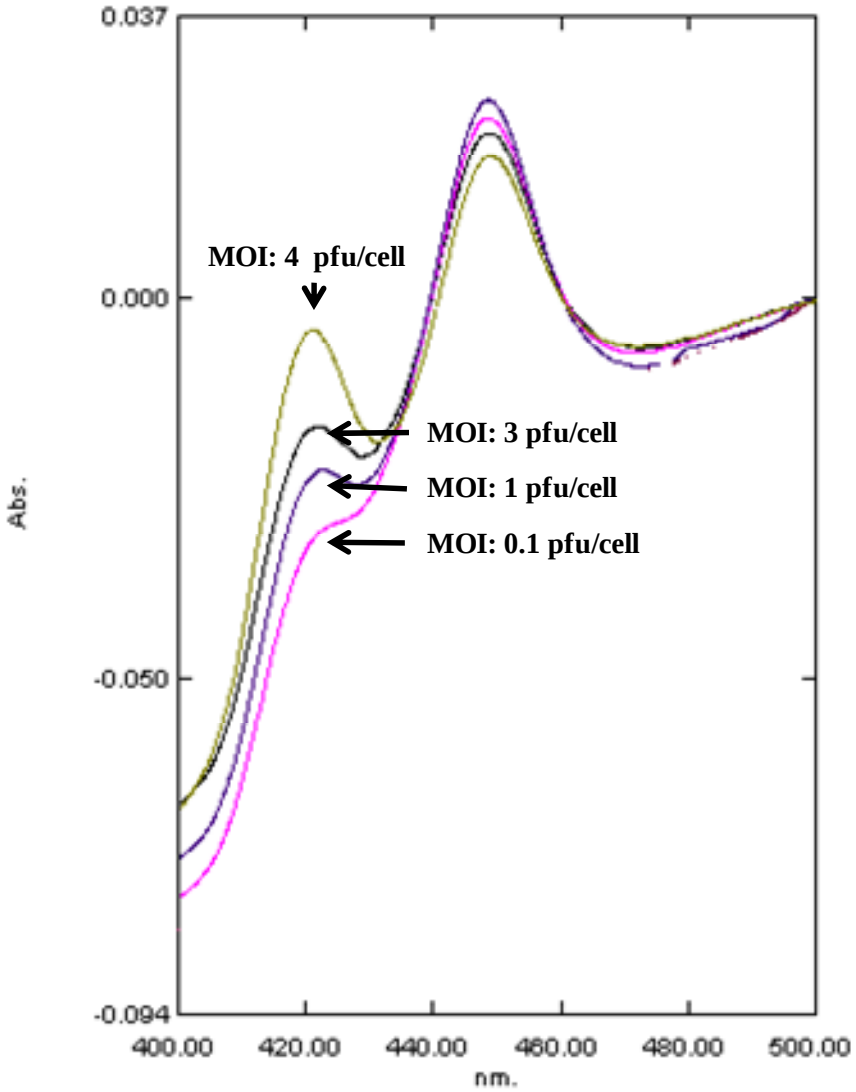

Figure 3.19. Optimization of CYP2D6 expression using different MOIs. Sf9 cells were infected with BV-2D6 using a range of MOIs (from 0.1 pfu/cell to 4 pfu/cell). The microsomes were prepared after 63 h of infection and were subjected to CO-binding assay as described in 'Materials and Methods' (Section Number 2.4.3).

3.10 Co-expression of CYP2D6 with the CPRs

After optimization of a particular BV-2D6 MOI that would allow a relatively high level of expression of spectrally active CYP2D6, the ability of different CPR species to transfer electrons to CYP2D6 and produce active enzymes was studied. Sf9 cells were infected with recombinant BV-2D6 alone at an MOI of 1 pfu/cell. In a second set of experiments, the cells were also co-infected with various BV-CPRs at an MOI that was 10-fold less (1×10^{-1} pfu/ cell) than the MOI used for BV-2D6 (MOI of 1 pfu/cell). The ratio of BV-2D6 to BV-CPR was maintained 10:1 in accordance with the published literature values (Chen et al. 1997). Haemin and δ-amino laevulinic acid were added 24 h post-infection to compensate for low levels of haem in insect cells as described in 'Materials and Methods'. Microsomes were prepared 63 h after infection and the total microsomal proteins were estimated by the Bradford method.

To confirm expression of recombinant proteins, microsomes obtained after infecting Sf9 cells with different baculovuruses were subjected to SDS-PAGE. Twenty-five μg of microsomal protein samples were separated on SDS-PAGE and protein bands were visualized by staining with Coomassie blue as described in 'Materials and Methods' (Section Number 2.4.5). Coomassie blue staining detected hRD, ΔhRDM and yRD proteins as well as the CYP2D6 protein (Figure 3.20).

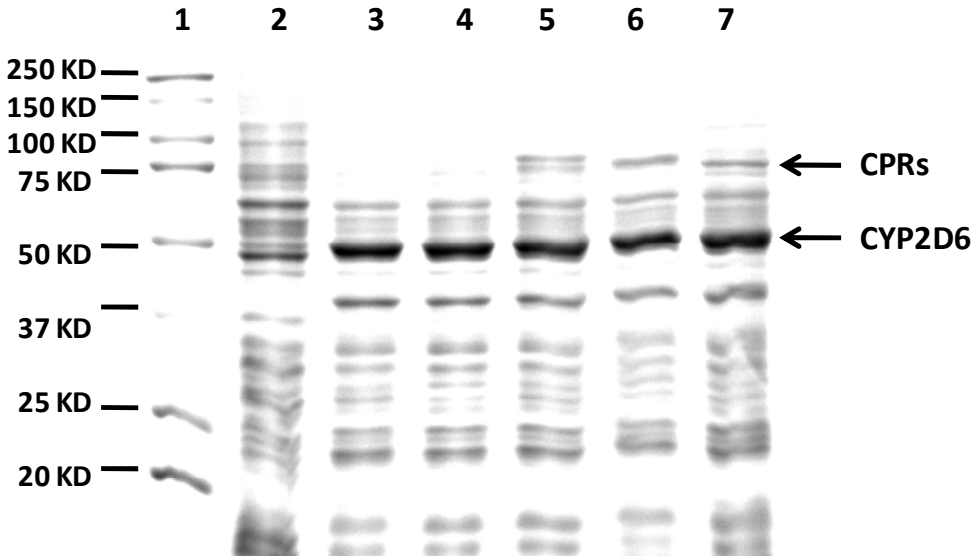

Figure 3.20. Coomassie staining of SDS-PAGE gels after subjecting Sf9 microsomal proteins that contain CYP2D6 and different CPRs to SDS-PAGE. 25 μg of microsomal proteins were separated per lane on 10% SDS-PAGE. Gels were stained with Coomassie G-250 as described in 'Materials and Methods' (Section Number 2.4.5). Lane 1, protein marker; Lane 2, control (microsomes that do not contain any recombinant proteins); Lane 3, CYP2D6 expressed alone; Lane 4, CYP2D6 co-expressed with ΔhRD; Lane 5, CYP2D6 co-expressed with hRD; Lane 6, CYP2D6 co-expressed with ΔhRDM; Lane 7, CYP2D6 co-expressed with yRD.

3.10.1 Amounts of CYP2D6 in microsomes where CPRs are co-expressed

The CYP2D6 holoprotein content was measured using CO-difference spectrophotometric analysis. The spectra were typical of spectrally active P450 proteins with a large peak at 450 nm and a very small peak at 420 nm (Figure 3.21). The

CYP2D6 spectral content was highest when it was expressed alone. A decrease in CYP2D6 content was observed when CYP2D6 was co-expressed with different CPRs. It appeared that the decrease in the content of spectrally active CYP2D6 is not of the same magnitude – the decrease seemed to depend on the specific CPR that is co-expressed (Table 3.2). It was observed from the spectral content that co-expression of yRD resulted in the lowest yield of CYP2D6. In comparison with native human CPR and its variants, yRD is found to be most destructive to the CYP. ΔhRD co-expression with CYP2D6 yielded the highest CYP content amongst all co-expressions. It is noteworthy that ΔhRD is absent in microsomal membranes and therefore may not contribute at all to the destruction of the microsome-bound CYP. Surprisingly, the CYP content in hRD co-expressed microsomes was ~20% lower than the CYP2D6 content in ΔhRDM co-expressed microsomes indicating that the variant human CPR, ΔhRDM, is less toxic to the CYP than wild-type hRD.

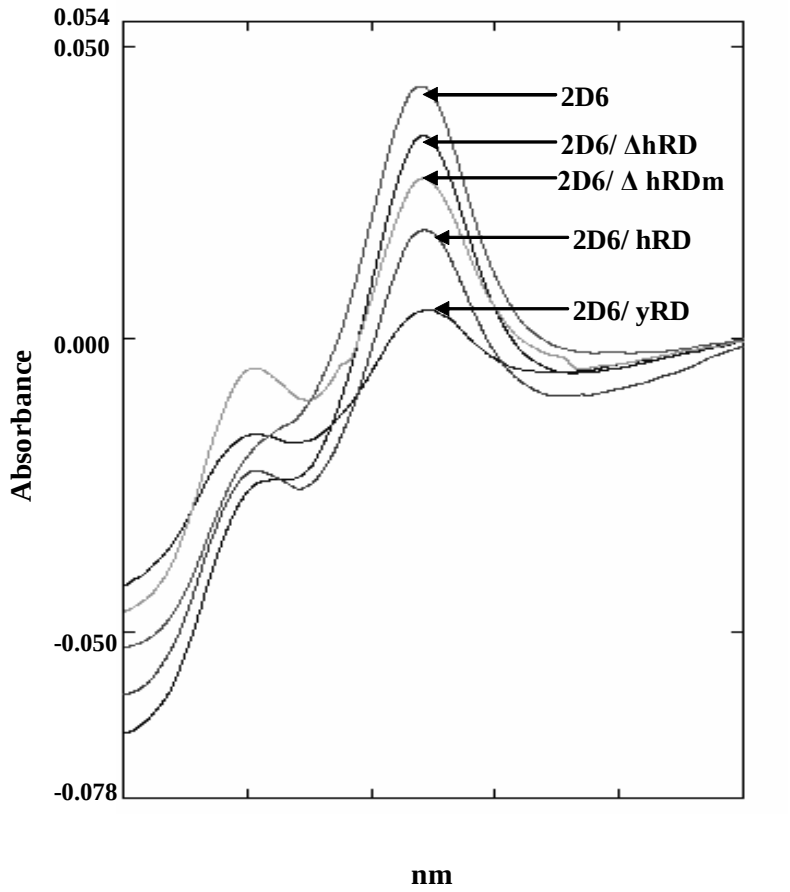

Figure 3.21. Reduced carbon monoxide difference spectra of CYP2D6 co-expressed with different CPRs. Sf9 cells were infected with BV-2D6 at an MOI of 1 pfu/cell and with BV-CPRs at an MOI of 0.1 pfu/cell. The cells were harvested at 63 h, microsomes were prepared and CYP content was measured using CO-difference spectra.

Table 3.2: Specific CYP2D6 content in microsomal samples where CYP2D6 was co-expressed with CPRs. CYP2D6 content was determined using CO-difference spectroscopy as described in 'Materials and Methods' (Section Number 2.4.3) and as depicted in Figure 3.21. Sf9 cells were co-infected with BV-2D6 at an MOI of 1 pfu/cell and with BV-CPRs at an MOI of 0.1, and microsomes were prepared at 63 h post-infection.

Microsome Samples	**CYP Content (pmol/mg protein)**
CYP2D6	513.6 ± 16.9
CYP2D6 + ΔhRD	479.0 ± 13.7
CYP2D6 + ΔhRDM	361.4 ± 15.0
CYP2D6 + hRD	300.4 ± 11.5
CYP2D6 + yRD	107.5 ± 7.9

Western blotting was performed to confirm the presence of the CYP isozyme, CYP2D6, in microsomal samples that co-express CYP2D6 and CPR. 1.5 μg of microsomal protein was separated on 10% SDS-PAGE and immuno-blotting was performed as described in 'Materials and Methods' (Section Number 2.4.6) by using antibodies specific to human CYP2D6. The blots were probed overnight with 1:2,000

dilution of mouse monoclonal antibody to CYP2D6 (BD-Gentest, Catalogue No A246) followed by incubation with 1:10,000 dilution of secondary antibody-Anti-mouse IgG-HRP conjugate. The blots were developed using luminol chemiluminescent substrate. The Western blot detected the CYP2D6 protein bands in all the microsomes that co-express CYP2D6 and a CPR (Figure 3.22). The band intensities were measured by means of densitometry on Bio-Rad's Quantity One software. The sharp decrease in spectrally active CYP2D6 in CPR co-expressed microsomes observed in reduced CO difference spectra is not observed on the Western blot where band intensities, as measured by densitometry, were not significantly different (Table 3.3). This means that apoprotein levels are not drastically affected. There is a slight difference between the CYP2D6 alone expressed band and the co-expressed CYP2D6 band intensities but this was not mirrored in the reduced CO-difference spectra. These results indicate that CPRs generally do not down-regulate or modulate CYP expression levels but are responsible specifically for the destruction of CYP2D6 holoenzyme (spectrally active enzyme). The destruction of CYP2D6 could be a result of CPR-initiated oxidative damage of microsomal proteins.

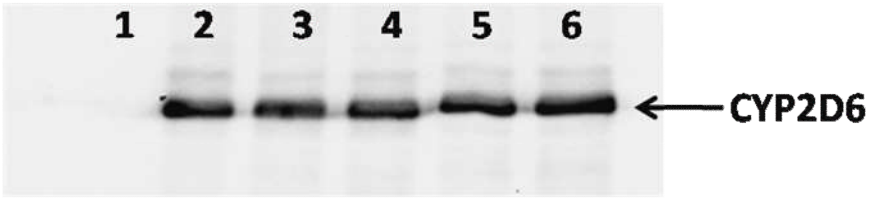

Figure 3.22. Comparison of the levels of CYP2D6 co-expressed with different CPR species in Sf9 insect cells, via Western blotting. 1.5 μg of microsomal proteins were loaded per lane on 10% SDS-PAGE and immuno-blotting was performed as described

in ‘Materials and Methods’ (Section Number 2.4.6) using antibody specific to human CYP2D6. Lane 1, control (microsomes from uninfected Sf9 cells); Lane 2, CYP2D6 co-expressed with yRD; Lane 3, CYP2D6 co-expressed with ΔhRDM; Lane 4, CYP2D6 co-expressed with hRD; Lane 5, CYP2D6 co-expressed with ΔhRD; Lane 6, CYP2D6 expressed alone without any CPR.

Table 3.3 The intensities of the CYP2D6 protein bands in the image shown in Figure 3.22 were measured by means of densitometry using Bio-Rad’s Quantity One software. The densities were measured at 6 different points on each protein band and the average values are presented as mean values ± STDEV.

Samples	**Average intensities**	**% of CYP2D6 alone**
CYP2D6	887 ± 116	100%
CYP2D6 + ΔhRD	853 ± 81	97%
CYP2D6 + ΔhRDM	738 ± 29	85%
CYP2D6 + hRD	773 ± 78	88%
CYP2D6 + yRD	805 ± 73	91%

3.10.2 CPR activities in microsomal samples which co-express CYP2D6

In order to find out the reductase activities in microsomal samples that co-express CYP2D6, reductase assays were performed as described in 'Materials and Methods' (Section Number 2.4.7) using both MTT and cytochrome *c*, as substrates. Reductase activity of yRD was highest amongst all the CPRs (Table 3.4). ΔhRD reductase activity was equal to control which was expected as the ΔhRD product does not anchor to microsomal membranes as revealed by Coomassie staining and Western blotting (see Section 3.5). The reductase activity of hRD is higher than ΔhRDM. However as seen earlier in the CO-difference spectra (Section 3.10.1), the strongest CPR, (yRD), results in the lowest yield of spectrally active CYP2D6. The second strongest CPR, (hRD), also results in a lower yield of spectrally active CYP2D6. Amongst all the CPRs studied, ΔhRDM appears to yield the highest content of spectrally active CYP2D6.

Table 3.4. Activities of NADPH-Cytochrome P450 reductase (CPR) exhibited by different CPR species when co-expressed with CYP2D6. Sf9 cells were co-infected with BV-2D6 and BV-CPRs and microsomes were prepared at 63 h. Reductase activities were measured by using MTT and cytochrome *c* as described in 'Materials and Methods' (Section Number 2.4.7). The moles of MTT and cytochrome *c* reduced per minute per mg of protein were calculated. Uninfected Sf9 cells were used as'Control'.

CPR	CPR Activity (nmol MTT reduced/min/mg protein)	CPR Activity (nmol cyt-*c* reduced/min/mg protein)
ΔhRD	21.2 ± 2.4	26.0 ± 1.6
ΔhRDM	308 ± 23.8	383.7 ± 27.2
hRD	425 ± 31.1	579.6 ± 51.7
yRD	584 ± 45.3	608.2 ± 68
Control	21.2 ± 1.1	24.1 ± 1.3

3.11 Measurement of reactive oxygen species

We speculated that the destruction of CYP2D6 holoenzyme by CPR could be a result of oxidative damage triggered by CPR. Therefore, to further investigate the reason behind this destruction, two parallel assays were set up to measure reactive oxygen species (ROS) in cells infected with BV-CPRs. ROS was measured using H_2DCFDA and Dihydrorhodamine-123 as substrates. As ΔhRD does not anchor to microsomal membranes, it was not studied any further.

Sf9 cells were infected with a range of MOIs (0.2 to 4.0 pfu/ml) of different BV-CPRs species for 72 h. At 72 h, the assay was performed as described in 'Materials and Methods' (Section Number 2.4.10). Percentage induction of ROS over control was calculated in baculovirus infected cells. The results obtained were in line with the results presented in Tables 3.2 and 3.4. The reductases, hRD and yRD, which are stronger than ΔhRDM (in terms of MTT and cytochrome *c* reduction) exhibited stronger induction of ROS in comparison with ΔhRDM (Figures 3.23 and 3.24).

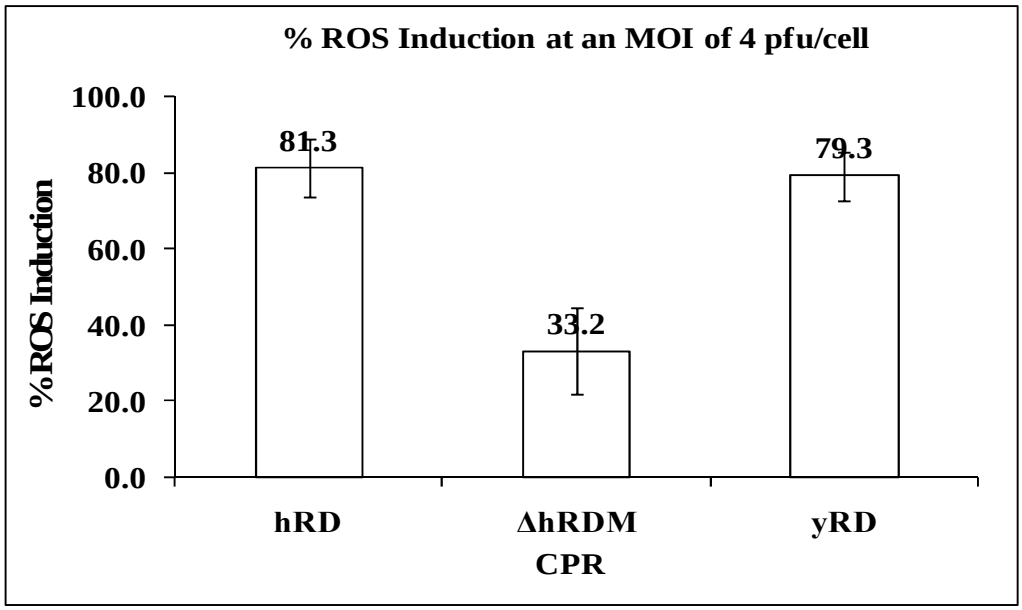

Figure 3.23. The ROS produced by different CPR species, as measured via the H_2DCFDA assay. ROS was measured using the H_2DCFDA dye as substrate. Sf9 cells were infected with a range of MOIs (0.2 to 4.0 pfu/ml) of different CPR species for 72 h. At 72 h, the H_2DCFDA assay was performed as described in 'Materials and Methods' (Section Number 2.4.10). The oxidation of intracellular non-fluorescent H_2DCF to highly fluorescent DCF was measured on a fluorometer. Blank values, indicating the fluorescence of the dye in PBS were subtracted from all the samples. Percentage induction over control was calculated in baculovirus infected cells.

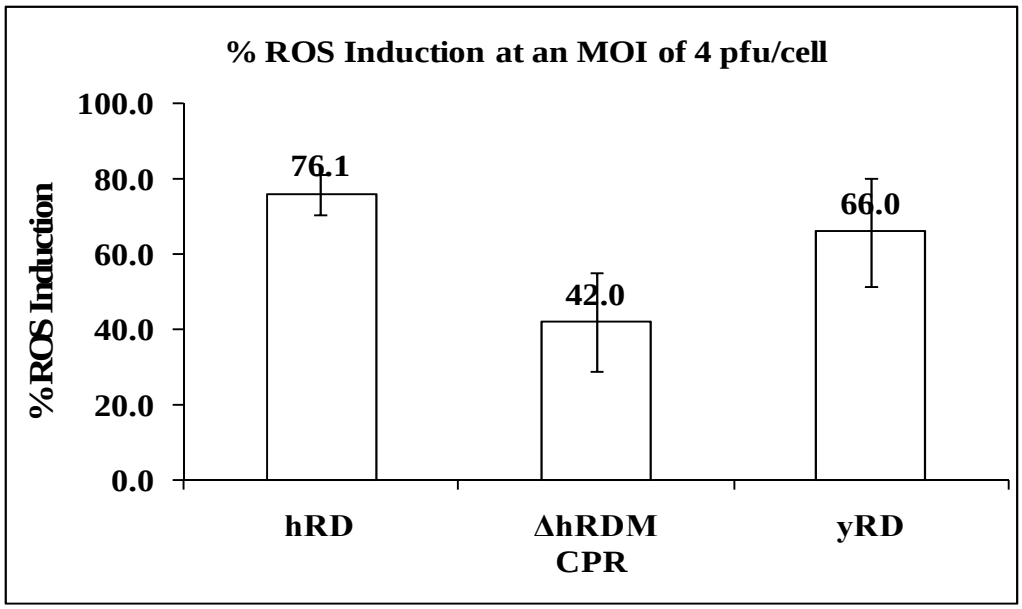

Figure 3.24. The ROS produced by different CPR species, as measured via the Dihydrorhodamine-123 assay. Sf9 cells were infected with a range of MOIs (0.2 to 4.0 pfu/ml) of different reductase species for 72 h. At 72 h, the Dihydrorhodamine-123 assay was performed as described in 'Materials and Methods' (Section Number 2.4.10). The oxidation of Dihydrorhodamine-123 to highly fluorescent rhodamine was measured on a fluorometer. Blank values, indicating the fluorescence of the dye in PBS were subtracted from all the samples. Percentage induction over control was calculated in baculovirus infected cells.

3.12 CYP2D6 enzymatic activities in the presence of CPRs

To compare the catalytic activity of recombinant CYP2D6 in microsomes that co-express CPRs, enzyme assays were performed using fluorogenic substrates. These involved kinetic analyses of CYP2D6 microsomes and were performed using three

different substrates, EOMCC, AMMC and CEC, as described below. 1.5 pmol of CYP2D6 was used per reaction and each reaction was performed in replicates. Kinetic progression of reactions was measured up to a period of 30 min.

3.12.1 EOMCC Assay

Kinetic studies with CYP2D6 microsomes (i.e. measurement of activities) were performed using the Vivid® fluorogenic substrate EOMCC (3-cyano-7-(ethoxymethoxy) coumarin) as per the standard Invitrogen Screening Kit protocol (Marks et al. 2002 and 2003). EOMCC is demethylated by human CYP2D6 to the fluorescent product 3-cyano-7-hydroxycoumarin (CHC). The reactions were carried out in a reaction volume of 100 µl/ well in 96-well black plates (Fisher Scientific, Catalogue No FB85083). The reaction was carried out at 37ºC in 100 mM potassium phosphate buffer pH 8.0, containing 10 µM EOMCC, 1.5 pmol CYP2D6 and the NADPH regenerating system (1.3 mM NADP+, 3.3 mM glucose-6-phosphate, 3.3 mM $MgCl_2$, 0.4U/ml glucose-6-phosphate dehydrogenase). The fluorescent values were recorded on the Biotek Synergy HT plate reader using an excitation wavelength of 400 nm (20 nm) and emission wavelength of 460 nm (40 nm). Changes in fluorescence were measured as relative fluorescence units (RFU). Kinetic progression of reactions was measured for 30 min (Figure 3.25 (B) and Table 3.5). Concentration of product formed was determined using CHC as a standard.

The standard curve of CHC was prepared using a range of concentrations of

CHC (0, 39.1, 78.1, 156.3, 312.5, 625, 1250 pmol/ ml). The assay for the standard was performed in 96-well black plates. The fluorescent values (RFU) were recorded on the Biotek Synergy HT plate reader using an excitation wavelength of 400 nm (20 nm) and emission wavelength of 460 nm (40 nm). Standard curve was plotted and used to convert the RFU measured with test samples to CHC concentrations. The standard curve is shown in Figure 3.25 (A).

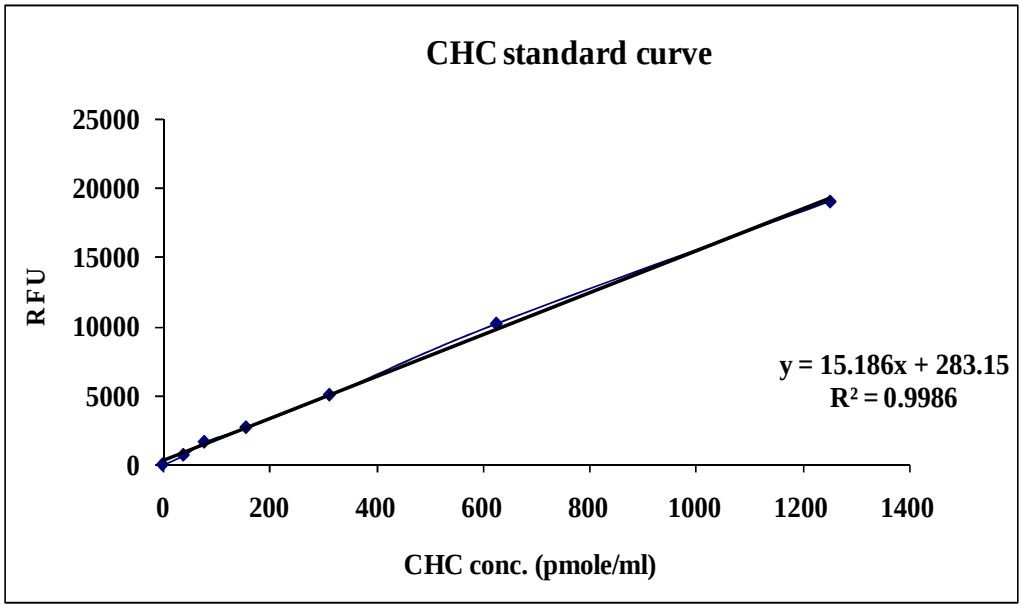

Figure 3.25 (A). CHC standard curve. The curve was plotted as described in Section 3.12.1.

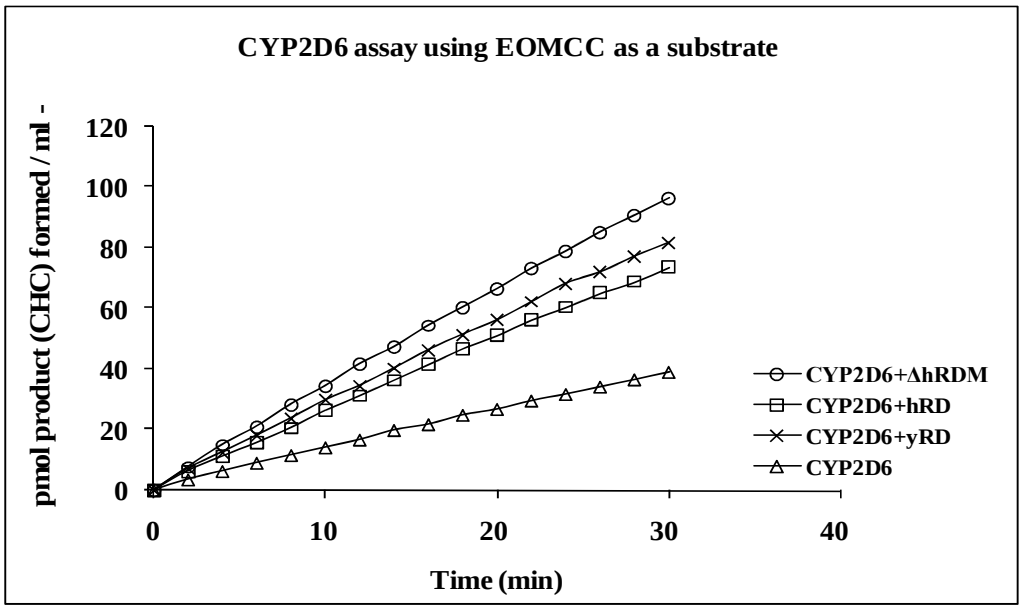

Figure 3.25 (B). Comparative kinetic analyses of CYP2D6 co-expressed with different CPRs, using EOMCC as a substrate. Sf9 cells were co-infected with CYP2D6 and different CPR species at an MOI of 1 and 0.1 pfu/ cells respectively. The activity of CYP2D6 co-expressed with various CPR species was measured using microsomes prepared at 63 h after baculovirus infection. EOMCC assay was performed as described in Section 3.12.1.

Table 3.5. CYP2D6 enzyme reaction rates in co-expressed microsomes, as tabulated from Figure 3.25 (B). Sf9 cells were co-infected with CYP2D6 and the CPR baculoviruses at an MOI of 1 and 0.1 pfu/ cell, respectively. The reaction rates were measured in microsomes prepared at 63h post-infection. EOMCC assay was performed as described in Section 3.12.1.

Microsomes	CYP2D6 reaction rates (pmole CHC formed/ min/ pmole of CYP2D6)
CYP2D6	0.08568
CYP2D6+hRD	0.16388
CYP2D6+ΔhRDM	0.21359
CYP2D6+yRD	0.18182

3.12.2 AMMC Assay

CYP2D6 microsomal activity was also measured using the 3-[2-(N,N-diethyl-N-methylammonium)ethyl]-7-methoxy-4-methylcoumarin (AMMC) fluorogenic substrate (Chauret et al, 2001). AMMC is demethylated by human CYP2D6 to the fluorescent product 3-[2-(N,N-diethyl-N-methylammonium)ethyl]-7-hydroxy-4-methylcoumarin (AHMC). The reactions were carried out in a reaction volume of 100 µl/ well in 96-well black plates (Fisher Scientific, Catalogue No FB85083). The reaction was carried

out at 37ºC in 100 mM potassium phosphate buffer pH 8.0, containing 1.5 μM AMMC, 1.5 pmol CYP2D6 and the NADPH regenerating system (1.3 mM NADP+, 3.3 mM glucose-6-phosphate, 3.3 mM $MgCl_2$, 0.4U/ml glucose-6-phosphate dehydrogenase). The fluorescent values were recorded on the Biotek Synergy HT plate reader using an excitation wavelength of 400 nm (20 nm) and emission wavelength of 460 nm (40 nm). Changes in fluorescence were measured as relative fluorescence units (RFU). Kinetic progression of reactions was measured for 30 min (Figure 3.26 (B) and Table 3.6).

The standard curve of AHMC was prepared using a range of concentrations of AHMC (0, 0.914, 8.222, 24.667, 74.0, 222.0, 666.0 pmol/ ml). The assay for the standard was performed in 96-well black plates. The fluorescent values (RFU) were recorded on the Biotek Synergy HT plate reader using an excitation wavelength of 400 nm (20 nm) and emission wavelength of 460 nm (40 nm). Standard curve was plotted and AHMC concentrations in test samples were measured using the equation from the standard curve. The standard curve is shown in Figure 3.26 (A).

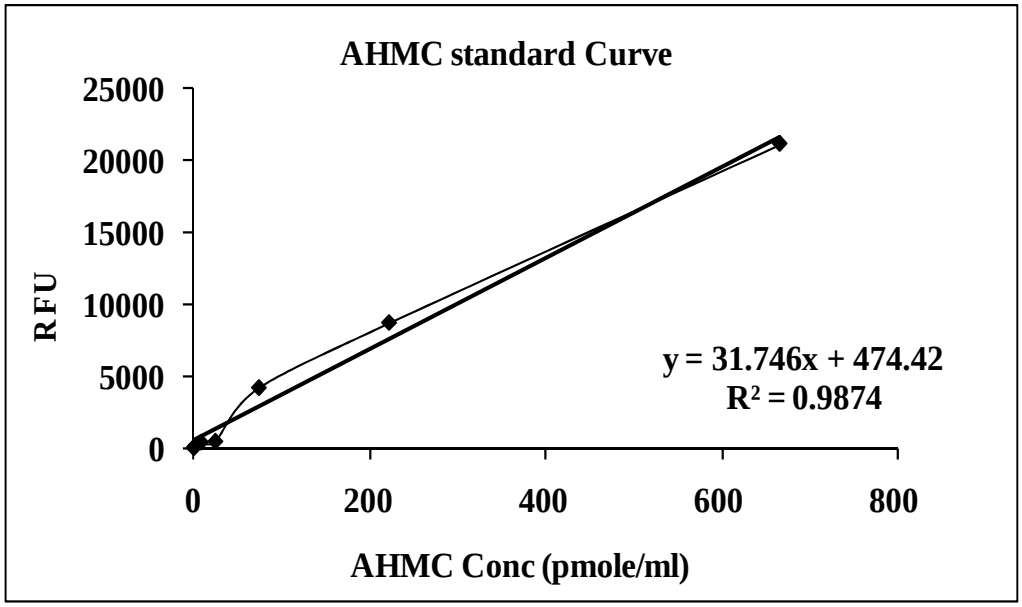

Figure 3.26 (A). AHMC standard curve. The curve was plotted as described in Section 3.12.2.

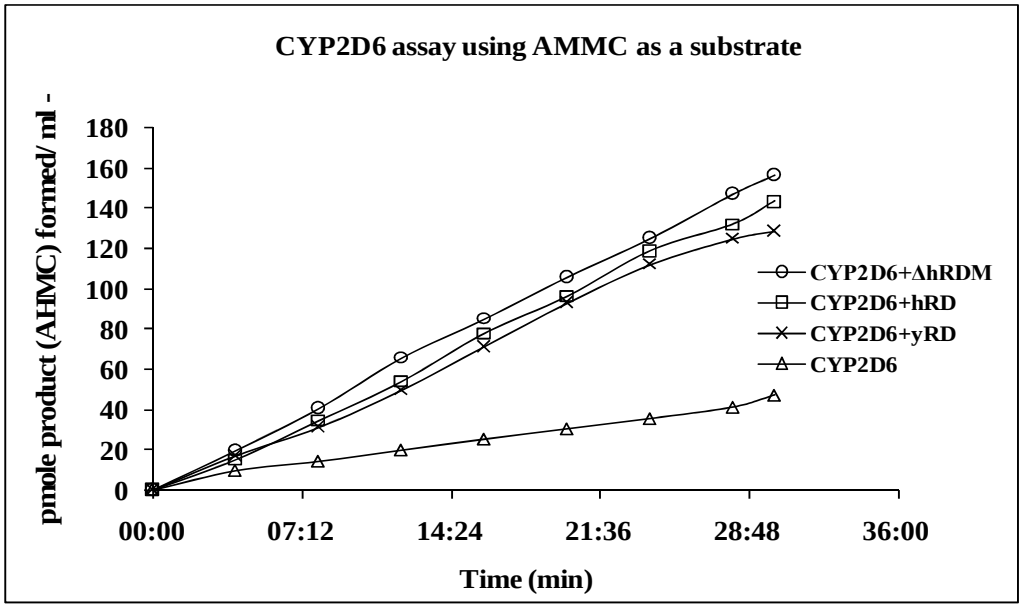

Figure 3.26 (B). Comparative kinetic analyses of CYP2D6 co-expressed with different CPRs, using AMMC as a substrate. Sf9 cells were co-infected with CYP2D6 and different CPR species at an MOI of 1 and 0.1 pfu/cell, respectively. The activity of

CYP2D6 expressed with various CPR species was measured using microsomes from cells infected with baculoviruses for 63 h. AMMC assay was performed as described in Section 3.12.2.

Table 3.6. CYP2D6 enzyme reaction rates in co-expressed microsomes, as tabulated from Figure 3.26 (B). Sf9 cells were co-infected with CYP2D6 and the CPR baculoviruses at an MOI of 1 and 0.1 pfu/ cell, respectively. The reaction rates were measured in microsomes prepared at 63h post-infection. AMMC assay was performed as described in Section 3.12.2.

Microsomes	CYP2D6 reaction rates (pmole AHMC formed/ min/ pmole of CYP2D6)
CYP2D6	0.09648
CYP2D6+hRD	0.32711
CYP2D6+ΔhRDM	0.35025
CYP2D6+yRD	0.30078

3.12.3 CEC Assay

CYP2D6 activity was measured using one more fluorogenic substrate, 3-cyano-7-ethoxycoumarin (CEC). CEC is metabolised mainly by CYP2C19 and CYP1A2 to a fluorescent product 3-cyano-7-hydroxycoumarin (CHC) (Yamamoto et al. 2003). However CEC is also metabolised by CYP2D6, though not specific for this CYP isozyme. The reactions were carried out in a reaction volume of 100 µl/ well in 96-well black plates (Fisher Scientific, Catalogue No FB85083). The reaction was carried out at 37ºC in 100 mM potassium phosphate buffer pH 7.4, containing 50 µM CEC, 1.5 pmol CYP2D6 and the NADPH regenerating system (1.3 mM NADP+, 3.3 mM glucose-6-phosphate, 3.3 mM $MgCl_2$, 0.4U/ml glucose-6-phosphate dehydrogenase). The fluorescent values were recorded on the Biotek Synergy HT plate reader using an excitation wavelength of 400 nm (20 nm) and emission wavelength of 460 nm (40 nm). Changes in fluorescence were measured as relative fluorescence units (RFU). Kinetic progression of reactions was measured for 30 min (Figure 3.27 and Table 3.7).

Standard curve was plotted and CHC concentrations in test samples were measured using the equation from the standard curve. The standard curve is shown in Figure 3.25 (A).

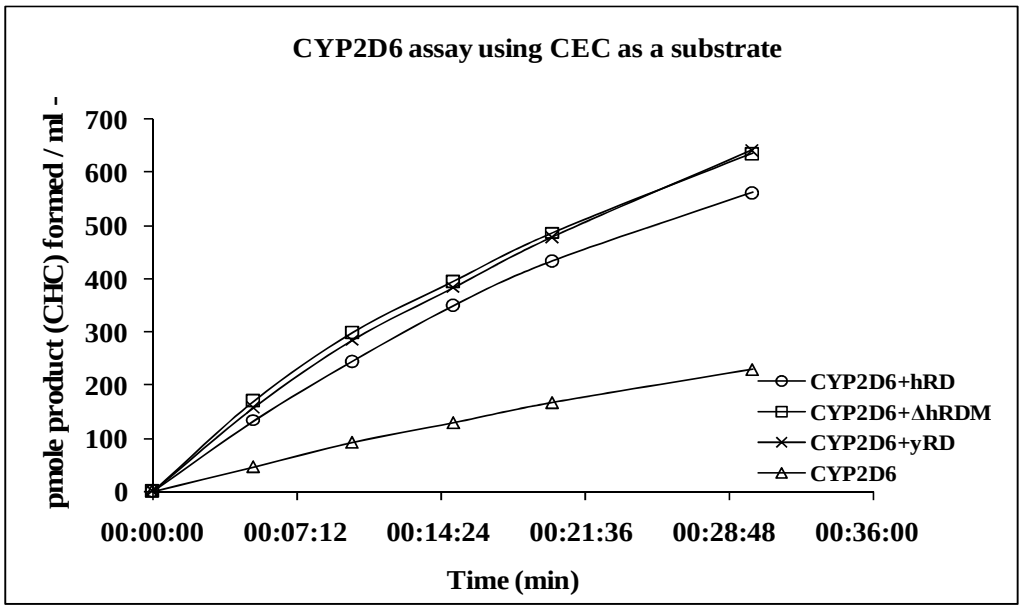

Figure 3.27: Comparative kinetic analyses of CYP2D6 co-expressed with different CPRs using CEC as a substrate. Sf9 cells were co-infected with CYP2D6 and different CPRs. The activity of CYP2D6 expressed with various CPR species was measured using microsomes from cells infected with baculoviruses for 63 h. CEC assay was performed as described in Section 3.12.3.

Table 3.7. CYP2D6 enzyme reaction rates in co-expressed microsomes, as tabulated from Figure 3.27. Sf9 cells were co-infected with CYP2D6 and the CPR baculoviruses at an MOI of 1 and 0.1 pfu/ cell, respectively. The reaction rates were measured in microsomes prepared at 63h post-infection. CEC assay was performed as described in Section 3.12.3.

Microsomes	CYP2D6 reaction rates (pmole CHC formed/ min/ pmole of CYP2D6)
CYP2D6	0.50897
CYP2D6+hRD	1.2472
CYP2D6+ΔhRDM	1.38
CYP2D6+yRD	1.3998

3.12.4 LC MS analysis of dextromethorphan O-demethylase activity of CYP2D6

The ability of the CYP2D6 co-expressed with hRD, ΔhRD and ΔhRDM to metabolise dextromethorphan, via its dextromethorphan O-demethylase activity, was studied using the assay described below.

Dextromethorphan O-demethylase activity was studied according to the method of Walsky and Obach (2004) with minor modifications. Dextromethorphan O-demethylase activity was measured in a 100 µl reaction mixture which contained 3.0 pmole of CYP2D6 co-expressed with various reductases, NADPH regenerating system (3.6 mM $NADP^+$, 6.6 mM glucose-6-phosphate, 6.6 mM magnesium chloride, 0.8U of glucose-6-phosphate dehydrogenase) and a range of concentrations of dextromethorphan (0.25 µM to 4.0 µM). This mixture was incubated at 37ºC for 20 min. At the end of this time point, the reaction was stopped by vigorous mixing with 100 µl of 0.05% formic acid in acetonitrile and incubation on ice for 10 min. The precipitated proteins were removed by centrifugation at 13,000X g.

Analysis of the resulting supernatants was carried out on an Agilent LC/MS single Quadrupole mass spectrophotometer equipped with an APCI/ESI multimode ionisation source. 20 µl of the supernatant was loaded for each run on an Agilent Eclipse XDB Zorbax C18 column. A 17 min linear gradient elution at a flow rate of 1.0 ml/min, using solvent A (0.05% formic acid) and solvent B (0.05% formic acid in acetonitrile), was used to detect dextrorphan (the metabolite) and dextromethorphan (the substrate). All assays were carried out in triplicate. The parameters of enzyme kinetics (Km, Vmax and efficiency of catalysis) were calculated using Graphpad Prism version 3.02 (2000).

CYP2D6 alone and CYP2D6 + ΔhRD co-expressed microsomes showed lack of ability to metabolise detromethorphan. This is justified as the presence of the electron

donor protein, CPR, is essential for CYP catalytic activity. The absence of ΔhRD on the microsomes could explain the results observed. In comparison to CYP2D6 + hRD co-expressed microsomes, the CYP2D6+ ΔhRDM has increased enzyme activity as seen by increased Vmax and thereby overall efficiency of catalysis (Table 3.8). No significant changes were observed in the Km values stating that the affinity for the substrate towards CYP2D6 holoenzyme has not changed but the higher coupling efficiency of ΔhRDM has resulted in increased Vmax thereby the quadrupling of the efficiency of catalysis.

Table 3.8. Efficiency of CYP2D6 enzyme mediated catalysis of dextromethorphan. CYP2D6 was co-expressed with hRD and ΔhRDM in Sf9 cells and the ability of the respective microsomes to metabolise dextromethorphan to dextrorphan was determined using procedures described in Section 3.12.4. Efficiency of catalysis was calculated using the ratio, Vmax/Km.

Microsome	**Vmax (pmol/min/ pmol CYP2D6)**	**Km (μM)**	**Vmax/Km(μl/min/pmol CYP2D6)**
CYP2D6	0	0	0
CYP2D6+ΔhRD	0	0	0
CYP2D6+hRD	0.764 ± 0.017	1.303 ± 0.489	0.586
CYP2D6+ΔhRDM	4.026 ± 0.279	1.436 ± 0.239	2.803

The enzyme assays in this Section clearly show that CYP2D6 activity is significantly higher in microsomes where CPR is co-expressed as compared to the microsomes where CYP2D6 is expressed alone. However there is a great deal of difference amongst samples that co-express the CYP and the different CPRs, as enumerated below.

1. Since the holoprotein content of CYP2D6 is very low when co-expressed with yRD, significantly more protein is needed to achieve 1.5 pmol enzyme concentrations in the reactions that are used for enzyme activities.
2. The reductase activity of the yeast CPR, yRD, is very strong but unfortunately it does not couple well with the human CYP2D6 (i.e. it provides poor CYP2D6 activity).
3. Although the reductase activity of the human CPR variant, ΔhRDM, is much lower than the human CPR (hRD) and the yeast CPR (yRD) as determined by MTT and cytochrome *c* assays, the reaction rates of CYP2D6 are supported better by ΔhRDM than the two more powerful reductases, hRD and yRD (Figures 3.25, 3.26, 3.27 and Table 3.8).

The only explanation for these results is that ΔhRDM is far more efficient in activating CYP2D6 than hRD and yRD.

3.13 Coupling efficiency of hRD, ΔhRDM and yRD with CYP2D6

The CPR activity of ΔhRDM, as measured by the MTT assay, in microsomes that co-express CYP2D6 and ΔhRDM is lower than the CPR activity in microsomes

that co-express CYP2D6 and hRD or yRD. Yet, our results indicate that ΔhRDM has a higher potential to activate CYP2D6 enzymatic reactions. To further highlight the property of this variant human CPR molecule, the coupling ability of ΔhRDM was determined in terms of percentage relative coupling efficiency.

Percentage coupling efficiency was calculated by dividing CYP activity in the EOMCC assay by CPR activity in the MTT assay. The coupling efficiency of the different CPRs was tabulated in comparison with ΔhRDM (ΔhRDM activity being considered as 100%; Figure 3.28). The coupling efficiency values clearly show that ΔhRDM couples better with CYP2D6 than the native, wild-type form of hRD. The lower levels of ROS induction by ΔhRDM (Figures 3.23 and 3.24) provide a valid reason for its higher coupling efficiency.

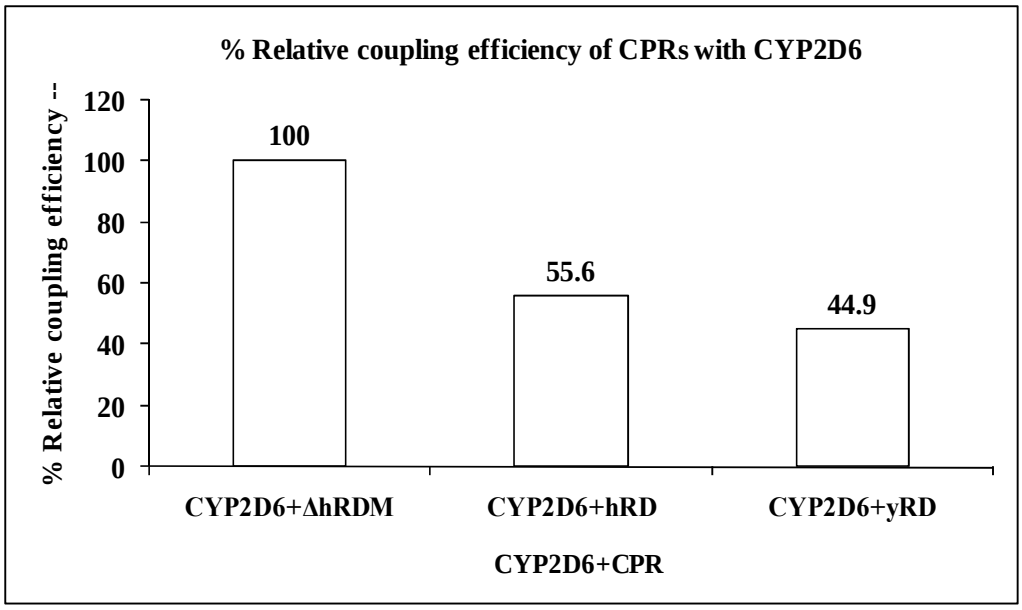

Figure 3.28. Percentage relative coupling efficiencies of different CPRs with CYP2D6 were calculated in comparison with ΔhRDM using microsomes that were prepared from Sf9 cells after 63 h of baculovirus infection. The product formed (CHC) from the EOMCC assay and CPR activity measured in the MTT assay were used for the calculations. CYP2D6 activity was divided by CPR activity and percentage relative coupling efficiency was determined.

3.14 Augmentation of CYP2D6 activity by changing the reductase ratios

Since ΔhRDM shows clear superiority over the two reductases hRD and yRD (being less destructive to the CYP2D6 holoprotein and having better reaction rates), we thought of increasing the ΔhRDM amounts during co-expression with CYP2D6.

Sf9 cells were seeded and infected in T75 flasks with BV-CYP2D6 and BV-ΔhRDM as described in 'Materials and Methods'. For co-infection, Sf9 cells were infected with BV-CYP2D6 with an MOI of 1.0 pfu/cell and with BV-CPR at two different MOIs of 1×10^{-1} pfu/cell (CYP2D6 to CPR ratio: 10:1) and 2×10^{-1} pfu/cell (CYP2D6 to CPR ratio: 5:1). Microsomes were prepared after 63 h and 1.5 pmol of CYP2D6 was used per reaction for the enzyme assays which were performed using CEC as a substrate. By doubling the MOI of BV-ΔhRDM during co-expression, substantial increase in rates of reaction were observed (Figure 3.29). A similar experiment was performed with CYP2D6 and hRD and again an increase in the reaction rates were observed (Figure 3.30). With doubling of MOIs of both BV-ΔhRDM and hRD, decrease in spectrally active CYP2D6 was observed. However, the spectrally active CYP2D6 at 5:1 ratio of CYP2D6 : ΔhRDM was much higher than the CYP2D6 obtained when the CYP2D6 : hRD ratio was 5:1 (Table 3.9).

Thus ΔhRDM clearly provides more room for improvement. It would definitely allow for further optimisation of experimental routes towards higher levels of CYP2D6 production on insect cell derived microsomal membranes together with much improved activity.

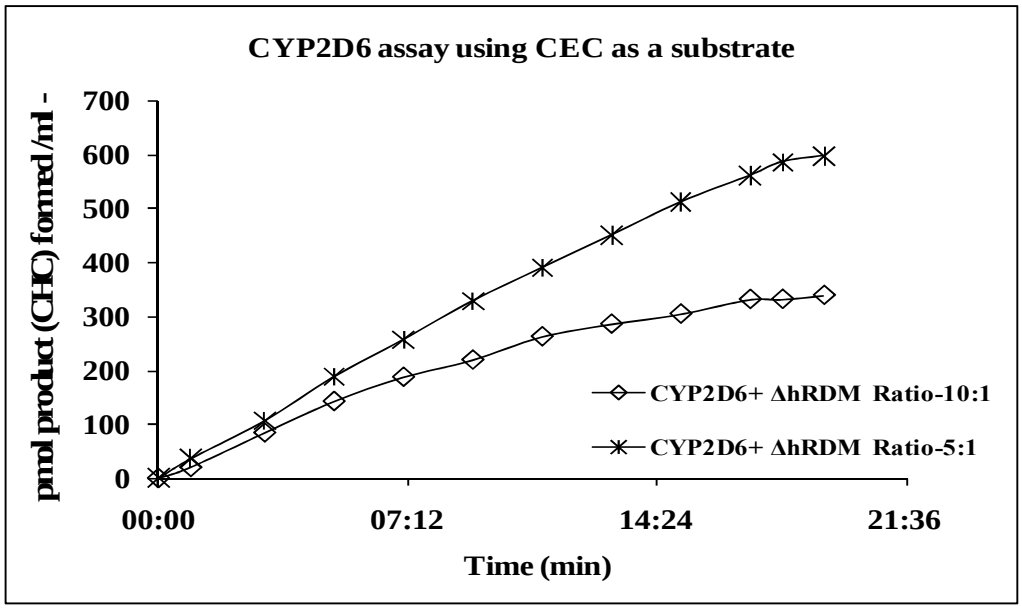

Figure 3.29. Kinetic analysis of CYP2D6 co-expressed with two different ratios of CYP to ΔhRDM, as shown in legend. CEC assay was performed using microsomes that were prepared from Sf9 cells after 63 h of baculovirus infection. Standard curve was plotted and CHC concentrations in test samples were measured using the equation from the standard curve. The standard curve is shown in Figure 3.24 (A).

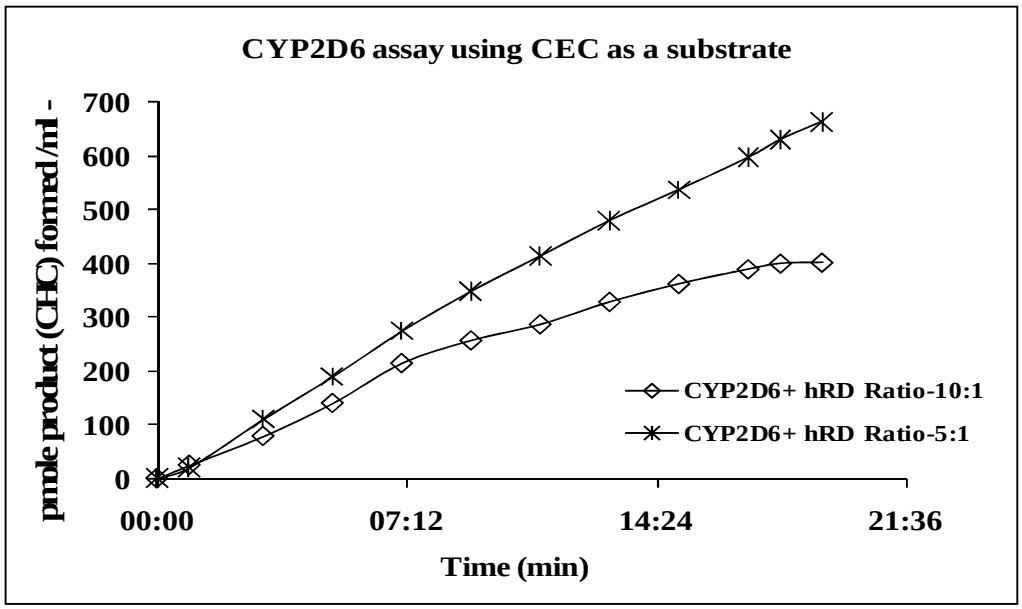

Figure 3.30. Kinetic analysis of CYP2D6 co-expressed with two different ratios of CYP to hRD, as shown in legend. CEC assay was performed using microsomes that were prepared from Sf9 cells at 63 h of baculovirus infection. Standard curve was plotted and CHC concentrations in test samples were measured using the equation from the standard curve. The standard curve is shown in Figure 3.24 (A).

Table 3.9. Comparison of the levels of CYP2D6 produced and CPR activities when CYP2D6 is co-expressed with hRD and ΔhRDM in two different ratios of CYP to CPR (10:1 and 5:1). Spectral analysis for the quantification of CYP and the assay for CPR were performed using microsomes that were prepared from Sf9 cells after 63 h of baculovirus infection.

Sample	CYP2D6 Content (nmol/mg protein)	CPR Activity (nmol MTT reduced/min/mg protein)
CYP2D6+hRD(10:1)	0.2027 ± 0.016	407 ± 29.3
CYP2D6+hRD(5:1)	0.0724 ± 0.009	620 ± 42.1
CYP2D6+ΔhRDM(10:1)	0.2710 ± 0.011	283 ± 18.0
CYP2D6+ΔhRDM(5:1)	0.1628 ± 0.008	550 ± 28.6

Insect cells can be grown in bioreactors and thus are able to produce large quantities of recombinant proteins. Bioreactors can be used for the expression of active CYPs and have application in large-scale bio-catalysis. Hence, higher CYP reaction rates are highly sought after not only in drug metabolism studies but also in the area of bio-transformations.

3.15 Augmentation of CYP2D6 activity by blending the reductase microsomes with CYP2D6 microsomes

In order to see if the activity of CYP2D6 could be augmented, we performed further experiments. Since Tni cells are capable of expressing significantly higher levels of recombinant proteins compared to other insect cell lines, we used this cell line for co-expression of the CYP and CPRs. The co-expression of CPR with a CYP results in CYP destruction, yet co-expression is essential for high catalytic activity of CYPs. We wanted to find out the consequence of blending additional CPR microsomes, during the process of microsomal preparations, to the microsomes that co-express the CYP, CPR enzymes.

Therefore, we co-infected Tni cells with BV-CYP2D6 (MOI of 1.0 pfu/ cell) and BV-ΔhRDM (MOI of 1×10^{-1} pfu/ cell). In a separate set of flasks, Tni cells were infected only with BV-hRD with an MOI of 1.0 pfu/ cell. The cells were processed and harvested as described in 'Materials and Methods'. At 63 h post-infection, cells were lysed and centrifuged to remove cell debris. The cell lysate from the co-expression experiment was blended with the lysate from cells infected only with hRD in 3:1 ratio (three parts of co-expression lysate and one part of hRD-expressed cell lysate). The blended mixture was then processed as described in 'Materials and Methods' and microsomes were prepared. Enzyme activity was assayed using 1.5 pmol of enzyme per reaction and AMMC as a substrate (Figure 3.31). By blending the enzymes in this way, it is likely that the organization of CYP and ΔhRDM on microsomal membranes is not

altered but that some extra reductase activity is provided to the system. Surprisingly, blending further increased the enzyme activity by about 40%.

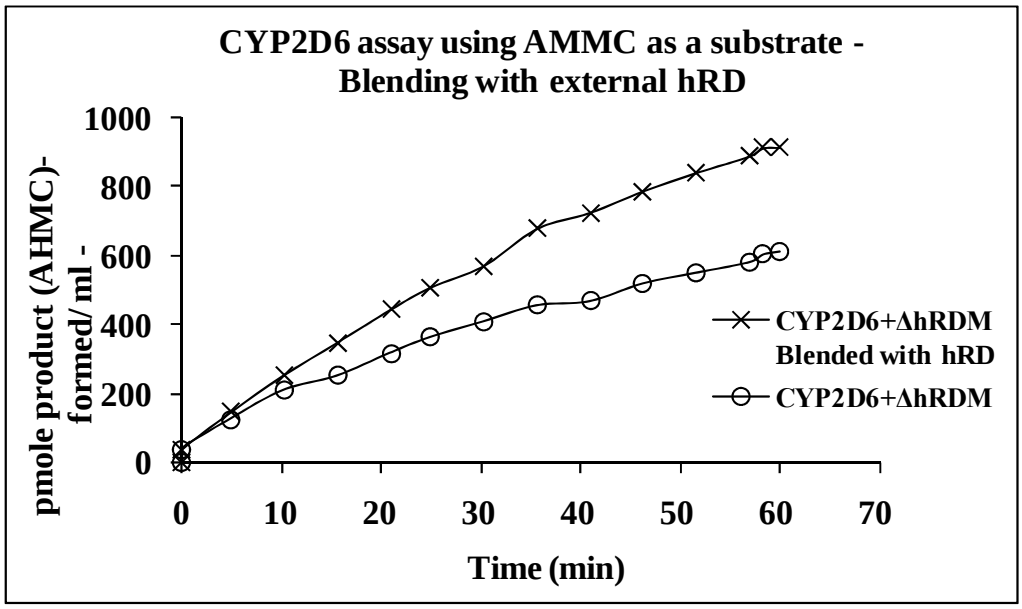

Figure 3.31. Comparative kinetic analysis of CYP2D6 co-expressed with ΔhRDM and blended with hRD as shown in legend. AMMC assay was performed using microsomes that were prepared from Tni insect cells after 63 h of baculovirus infection. CYP to CPR ratio for blending was 3:1. Standard curve was plotted and AHMC concentrations in test samples were measured using the equation from the standard curve. The standard curve is shown in Figure 3.25 (A).

3.16 Spinner culture for co-expression of CYP2D6 and ΔhRDM in Tni cells

Expression level of heterologous proteins in Tni cells is known to be higher than Sf9 and Sf21 cells. As ΔhRDM couples better with CYP2D6, a scale-up experiment

using spinner culture was set up for co-expression of CYP2D6 with ΔhRDM in Tni cells. Spinner cultures were set up as described in 'Materials and Methods' (Section Number 2.3.6). The cells were seeded at a density of 1.25 x 10^6 cells/ ml in Express Five™ medium. Total culture volume was 250 ml in 500 ml spinner flask with a vertical impeller.

It has been reported that cells in suspension require lower MOI for expression of spectrally active CYPs than that is required for adherent cultures (Crespi and Miller, 1999). In line with this, the cells were co-infected with BV-CYP2D6 at an MOI of 0.3 pfu/ml and with BV-ΔhRDM at an MOI of 0.03 (10 times less). In previous experiments, the adherent cells were infected with BV-CYP2D6 at an MOI of 1 pfu/cell but in this experiment the cells in suspension were infected with lower MOI (0.3 pfu/cells). The spinner flask was incubated at 27°C with constant stirring at 90 rpm. 24 h post-infection haemin was added to a final concentration of 2.5 µg/ml. Microsomes were prepared 63 h post-infection and after measuring protein concentrations and CYP content, EOMCC assay was performed to measure CYP2D6 catalytic activity (as described in Section 3.12.1). Results from this scale-up experiment were similar to that obtained from earlier small scale co-expression studies with CYP2D6 and ΔhRDM (Figure 3.32). It shows that CYP expression can efficiently be scaled up using lower MOIs to produce enzymatically active protein.

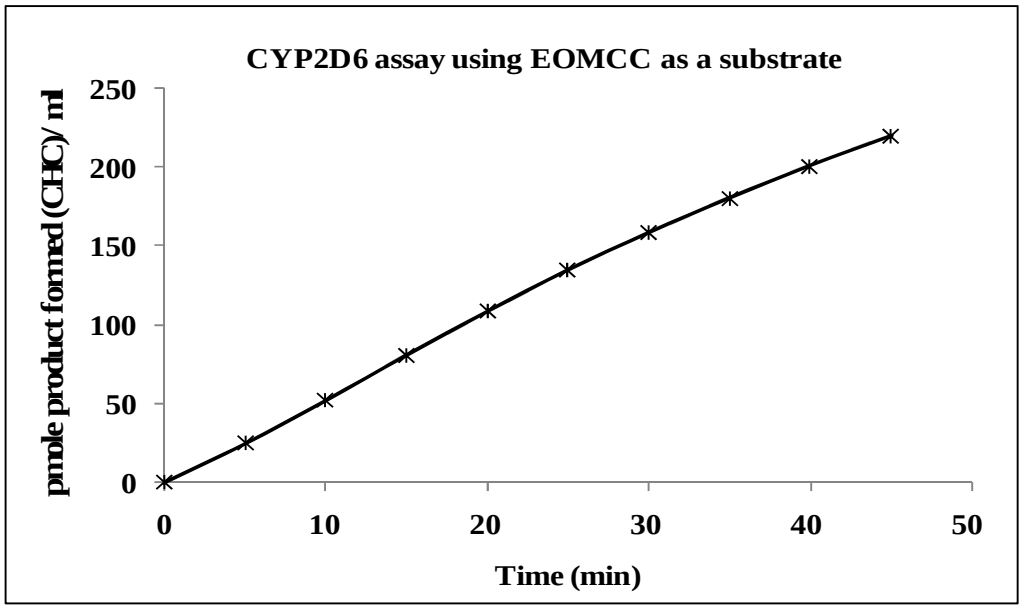

Figure 3.32. Kinetic analysis of CYP2D6 co-expressed with ΔhRDM, in a spinner flask, using EOMCC as a substrate. Tni cells in a spinner flask were co-infected with CYP2D6 and ΔhRDM at an MOI of 0.3 and 0.03 pfu/ cells, respectively. The activity of CYP2D6 co-expressed with ΔhRDM was measured using microsomes prepared at 63h after baculovirus infection. EOMCC assay was performed as described in Section 3.12.1.

3.17 Conclusion

With the exception of some plants, a single CPR of a particular eukaryotic species interacts with all other cytochrome P450s enzymes of the same species (Benveniste, 1991). Therefore, understanding the process by which this interaction occurs is an important biological goal.

In this study we have cloned and expressed CYP2D6 with native human CPR (hRD), two variants of native human CPR (ΔhRD and ΔhRDM) and yeast CPR (yRD) in Sf9 insect cells. The human CPR-variant, ΔhRD from which the N-terminal 24 amino acids have been removed do not anchor to microsomal membranes. Interestingly however, the other variant, ΔhRDM (which also lacks the N-terminal 24 amino acids but has a 17-amino acid sequence which includes the 12-amino acid *c*-myc tag epitope attached at the C-terminal end of ΔhRD) regains the ability to anchor to microsomal membranes. The *c*-myc tag at the C-terminal of the fusion protein, ΔhRDM must be somehow involved in the tertiary structure of the protein and helping the protein to anchor to the microsomal membranes. It is possible that the C-terminal tag is the source of the ΔhRDM's activity. Our experiments have consistently failed to show any reductase activity for ΔhRD even in the soluble cytosolic fraction of the cell lysate (results not shown).

The *c*-myc tag is generally used as an epitope tag and can be added to either the N-terminus or C-terminus of a known protein coding sequence. The tag is recognised

by antibodies raised against the 12-amino acid *c*-myc peptide epitope (9E10) and can be used to localize tagged proteins in cells. Although the tagged protein is merely a fusion protein between the expressed protein and the tag, its expression may not be regulated in the same way as would occur *in vivo* since the fusion protein is usually expressed under the control of a heterologous promoter. This could result in the abnormal expression of the tagged protein. Some previous studies have shown that an epitope tag may or may not affect a target protein activity or its folding and topology (Sells and Chernoff, 1995; Jarvik and Telmer, 1998; Chavand et al., 2001). In this study we have demonstrated that the C-terminal *c*-myc tag in ΔhRDM exhibits an unusual phenomenon, that is, allows the N-terminally truncated reductase ΔhRD to bind again to microsomal membranes.

The insect cell-baculovirus expression system has been used for expression of a range of recombinant proteins. But expression of CYPs in the baculovirus expression system provides some unique advantages. Insect cells can be co-infected with two or more recombinant baculoviruses, and so CYP to CPR ratio can be changed by altering the MOI for each virus (Tamura, 1992). In this study we have expressed CYP2D6 with human CPR and its engineered variants (Figure 3.2) and also with yeast NADPH cytochrome P450 reductase (yRD). All the CPRs have different reduction potentials as measured by the MTT assay. However when these CPRs were co-expressed with the CYP2D6 and the CYP activity was measured using enzyme assays, we found that the strength of the reductase does not determine CYP activity – it is the ability of CPR to couple with CYP which is crucial.

The yeast CPR (yRD) appears to have the strongest reduction potential but it is extremely destructive to CYP2D6. It also does not offer a better reaction rate in CYP2D6 assays implying that it fails to couple well with CYP2D6. The destruction of the CYP2D6 by yeast and human CPRs is significant which is reflected in the decrease in CYP2D6 spectral content when CYP, CPR proteins are co-expressed. This is in comparison with the spectral content obtained when CYP2D6 is expressed alone.

Based on the CYP2D6 enzyme assays, percentage relative coupling efficiency and efficiency of catalysis it can be concluded that the ΔhRDM, which has the weakest reduction potential, surprisingly provides the best CYP2D6 reaction rates in comparison with the two wild-type CPRs – hRD and yRD. We find that ΔhRDM not only couples far better to CYP2D6 than the native human CPR, hRD. But also yields higher levels of CYP2D6 with far less destruction of the CYP.

All the CPRs studied did decrease the CYP holoenzyme but the apoprotein levels were found to be unaffected (Figure 3.22). We were able to show the possible cause of CYP2D6 destruction by CPRs. The reactive oxygen species (ROS) assays clearly indicated that the cause of CYP2D6 destruction is likely to be oxidative damage caused by CPRs. Based on the results obtained, this chapter clearly illustrates that peak enzymatic activity cannot just be obtained by increasing the MOI of the CPR baculovirus. Coupling efficiency of a CPR is extremely important to achieve the best enzymatic activity of the CYP.

In conclusion ΔhRDM, a genetically engineered variant of human CPR offers advantages of high-level expression of CYP2D6 with better reaction rates. ΔhRDM also offers an improvement in the ratio of spectrally active CYP2D6 to spectrally inactive CYP2D6.

Chapter 4 Interaction of human and yeast NADPH cytochrome P450 reductases with human CYP3A4 on ER membranes of insect cells

4.1 Introduction

Cytochrome P450 enzymes (CYPs) belong to a superfamily of haem binding monooxygenase enzymes involved in metabloism of xenobiotics such as toxins, carcinogens and drugs as well as in the biosynthesis of cholesterol, vitamins and steroids (Wolf et al 1986; Shou et al. 2001). Biotransformation of these xenobiotics and endobiotics by CYPs requires supply of reducing equivalents from its redox partner NADPH cytochrome P450 reductase (CPR). The CPR contains FMN, FAD and NADPH binding domains and electrons are transferred from NADPH to FAD to FMN and finally to CYP. The interaction between CYP and CPR occurs on the surface of the endoplasmic reticulum (ER). Electrostatic (Shen and Kasper 1995), hydrophobic and van der Waals forces (Voznesensky and Schenkman 1994) have been implicated as determinants of this interaction. However CYP-CPR interaction and the formation of a productive monooxygenase complex remain poorly understood (Deeni et al. 2001). Both CYP and CPR contain N-terminal hydrophobic domains that allow anchoring to the microsomes (ER membranes) which appears to be important for correct spatial orientation of the redox centres for effective electron transfer.

In comparison with other CYPs, human CYP3A4 exhibits negligible catalytic activity when co-expressed alone in the presence of yeast's endogenous CPR in yeast

cells. This was explained by the possibility that CYP3A4 forms two dimensional aggregates on yeast microsomal membranes, thereby inhibiting interaction with the endogenous yeast CPR (Hayashi et al 2000). It was observed that only a fusion between human CYP3A4 and yeast CPR permitted measurable catalytic activity. In the presence of human cytochrome b_5, the catalytic efficiency of CYP3A4 (in the CYP3A4–yeast CPR fusion) towards its substrates was appreciably enhanced (Hayashi et al 2000) which corroborated earlier findings that human cytochrome b_5 plays a major role in the catalytic activity of CYP3A4 (Truan et al 1993; Voice et al 1999).

It seems that in all CYP–CPR fusion constructs, the CYP domain is anchored to the microsomes and the C-terminal reductase (shorn off its own N-terminal membrane anchor) moves flexibly lying on the cytoplasmic side (Yabusaki 1995). Since the fused enzyme is expressed as a single polypeptide chain, the reductase domain of CPR and the haem domain of CYP are probably forced to remain in close proximity rather than associating with each other via natural interactions on ER membranes which happens when the two enzymes, CYP and CPR, are expressed as separate entities.

There are a number of reports on the co-expression of the yeast CPR and a human CYP on yeast microsomes and their resultant activities (Eugster and Sengstag 1993; Ellis et al 1992; Renaud et al 1990; Brian et al 1990) – they vary from being quite good to extremely poor (our own unpublished observations). To the best of our knowledge, the possible interaction of the yeast CPR with a human CYP on insect cell microsomes has never been studied before although a variety of different eukaryotic

(mainly mammalian) CPRs have been co-expressed with human CYPs in insect cells (Wang et al. 1996; Lee et al. 1995; Paine et al 1996; Schwarz et al. 2001).

We specifically chose to further understand the interaction of yeast CPR with human CYP3A4 in insect cells with the knowledge that there have been some inexplicable hurdles towards the co-expression of these two enzymes, as separate entities, in baker's yeast. Hence, human CYP3A4 and cytochrome b_5 were co-expressed in an insect cell system and a comparative study was performed between their interactions with human and yeast CPR. Cytochrome b_5 is known to stimulate CYP3A4 activity towards its substrates (Voice et al 1999).

The CYP3A4 enzyme is the most abundant drug-metabolizing CYP in human liver, consisting of about 30-40% of the total hepatic CYP content (Shimada et al, 1994; Imaoka et al. 1996). Apart from the liver, CYP3A4 is also an intestinal phase I enzyme (Kolars et al. 1992) that metabolises approximately 50% of currently marketed drugs (Bertz and Granneman 1997). A number of important drugs have been identified as substrates, inducers and/or inhibitors of CYP3A4. The substrates of CYP3A4 include drugs, such as quinidine, nifedipine, diltiazem, lidocaine, lovastatin, erythromycin, cyclosporin, triazolam, and midazolam, and endogenous substances that include testosterone, progesterone, and androstenedione (Pelkonen et al. 1998, Guengerich 1999). It also activates procarcinogens, including aflatoxin B_1 (Aoyama et al. 1990), polycyclic aromatic hydrocarbons (PAHs) (Kapucuoglu et al. 2003), 4-(methylnitrosamino)-1-(3-pyridyl)-1-butanone (NNK) (Hecht 1999), and 6-

aminochrysene (Yamazaki et al. 1995). CYP3A4 is induced in human hepatocytes by rifampicin (Morel et al. 1990, Schuetz et al. 1993), dexamethasone (Pichard et al. 1992, Schuetz et al. 1993, Kocarek et al. 1995), and phenobarbital (Schuetz et al. 1993, Kocarek et al. 1995). CYP3A4 is also induced *in vivo* by rifampicin and barbiturates in the liver (Perrot et al. 1989, Ged et al. 1989) and by rifampicin in the small intestine (Kolars et al. 1992).

As CYP3A4 is the most abundant and most important CYP in the human liver, the inhibition or induction of CYP3A4 by drugs often causes unfavourable drug-drug interactions and can lead to fatal toxicity. Detection of possible CYP3A4 inhibitors and inducers during the early stages of drug development is critical in preventing potential drug-drug interactions and side effects. Clinicians are encouraged to have a sound knowledge of the drugs that behave as substrates, inhibitors or inducers of CYP3A4. They ought to be prescribed judiciously with close monitoring so as to avoid possible interactions between drugs that are inhibitors and inducers of CYP3A4. It is often necessary to use such drugs simultaneously (Zhou 2008).

In this Chapter, we show the interactions of both yeast and human CPR with human CYP3A4 using the baculovirus expression system. We have explored the ability of the two CPRs to transfer electrons to an artificial substrate MTT and then extended the observations to a physiological substrate, CYP3A4. Previously it has been reported that human CYP levels are drastically reduced when it is co-expressed with CPR in the baculovirus expression system (Chen et al 1997; Wang et al 1996; Paine et al 1996).

We have also found in our studies in Chapter 3 that oxidative damage caused by CPRs is responsible for reduction in CYP holoprotein content. We find here a similar effect when a human CYP and the human CPR are co-expressed together. However in the case of yeast CPR, we find that oxidative damage is not the complete reason behind it being unable to support CYP3A4's catalytic activity.

4.2 Gene cloning in basic vectors

The cytochrome P450 3A4 (CYP3A4) and cytochrome b_5 genes were isolated by PCR from a human liver cDNA library (Life Technology, Catalogue No 10422-012). The *CYP3A4* gene was isolated with the forward primer (5'- GCAGATCT**GC CACC**ATGGCT CTCATCCCAG ACTTGGCC -3', the *BglII* site and the Kozak sequence are marked with an underline and bold letters, respectively), and the reverse primer (5'-ATGTCGACTC AGGCTCCACT TACGGTGCC -3', the *Sal*I site is underlined). The *cytochrome b_5* gene was isolated with the forward primer (5'-CGGGATCC**GC CACC**ATGGCA GAGCAGTCGG ACGAGG -3', the *BamHI* site and the Kozak sequence are marked with an underline and bold letters, respectively) and the reverse primer (5'-GCTCTAGATC AGTCCTCTGC CATGTATAGG CGATAC -3', the *XbaI* site is underlined). The genes coding for human NADPH P450 reductase (hRD), its variants (ΔhRD and ΔhRDM) and the yeast NADPH P450 reductase (yRD) were cloned earlier and are described in Chapter 3.

The genes were amplified using the above mentioned primers, as described in 'Materials and Methods' (Section Number 2.2.2). The PCR products were run on an agarose gel containing ethidium bromide, and DNA fragments of expected size were isolated and purified using Qiagen gel extraction kit according to the manufacturer's protocol. The purified DNA fragments were digested with the corresponding restriction enzymes and after digestion run again on an agarose gel containing ethidium bromide. The digested DNA fragments were purified using the Qiagen gel extraction kit. The *CYP3A4* and *cytochrome* b_5 genes were then directionally ligated using T4 DNA ligase into pSP73 and pBluescript KS+, respectively (digested with the same restriction enzymes with which the corresponding genes were digested). The ligation mixture was used for transforming *E. coli* DH5α competent cells, and colonies containing the correct recombinant constructs were identified via restriction analysis. Plasmids were extracted from positive clones. The experimental methods employed are described in 'Materials and Methods'. The gene sequences were confirmed by DNA sequencing and further alignment of sequences obtained with reference sequences in the NCBI database. The resultant plasmids were named pSP73/BglII-Sal/CYP3A4 (Figure 4.1) and pBluKS+/Bam-Xba/b_5 (Figure 4.2).

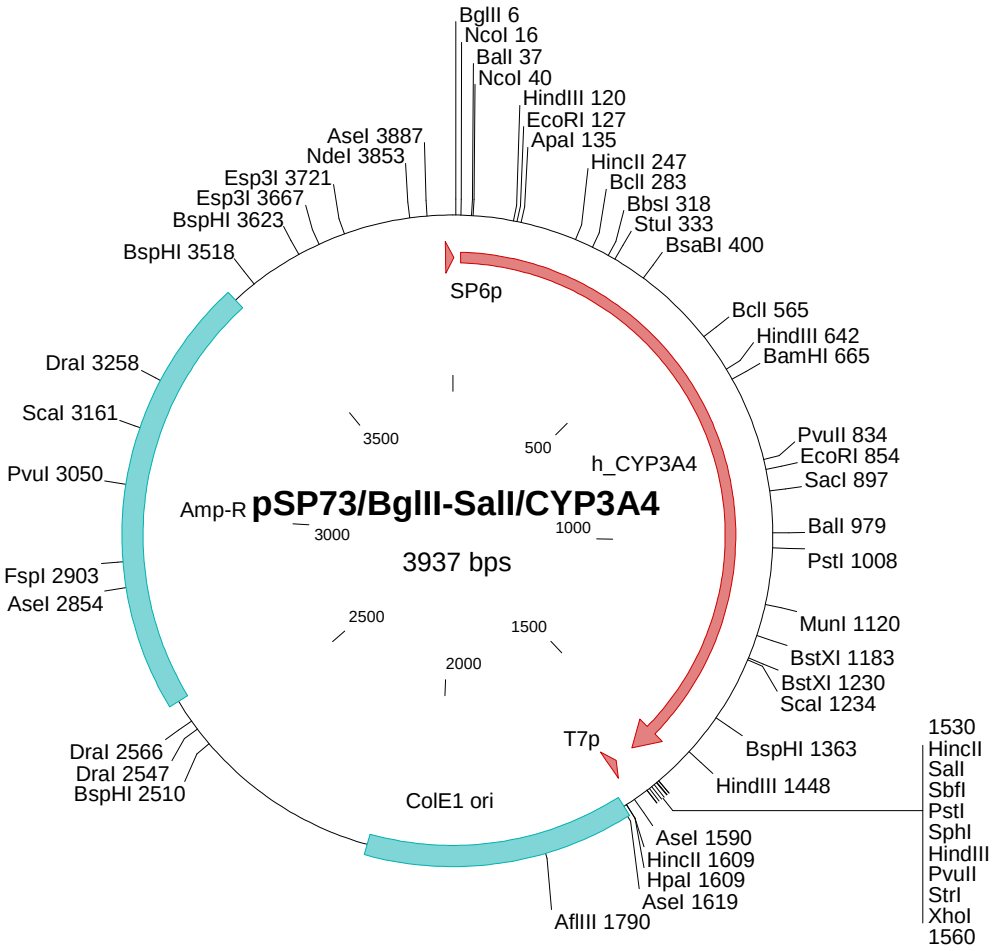

Figure 4.1. The plasmid map of pSP73/BglII-Sal/CYP3A4.

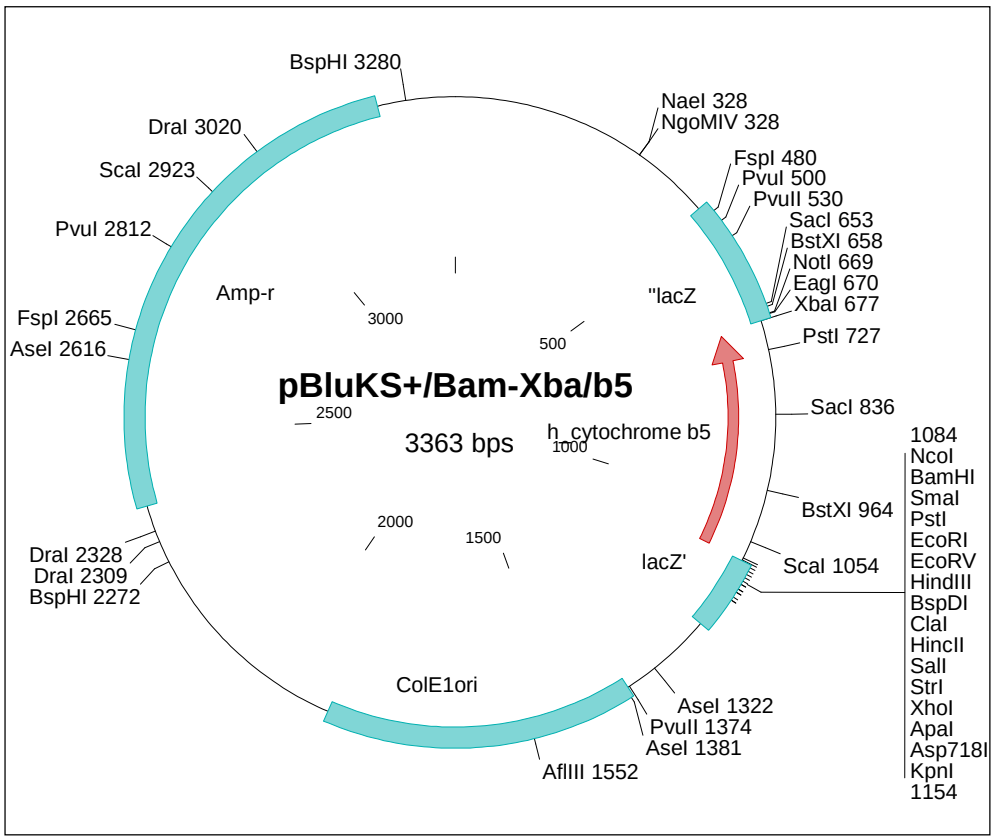

Figure 4.2. The plasmid map of pBluKS+/Bam-Xba/b_5.

4.3 Sub-cloning of genes in baculovirus transfer vector

The *CYP3A4* and *cytochrome* b_5 genes were isolated from pSP73/BglII-SalI/CYP3A4 and pBluKS+/Bam-Xba/b_5 using sets of *Bgl*II, *Sal*I and *BamH*I, *Xba*I restriction enzymes, respectively. The pFastBac1 vector was digested with *BamH*I, *Sal*I for *CYP3A4* cloning and with *BamH*I, *Xba*I for human *cytochrome* b_5 cloning. The digested fragments of *CYP3A4* and *cytochrome* b_5 genes were gel purified and used for ligation into linearised pFastBac1 (digested with the appropriate restriction enzymes). The ligation mixture was used for transforming *E. coli* DH5α competent cells and transformants were screened by restriction analysis. The cDNAs in the pFastBac1

vector were cloned under the control of a polyhedrin promoter. The resultant recombinant donor vectors were named pFastBac1/CYP3A4 (Figure 4.3) and pFastBac1/Bam-Xba/b_5 (Figure 4.4).

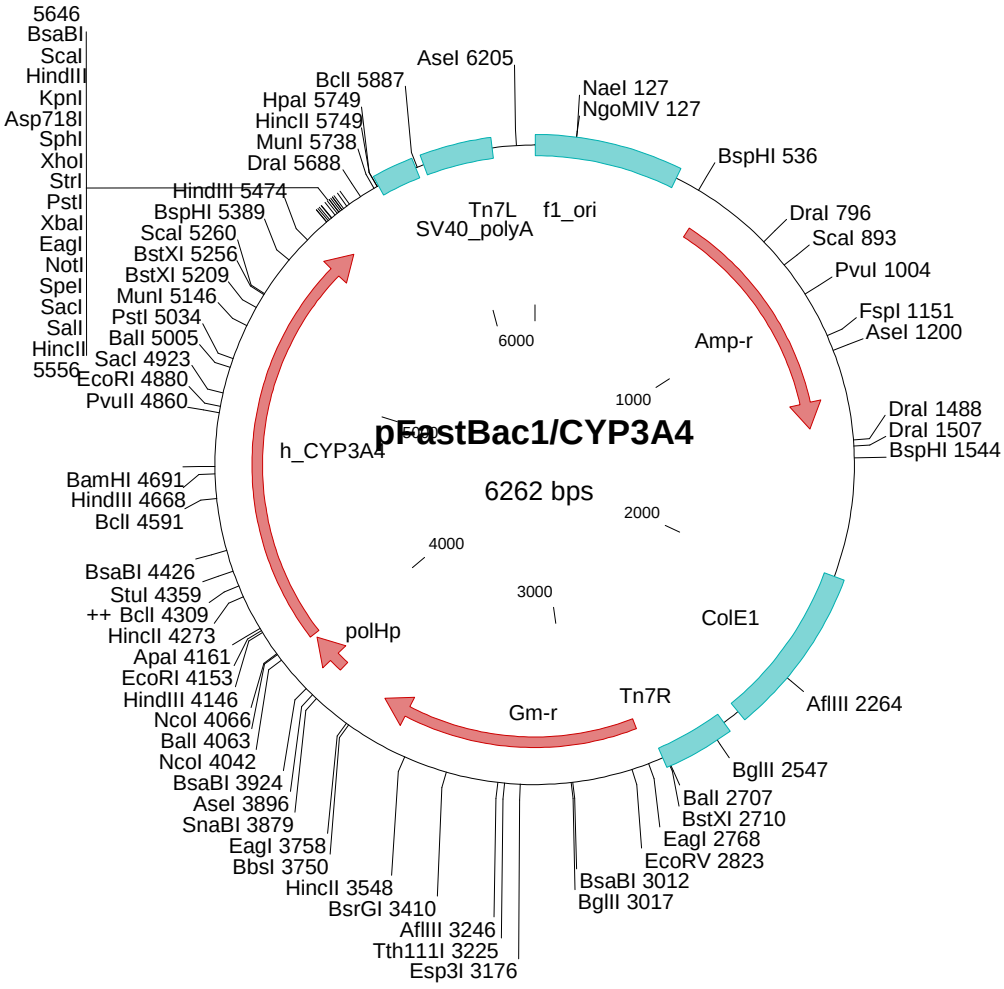

Figure 4.3. The plasmid map of pFastBac1/CYP3A4, the *Bgl*II-*Sal*I human *CYP3A4* fragment being cloned in *BamH*I-*Sal*I digested pFastBacI.

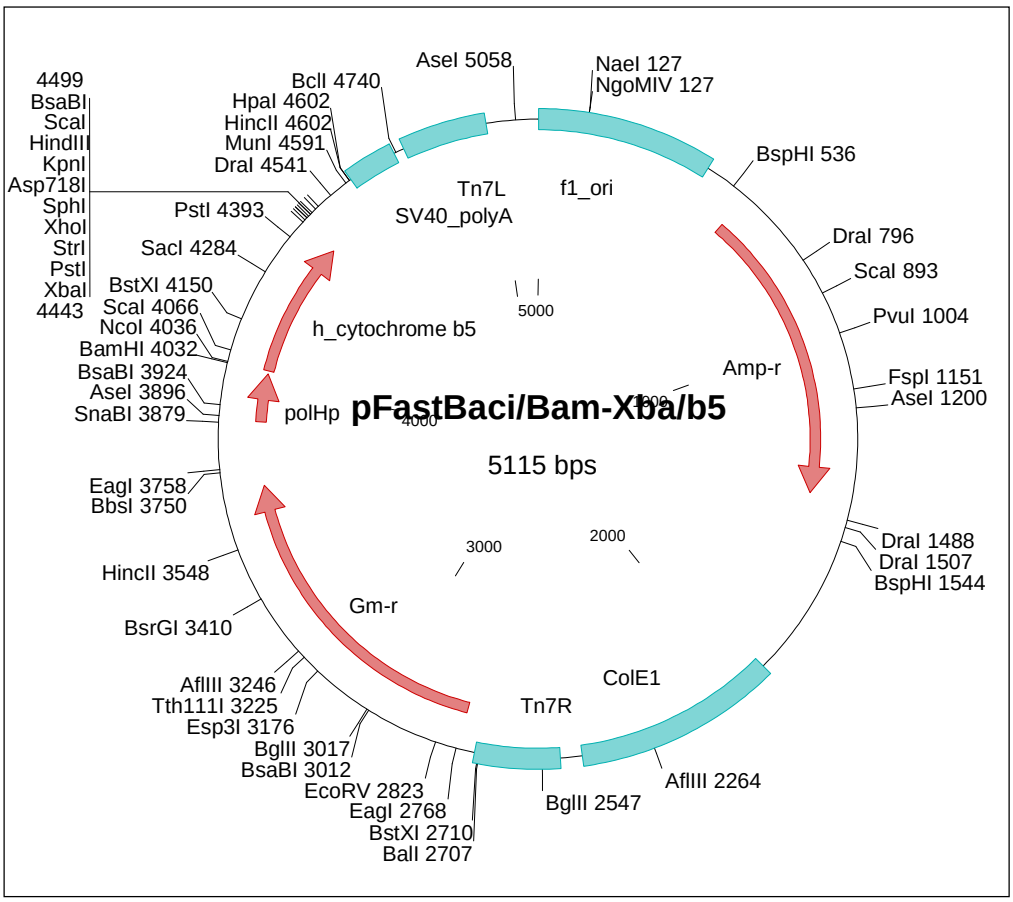

Figure 4.4. The plasmid map of pFastbac1/Bam-Xba/b_5, the *BamH*I-*Xba*I human b_5 fragment being cloned in *BamH*I-*Xba*I digested pFastBacI

4.4 Generation of bacmid constructs and baculoviruses

The recombinant donor vectors, named pFastBac1/CYP3A4 and pFastBac1/Bam-Xba/b_5 were transposed on to *E. coli* DH10Bac competent cells. DH10Bac cells contain a baculovirus shuttle vector (bacmid DNA) and a helper plasmid, and allow generation of a recombinant bacmid by site-specific transposition. The propagation of recombinant bacmid in DH10Bac was identified by white colour in the presence of a chromogenic substrate Bluo-gal and the inducer IPTG. The white

colonies were streaked a second time on Bluo-gal plates and after confirming the phenotype, recombinant bacmids were isolated and confirmed by PCR analysis. PCR was performed using M13 forward primer (5' -GTTTTCCCAGTCACGAC- 3') and gene-specific reverse primers (Figure 4.5).

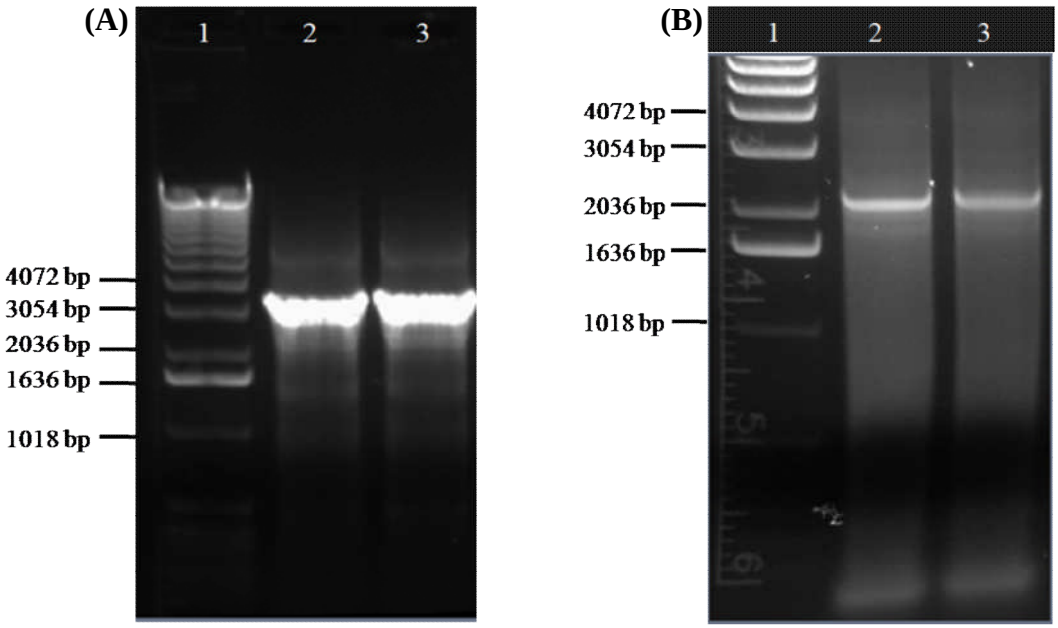

Figure 4.5. Confirmation of *CYP3A4* and *cytochrome b_5* gene transposition on bacmids via PCR. PCR was performed using a set of M13 forward and gene-specific reverse primers. PCR was performed as described in 'Materials and Methods' (Section Number 2.2.2). After transposition on bacmids, the expected DNA fragment size for *CYP3A4* gene is ~3000 bp and for cytochrome b5, ~2000 bp. (A): Lane 1, 1 kb DNA ladder; Lane 2, clone No 1 of CYP3A4 bacmid; Lane 3, clone No 2 of CYP3A4 bacmid. (B): Lane 1, 1 kb DNA ladder; Lane 2, clone No 1 of cytochrome b_5 bacmid; Lane 3, clone No 2 of cytochrome b_5 bacmid.

In order to generate baculoviruses, Sf9 cells were transfected with recombinant bacmids as described in 'Materials and Methods' (Section Number 2.2.14). Hereafter, CYP3A4 baculovirus is referred to as BV-CYP3A4 and cytochrome b_5 baculovirus is referred as BV-cyt-b_5. The baculoviruses produced in Sf9 cells were subjected to two more rounds of amplification by infecting the cells with baculoviruses for 96 h. The baculovirus titration was performed using plaque assay and titres of the baculovirus stocks were determined. The experimental methods employed are detailed in 'Materials and Methods'.

4.5 Expression of CYP3A4 and cytochrome b_5 in Sf9 cells

Following amplification and titration of recombinant baculoviruses, Sf9 cells were infected with BV-CYP3A4 at an MOI of 1.0 pfu/cell. In a separate experiment, Sf9 cells were infected with BV-cyt-b_5 at an MOI of 1.0 pfu/cell. To compensate for low endogenous levels of haem in insect cells, haemin (2 μg/ ml) and δ-amino levulinic acid (100μM) were added 24 hour post-infection to the cells for expression of CYP3A4. Cells were harvested 63 h post-infection and the microsomes were prepared.

Coomassie staining was performed to confirm expression of CYP3A4 and cytochrome b_5 proteins. Microsomes (20 μg microsomal protein/ lane) were separated on 10% sodium dodecyl sulfate-polyacrylamide gel and protein bands were visualized (Figure 4.6) by staining with Coomassie G-250 and several de-staining steps, as described in 'Materials and Methods' (Section Number 2.4.5). Commassie staining of

microsomal protein fractions prepared from recombinant baculovirus infected insect cells detected CYP3A4 and cytochrome b_5 protein bands. The size of the protein bands was consistent with the molecular weight predicted from the cDNA sequence.

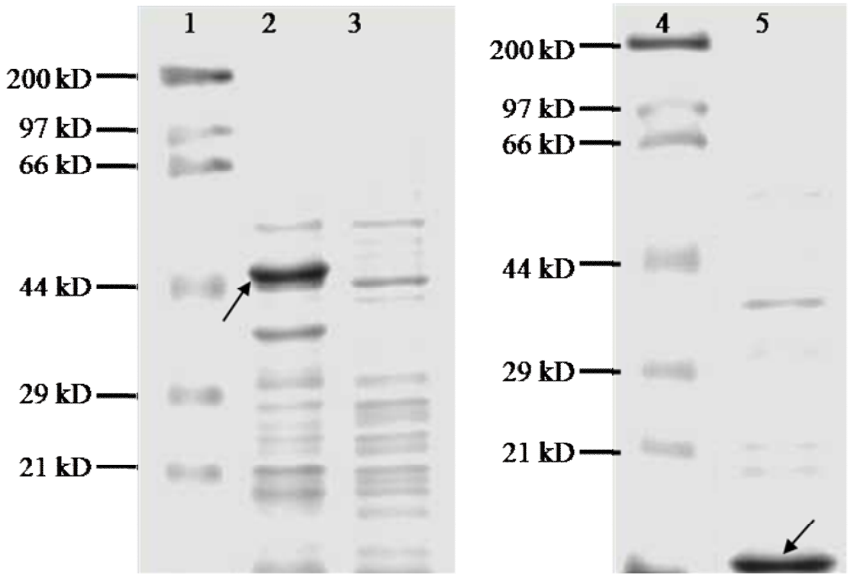

Figure 4.6. SDS-PAGE gel analysis of CYP3A4 and cytochrome b_5 proteins. 25 µg microsomal fractions of the proteins expressed in Sf9 cells were loaded per lane on 10% SDS-PAGE. Gels were stained with Coomassie blue G-250 as described in 'Materials and Methods' (Section Number 2.4.5). Lane 1, protein marker; Lane 2, CYP3A4; Lane 3, negative control; Lane 4, protein marker; Lane 5, cytochrome b_5.

4.6 Co-expression of CYP3A4 with the CPRs and cytochrome b_5 in Sf9 cells

In human liver microsomes CYP levels far exceed the levels of NADPH

cytochrome P450 reductase (CPR) by a 10:1 to 20:1 ratio (Estabrook et al 1971). In line with this, while co-infecting Sf9 cells with BV-CYP3A4 and BV-CPR (hRD, ΔhRD, ΔhRDM and yRD), multiplicity of infection (MOI) for BV-CPR was kept 10 times less (0.1 pfu/cell) than that of CYP3A4 (1 pfu/cell). For co-expression of the third protein cytochrome b_5, the baculovirus BV-cyt-b_5 was used at an MOI of 0.1 pfu/ cell. To compensate for low endogenous levels of haem in insect cells, haemin (2 µg/ ml) and δ-amino levulinic acid (100µM) were added 24 hour post-infection to the cells for expression of CYP3A4. Cells were harvested after 63 h and microsomes were prepared. The experimental methods employed are detailed in 'Materials and Methods'. Experiments related to Western blotting and Coomassie staining for expression of the individual proteins hRD, ΔhRD, ΔhRDM and yRD were presented in Chapter 3.

Western blotting was performed for CYP3A4 using the co-expressed microsomes. For Western blotting, the microsomes prepared from the baculovirus infected Sf9 cells as described above were separated on 10% sodium dodecyl sulfate-polyacrylamide gel (1.5 µg microsomal protein/ lane). The proteins were transferred to Immobilon P membrane (Millipore) by the semi-dry transfer method. The membrane was blocked overnight at 4ºC with 5% non-fat dry milk in PBS. The blot was then probed with 1:2,500 dilution of mouse polyclonal antibody to CYP3A (Gentest, Catalogue No 458258). Then the blot was incubated with 1:7,500 dilution of secondary antibody – anti-mouse IgG-HRP conjugate (Santa Cruz Biotechnology, Catalogue No SC-2302). The blot was incubated with luminol chemiluminescent substrate for a short time. Chemiluminescence was captured (Figure 4.7) on Gel Doc™ (Bio-Rad). Human CYP3A4 protein bands reacted with the CYP3A-specific antibodies in Western blot

analysis. The protein band intensities were measured by densitometry using Quantity-one software from Bio-Rad.

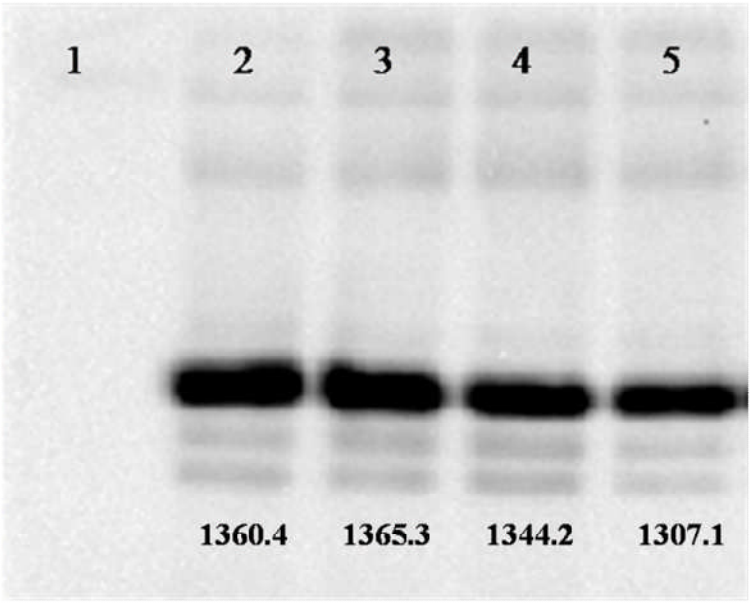

Figure 4.7. Immunoblot analysis of CYP3A4 co-expressed with different CPR species in Sf9 insect cells. Sf9 cells were infected with CYP and CPR baculoviruses at an MOI of 1 pfu/cell and 0.1 pfu/cell respectively. The cells were also co-infected with a third virus, encoding cytochrome b_5, at an MOI of 0.1 pfu/cell. 63 h post-infection microsomes were prepared. 1.5 μg of microsomal fractions were loaded per lane on 10% SDS-PAGE and immunoblotting was performed as described in 'Materials and Methods' (Section Number 2.4.6) by using antibodies that recognise human CYP3A4. The numbers below the bands show band intensities in arbitrary units. Lane 1, negative control; Lane 2, CYP3A4 expressed with cytochrome b_5; Lane 3, CYP3A4 and cytochrome b_5 co-expressed with hRD; Lane 4, CYP3A4 and cytochrome b_5 co-expressed with ΔhRDM; Lane 5, CYP3A4 and cytochrome b_5 co-expressed with yRD.

4.7 Amounts of CYP3A4 in microsomes that co-express different CPRs

The insect cells were infected with recombinant baculovirus encoding CYP3A4 alone (MOI 1.0) and were also co-infected with baculoviruses encoding cytochrome b5 (MOI 0.1) and human CPR or yeast CPR (MOI 0.1). Microsomes were prepared 63-h post-infection and the protein concentrations were determined by a modified Bradford method (Bradford 1976). The microsomes were diluted to a protein concentration of 1 mg/ml with 100 mM potassium phosphate buffer (pH 7.4), 20% (vol/vol) glycerol. Then a few grains of sodium dithionite were added and a baseline recorded on dual wavelength spectrophotometer (Shimadzu UV-2401PC). CYP3A4 holoprotein contents were spectrophotometrically measured as reduced carbon monoxide (CO) spectra (Omura & Sato 1964) using 91 mM^{-1} cm^{-1} as extinction coefficient. The experimental methods employed are detailed in 'Materials and Methods' (Section Number 2.4.3).

Figure 4.8 and Table 4.1 summarise CYP3A4 content when co-expressed only with cytochrome b_5 and when co-expressed with human or yeast CPRs. The co-expression of CYP3A4 with CPRs results in decrease in spectrally active CYP3A4 levels (holoprotein levels). CYP3A4 content is highest when co-expressed only with cytochrome b_5. CYP3A4 content was higher when co-expressed with ΔhRDM in comparison to CYP3A4 content when co-expressed with hRD or yRD. However it is interesting to note that similar to CYP2D6 (results presented in Chapter-3), CYP3A4 apoprotein levels as measured by densitometry from the immunoblot **(**Figure 4.7**)** do not change irrespective of the CPR (human or yeast) that is co-expressed with CYP3A4.

These results suggest that CPR does not regulate the CYP expression levels in any way but is responsible for decrease in spectrally active enzyme i.e. holoprotein. CYP3A4 holoprotein destruction by ΔhRDM is found to be much less than that caused by hRD and yRD. Although ΔhRD does not anchor on the microsomal membranes, it has some destructive effect on CYP3A4 holoenzyme as compared to cells that produce CYP3A4 in the absence of any CPR (i.e. CYP3A4 + b5). Experimental evidence, presented in Chapter 3, correlates reactive oxygen species induced by CPRs as being responsible for their destructive effects.

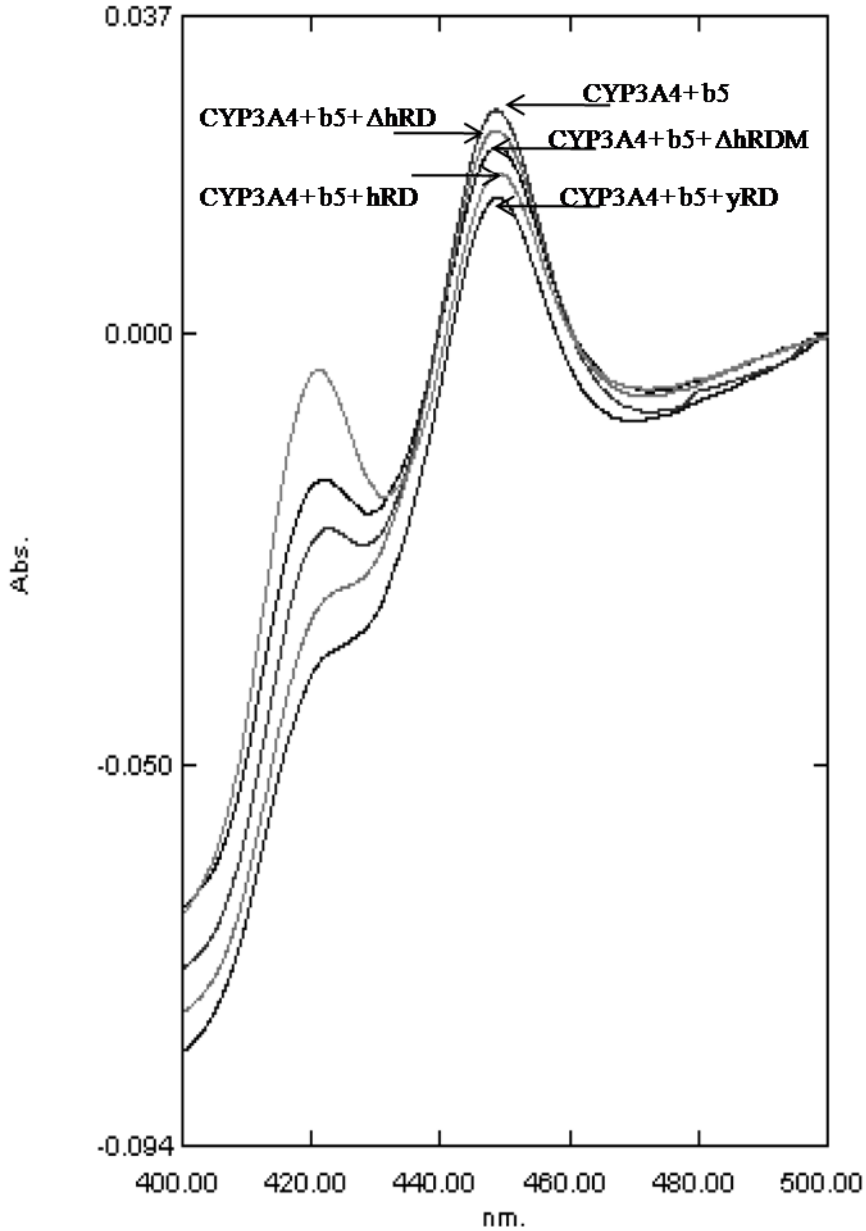

Figure 4.8. Reduced carbon monoxide difference spectra of CYP3A4. Sf9 cells infected with CYP3A4, cytochrome b_5 and CPR baculoviruses at an MOI of 1, 0.1 and 0.1 pfu/ cell, respectively. The cells were harvested 63 h post-infection and microsomes were prepared. CYP content was measured by reduced carbon monoxide difference spectra as described in 'Materials and Methods' (Section Number 2.4.3).

Table 4.1. CYP3A4 content in microsomal samples as determined by reduced CO-difference spectroscopy. Sf9 cells were co-infected with CYP3A4, cytochrome b_5 and CPR baculoviruses at an MOI of 1.0 pfu/cell, 0.1 pfu/cell and 0.1 pfu/cell, respectively. Microsomes were prepared 63 h post-infection as described in 'Materials and Methods' (Section Number 2.4.1). Data are presented as mean values ± STDEV.

Microsomes	CYP content (pmole/mg protein)
CYP3A4+ b_5	512.10 ± 18.3
CYP3A4+hRD+ b_5	251.01 ± 21.7
CYP3A4+ΔhRD+ b_5	455.83 ± 31.1
CYP3A4+ΔhRDM+ b_5	339.00 ± 26.9
CYP3A4+yRD+ b_5	247.61 ± 19.2

4.8 Measurement of cytochrome b_5 in microsomes that co-express CYP3A4 and CPRs

Cytochrome b_5 content in microsomes that co-express CYP3A4 and different CPRs was measured spectrophotometrically according to procedures published before (Strittmatter and Velick 1956; Holmans et al. 1994, Shet et al. 1994). Reduced cytochrome b_5 absorbs at 424 nm. The microsomes were diluted to a protein

concentration of 1 mg/ml in 100 mM potassium phosphate buffer (pH 7.4), 20% glycerol. The diluted suspension was divided equally in two cuvettes (reference and sample cuvette). The cuvettes were placed in the dual wavelength spectrophotometer. The baseline was recorded by scanning samples from 400 nm to 500 nm. A few grains of sodium dithionite were then added to the sample cuvette in order to reduce cytochrome b5. The difference spectrum between the two cuvettes was scanned again from 400 nm to 500 nm and recorded. The absorbance difference between 424 nm and 408 nm was calculated and b_5 content in microsomal suspension was measured using 112 mM^{-1} cm^{-1} as extinction coefficient.

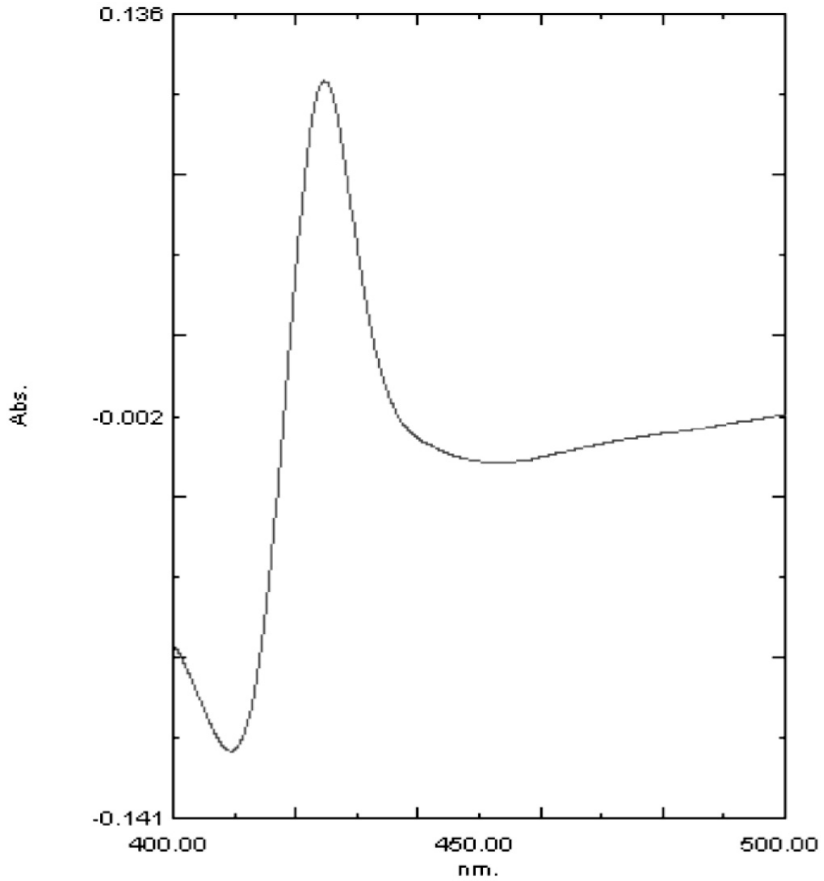

Figure 4.9. A typical difference spectra of cytochrome b_5. Sf9 cells were infected with CYP3A4 and cytochrome b_5 baculoviruses at an MOI of 1 and 0.1 pfu/ cell, respectively. The cells were harvested 63 h post-infection and microsomes were prepared. Cytochrome b_5 content was measured by reduced difference spectra as described in Section 4.8.

Table 4.2. Cytochrome b_5 content in microsomal samples as determined by spectroscopy. Sf9 cells were co-infected with CYP3A4, CPR and cytochrome b_5 baculoviruses at an MOI of 1.0 pfu/cell 0.1 pfu/cell and 0.1 pfu/cell, respectively. Microsomes were prepared 63 h post-infection and cytochrome b_5 content was measured as described in 'Materials and Methods' (Section Number 2.4.1). Data are presented as mean values ± STDEV.

Microsomes	Cytochrome b_5 content (pmole/mg protein)
CYP3A4+ b_5	289.0 ± 11.3
CYP3A4+hRD+ b_5	275.7 ± 16.8
CYP3A4+ΔhRDM+ b_5	278.6 ± 16.1
CYP3A4+yRD+ b_5	288.9 ± 14. 5

4.9 Stimulation of CYP3A4 activity by cytochrome b_5

Cytochrome b_5 has been shown to stimulate CYP3A4 activity towards its substrates (Voice et al 1999). We have co-expressed cytochrome b_5 with CYP3A4 and have observed augmentation of CYP3A4 activity towards demethylation of DBOMF. The Sf9 cells were infected with recombinant baculovirus encoding CYP3A4 alone (MOI 1.0 pfu/cell). In the second set of experiments, Sf9 cells were co-infected with

CYP3A4 baculovirus (MOI 1.0 pfu/cell) and ΔhRDM baculovirus (MOI 0.1 pfu/cell). In the third set of experiments, Sf9 cells were co-infected with CYP3A4 baculovirus (MOI 1.0 pfu/cell), ΔhRDM baculovirus (MOI 0.1 pfu/cell) and cytochrome b_5 baculovirus (MOI 0.1 pfu/cell). Microsomes were prepared 63-h post-infection, CYP content was measured and the microsomes were used for measuring CYP3A4 catalytic activity in DBOMF assay.

The production of the metabolite fluorescein, by dealkylation of Vivid® fluorogenic substrate dibenzyl-oxymethyl-fluorescein (DBOMF) was measured for 10 min at 37ºC. The assay was performed as per the standard Invitrogen Screening Kit protocol. The reactions were carried out at 37ºC in a reaction volume of 0.1 ml/well in 96-well black plates. The assay mixture contained 100 mM Potassium phosphate buffer pH 8.0, containing 10 µM DBOMF, 1.0 pmole CYP3A4 and the NADPH regenerating system (1.3 mM NADP+, 3.3 mM G6P, 3.3 mM Mg Cl_2, 0.4U/ml G6PDH). Fluorescein formation was measured fluorometrically on the Biotek Synegy HT plate reader (excitation wavelength of 485/20 nm and emission wavelength of 528/20 nm). Changes in fluorescence were recorded for 10 min as relative fluorescence units (RFU). Fluorescein, the metabolite of DBOMF, was used to generate a standard curve.

The standard curve of fluorescein was prepared using a range of concentrations of fluorescein (0, 39.1, 78.1, 156.3, 312.5, 625, 1250 pmol/ ml). The assay for generation of the standard was performed in 96-well black plates. The fluorescent values (RFU) were recorded on the Biotek Synegy HT plate reader using an excitation

wavelength of 485/20 nm and emission wavelength of 528/20 nm. Standard curve was plotted and fluorescein concentrations in test samples were measured using the equation from the standard curve. The standard curve is shown in Figure 4.10 (A).

Co-expression of cytochrome b_5 with CYP3A4 and ΔhRDM significantly improved the CYP3A4 catalytic activity which is in agreement with the reports that cytochrome b_5 stimulates CYP3A4 catalytic activity towards its substrates (Figure 4.10 (B); Table 4.3).

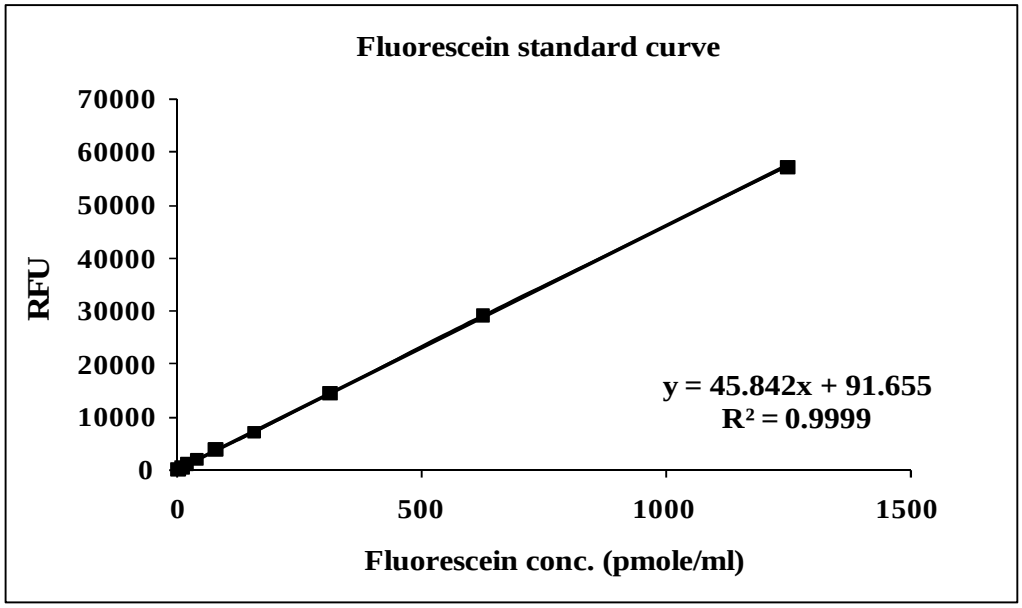

Figure 4.10 (A). The fluorescein standard curve. The curve was generated as described in Section 4.9.

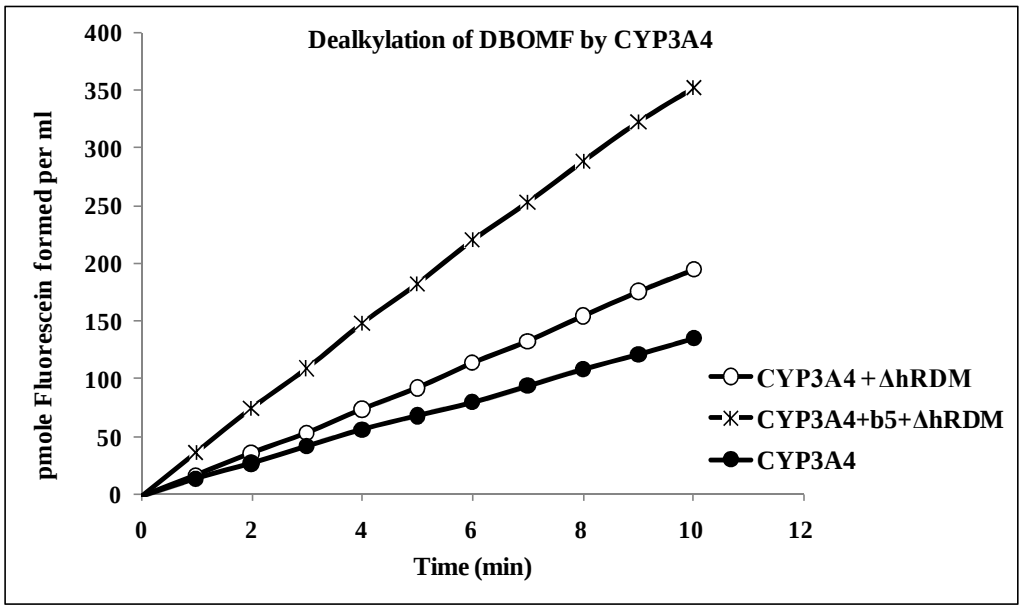

Figure 4.10 (B). Increase in CYP3A4 catalytic activity by co-expression of the third protein cytochrome b_5 in Sf9 cells. Sf9 cells were infected with CYP3A4 alone, co-infected with ΔhRDM and also co-infected with cytochrome b_5 as described in Section 4.9. The catalytic activity of CYP3A4 was measured in microsomes prepared at 63h post-infection. DBOMF assay was performed as described in Section 4.9.

Table 4.3. CYP3A4 enzyme reaction rates in co-expressed microsomes, as tabulated from Figure 4.10 (B). Sf9 cells were infected with CYP3A4 alone, co-infected with ΔhRDM and also co-infected with cytochrome b_5 as described in Section 4.9. The enzyme reaction rates were measured in DBOMF assay. DBOMF assay was performed as described in Section 4.9.

Microsomes	CYP3A4 reaction rates (pmole fluorescein formed/ min/ pmole of CYP3A4)
CYP3A4	1.351
CYP3A4+ ΔhRDM	1.973
CYP3A4+ΔhRDM+ b_5	3.5508

4.10 NADPH-cytochrome P450 reductase (CPR) activity assay

NADPH-cytochrome P450 reductase (CPR) activities of human and yeast CPRs in co-expressed microsomes were measured by the reduction of the tetrazolium salt, MTT as described in 'Materials and Methods' (Section Number 2.4.7). In CYP3A4 and CPR co-expressed microsomes, reduction potential of yRD is higher than that of hRD (Table 4.4), which means yRD can reduce MTT more efficiently than hRD. However, the amount of CYP3A4 holoprotein in cells co-producing yRD is the same as in cells that co-express hRD (Table 4.1). Both the CPRs, hRD and yRD reduce holoprotein content with equal magnitude without decreasing the apoprotein levels (Figure 4.7).

Both the CPRs must be causing oxidative damage to microsomal proteins which results in decrease in holoprotein levels. Reduction potential of ΔhRDM towards MTT is lower than hRD and yRD. Concomitantly, the amount of CYP3A4 holoprotein in cells co-producing ΔhRDM is higher than that in cells that co-express hRD or yRD (Table 4.1). As ΔhRD does not anchor to the microsomal membranes, the microsomes prepared from cells co-expressing ΔhRD do not show any microsomal reductase activity.

Table 4.4. NADPH cytochrome P450 reductase (CPR) activities exhibited by yeast and human CPRs in CYP3A4 co-expressed microsomes. Sf9 cells were co-infected with CYP3A4 baculoviruses (MOI 1.0 pfu/cell), cytochrome b5 baculoviruses (MOI 0.1 pfu/cell), CPR baculoviruses (MOI 0.1 pfu/cell) and microsomes were prepared 63 h post-infection. CPR activity was measured using MTT as described in 'Materials and Methods' (Section Number 2.4.7). The moles of MTT reduced per minute per mg of protein were calculated.

CPR Species	Reductase activity (nmole MTT reduced/min/mg protein)
CYP3A4+ b_5	21.2 ± 1.3
CYP3A4+hRD+ b_5	238.9 ± 31.7
CYP3A4+ΔhRD+ b_5	19.7 ± 1.9
CYP3A4+ΔhRDM+ b_5	169.9 ± 18.3
CYP3A4+yRD+ b_5	295.8 ± 29.9

4.11 CYP3A4 enzymatic activities in the presence of CPRs and cytochrome b_5 – DBOMF dealkylation activity

DBOMF dealkylation activities were determined in microsomal fractions prepared from Sf9 cells co-infected for 63 h with CYP3A4+b_5, CYP3A4+b_5+hRD, CYP3A4+b_5+ΔhRD, CYP3A4+b_5+ΔhRDM and CYP3A4+b_5+yRD baculoviruses. The production of the metabolite fluorescein from Vivid® fluorogenic substrate dibenzyl-oxymethyl-fluorescein (DBOMF) was measured for 15 min at 37ºC. The assay was performed as per the standard Invitrogen Screening Kit protocol. The reactions were carried out at 37ºC in a reaction volume of 100 µl/well in 96-well black plates. The assay mixture contained 100 mM Potassium phosphate buffer pH 8.0, containing 10 µM DBOMF , 1.0 pmole CYP3A4 and the NADPH regenerating system (1.3 mM NADP+, 3.3 mM G6P, 3.3 mM $MgCl_2$, 0.4U/ml G6PDH). Fluorescein formation was measured fluorometrically on the Biotek Synergy HT plate reader (excitation wavelength of 485/20 nm and emission wavelength of 528/20 nm). Changes in fluorescence were recorded for 10 min as relative fluorescence units (RFU). Metabolite of DBOMF, fluorescein, was used to generate a standard curve (Figure 4.10 (A)).

CYP3A4+b_5 showed minimal activity whereas both CYP3A4+b_5+hRD and CYP3A4+b_5+ΔhRDM exhibited much higher DBOMF dealkylation activity. However, the catalytic activity of CYP3A4+b_5, in the presence of hRD and ΔhRDM, is significantly higher than that in the presence of yRD (Figure 4.11 and Table 4.5), which is not consistent with the fact that yRD shows higher MTT reduction potential than hRD (Table 4.4). This observation indicates that the cause of poor CYP3A4 activity in the

presence of yRD cannot be due only to oxidative damage since yRD and hRD show similar ROS induction potential, as shown in Chapter 3 (therefore, one would expect the same magnitude of oxidative damage to the CYP). It is more likely that, in the specific intracellular environment of insect cells, co-expressed CYP3A4 and yRD do not form the correct spatial orientation that would support human CYP catalytic activity.

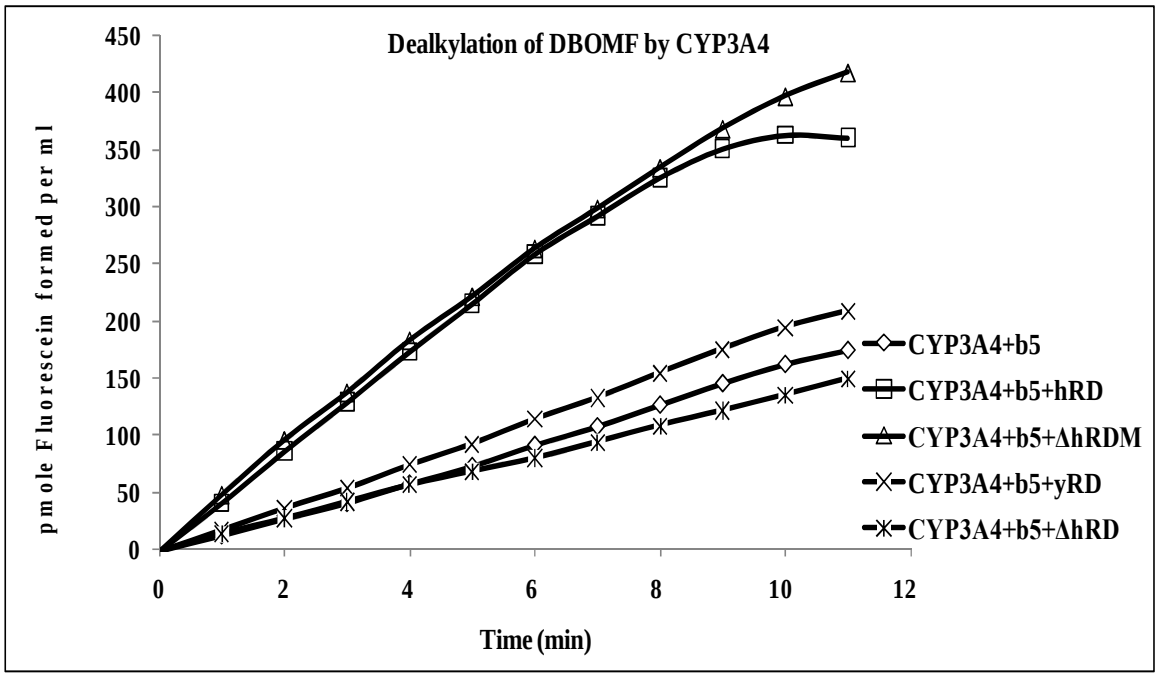

Figure 4.11. Kinetic analysis of CYP3A4 catalytic activity towards dealkylation of DBOMF. Sf9 cells were co-infected with CYP3A4, cytochrome b_5 and the CPR baculoviruses at an MOI of 1, 0.1 and 0.1 pfu/ cell, respectively. The catalytic activity of CYP3A4 was measured in microsomes prepared at 63h post-infection. DBOMF assay was performed as described in Section 4.11.

Table 4.5. CYP3A4 enzyme reaction rates in co-expressed microsomes, as tabulated from Figure 4.11. Sf9 cells were co-infected with CYP3A4, cytochrome b_5 and the CPR baculoviruses at an MOI of 1, 0.1 and 0.1 pfu/ cell, respectively. The reaction rates were measured in microsomes prepared at 63h post-infection. DBOMF assay was performed as described in Section 4.9.

Microsomes	CYP3A4 reaction rates (pmole fluorescein formed/ min/ pmole of CYP3A4)
CYP3A4+ b_5	1.653
CYP3A4+hRD+ b_5	3.536
CYP3A4+ΔhRD+ b_5	1.353
CYP3A4+ΔhRDM+ b_5	3.851
CYP3A4+yRD+ b_5	1.955

4.12 Measurement of reactive oxygen species (ROS) induction by CPR in presence of cytochrome b_5

The experiments presented in Chapter 3 show that ROS induced by CPRs are responsible for CYP holoenzyme destruction. The results presented in Chapter 3 also show that ROS induced by yRD and hRD was higher than ROS induced by ΔhRDM. Like CYP2D6, as described in Chapter 3, CYP3A4 holoenzyme levels changed

depending on which reductase species was co-expressed (Table 4.1). yRD and hRD co-expression resulted in lower CYP3A4 holoenzymes content than with ΔhRDM co-expression. CYP3A4 holoenzyme content was not significantly different when co-expressed with yRD or hRD. Despite this, CYP3A4 catalytic activity supported by yRD was minimal (Figure 4.11).

To determine whether the oxidative damage to CYP3A4 by CPRs is accelerated by co-expressing the third protein cytochrome b_5, reactive oxygen species (ROS) in cells infected with CPR and cytochrome b_5 baculoviruses were measured. The fluorescent dye 2',7'-dichlorodihydrofluorescein diacetate (H_2DCFDA) was used for measuring reactive oxygen species induction in Sf9 cells. Sf9 cells were seeded in 96-well tissue culture grade black plates at a density of 20,000 cells/well. After cell attachment on the substratum, they were infected with hRD, ΔhRDM and yRD baculoviruses (at an MOI of 2 pfu/cell) and also co-infected with cytochrome b_5 baculovirus (at an MOI of 0.2 pfu/ml) for 72 h. At 72 h, medium was removed from the wells and 100 µl of 10 µM H_2DCFDA in PBS was added to each well. The plate was again incubated for 30 min to allow the dye to enter the cells. The oxidation of intracellular non-fluorescent H_2DCF to highly fluorescent DCF was measured on a fluorometer (Bio-Tek). Excitation 485/20 nM and emission 528/20 nM filter sets were used to measure the fluorescence. Blank values, indicating the fluorescence of the dye in PBS (blank without cells), were subtracted from all samples. Percentage inductions of ROS in baculovirus-infected cells over control cells (without baculovirus infection) were calculated.

yRD and hRD exhibited stronger induction of ROS than ΔhRDM. However, co-expression of b5 with CPRs did not noticeably alter the ROS levels induced by CPRs in insect cells (Table 4.6).

Table 4.6. Measurement of ROS induction by hRD, ΔhRDM and yRD. ROS was measured by using H_2DCFDA dye. Sf9 cells were infected with CPR baculoviruses (at an MOI of 2 pfu/ml) and also co-infected with cytochrome b_5 baculoviruses (at an MOI of 0.2 pfu/ml) for 72 h. At 72 h, H_2DCFDA assay was performed as described in Materials and Methods (Section Number 2.4.10). The oxidation of intracellular non-fluorescent H_2DCF to highly DCF was measured on a fluorometer as described in Section 4.12.

Microsomes	Percentage ROS Induction
hRD	34.45 ± 4.6
hRD+b_5	31.95 ± 1.6
ΔhRDM	16.395 ± 0.56
ΔhRDM+b_5	17.56 ± 3.9
yRD	44.45 ± 1.3
yRD+b_5	46.35 ± 4.45

4.13 Coupling efficiency of the two CPRs, hRD and ΔhRDM, with CYP3A4

Although activities supported by hRD and ΔhRDM of CYP3A4 as measured by DBOMF dealkylation assays are similar, the reduction potential of both the reductases towards MTT is different. Reduction potential of ΔhRDM towards MTT is much lower than that of hRD and yRD which indicates that CYP3A4 activity supported by per unit of ΔhRDM is better than that supported by hRD or yRD. This observation is presented in terms of coupling efficiencies of hRD, ΔhRDM and yRD with CYP3A4.

To calculate the percent coupling efficiency, the CYP3A4 activity in DBOMF assay was divided by CPR activity in the MTT assay. The percent relative coupling efficiency for hRD and yRD was calculated in comparison with ΔhRDM, considering ΔhRDM activity as 100% (Table 4.7). The percent coupling efficiency values show that ΔhRDM couples better with CYP3A4 than its native form hRD. The percent coupling efficiency of yRD with CYP3A4 is extremely poor in comparison to ΔhRDM.

Table 4.7. Percentage relative coupling efficiency of hRD and yRD with CYP3A4 was calculated in comparison with ΔhRDM using microsomes that were prepared from Sf9 cells after 63 h of baculovirus infection. The product formed (fluorescein) from the DBOMF assay and CPR activity measured in the MTT assay were used for the calculations. CYP3A4 activity was divided by CPR activity and percent relative coupling efficiency was calculated.

Microsomal samples	Percentage Relative coupling efficiency
CYP3A4+ ΔhRDM+ b_5	100
CYP3A4+ hRD+ b_5	65.31
CYP3A4+ yRD+ b_5	29.17

4.14 Conclusions

Cytochrome P450 enzymes (CYPs) require an electron donor enzyme, a NADPH cytochrome P450 reductase (CPR), to support their catalytic activities. The baker's yeast, *Saccharomyces cerevisiae*, has been widely used for many years for expression of human CYPs because it contains intracellular compartments like the endoplasmic reticulum that are similar to those in human cells. Yeast also contains a CPR, the electron donor enzyme, which is quite similar to that present in humans.

In the past three decades, many scientific papers have been published on the expression of human and mammalian cytochrome P450 enzymes in yeast. Most of these studies have used the yeast CPR as an electron donor to activate human CYPs (Yabusaki et al 1995; Ellis et al 1992). There are a number of reports on the co-expression of the yeast CPR and a human CYP so as to obtain active CYPs on yeast microsomes (Eugster et al 1993; Ellis et al 1992; Renaud et al 1990; Brian et al 1990). These activities vary from being quite good to extremely poor (also our own unpublished observations).

Our results in Chapter 3 indicated that the yeast CPR, yRD, could act as an efficient alternative electronic donor to the human CPR, hRD, for the general activation of human CYPs. We wanted to explore if the results obtained from co-expression studies of yRD and CYP2D6, which express optimal activity in the absence of cytochrome b_5, are applicable in the context of another CYP where the presence of

cytochrome b_5 is essential. We chose CYP3A4, which is also widely used for drug metabolism studies, for these studies. We therefore co-expressed the yeast CPR and human CYP3A4 enzymes in insect cells along with cytochrome b_5.

The beauty of insect cell expression systems using baculoviruses is that one can vary the CYP to CPR ratio by infecting the cells with baculoviruses at different MOIs. In this Chapter we have co-expressed different human CPRs (hRD, ΔhRD and ΔhRDM) with human CYP3A4 at optimal MOIs and have compared our results with experiments that allow co-expression of the yeast CPR (yRD) and CYP3A4 using similar MOIs. All co-expression studies were performed in the presence of human cytochrome b_5.

Reduction in human CYP levels has been reported when CYPs are co-expressed with CPR in baculovirus expression systems (Chen et al 1997; Wang et al 1996; Paine et al 1996). Our results are in agreement with these reports. We have linked this effect to the increased production of hydroxyl radicals. However in the case of yRD, we find that oxidative damage to CYP3A4 may not be the complete reason behind yRD's inability to support CYP3A4 activity. The yRD enzyme activity towards its artificial substrate MTT was higher than hRD and ΔhRDM, which shows that yeast CPR is expressed in insect cells with very good reduction potential.

CYP3A4, when co-expressed with hRD or ΔhRDM, on insect cell microsomes exhibits strong catalytic activity towards de-alkylation of DBOMF (Figure 4.11)

whereas CYP3A4 co-expressed with yRD manifests extremely poor activity. This observation would indicate that yRD is unable to couple efficiently with human CYP3A4. The CYP3A4 activity in presence of cytochrome b_5 and yeast CPR is nearly as low as the activities observed in the microsomes that co-express CYP3A4 and b_5.

Our results from the H2DCFDA assay show that both yRD and hRD induce higher amounts of reactive oxygen species than ΔhRDM (Table 4.4). In spite of similar amounts of CYP3A4 holoprotein content in microsomes co-expressing yRD and hRD (Table 4.1), CYP3A4 catalytic activity in the presence of yRD is unusually poor as compared to CYP3A4 activity in the presence of hRD (Figure 4.11). Therefore, it is very likely that oxidative damage is not the complete reason for the poor CYP3A4 catalytic activity in the presence of yRD. It is possible that the specific intracellular environment in insect cells may not support the interaction of yRD with human CYP3A4 in the presence of human cytochrome b_5.

This may suggest the importance for a CYP and the CPR to have correct spatial orientation of their redox centres for effective electron transfer. Possibly, the human CYP3A4 and the yeast CPR do not form the correct spatial orientation on the surface of the insect cell microsomes, in the presence of human cytochrome b_5, that would allow effective electron transfer to the CYP3A4 active site. Recently, protein crystal structure of yeast CPR has been solved which reveals that it has a second FMN binding site at the interface of the connecting and FMN binding domains. The two FMN binding domains have different accessibilities to the bulk solvent and different amino acid environments

(Lamb et al 2006). Electrostatic forces have been shown experimentally to limit accessibility of electron transfer sites on CPR for its charged redox partners (Voznesensky and Schenkman 1994). One could speculate that the human cytochrome b_5, bound to CYP3A4, plays a major role in hindering the transfer of electrons from the yeast CPR, yRD, to the CYP3A4 active site.

In conclusion, our findings demonstrate that (1) yRD perceptibly lacks the ability to support human CYP3A4 catalytic activity on insect cell ER membranes, in the presence of cytochrome b_5; (2) oxidative damage cannot be the only reason behind yeast CPR being unable to support CYP3A4 activity; (3) in comparison with yRD, hRD and ΔhRDM are probably the best redox partners for a human CYP which demands cytochrome b_5 for manifestation of optimal activity – this could be due to the inability of CYP3A4 and yRD to form a mutually correct spatial orientation in the intracellular endoplasmic reticular environment afforded by insect cells; (4) the variant hRD enzyme, ΔhRDM, appears to be far superior to the wild-type hRD in terms of its ability to couple with CYP3A4 and to produce higher amounts of a spectrally-active, catalytically-useful CYP enzyme.

Chapter-5 Interaction of CYP1A1, CYP1B1, CYP1A2, CYP2C8 and CYP2E1 with the CPRs in Sf9 cells

5.1 Introduction

The multiple isoforms of cytochrome P450 enzymes metabolise a wide variety of xenobiotic compounds such as drugs and carcinogens, as well as endobiotics such as prostaglandins and steroids. Microsomal P450-mediated monooxygenase activity supported by NADPH requires an interaction between flavoprotein NADPH-cytochrome P450 reductase (CPR) and cytochrome P450 (CYP). These proteins have been identified as the simplest system that possesses monooxygenase function; however, little is known about the organisation of these proteins on microsomal membranes (Backes and Kelley 2003).

The results presented in Chapters 3 and 4 show that CPRs are responsible for reduction in spectrally active CYP enzymes and they also modulate CYP catalytic activity. In the case of CYP2D6 and CYP3A4 we have observed different magnitudes of decrease in the CYP holoprotein levels depending on which CPR species is co-expressed. It has been shown in protein binding assays, where affinities of various human CYPs for human CPR were studied, that there are differences in the interactions of CYP enzymes with the accessory proteins, CPR and cytochrome b_5 (Shimada et al. 2005).

Our objective was to perform a comparative study of the interactions of individual CYPs with diverse CPRs so as to determine if there are any subtle differences in the affinity of a specific CYP for a CPR. In order to conduct this type of study, we have taken the approach of ascertaining a particular CYP's ability to couple with a CPR via measurement of CYP enzyme catalytic activities. By studying CYP coupling efficiencies, it would be possible to investigate the comparative ability of CPRs to support individual CYP catalytic activities. This will possibly aid in our aim to develop an improved cytochrome P450 expression system by defining a superior CPR that would generally allow improved CYP catalytic activities.

In order to elucidate the ability of CPRs to couple with individual CYPs, we studied the CPRs viz. hRD, ΔhRDM and yRD in the context of three other CYPs – CYP1B1, CYP1A2 and CYP2E1. As ΔhRD does not anchor on the microsomal membranes, it was not pursued any further. After having obtained indications that ΔhRDM indeed could be a superior CPR, we went on to study enzyme activities of CYP1A1 and CYP2C8 in the context of ΔhRDM only. In the case of CYP2E1 and CYP2C8, apart from CPR, a third protein cytochrome b_5 was also co-expressed. Cytochrome b_5 is known to augment CYP2C8 and CYP2E1 mediated monooxygenase reactions (Porter, 2002).

About half of the 57 human CYP isoforms belong to the families 1, 2 and 3 (Nelson, 1999). The majority of CYP isoforms in these families are involved in xenobiotic metabolism (Gonzalez 1992; Capdevila et al. 2000). Most of the CYPs are

expressed in the human liver, but some are also expressed in extra-hepatic tissues (Raunio et al. 1995). The expression is predominant in the liver, probably due to its major role in the utilisation of all ingested substances by the human organism. Expression of CYPs in extra-hepatic tissues, such as lung and skin possibly act as the first line of defence against exogenous compounds.

5.1.1 CYP1 family

CYP1A1, CYP1A2 and CYP1B1, together form the CYP1 family (Nelson et al. 1996). The CYP1 family members are induced by polycyclic aromatic hydrocarbons (PAH), 2,3,7,8-Tetrachlorodibenzo-*p*-dioxin (TCDD) (Schmidt and Bradfield 1996), and cigarette smoking (Willey et al. 1997; Zevin and Benowitz 1999). All the three isoforms are transcriptionally regulated by the aryl hydrocarbon receptor-aryl hydrocarbon receptor nuclear translocator pathway (AHR-ARNT pathway) (Schmidt and Bradfield 1996). They can metabolise PAHs into carcinogenic intermediates (Shimada et al. 1996) and thus they are implicated in the formation of chemically caused cancers (Nebert et al. 1996). From the CYP1 family we have studied CYP1A1, CYP1A2 and CYP1B1 in conjunction with the different CPRs; the results of their affinities towards the CPRs are presented in this chapter.

5.1.1.1 CYP1A1

Constitutive expression of CYP1A1 in the human liver and in extra-hepatic tissues is very low (Edwards et al. 1998). However it is highly inducible by PAHs and

also by cigarette smoke (Anttila et al. 1991). It is inducible by AHR ligands in many tissues including lung, lymphocytes, mammary gland, and placenta (Raunio et al. 1995). In human primary hepatocytes, CYP1A1 is induced by the AHR agonists, PAH, 3-methylcholanthrene and omeprazole (Rodríguez-Antona et al. 2000; Bowen et al. 2000). CYP1A1 is responsible for the activation of pro-carcinogens, and have been linked with chemical-induced cancers such as lung cancer (Raunio et al. 1995).

5.1.1.2 CYP1A2

CYP1A2 is one of the main drug metabolising enzymes and is responsible for metabolism of several drugs (Landi et al. 1999). It is known to be expressed only in liver (Raunio et al. 1995) and constitutes quite a substantial amount (about 13%) of the total hepatic CYP content (Shimada et al. 1994, Imaoka et al. 1996). It activates PAHs, nitrosamines, aflatoxin B_1, and especially aryl amines into forms that can bind to DNA and produce mutations (Aoyama et al. 1990; Shimada et al. 1996; Macé et al. 1997; Hammons et al. 1997; Hecht 1998). The regulation of CYP1A2 is observed to be both AHR-ARNT–dependent and independent and is induced by cigarette smoke, charbroiled meat, indole-3-carbinol (contained in cruciferous vegetables), phenytoin, rifampicin, and omeprazole (Landi et al. 1999).

5.1.1.3 CYP1B1

The expression of CYP1B1 in human liver is nonexistent (Sutter et al. 1994; Shimada et al. 1996; Hakkola et al. 1997; Edwards et al. 1998; Tang et al. 1999).

However it expresses in many other tissues such as kidney, prostate, mammary gland, and ovary (Sutter et al. 1994; Shimada et al. 1996; Tang et al. 1999). CYP1B1 is also responsible for the metabolism of PAHs and aryl amines (Shimada et al. 1996). It is known to overexpress in cancer tumours (Murray et al. 1997). The induction of CYP1B1 is regulated by the AHR-ARNT pathway (Sutter et al. 1994; Savas and Jefcoate 1994), although the responses of CYP1B1 to AHR ligands differ from those of CYP1A1 (Hakkola et al. 1997).

5.1.2 CYP2 family

The human CYP2 family is a heterogeneous group of enzymes and contains the subfamilies CYP2A, CYP2B, CYP2C, CYP2D, CYP2E, CYP2F, and CYP2J (Nelson et al. 1996) and accounts for about 20% of the human total liver CYP content (Shimada et al. 1994, Imaoka et al. 1996). CYP2B6, CYP2D6, CYP2E1, CYP2F1, and CYP2J2 are the only functional members in their respective subfamilies, whereas the CYP2A subfamily contains two functional enzymes (CYP2A6 and CYP2A13) and CYP2C subfamily contains four functional enzymes (CYP2C8, CYP2C9, CYP2C18 and CYP2C19). Unlike the CYP1 family, the members of the CYP2 family do not share similar features of regulation. The substrate and tissue specificities of these enzymes also differ markedly (Nelson et al. 1996).

From the CYP2 family we have studied the expression of CYP2D6 and CYP2E1 in conjunction with the CPRs, hRD, ΔhRDM and yRD, whereas CYP2C8 has been

expressed only in conjunction with ΔhRDM. The results from CYP2D6 have already been presented in Chapter 3 but the results from CYP2C8 and CYP2E1 are presented in this chapter.

5.1.2.1 CYP2C

CYP2C8 is known to catalyse 6-alpha hydroxylation of taxol, a drug used in treating breast cancer. CYP2C9 is the main CYP2C present in the human liver, followed by CYP2C8 and CYP2C19 (Edwards et al. 1998). The CYP2C18 protein is not expressed in the liver (Richardson et al. 1997). CYP2C mRNA and protein are induced in primary hepatocytes by phenobarbital and rifampicin (Morel et al. 1990; Chang et al. 1997). Pharmaceutical substrates for CYP2C include diazepam, omeprazole, mephenytoin, tolbutamide, and warfarin (Guengerich 1995) as well as many non-steroidal anti-inflammatory drugs (Pelkonen et al. 1998). Selective substrates include taxol for CYP2C8, tolbutamide for CYP2C9, and mephenytoin for CYP2C19 (Pelkonen et al. 1998).

5.1.2.2 CYP2E1

CYP2E1 is the only isoform in this subfamily (Nelson et al. 1996). About 7% of the liver CYP content consists of CYP2E1 (Shimada et al. 1994; Imaoka et al. 1996). It is also expressed in lung and brain (Raunio et al. 1995). The CYP2E1 enzyme has been studied extensively due to its role in the metabolism of ethanol and also as an activator of chemical carcinogens (Lieber 1997). Most of the over 70 substrates demonstrated are

small and hydrophobic compounds (Ronis et al. 1996) that include a few pharmaceuticals such as paracetamol, chlorzoxazone, enflurane, and halothane (Guengerich 1995). Disulfiram is a clinically used inhibitor of CYP2E1 (Guengerich and Shimada 1991).

Many substrates of CYP2E1 are also CYP2E1-inducing agents – they include acetone, ethanol, pyridine, pyrazole, and isoniazid (Ronis et al. 1996). Ethanol intake increases the human CYP2E1 content in the liver (Perrot et al. 1989), and it is also induced in lymphocytes of insulin-dependent diabetics (Song et al. 1990).

5.2 Outline of the chapter

The results obtained with CYP2D6 and CYP3A4 and their interactions with the CPRs have been presented in Chapters 3 and 4. The findings presented in those chapters show that ROS induced by CPRs is responsible for decrease in CYP holoprotein content and ΔhRDM is relatively superior in terms of its ability to produce high levels of a spectrally active CYP as well as in terms of its ability to support CYP2D6 and CYP3A4 catalytic activities. We have also shown that co-expression of cytochrome b_5 does not increase or decrease the CPR's potential to induce ROS and thus may not have any role in causing damage to CYP holoprotein.

The ability of the CPRs to couple with individual CYPs was studied by co-expressing CPRs viz. hRD, ΔhRDM and yRD in the context of the three more CYPs – CYP1B1, CYP1A2 and CYP2E1. We also studied CYP1A1 and CYP2C8 but only in the context of ΔhRDM. The experiments that describe gene cloning and protein expression, measurement of CYP holoprotein contents and enzyme activities, and determination of coupling efficiencies are presented in this chapter. General experimental methodologies have already been highlighted in the 'Materials and Methods' chapter. However, methods which pertain to the specific CYPs in this chapter are also described here.

5.3 Gene cloning into pBluescript KS+ and pFastBac1

5.3.1 CYP1A1 cloning

Cytochrome P450 1A1 (CYP1A1) cDNA was isolated in our laboratory previously by PCR from a human liver cDNA library (Life Technology, Catalogue No 10422-012). CYP1A1 was isolated with the forward primer (5'- ATGGATCC**GC CACC**ATGCTT TTCCCAATCT CCATGTCGGC -3', the *BamHI* site and the Kozak sequence are marked with an underline and bold letters, respectively), and the reverse primer (5'-ATGTCGACCT AAGAGCGCAG CTGCATTTGG AAGTGC -3', the *Sal*I site is underlined).

The cDNA was further amplified using the above mentioned primers as described in 'Materials and Methods' (Section Number 2.2.2). The PCR product was

run on an agarose gel containing ethidium bromide and the DNA fragment of expected size was isolated and purified using Qiagen gel extraction kit according to the manufacturer's protocol. The purified DNA fragment was digested with *BamH*I and *Sal*I restriction enzymes and after digestion run again on an agarose gel that contained ethidium bromide. The digested DNA fragment was purified using a Qiagen gel extraction kit. CYP1A1 cDNA was then directionally ligated using T4 DNA ligase into pBluescript KS+ (digested with *BamH*I, *Sal*I). The ligation mixture was used for transforming *E. coli* DH5α competent cells, and colonies containing the correct recombinant constructs were identified with restriction analysis. Plasmids were extracted from positive clones. The experimental methods employed are detailed in 'Materials and Methods'. The cDNA sequence was confirmed by DNA sequencing and its alignment with reference sequence in the NCBI database. The resultant plasmid was named pBluKS+/Bam-Sal/CYP1A1 (Figure 5.1).

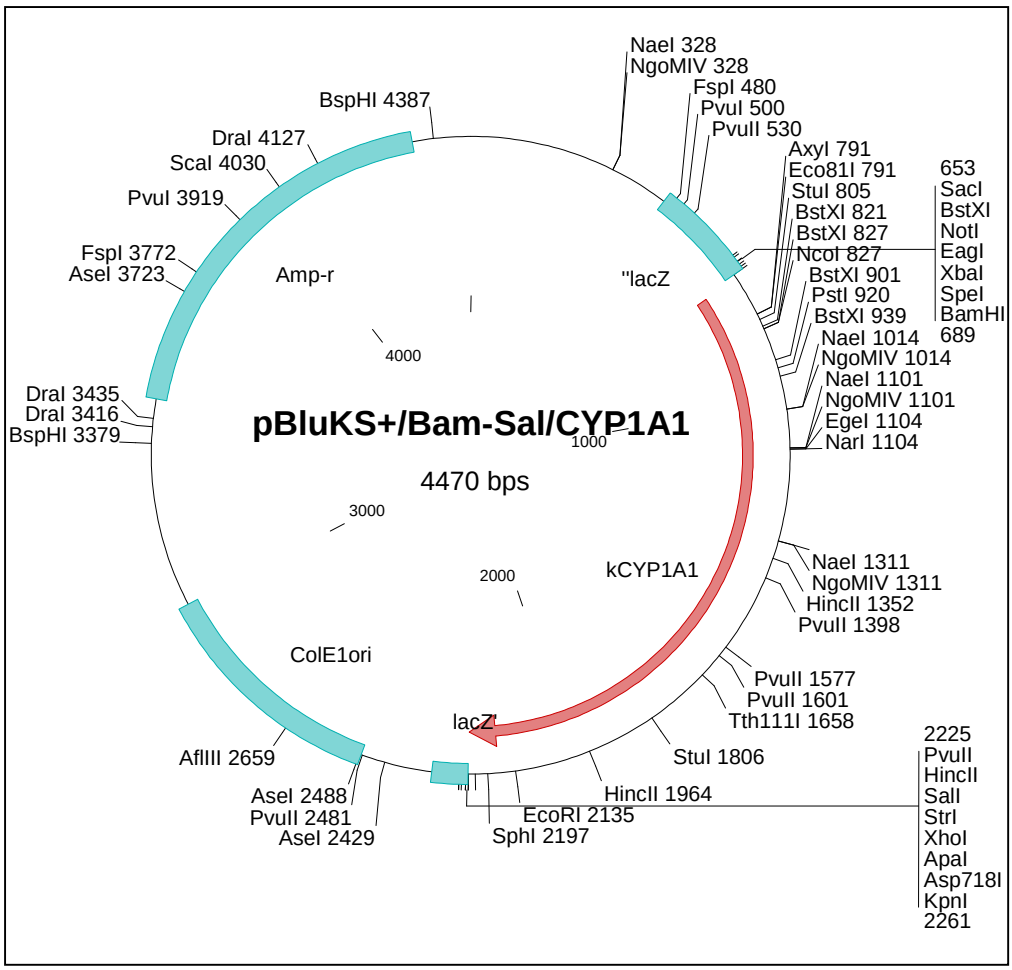

Figure 5.1. The plasmid map of pBluKS+/Bam-Sal/CYP1A1.

For subcloning CYP1A1 into the transfer vector, the *CYP1A1* gene was isolated from pBluKS+/Bam-Sal/CYP1A1 using the restriction enzymes, *BamH*I and *Sal*I. The digested fragment of CYP1A1 was gel purified and used for ligation into pFastBac1 (cut with *BamH*I, *Sal*I). The ligation mixture was used for transforming *E. coli* DH5α competent cells, and transformants were screened via restriction analysis (Figure 5.2(A)). The cDNA in the pFastBac1 vector was cloned under the control of polyhedrin promoter. The resultant recombinant transfer vector was named pFastBac1/Bam-Sal/CYP1A1 (Figure 5.2(B)).

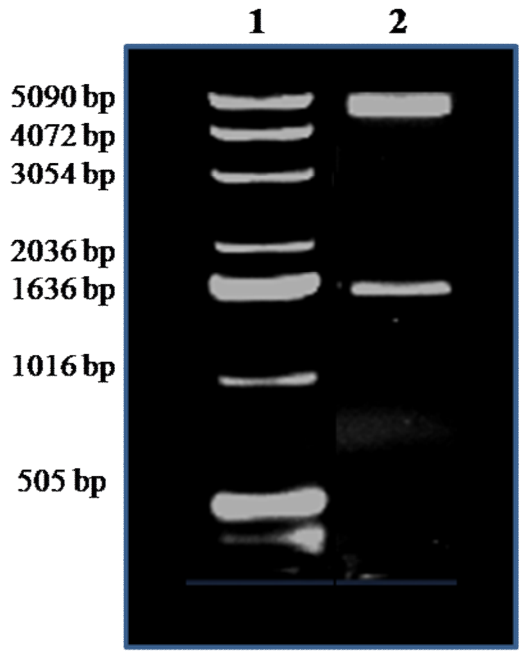

Figure 5.2 (A). Assessment of pFastBac1/Bam-Sal/CYP1A1 plasmid veracity by diagnostic restriction enzyme digestion. Digestion of pFastBac1/Bam-Sal/CYP1A1 construct by *BamH*I and *Sal*I (performed as described in 'Materials and Methods') produces two expected fragments of 4738 bp and 1551 bp**.** Lane 1, 1.0 kb DNA ladder for sizing linear double-stranded DNA fragments (Invitrogen, catalogue No- 15615-016); Lane 2, pFastBac1/Bam-Sal/CYP1A1 digested with *BamH*I, *Sal*I, expected fragments being 4738 bp and 1551 bp.

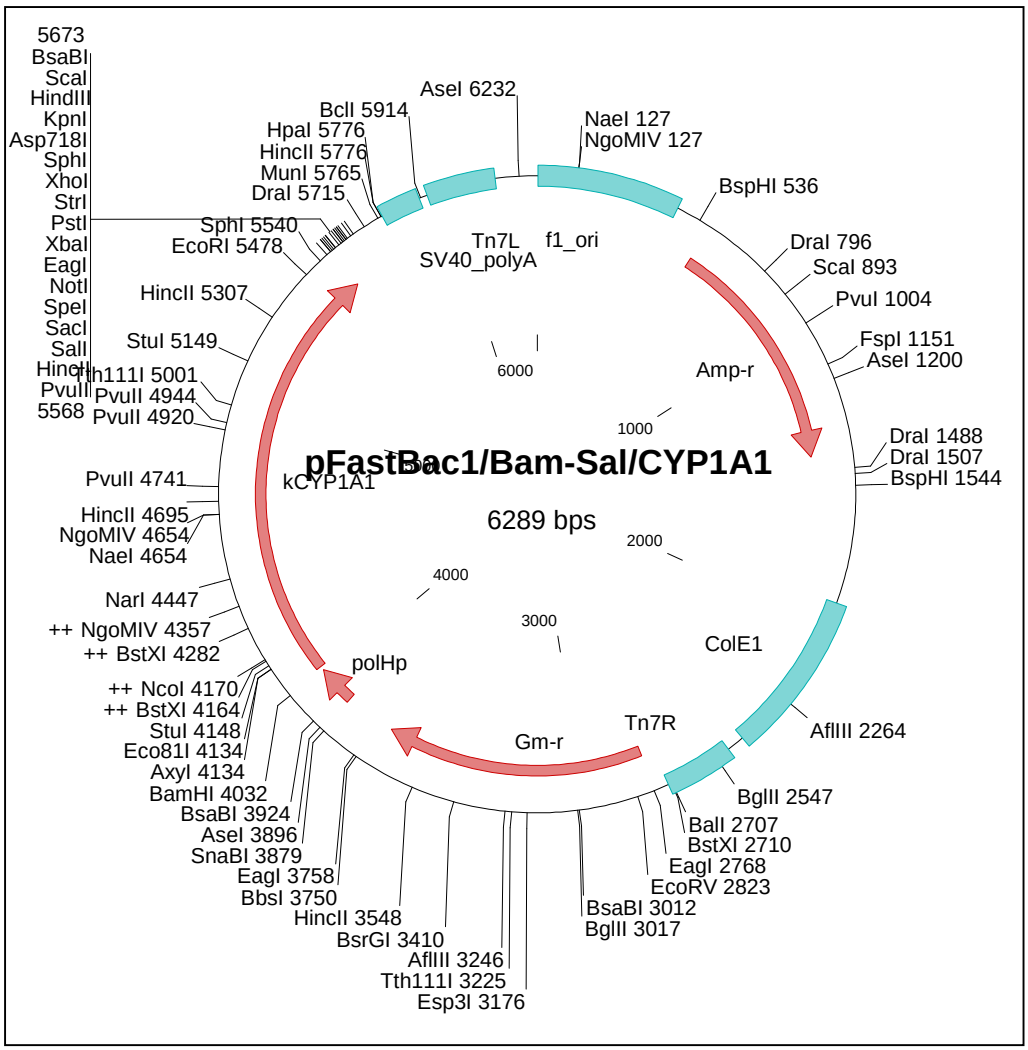

Figure 5.2 (B). The plasmid map of pFastBac1/Bam-Sal/CYP1A1.

5.3.2 CYP1B1 cloning

Cytochrome P450 1B1 (CYP1B1) cDNA was isolated in our laboratory previously by PCR from a human liver cDNA library (Life Technology, Catalogue No 10422-012). CYP1B1 was isolated with the forward primer (5'- ATGGATCC**GC CACC**ATGGGC ACCAGCCTCA GCCCGAACG -3', the *BamHI* site and the Kozak sequence are marked with an underline and bold letters respectively), and the reverse

primer (5'-ATGTCGACTT ATTGGCAAGT TTCCTTGGCT TG -3', the *Sal*I site is underlined).

The gene was amplified using the above mentioned primers as described in 'Materials and Methods' (Section Number 2.2.2). The PCR product was run on an agarose gel containing ethidium bromide (0.1 µg/ml) and the DNA fragment of expected size was isolated and purified using Qiagen gel extraction kit according to the manufacturer's protocol. The purified DNA fragment was digested with the restriction enzymes, *BamH*I, *Sal*I, and after digestion run again on an agarose gel that contained ethidium bromide. The digested cDNA fragment was purified using a Qiagen gel extraction kit. CYP1B1 cDNA was then directionally ligated using T4 DNA ligase into pBluescript KS+ (digested with *BamH*I-*Sal*I). The ligation mixture was transformed into *E. coli* DH5α competent cells, and colonies containing the correct recombinant constructs were identified with restriction analysis. Plasmids were extracted from positive clones. The experimental methods employed are detailed in 'Materials and Methods' (Section Number 2.2.11). The cDNA sequence was confirmed by DNA sequencing and its alignment with the reference sequence in the NCBI database. The resultant plasmid was named pBluKS+/Bam-Sal/CYP1B1 (Figure 5.3).

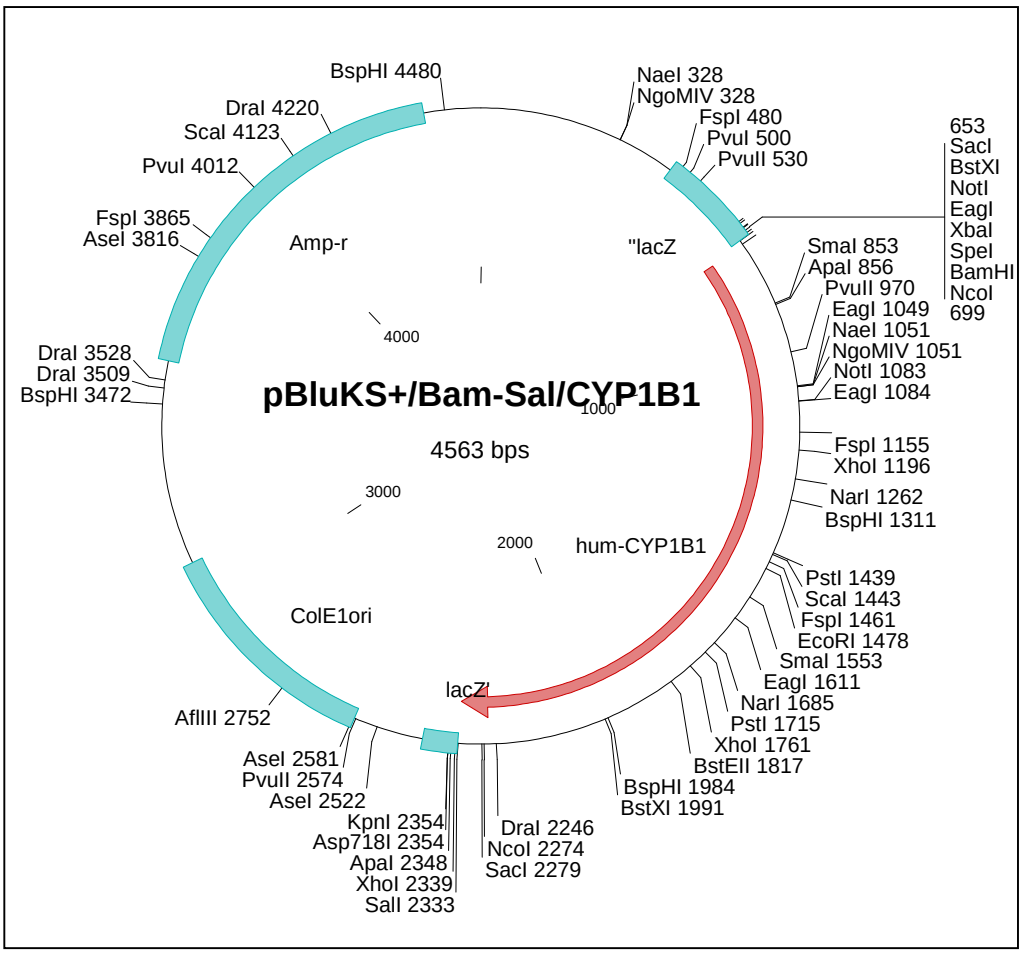

Figure 5.3. The plasmid map of pBluKS+/Bam-Sal/CYP1B1.

For subcloning of CYP1B1 into the transfer vector, the *CYP1B1* cDNA was isolated from pBluKS+/Bam-Sal/CYP1B1 using the set of restriction enzymes, *BamH*I and *Sal*I. The digested fragment of CYP1B1 was gel purified and used for ligation into pFastBac1 (cut with *BamH*I, *Sal*I). The ligation mixture was transformed into *E. coli* DH5α competent cells, and transformants were screened with restriction analysis (Figure 5.4(A)). The cDNA in the pFastBac1 vector was cloned under the control of polyhedrin promoter. The resultant recombinant transfer vector was named pFastBac1/Bam-Sal/CYP1B1 (Figure 5.4(B)).

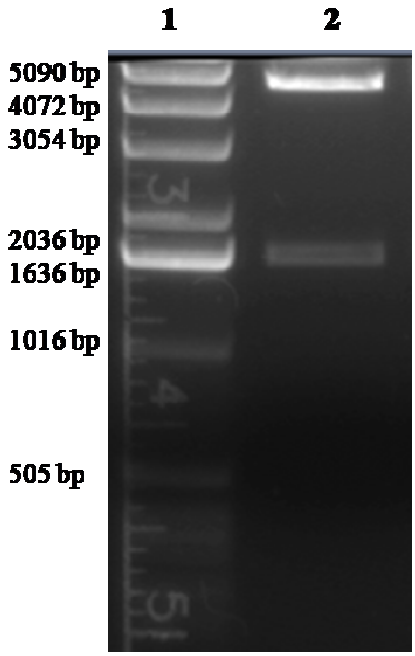

Figure 5.4 (A). Assessment of the pFastBac1/Bam-Sal/CYP1B1 plasmid veracity by diagnostic restriction enzyme digestion. Digestion of pFastBac1/Bam-Sal/CYP1B1 construct by *BamH*I, *Sal*I produces two expected fragments of 4738 bp and 1644 bp**.** The diagnostic restriction digestion was performed as described in 'Materials and Methods' (Section Number 2.2.4). Lane 1, 1.0 kb DNA ladder for sizing linear double-stranded DNA fragments (Invitrogen, Catalogue No 15615-016); Lane 2, pFastBac1/CYP1B1 digested with *BamH*I, *Sal*I, expected fragments being 4738 bp and 1644 bp.

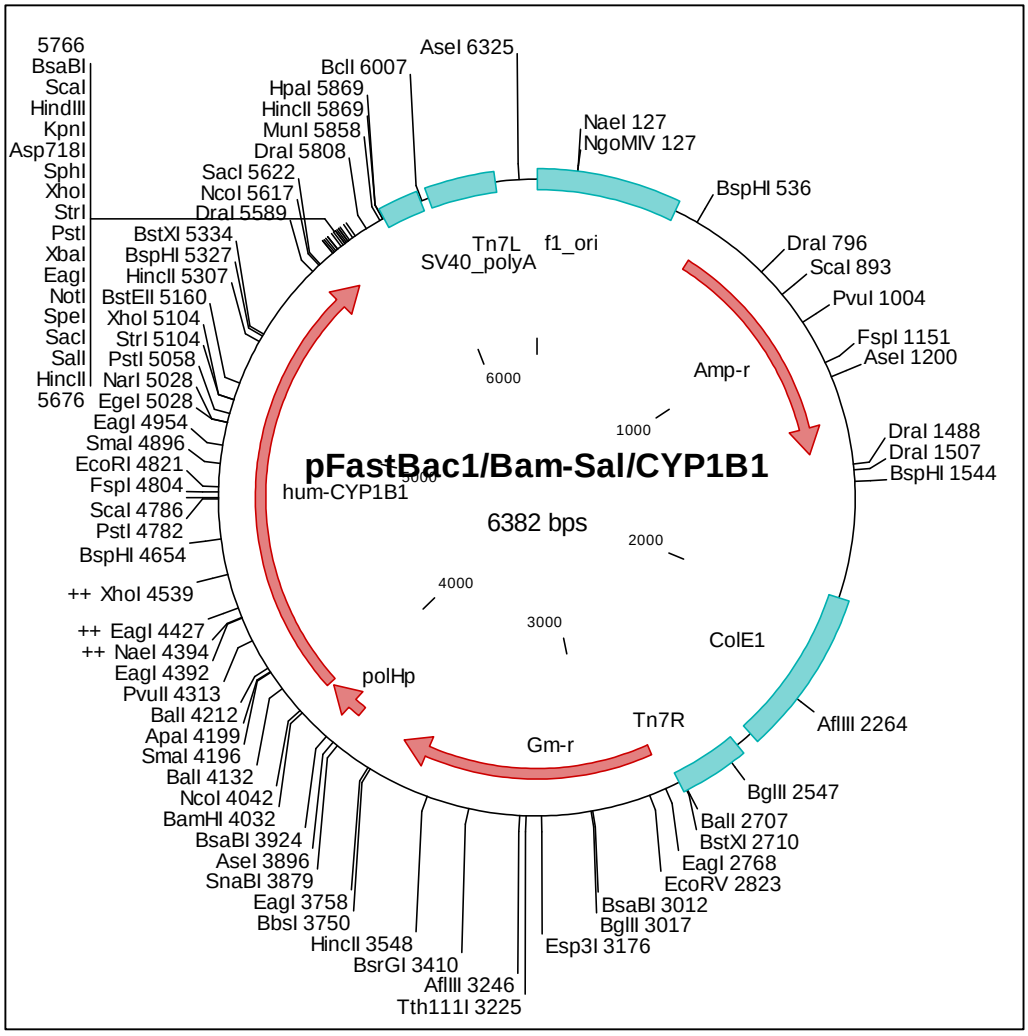

Figure 5.4 (B). The plasmid map of pFastBac1/Bam-Sal/CYP1B1.

5.3.3 CYP1A2 cloning

Human cDNA ORF clone for cytochrome P450 1A2 (CYP1A2, Reference ID: NM_000761) in pCMV6-XL4 vector was procured from Origene (Catalogue No SC119671). CYP1A2 cDNA was then isolated from the pCMV6-XL4 vector with the forward primer (5'- ATGGATCC**GC CACC**ATGGCA TTGTCCCAGT CTGTTCCC -3', the *BamHI* site and the Kozak sequence are marked with an underline and bold

letters, respectively), and the reverse primer (5'-ATCTCGAGTC AGTTGATGGA GAAGCGCAGC CGCGCC -3', the *Xho*I site is underlined).

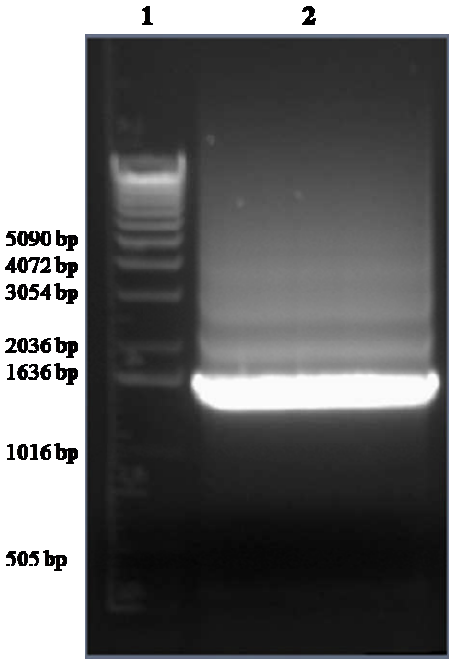

Figure 5.5 (A). CYP1A2 PCR amplified fragment generated by using CYP1A2 forward and reverse primers. The PCR and agarose gel electrophoresis was performed as described in 'Materials and Methods'. Lane 1, 1.0 kb DNA ladder for sizing linear double-stranded DNA fragments (Invitrogen, catalogue No- 15615-016); Lane 2, 1615 bp PCR fragment of CYP1A2.

The PCR product was run on an agarose gel (Figure 5.5(A)), containing ethidium bromide and DNA fragment of expected size (1615 bp) was isolated and purified using a Qiagen gel extraction kit according to the manufacturer's protocol. The purified DNA fragment was digested with the restriction enzymes, *BamH*I, *Xho*I and after digestion run again on an agarose gel that contained ethidium bromide. The digested DNA fragment was purified using a Qiagen gel extraction kit. *CYP1A2* gene

was then directionally ligated using T4 DNA ligase into pBluescript KS+ (digested with *BamH*I-*Xho*I). The ligation mixture was transformed into *E .coli* DH5α competent cells, and colonies containing the correct recombinant constructs were identified with restriction analysis (Figure 5.5 (B)). Plasmids were extracted from positive clones. The experimental methods employed are detailed in 'Materials and Methods'. The resultant plasmid was named pBluKS+/Bam-Xho/CYP1A2 (Figure 5.5 (C)).

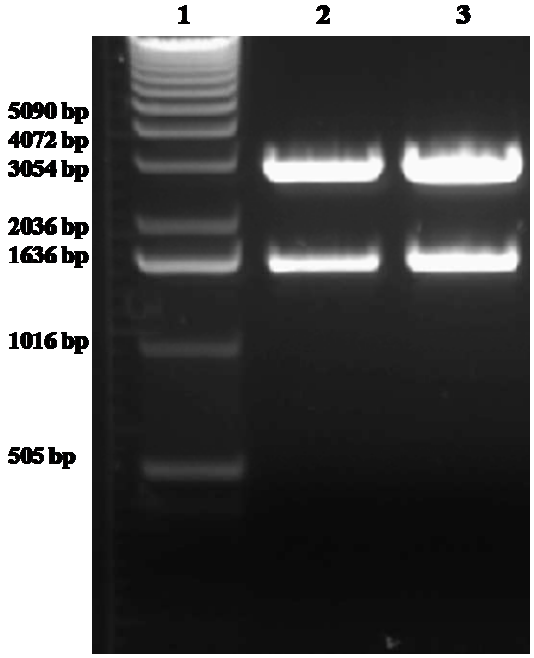

Figure 5.5 (B). Assessment of the pBluKS+/Bam-Xho/CYP1A2 plasmid veracity by diagnostic restriction enzyme digestion. Digestion of pBluKS+/Bam-Xho/CYP1A2 construct by *BamH*I, *Xho*I produces two expected fragments of 2913 bp and 1615 bp**.** The diagnostic restriction enzyme digestion was performed as described in 'Materials and Methods' (Section Number 2.2.4). Lane 1, 1.0 kb DNA ladder for sizing linear double-stranded DNA fragments (Invitrogen, Catalogue No 15615-016). Lane 2, Clone #1, pBluescript KS+/CYP1A2 digested with *BamH*I, *Xho*I, expected fragments being

2913 bp and 1615 bp; Lane 3, Clone #2, pBluescript KS+/CYP1A2 digested with *BamH*I, *Xho*I, expected fragments being 2913 bp and 1615 bp.

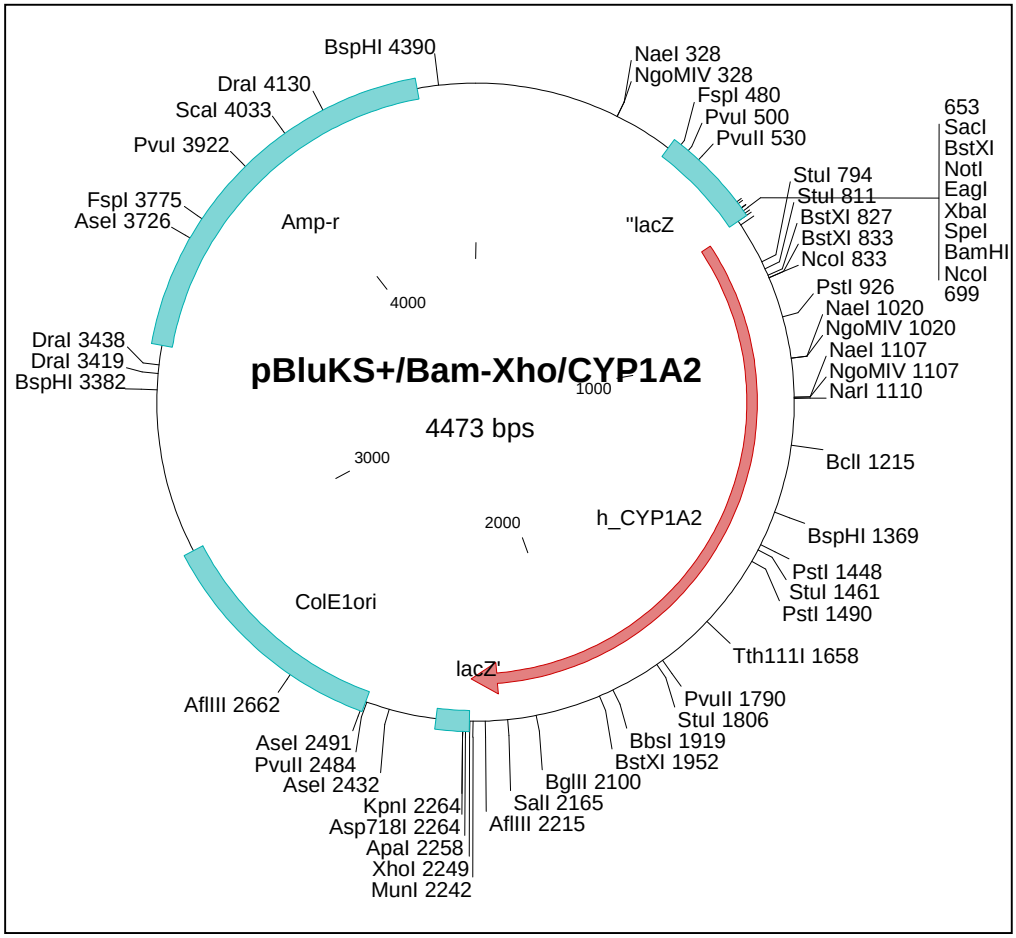

Figure 5.5 (C). The plasmid map of pBluKS+/Bam-Xho/CYP1A2.

For subcloning of CYP1A2 into the transfer vector, the *CYP1A2* gene was isolated from pBluKS+/Bam-Xho/CYP1A2 using the set of restriction enzymes, *BamH*I, *Xho*I. The digested fragment of *CYP1A2* was gel purified and used for ligation into pFastBac1 (cut with *BamH*I, *Xho*I). The ligation mixture was transformed into *E. coli* DH5α competent cells, and transformants were screened with restriction enzyme analysis (Figure 5.6(A)). The cDNA in the pFastBac1 vector was cloned under the

control of polyhedrin promoter. The resultant recombinant transfer vector was named pFastBac1/Bam-Xho/CYP1A2 (Figure 5.6 (B)).

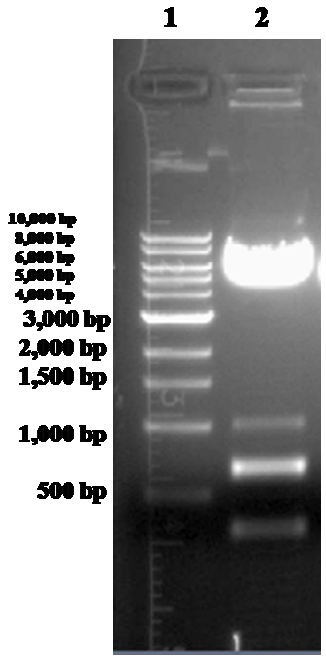

Figure 5.6 (A). Assessment of the pFastBac1/Bam-Xho/CYP1A2 plasmid veracity by diagnostic restriction enzyme digestion. Digestion of pFastBac1/Bam-Xho/CYP1A2 construct by *Stu*I produces five expected fragments of 5292 bp, 1012 bp, 650 bp, 345 bp and 17 bp**.** The 17 bp fragment cannot be seen on the gel as the size of the fragment is very small. The diagnostic restriction digestion was performed as described in 'Materials and Methods' (Section Number 2.2.4). Lane 1, 1.0 kb DNA ladder for sizing linear double-stranded DNA fragments (NEB, catalogue No- N3232S); Lane 2, pFastBac1/Bam-Xho/CYP1A2 digested with *Stu*I, expected fragments are 5292 bp, 1012 bp, 650 bp, 345 bp and 17 bp.

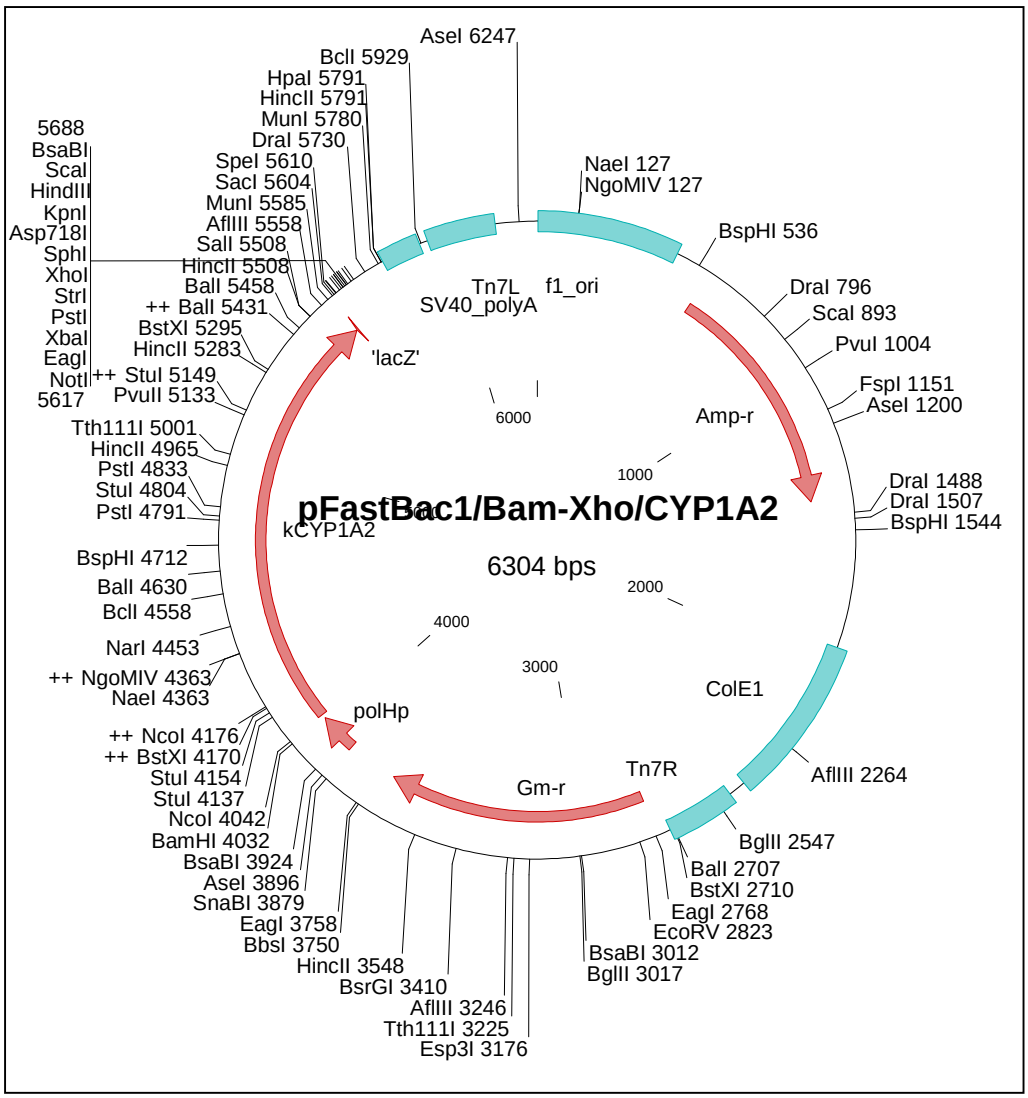

Figure 5.6 (B). The plasmid map of pFastBac1/Bam-Xho/CYP1A2.

5.3.4 CYP2C8 cloning

Cytochrome P450 2C8 (*CYP2C8*) gene was isolated in our laboratory previously by PCR from a human liver cDNA library (Life Technology, Catalogue No 10422-012). *CYP2C8* was isolated with the forward primer (5'- CGACTAGT**GC CACC**ATGGAA CCTTTTGTGG TCCTGGTGCT GTG -3', the *SpeI* site and the Kozak sequence are marked with an underline and bold letters, respectively), and the reverse primer (5'-

CCGCTCGAGT CAGACAGGGA TGAAGCAGAT CTGGTATGAG -3', the *Xho*I site is underlined).

The cDNA was further amplified using above mentioned primers as described in 'Materials and Methods' (Section Number 2.2.2). The PCR product was run on an agarose gel containing ethidium bromide and the DNA fragment of expected size was isolated and purified using a Qiagen gel extraction kit according to the manufacturer's protocol. The purified DNA fragment was digested with *Spe*I, *Xho*I restriction enzymes and after digestion run again on an agarose gel that contained ethidium bromide. The digested DNA fragment was purified using a Qiagen gel extraction kit. The *CYP2C8* gene was then directionally ligated using T4 DNA ligase into pBluescript KS+ (cut with *Spe*I-*Xho*I). The ligation mixture was transformed into *E. coli* DH5α competent cells, and colonies containing the correct recombinant constructs were identified with restriction enzyme analysis. Plasmids were extracted from positive clones. The experimental methods employed are detailed in 'Materials and Methods'. The gene sequence was confirmed by DNA sequencing and its alignment with reference sequence in the NCBI database. The resultant plasmid was named pBluKS+/Spe-Xho/CYP2C8 (Figure 5.7).

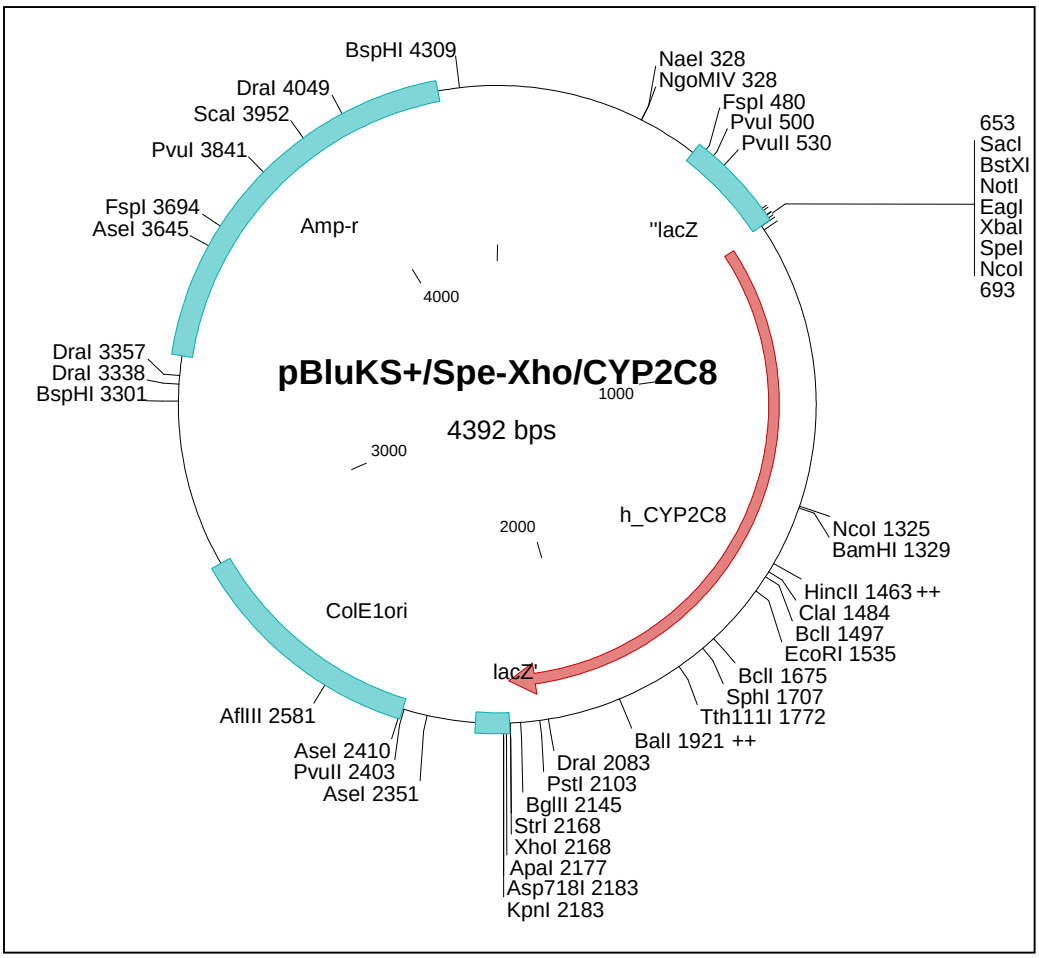

Figure 5.7. The plasmid map of pBluKS+/Spe-Xho/CYP2C8.

For subcloning of *CYP2C8* into the transfer vector, the *CYP2C8* gene was isolated from pBluKS+/Spe-Xho/CYP2C8 using the set of restriction enzymes, *Spe*I, *Xho*I. The digested fragment of CYP2C8 was gel purified and used for ligation into pFastBac1 (cut with *Spe*I, *Xho*I). The ligation mixture was transformed into *E. coli* DH5α competent cells, and transformants were screened via restriction enzyme analysis (Figure 5.8 (A)). The cDNA in the pFastBac1 vector was cloned under the control of polyhedrin promoter. The resultant recombinant transfer vector was named pFastBac1/Spe-Xho/CYP2C8 (Figure 5.8 (B)).

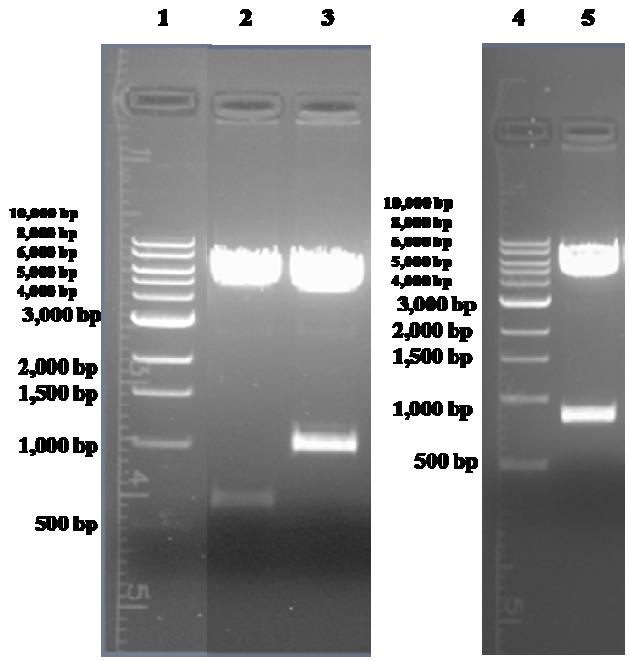

Figure 5.8 (A). Assessment of the pFastBac1/Spe-Xho/CYP2C8 plasmid veracity by diagnostic restriction enzyme digestion. All the expected DNA fragments were observed on the gel. The diagnostic restriction enzyme digestion was performed as described in 'Materials and Methods' (Section Number 2.2.4). Lane 1, 1.0 kb DNA ladder for sizing linear double-stranded DNA fragments (NEB, catalogue No- N3232S); Lane 2, pFastBac1/Spe-Xho/CYP2C8 digested with *Nco*I, expected fragments being 5592 bp and 632 bp; Lane 3, pFastBac1/Spe-Xho/CYP2C8 digested with *Afl*III, expected fragments being 5242 bp and 982 bp; Lane 4, 1.0 kb DNA ladder for sizing linear double-stranded DNA fragments (NEB, Catalogue No N3232S); Lane 5, pFastBac1/Spe-Xho/CYP2C8 digested with *Hpa*I, expected fragments being 5375 bp and 849 bp.

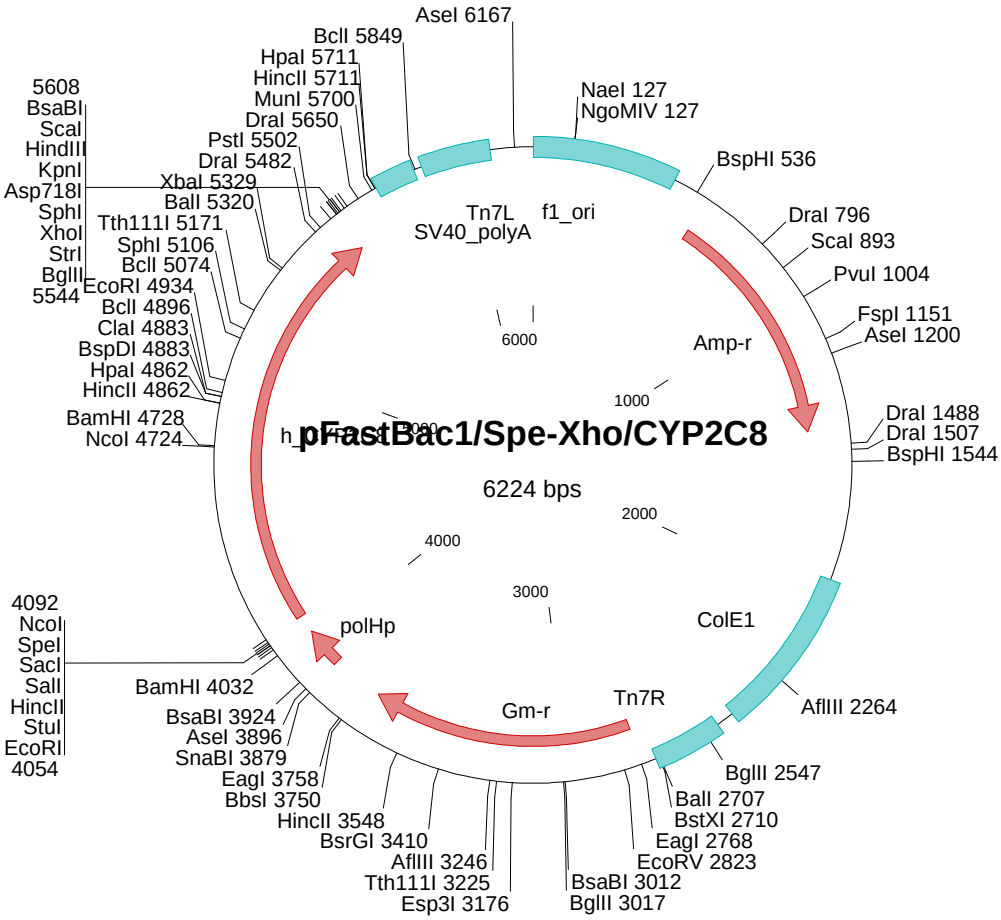

Figure 5.8 (B). The plasmid map of pFastBac1/Spe-Xho/CYP2C8.

5.3.5 CYP2E1 cloning

Cytochrome P450 2E1 (*CYP2E1*) gene was isolated in our laboratory previously by PCR from a human liver cDNA library (Life Technology, Catalogue No 10422-012). *CYP2E1* was isolated with the forward primer (5'- GAAGATCT**GC CACC**ATGTCT GCCCTCGGAG TGACCGTGGC CCT -3', the *Bgl*II site and the Kozak sequence are marked with an underline and bold letters, respectively), and the reverse primer (5'- ATCTCGAGTC ATGAGCGGGG AATGACACAG -3', the *Xho*I site is underlined).

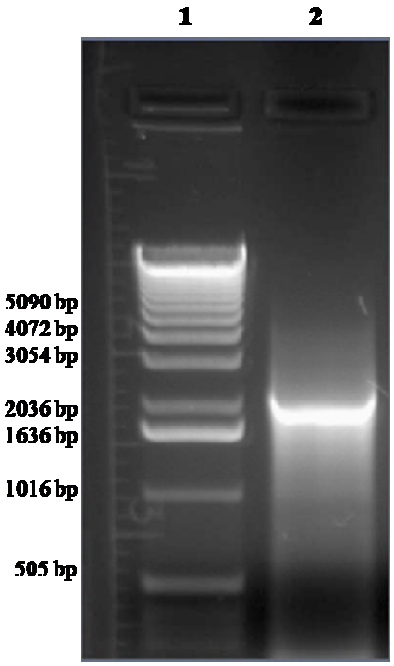

Figure 5.9 (A). *CYP2E1* PCR amplified fragment generated by using *CYP2E1* forward and reverse primers. The PCR and agarose gel electrophoresis was performed as described in 'Materials and Methods'. Lane 1, 1.0 kb DNA ladder for sizing linear double-stranded DNA fragments (Invitrogen, Catalogue No 15615-016); Lane 2, PCR fragment of *CYP2E1*.

The cDNA was amplified using above mentioned primers as described in 'Materials and Methods' (Section Number 2.2.2). The PCR product was run on an agarose gel (Figure 5.9(A)) containing ethidium bromide and the DNA fragment of expected size was isolated and purified using a Qiagen gel extraction kit according to the manufacturer's protocol. The purified DNA fragment was digested with the restriction enzymes, *Bgl*II, *Xho*I and after digestion run again on an agarose gel that contained ethidium bromide. The digested DNA fragment was purified using a Qiagen

gel extraction kit. *CYP2E1* cDNA was then directionally ligated using T4 DNA ligase into pSP73 (digested with *Bgl*II-*Xho*I). The ligation mixture was transform into *E. coli* DH5α competent cells and colonies containing the correct recombinant constructs were identified with restriction enzyme analysis (Figure 5.9 (B)). Plasmids were extracted from positive clones. The experimental methods employed are detailed in 'Materials and Methods' (Section Number 2.2.11). The gene sequence was confirmed by DNA sequencing and its alignment with reference sequence in the NCBI database. The resultant plasmid was named pSP73/Bgl-Xho/CYP2E1 (Figure 5.9 (C)).

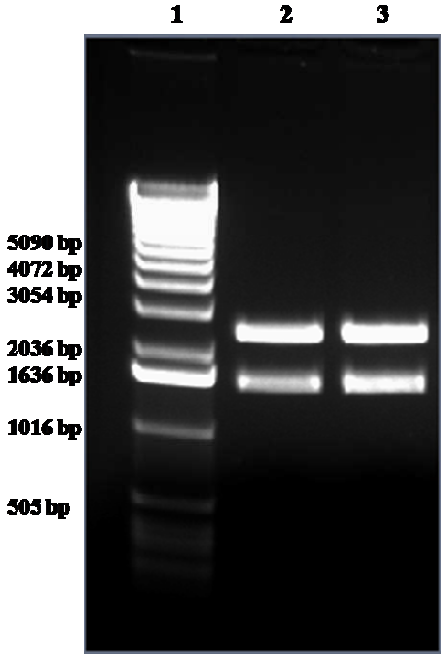

Figure 5.9 (B). Assessment of the pSP73/Bgl-Xho/CYP2E1 plasmid veracity by diagnostic restriction enzyme digestion. Digestion of pSP73/Bgl-Xho/CYP2E1 construct by *Bgl*II, *Xho*I produces two expected fragments of 2383 bp and 1494 bp**.** The diagnostic restriction enzyme digestion was performed as described in 'Materials and Methods' (Section Number 2.2.4). Lane 1, 1.0 kb DNA ladder for sizing linear double-

stranded DNA fragments (Invitrogen, Catalogue No 15615-016); Lane 2, Clone #1, pSP73/BglII-XhoI/CYP2E1 digested with *Bgl*II, *Xho*I, expected fragments being 2383 bp and 1494 bp; Lane 3, Clone #2, pSP73/BglII-XhoI/CYP2E1 digested with *Bgl*II, *Xho*I, expected fragments being 2913 2383 bp and 1494 bp.

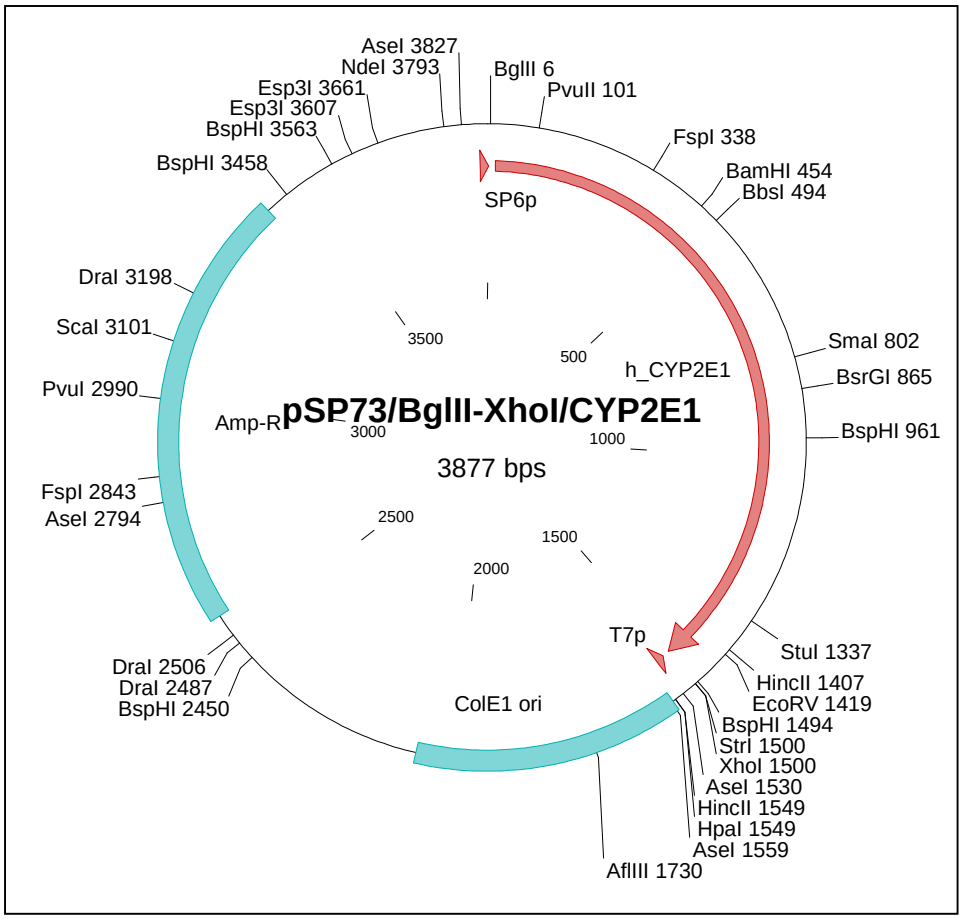

Figure 5.9 (C). The plasmid map of pSP73/BglII-XhoI/CYP2E1.

For subcloning of *CYP2E1* into the transfer vector, the *CYP2E1* gene was isolated from pSP73/BglII-XhoI/CYP2E1 using the set of restriction enzymes *Bgl*II, *Xho*I. The digested fragment of *CYP2E1* was gel purified and used for ligation into pFastBac1 (cut with *BamH*I, *Sal*I which have compatible sticky ends to *Bgl*II, *Xho*I –

but once the vector is ligated to the gene insert, the gene cannot be re-isolated from the resultant plasmid). The ligation mixture was transformed into *E. coli* DH5α competent cells, and transformants were screened with restriction analysis (Figure 5.10 (A)). The cDNA in the pFastBac1 vector was cloned under the control of polyhedrin promoter. The resultant recombinant transfer vector was named pFastBac1/CYP2E1 (Figure 5.10 (B)).

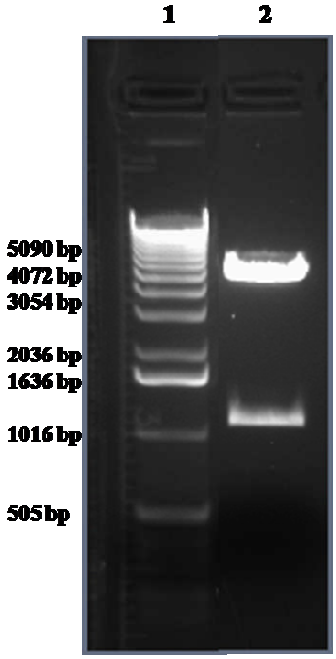

Figure 5.10 (A). Assessment of the pFastBac1/CYP2E1 plasmid veracity by diagnostic restriction enzyme digestion. Digestion of pFastBac1/CYP2E1 construct by *BamH*I-*Xba*I produces two expected fragments of 5152 bp and 1080 bp**.** The diagnostic restriction enzyme digestion was performed as described in 'Materials and Methods' (Section Number 2.2.4). Lane 1, 1.0 kb DNA ladder for sizing linear double-stranded DNA fragments (Invitrogen, Catalogue No 15615-016); Lane 2, pFastBac1/CYP2E1 digested with *BamH*I, *Xba*I, expected fragments being 5152 bp and 1080 bp.

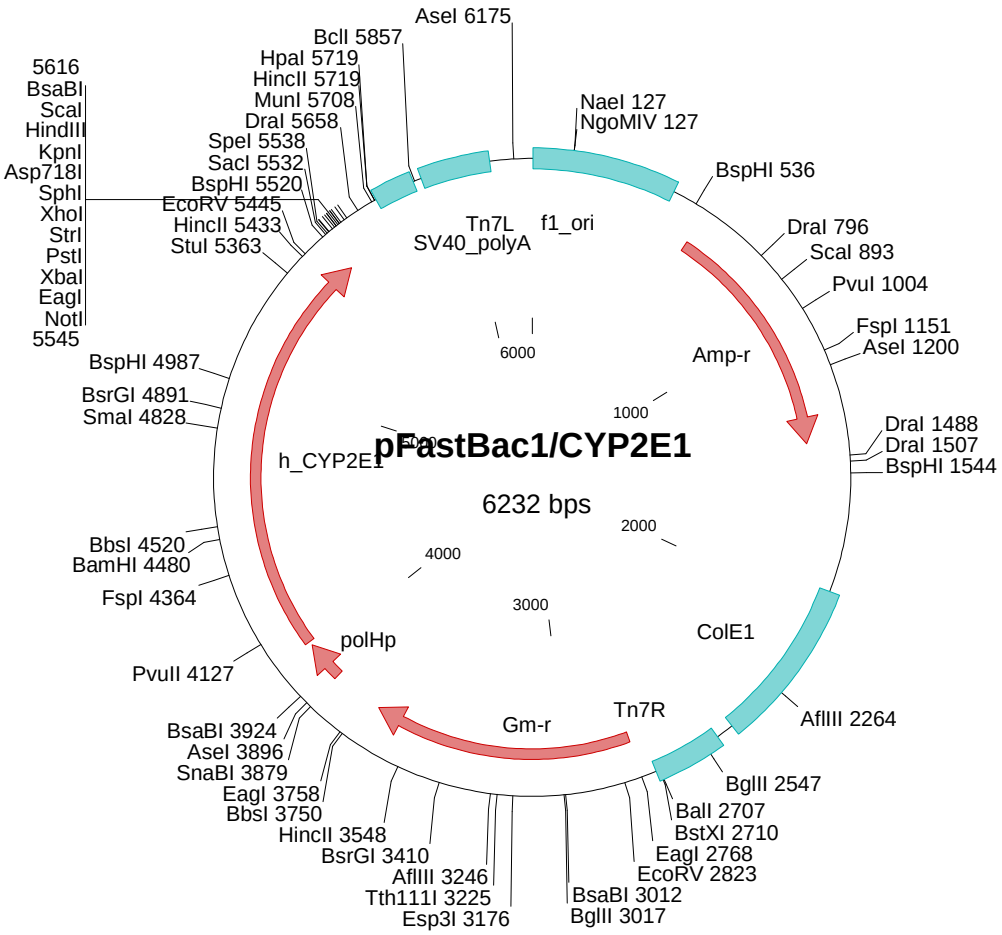

Figure 5.10 (B). The plasmid map of pFastBac1/CYP2E1.

5.4 Generation of bacmid Constructs and baculoviruses

The recombinant transfer vectors, named pFastBac1/Bam-Sal/CYP1A1, pFastBac1/Bam-Sal/CYP1B1, pFastBac1/Bam-Xho/CYP1A2, pFastBac1/Spe-Xho/CYP2C8 and pFastBac1/CYP2E1 were transposed into DH10Bac competent cells. DH10Bac cells contain a baculovirus shuttle vector (bacmid DNA) and a helper plasmid which allow generation of a recombinant bacmid by site-specific transposition. The propagation of recombinant bacmid in *E. coli* DH10Bac was identified by white colour

in the presence of a chromogenic substrate-Bluo-gal and the inducer IPTG. The white colonies were streaked a second time on the Bluo-gal plates and after confirming the white phenotype, recombinant bacmids were isolated and confirmed by PCR analysis. PCR was performed using M13 forward primer (5'GTTTTCCCAGTCACGAC 3') and gene specific reverse primers (Figure 5.11) or gene specific forward and reverse primers as indicated.

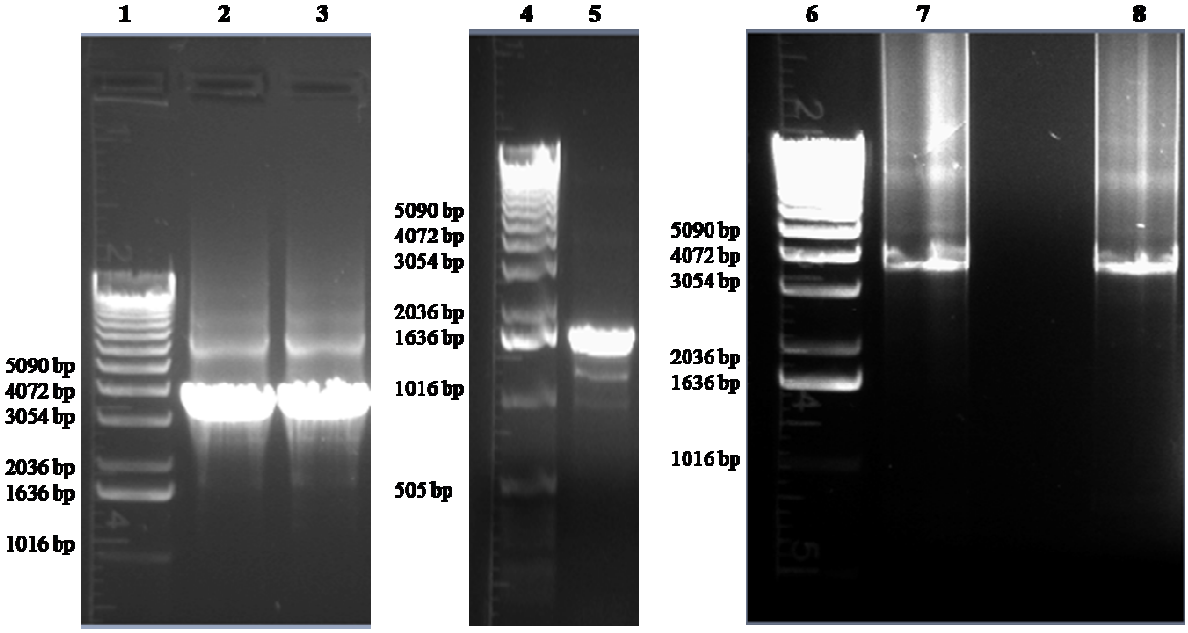

Figure 5.11. Confirmation of *CYP1A1*, *CYP1A2*, *CYP1B1*, *CYP2E1* and *CYP2C8* gene transpositions on to bacmids. All the CYP recombinations on bacmid were confirmed by PCR which were performed as described in 'Materials and Methods' (Section Number 2.2.16). Lane 1, 1 kb DNA ladder for sizing linear double-stranded DNA fragments (Invitrogen, Catalogue No 15615-016); Lane 2, CYP1A1 recombinant bacmid confirmation, PCR was performed using set of M13 forward and gene specific reverse primers. Expected PCR fragment size for CYP1A1 transposition confirmation is ~3200 bp; Lane 3, CYP1A2 recombinant bacmid confirmation, PCR was performed

using set of M13 forward and gene specific reverse primers. Expected PCR fragment size for CYP1A2 transposition confirmation is ~3200 bp; Lane 4, 1 kb DNA ladder for sizing linear double-stranded DNA fragments (Invitrogen, Catalogue No 15615-016); Lane 5, CYP1B1 recombinant bacmid confirmation, PCR was performed using gene specific forward and reverse primers. Expected PCR fragment size for CYP1B1 transposition confirmation is 1644 bp; Lane 6, 1 kb DNA ladder for sizing linear double-stranded DNA fragments (Invitrogen, Catalogue No 15615-016); Lane 7, CYP2E1 recombinant bacmid confirmation, PCR was performed using a set of M13 forward and gene specific reverse primers. Expected PCR fragment size for CYP2E1 transposition confirmation is ~3200 bp; Lane 8, CYP2C8 recombinant bacmid confirmation, PCR was performed using a set of M13 forward and gene specific reverse primers. Expected PCR fragment size for CYP2C8 transposition confirmation is ~3200 bp.

In order to generate baculoviruses, Sf9 cells were transfected with recombinant bacmids as described in 'Materials and Methods' (Section Number 2.3.7). Hereafter, CYP baculovirus is referred to as BV-CYP. The baculoviruses produced in Sf9 cells by initial transfections were subjected to two more rounds of amplification by infecting the cells with baculoviruses for 96 h. The baculovirus titration was performed using plaque assay and titres of the baculovirus stocks were determined. The experimental methods employed are detailed in 'Materials and Methods'.

5.5 Expression of CYP1A1, CYP1B1, CYP1A2, CYP2C8 and CYP2E1 in Sf9 cells

Following amplification and titration of recombinant baculoviruses, Sf9 cells were infected with CYP baculoviruses in separate experiments. The cells were incubated in a 27°C humidified incubator. To compensate for low endogenous levels of haem in insect cells, haemin (2 µg/ ml) and δ-amino levulinic acid (100µM) were added 24 h post-infection to the cells. Cells were harvested 63 h post-infection and the microsomes were prepared. The experimental methods employed are detailed in 'Materials and Methods'.

The presence of the individual CYPs in different microsomes was confirmed by Coomassie staining. Microsomes (20 µg of microsomal proteins/ lane) were separated on 10% sodium dodecyl sulfate-polyacrylamide gel and protein bands were visualised by staining with Coomassie G-250 followed by several de-staining steps as described in 'Materials and Methods' (Section Number 2.4.5). Commassie staining of microsomal protein fractions prepared from recombinant baculovirus infected insect cells detected CYP1A1, CYP1B1, CYP1A2, CYP2C8 and CYP2E1 protein bands (Figure 5.12 (A) and (B)). The size of the protein bands was consistent with the molecular weights predicted from the cDNA sequences.

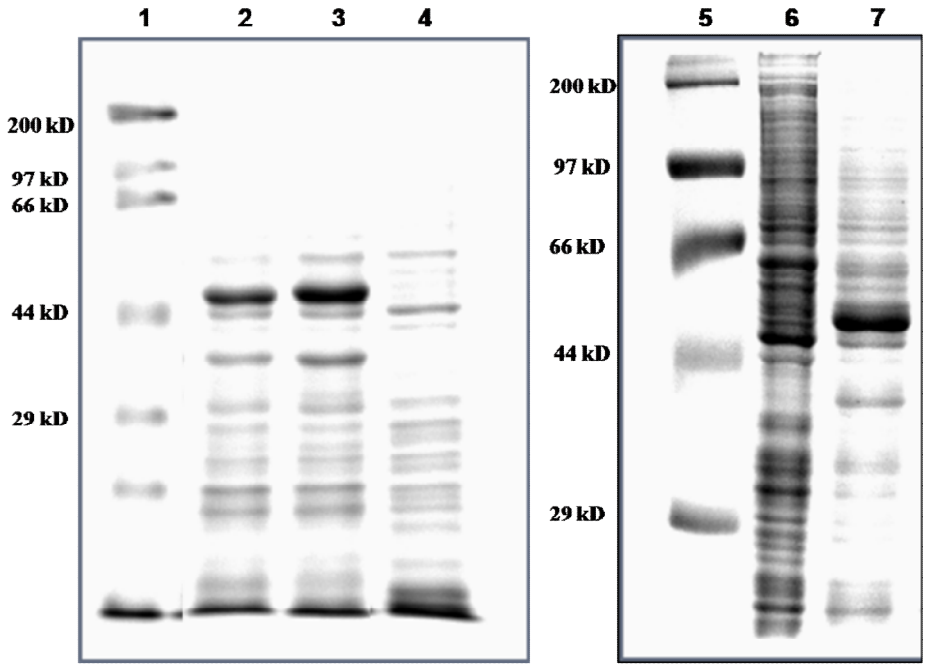

Figure 5.12 (A). SDS-PAGE gel analysis of CYP1A1, CYP2E1 and CYP2C8 proteins. 20 µg of microsomal fractions of the proteins expressed in Sf9 cells were loaded per lane on 10% SDS-PAGE. Gels were stained with Coomassie blue G-250 as described in 'Materials and Methods' (Section Number 2.4.5). Lane 1; protein marker (Santa Cruz Biotechnology, Catalogue No sc-2361); Lane 2, CYP1A1; Lane 3, CYP2E1; Lane 4, negative control (proteins from cells infected with baculovirus encoding no foreign gene) ; Lane 5, protein marker (Santa Cruz Biotechnology, catalogue No: sc-2361). Lane 6, negative control (proteins from cells infected with baculovirus encoding no foreign gene); Lane 7, CYP2C8.

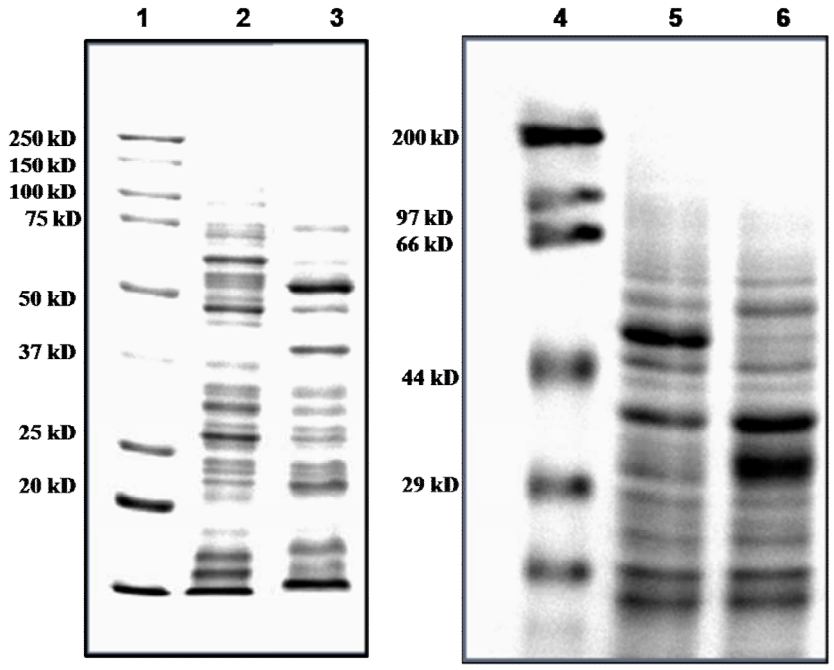

Figure 5.12 (B). SDS-PAGE gel analysis of CYP1B1 and CYP1A2 proteins. 20 µg of microsomal fractions of the proteins expressed in Sf9 cells were loaded per lane on 10% SDS-PAGE. Gels were stained with Coomassie blue G-250 as described in 'Materials and Methods' (Section Number 2.4.5). Lane 1, protein marker (Bio-Rad, Catalogue No 161-0375); Lane 2, negative control (proteins from cells infected with baculovirus encoding no foreign gene); Lane 3, CYP1A2; Lane 4, protein marker (Santa Cruz Biotechnology, catalogue No: sc-2361); Lane 5, CYP1B1; Lane 6, negative control (proteins from cells infected with baculovirus encoding no foreign gene).

5.6 Co-expression of CYPs with the CPRs in Sf9 cells

As presented in Chapters 3 and 4, ΔhRD does not anchor on to the microsomal membranes – therefore, it was not pursued further. CYP1B1, CYP1A2 and CYP2E1

were studied in the context of three different CPR species viz. hRD, ΔhRDM and yRD, whereas CYP1A1 and CYP2C8 were studied only in the context of ΔhRDM. In the human liver microsomes, CYP levels are found to be exceeding the levels of NADPH cytochrome P450 reductase by a 10:1 to 20:1 ratio (Estabrook et al 1971). In line with this, while co-infecting Sf9 cells with BV-CYP and BV-CPR, multiplicity of infection (MOI) for BV-CPR was kept 10 times less (1×10^{-1} pfu/cell) than that for CYPs (1 pfu/cell). Cytochrome b_5 is known to augment CYP2C8 and CYP2E1 catalytic activity. For the co-expression of the third protein (cytochrome b_5) with CYP2C8 and CYP2E1, the MOI of BV-cyt-b_5 was kept at 0.1 pfu/ cell. To compensate for low endogenous levels of haem in insect cells, haemin (2 μg/ ml) and δ-amino levulinic acid (100μM) were added 24 hour post-infection. Cells were harvested after 63 h and the microsomes were prepared. The experimental methods employed are detailed in 'Materials and Methods'. Western blot and Coomassie staining experiments for hRD, ΔhRDM and yRD were presented in Chapter 3 and Coomassie staining for cytochrome b_5 was presented in Chapter 4.

After co-expression with CPRs, Western blotting was performed for CYP1A2 and CYP2E1 microsomes. For Western blotting, the microsomes prepared from the baculovirus infected Sf9 cells were separated on 10% sodium dodecyl sulfate-polyacrylamide gel (1.5 μg microsomal protein/ lane). The proteins were transferred to Immobilon-P membrane (Millipore) by semi-dry transfer method. The membrane was blocked overnight at 4ºC with 5% non-fat dry milk in PBS. The blot for CYP1A2 was probed with goat anti-rat CYP1A1 polyclonal antibody (BD-Gentest, Catalogue No 458124) at a 1:2500 dilution followed by exposure to donkey anti-goat HRP-conjugated

secondary antibody (Santa Cruz Biotechnology, Catalogue No sc-2304) at a 1:7500 dilution. The blot for CYP2E1 was probed with goat anti-rat CYP2E1 polyclonal antibody (BD-Gentest, Catalogue No 458216) at a 1:2500 dilution followed by exposure to donkey anti-goat HRP-conjugated secondary antibody (Santa Cruz Biotechnology, Catalogue No sc-2304) at a 1:7500 dilution. The blots were incubated with luminal, a chemiluminescent substrate, for short period of time. Chemiluminescence was captured (Figure 5.13 (A) and (B)) on Gel Doc™, Bio-Rad. Human CYP protein bands reacted with the corresponding antibodies in Western blot analysis. The protein band intensities were measured by densitometry using 'Quantity One' software from Bio-Rad.

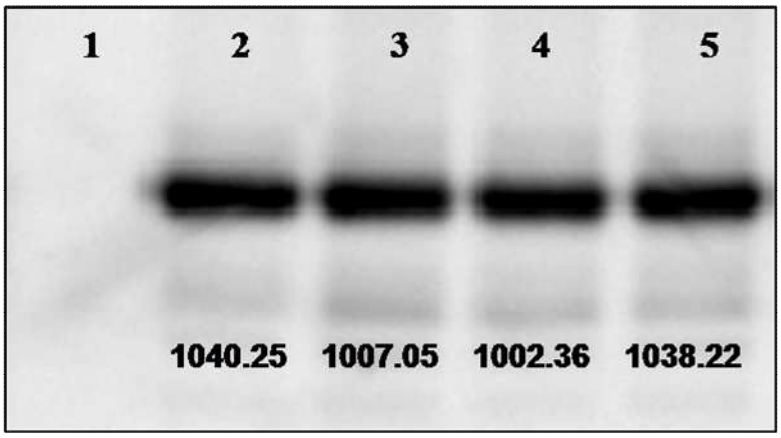

Figure 5.13 (A). Immunoblot analyses of CYP1A2 co-expressed with different CPR species in Sf9 insect cells. Sf9 cells were infected with CYP and CPR baculoviruses at an MOI of 1 pfu/cell and 0.1 pfu/cell, respectively. Microsomes were prepared 63 h post-infection. 1.5 μg of microsomal fractions were loaded per lane on 10% SDS-PAGE and immunoblotting was performed as described in 'Materials and Methods'

(Section Number 2.4.6). The numbers below the bands show band intensities in arbitrary units. Lane 1, negative control (proteins from cells infected with baculovirus encoding no foreign gene); Lane 2, CYP1A2 expressed alone; Lane 3, CYP1A2 co-expressed with hRD; Lane 4, CYP1A2 co-expressed with ΔhRDM; Lane 5, CYP1A2 co-expressed with yRD.

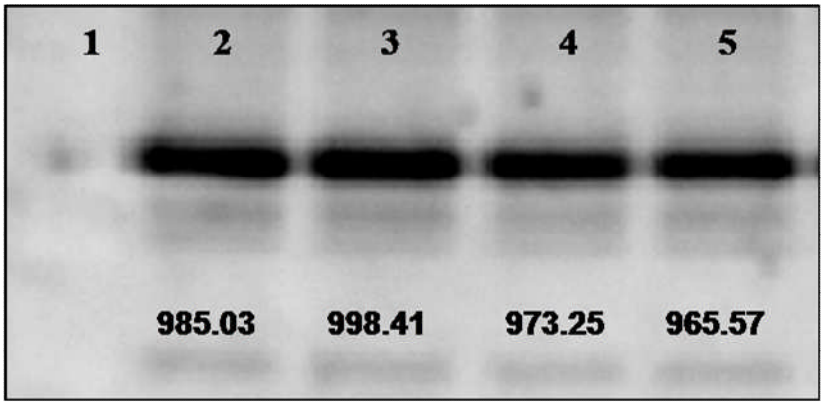

Figure 5.13 (B). Immunoblot analyses of CYP2E1 co-expressed with different CPR species in Sf9 insect cells. Sf9 cells were infected with CYP and CPR baculoviruses at an MOI of 1 pfu/cell and 0.1 pfu/cell, respectively. Microsomes were prepared 63 h post-infection. 1.5 μg of microsomal fractions were loaded per lane on 10% SDS-PAGE and immunoblotting was performed as described in 'Materials and Methods' (Section Number 2.4.6). The numbers below the bands show band intensities in arbitrary units. Lane 1, negative control (proteins from cells infected with baculovirus encoding no foreign gene); Lane 2, CYP2E1 co-expressed with cytochrome b_5; Lane 3, CYP2E1 co-expressed with cytochrome b_5 and hRD; Lane 4, CYP2E1 co-expressed with

cytochrome b_5 and ΔhRDM; Lane 5, CYP2E1 co-expressed with cytochrome b_5 and yRD.

5.7 CYP amounts and their catalytic activities supported by hRD, ΔhRDM and yRD

The insect cells were infected with CYP (BV-CYP1B1, BV-CYP1A2 and BV-CYP2E1) recombinant baculoviruses alone (MOI: 1.0 pfu/cell) and also co-infected with hRD or ΔhRDM or yRD baculoviruses (MOI: 0.1 pfu/cell). CYP1A1 and CYP2C8 were studied only with one CPR, i.e. ΔhRDM. In case of CYP2C8 and CYP2E1, cells were also co-infected with a third baculovirus, BV-cyt-b_5 (MOI: 0.1). Haemin (2 μg/ ml) and δ-amino levulinic acid (100μM) were added 24 h post-infection to compensate for low endogenous levels of haem. Microsomes were prepared 63-h post-infection and the protein concentrations were determined by a modified Bradford method (Bradford 1976). The microsomes were diluted to a protein concentration of 1 mg/ml with 100 mM potassium phosphate buffer (pH 7.4), 20% (vol/vol) glycerol. Then a few grains of sodium dithionite were added and a baseline recorded on a dual wavelength spectrophotometer (Shimadzu UV-2401PC). CYP holoprotein contents were spectrophotometrically measured as reduced carbon monoxide (CO) difference spectra (Omura and Sato 1964) using 91 mM^{-1} cm^{-1} as the extinction coefficient. The experimental methods have been described in detail in 'Materials and Methods'. Carbon monoxide difference spectra of CYPs expressed on their own are presented in Figure 5.14.

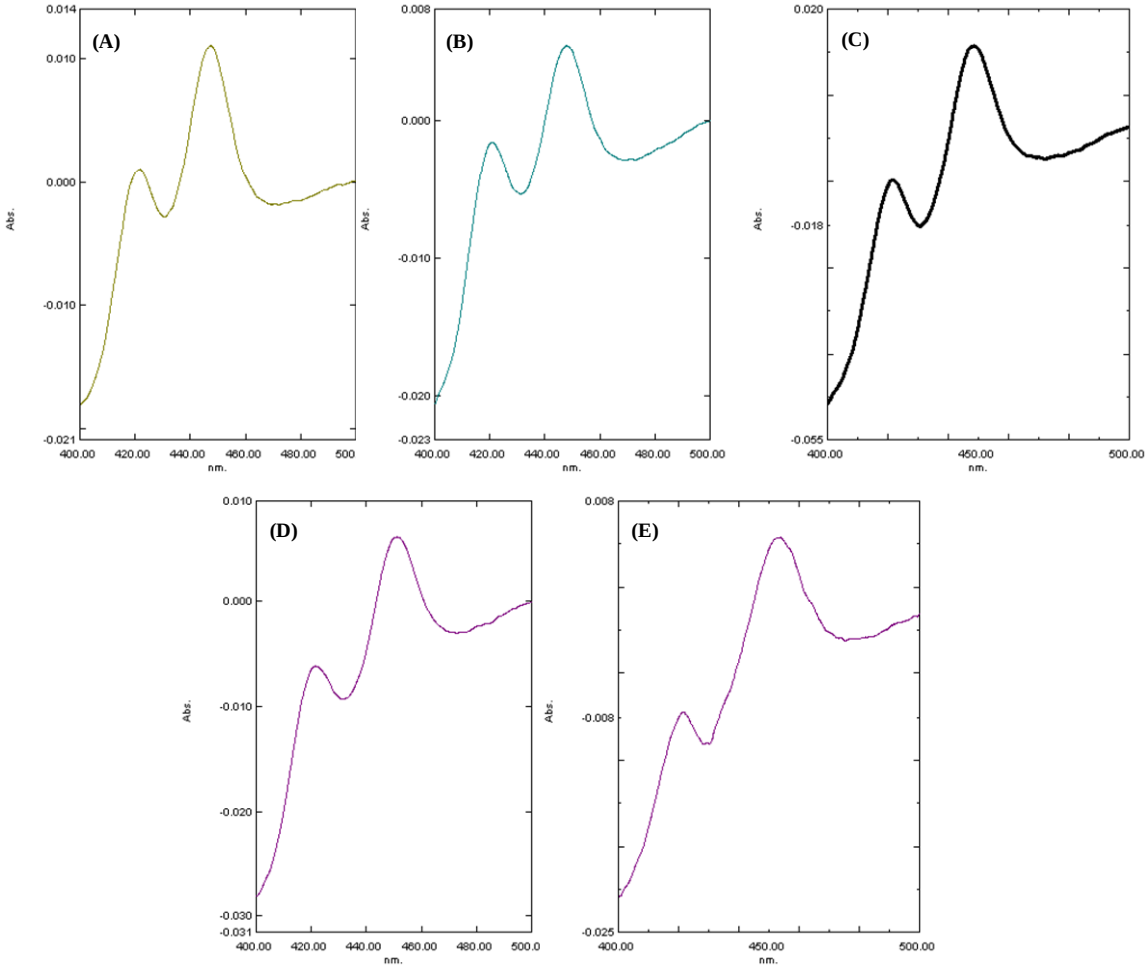

Figure 5.14. Reduced carbon monoxide difference spectra of CYPs. Sf9 cells were infected with CYP baculoviruses at an MOI of 1 pfu/ cell. 63 h post-infection, the cells were harvested and microsomes were prepared. CYP content was measured by reduced carbon monoxide difference spectra as described in 'Materials and Methods' (Section Number 2.4.3). (A) CYP1A1 CO-difference spectrum, (B) CYP1B1 CO-difference spectrum, (C) CYP1A2 CO-difference spectrum, (D) CYP2C8 CO-difference spectrum and (E) CYP2E1 CO-difference spectrum.

5.7.1 CYP1B1 interactions with hRD, ΔhRDM and yRD

CYP1B1 was expressed with and without the CPRs, microsomes were prepared and CYP contents were measured by carbon monoxide difference spectroscopy as described above. Table 5.1 shows specific contents of CYP1B1 when expressed with and without the CPRs.

Table 5.1. CYP1B1 content in microsomal samples, determined by reduced CO-difference spectroscopy. Sf9 cells were co-infected with CYP and CPR baculoviruses at an MOI of 1 and 0.1 pfu/ cell respectively. Microsomes were prepared 63 h post-infection as described in 'Materials and Methods' (Section Number 2.4.1). Data are presented as mean values ± STDEV.

Microsomes	specific content of CYP1B1 (pmole/mg protein)
CYP1B1	1287.56 ± 96.3
CYP1B1+ hRD	630.94 ± 52.9
CYP1B1+ ΔhRDM	940.91 ± 66.2
CYP1B1+ yRD	644.10 ± 61.7

The results, indicating that co-expression of CYPs with CPRs results in decrease in spectrally active CYP levels (holoprotein levels), are in agreement with what we observed in Chapters 3 and 4,. CYP content is highest when expressed without CPR. However, in microsomes which co-express CPRs, it is observed that CYP1B1 content is

higher when it is co-expressed with ΔhRDM in comparison to the CYP content obtained after co-expression with hRD or yRD (see Table 5.1). This implies that the destruction of CYP1B1 holoprotein by ΔhRDM is far less than that caused by hRD and yRD. In Chapter 3, experimental evidence has been presented that correlates the destruction of CYPs with reactive oxygen species that are induced by CPRs.

The catalytic activities of CYP1B1 co-expressed with CPRs were measured using the ethoxyresorufin-O-deethylase (EROD) assay (Klotz et al. 1984). CYP1B1 converts 7-ethoxyresorufin (7-ER) to resorufin in the presence of NADPH and oxygen and the assay is well known as the EROD assay. The amount of resorufin produced is measured fluorometrically and it reflects the level of 7-ethoxyresorufin o-deethylase activities. Both, CYP1B1 and CYP1A1 can catalyse deethylation of the substrate 7-ethoxyresorufin (7-ER) to form the product resorufin, which exhibits fluorescence at excitation wavelength of 530 nm and emission wavelength of 590 nm.

The production of the metabolite resorufin, by deethylation of the fluorogenic substrate 7-ethoxyresorufin was measured for 30 min. The assay was performed as described before (Klotz et al. 1984). The reaction kinetics was carried out at 37ºC in a reaction volume of 100 µl/well in 96-well black plates with transparent flat bottom (Fisher, Catalogue No FB86083). The assay mixture contained 100 mM Potassium phosphate buffer pH 7.4, containing 5 µM 7-ethoxyresorufin , 1.5 pmole CYP1B1 and the NADPH regenerating system (1.3 mM NADP+, 3.3 mM G6P, 3.3 mM $MgCl_2$, 0.4U/ml G6PDH). Resorufin formation was measured fluorometrically on the Biotek

Synegy HT plate reader (excitation wavelength of 528/20 nm and emission wavelength of 590/20 nm). Changes in fluorescence were recorded for 30 min as relative fluorescence units (RFU).

The metabolite of 7-ER, resorufin, was used to generate a standard curve – it was prepared using a range of concentrations of resorufin (1.82, 5.5, 16.5, 49.4, 148.1, 444.4, 1333.3 and 4000 pmole/100 µl reaction volume). The end-point assays were performed in 96-well black plates. The fluorescent values (RFU) were recorded on the Biotek Synegy HT plate reader using an excitation wavelength of 528/20 nm and emission wavelength of 590/20 nm. The standard curve was plotted (Figure 5.15 (A)) and resorufin concentrations in test samples (Figure 5.15 (A)) were measured using the equation from the standard curve.

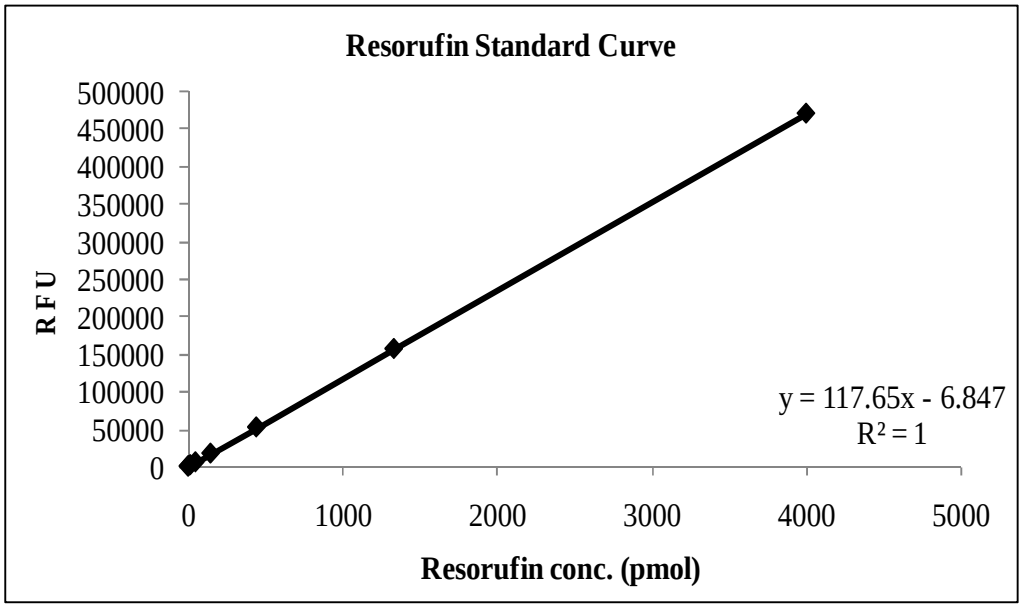

Figure 5.15 (A). The resorufin standard curve. The curve was prepared as described in Section 5.7.1.

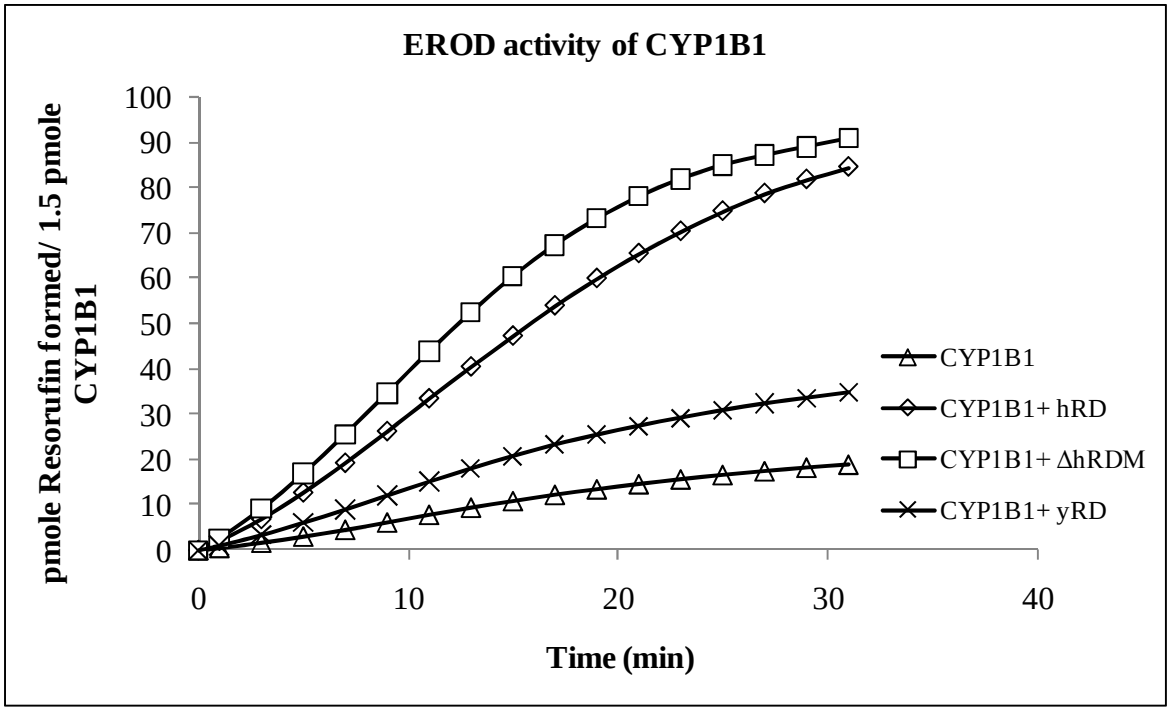

Figure 5.15 (B). Kinetic analysis of CYP1B1 catalytic activities in the EROD assay. Sf9 cells were co-infected with CYP1B1 and the CPR baculoviruses at an MOI of 1 and 0.1 pfu/ cell, respectively. The catalytic activities of CYP1B1 were measured in microsomes prepared at 63h post-infection. EROD assay was performed as described in Section 5.7.1.

Table 5.2. CYP1B1 enzyme reaction rates in co-expressed microsomes. Sf9 cells were co-infected with CYP1B1 and the CPR baculoviruses at an MOI of 1 and 0.1 pfu/ cell, respectively. The reaction rates were measured in microsomes prepared at 63h post-infection. EROD assay was performed as described in Section 5.7.1.

Microsomes	CYP1B1 reaction rates (pmole resorufin formed/ min/ pmole of CYP1B1)
CYP1B1	0.4292
CYP1B1+hRD	1.9462
CYP1B1+ΔhRDM	2.1176
CYP1B1+yRD	0.7897

NADPH-cytochrome P450 reductase activities of human and yeast CPRs in CYP1B1 co-expressed microsomes were measured by the reduction of the tetrazolium salt, MTT, as described in 'Materials and Methods' (Section Number 2.4.7). In CYP and CPR co-expressed microsomes, reduction potential of yRD was similar to that of hRD (Table 5.2), which means yRD can reduce MTT as efficiently as hRD. This observation is in line with similar levels of decrease in CYP1B1 holoprotein content in the presence of either yRD or hRD (Table 5.1). Both the CPRs probably cause oxidative damage to microsomal proteins which results in decrease in holoprotein levels. Reduction potential of ΔhRDM towards MTT is comparatively lower than hRD and yRD.

Table 5.3. NADPH cytochrome P450 reductase activities exhibited by hRD, ΔhRDM and yRD in CYP1B1 co-expressed microsomes. Sf9 cells were co-infected with CYP1B1 baculoviruses (MOI 1.0 pfu/cell) and CPR baculoviruses (MOI 0.1 pfu/cell) and microsomes were prepared 63 h post-infection. Reductase activity was measured by using MTT as described in Materials and Methods (Section Number 2.4.7). The moles of MTT reduced per minute per mg of protein were calculated.

CPR Species	Reductase activity (nmole MTT reduced/min/mg protein)
CYP1B1	14.5 ± 3.2
CYP1B1+ hRD	250.6 ± 47.1
CYP1B1+ ΔhRDM	173.1 ± 31.0
CYP1B1+ yRD	260.5 ± 39.3

As observed in Figure 5.15 (B) and Table 5.2, hRD and ΔhRDM supported CYP1B1 catalytic activity far better than yRD. However NADPH cytochrome P450 reductase activity of yRD as measured by the MTT assay (Table 5.2) is high. This observation again indicates that reduction potential of yRD towards MTT is not directly proportional to its ability to couple with a CYP. To highlight the ability of CPRs to support CYP1B1 activity, their coupling efficiency with CYP1B1 was calculated by using the following formula,

Coupling efficiency = CYP1B1 activity in EROD assay⁄CPR activity in MTT assay

As the coupling efficiency of ΔhRDM was highest among the three CPRs, percentage relative coupling efficiency for hRD and yRD was calculated in comparison with ΔhRDM, considering ΔhRDM activity as 100% (Table 5.4). The percent coupling efficiency values show that ΔhRDM couples better with CYP1B1 than its native form, hRD, and yeast reductase, yRD. The lower level of ROS induction by ΔhRDM (as depicted in Figures 3.22 and 3.23 in Chapter 3) correlates to its higher coupling efficiency. ROS induced by CPRs is responsible for a decrease in CYP holoproein content and possibly it is also responsible for uncoupling of CYP catalytic activity (as observed in the CYP enzyme assays).

Table 5.4. Percent relative coupling efficiency of hRD, ΔhRDM and yRD with CYP1B1. CYP1B1 activity in the EROD assay and CPR activity measured in the MTT assay were used for the calculations. CYP1B1 activity was divided by CPR activity and percent relative coupling efficiency was measured.

Microsome samples	% Relative coupling efficiency
CYP1B1+ ΔhRDM	100
CYP1B1+ hRD	63.49
CYP1B1+ yRD	24.78

5.7.2 CYP1A2 interactions with hRD, ΔhRDM and yRD

CYP1A2 was expressed with and without the CPRs, microsomes were prepared and CYP1A2 holoprotein contents were measured by carbon monoxide difference spectroscopy as described in Section 5.7. Table 5.5 shows specific contents of CYP1A2 when expressed with and without CPRs.

Table 5.5. CYP1A2 specific content in microsomal samples, determined by reduced CO-difference spectroscopy. Sf9 cells were co-infected with CYP and CPR baculoviruses at an MOI of 1 and 0.1 pfu/ cell, respectively. Microsomes were prepared 63 h post-infection as described in 'Materials and Methods' (Section Number 2.4.1). Data are presented as mean values ± STDEV.

Microsomes	Specific content of CYP1A2 (pmole/mg protein)
CYP1A2	1577.66 ± 88.3
CYP1A2+ hRD	644.41 ± 54.0
CYP1A2+ ΔhRDM	1162.21 ± 75.1
CYP1A2+ yRD	369.05 ± 31.5

Like the other CYPs studied, CYP1A2 holoprotein content was highest when it was expressed alone and the CYP holoprotein content was lower when CYP1A2 was co-expressed with the CPRs. However decrease in holoprotein content in yRD co-expressed microsomes was four fold, which indicates that yRD is extremely destructive

to CYP1A2 on insect cell microsomes. In comparison with hRD, genetically modified CPR, ΔhRDM, seems to yield substantially higher amounts of CYP1A2 holoprotein. The CYP1A2 content in hRD co-expressed microsomes was 2.5 fold lower than in the microsomes which contained only CYP1A2. Decrease in CYP1A2 holoprotein content by hRD and yRD is highest among all the CYPs that we studied which indicates that CYP-CPR interactions vary depending on the CYP isoform.

In order to compare the ability of different CPR species to transfer electrons to CYP1A2, enzyme assays were performed using the fluorogenic substrate, 3-cyano-7-ethoxycoumarin (CEC). CEC is metabolized mainly by CYP2C19 and CYP1A2 to a fluorescent product 3-cyano-7-hydroxycoumarin (CHC). However, CEC is also metabolized by CYP2D6, though not specific to the enzyme. The reactions were carried out in a reaction volume of 100 µl/ well in 96-well black plates with transparent flat bottom (Fisher Scientific, Catalogue No FB85083) at 37°C in 100 mM potassium phosphate buffer pH 7.4, containing 3 µM CEC, 1.0 pmole CYP1A2 and the NADPH regenerating system (1.3 mM NADP+, 3.3 mM glucose-6-phosphate, 3.3 mM $MgCl_2$, 0.4U/ml glucose-6-phosphate dehydrogenase). The fluorescent values were recorded on the Biotek Synegy HT plate reader using an excitation wavelength of 400 nm (20 nm) and emission wavelength of 460 nm (40 nm). Changes in fluorescence were measured as relative fluorescence units (RFU). Kinetic progression of reactions was measured for 30 min (Figure 5.16 (B) and Table 5.6). Standard curve was plotted and CHC concentrations in test samples were measured using the equation from the standard curve. The standard curve is shown in Figure 5.16 (A).

The standard curve of CHC was prepared using a range of concentrations of CHC (0, 39.1, 78.1, 156.3, 312.5, 625, 1250 pmole/ ml). The assays for generation of the standard curve were performed in 96-well black plates. The fluorescent values (RFU) were recorded on the Biotek Synegy HT plate reader using an excitation wavelength of 400 nm (20 nm) and emission wavelength of 460 nm (40 nm).

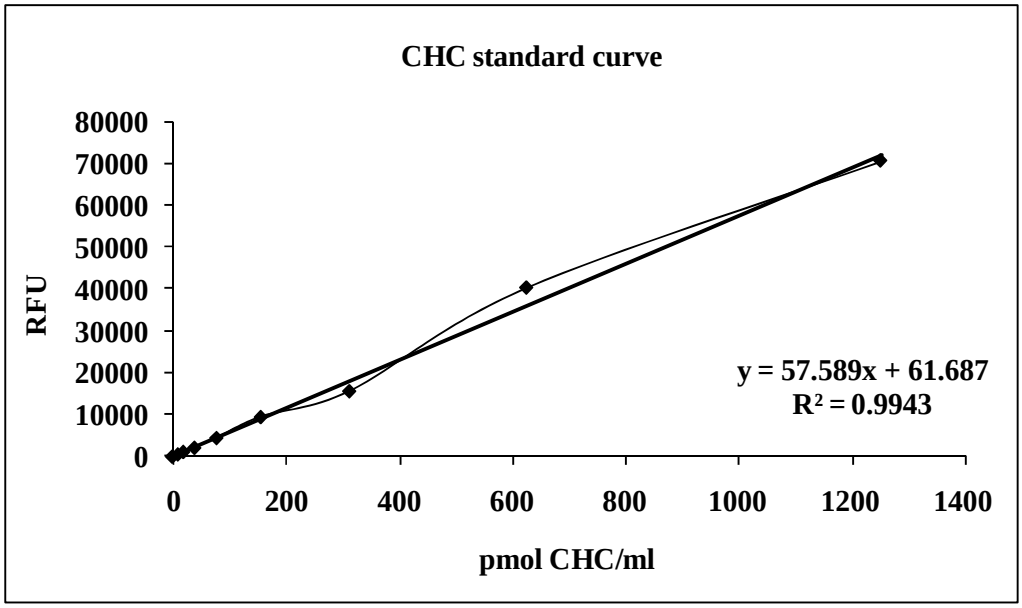

Figure 5.16 (A). CHC standard curve. The curve was prepared as described in Section 5.7.2.

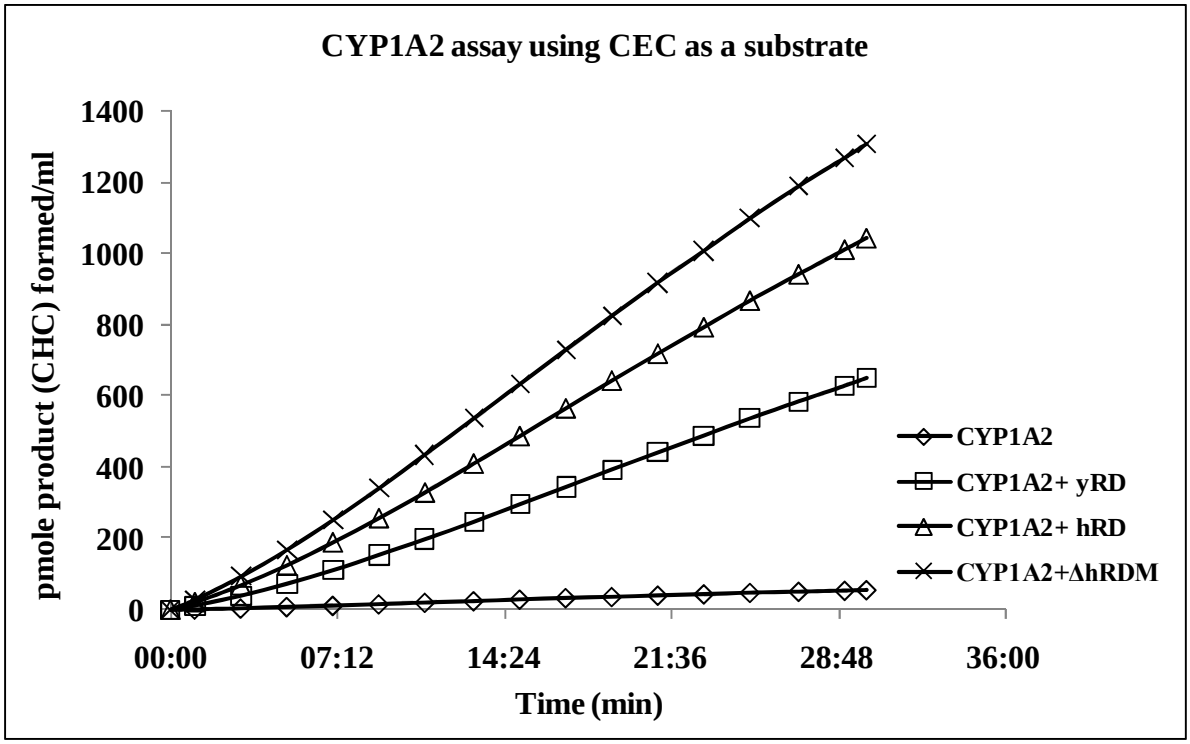

Figure 5.16 (B). Kinetic analysis of CYP1A2 catalytic activities using CEC as a substrate. Sf9 cells were co-infected with CYP1A2 and the CPR baculoviruses at an MOI of 1 and 0.1 pfu/ cell, respectively. The catalytic activities of CYP1A2 were measured in microsomes prepared at 63h post-infection. The enzyme assay was performed as described in Section 5.7.2.

Table 5.6. CYP1A2 enzyme reaction rates in co-expressed microsomes. Sf9 cells were co-infected with CYP1A2 and the CPR baculoviruses at an MOI of 1 and 0.1 pfu/ cell, respectively. The reaction rates were measured in microsomes prepared at 63h post-infection. CEC assay was performed as described in Section 5.7.2.

Microsomes	CYP1A2 reaction rates (pmole CHC formed/ min/ pmole of CYP1A2)
CYP1A2	0.194
CYP1A2+hRD	3.590
CYP1A2+ΔhRDM	4.510
CYP1A2+yRD	2.246

In order to find out the reductase activities of CPRs in co-expressed microsomes, reductase assays were performed as described in 'Materials and Methods' (Section Number 2.4.7) using MTT as a substrate. Reductase activities of hRD and yRD were comparable and reductase activity of ΔhRDM was lower than that of hRD or yRD (Table 5.7). However as seen in CO binding difference spectra, co-expression with the stronger CPRs, hRD and yRD, yield very low CYP1A2 holoprotein. Once again amongst all the three CPRs studied, co-expression with ΔhRDM appears to yield highest content of CYP1A2 holoprotein. Albeit the levels of CYP1A2 holoprotein change (Table 5.5), apoprotein levels of CYP1A2 remain unchanged (Figure 5.13 (A)). The observation that CPRs cause destruction to CYP holoprotein levels without changing apoprotein levels seems to be common to all the CYPs that we studied. This

finding again emphasises that CPRs do not modulate CYP expression levels but are responsible for CYP holoprotein destruction by means of reactive oxygen species.

Table 5.7. NADPH cytochrome P450 reductase activities exhibited by hRD, ΔhRDM and yRD in CYP1A2 co-expressed microsomes**.** Sf9 cells were co-infected with CYP1A2 baculoviruses (MOI 1.0 pfu/cell) and CPR baculoviruses (MOI 0.1 pfu/cell) and microsomes were prepared 63 h post-infection. Reductase activity was measured using MTT as described in 'Materials and Methods' (Section Number 2.4.7). The moles of MTT reduced per minute per mg of protein were calculated.

CPR Species	Reductase activity (nmole MTT reduced/min/mg protein)
CYP1A2	10.6 ± 2.1
CYP1A2+ hRD	238.1 ± 19.7
CYP1A2+ ΔhRDM	100.9 ± 12.0
CYP1A2+ yRD	201.8 ± 23.5

It is noticeable from the Figure 5.16 (B) and Table 5.6 that ΔhRDM is more efficient than hRD and yRD in terms of its ability to support CYP1A2 catalytic activity or couple with the CYP. To compare the abilities of the CPRs to support CYP1A2 activity, their coupling efficiencies with CYP1A2 were calculated by using the following formula,

Coupling efficiency = CYP1A2 activity in CEC assay⁄CPR activity in MTT assay

As the coupling efficiency of ΔhRDM was highest among the three CPRs, percentage relative coupling efficiency for hRD and yRD was calculated in comparison with ΔhRDM, considering ΔhRDM activity as 100% (Table 5.8). Though coupling efficiency of yRD appears to be close to hRD, it is extremely destructive to the CYP1A2 holoprotein resulting in very low levels of spectrally active CYP1A2.

Table 5.8. Percent relative coupling efficiency of hRD, ΔhRDM and yRD with CYP1A2. CYP1A2 activity in the CEC assay and CPR activity measured in the MTT assay were used for the calculations. CYP1A2 activity was divided by CPR activity and percent relative coupling efficiency was measured.

Microsome samples	% Relative coupling efficiency
CYP1A2+ ΔhRDM	100
CYP1A2+ hRD	33.73
CYP1A2+ yRD	24.9

5.7.3 CYP2E1 interactions with hRD, ΔhRDM and yRD

CYP2E1 and cytochrome b_5 were expressed with and without the CPRs, microsomes were prepared and CYP2E1 holoprotein contents were measured by carbon monoxide difference spectroscopy as described in Section 5.7. Table 5.9 shows specific

contents of CYP2E1 when expressed with and without CPRs. It was observed that like other CYPs, CYP2E1 holoprotein levels change when co-expressed with the CPRs. However CYP1E1 apoprotein levels as measured by densitometry from the immunoblot **(**Figure 5.13 (B)**)** do not change regardless of co-expression with hRD, or ΔhRDM or yRD. These results confirm that CPRs do not regulate the CYP expression at the transcription level but are responsible for decrease in spectrally active enzyme i.e. holoprotein.

Table 5.9. CYP2E1 specific content in microsome samples, determined by reduced CO-difference spectroscopy. Sf9 cells were co-infected with CYP and CPR baculoviruses at an MOI of 1 and 0.1 pfu/ cell respectively. Microsomes were prepared 63 h post-infection as described in Materials and Methods (Section Number 2.4.1). Data are presented as mean values ± STDEV.

Microsomes	Specific content of CYP2E1 (pmole/mg protein)
CYP2E1+ b_5	1009.16
CYP2E1+ b_5 + hRD	471.88
CYP2E1+ b_5 + ΔhRDM	583.33
CYP2E1+ b_5 + yRD	453.49

Kinetic studies with CYP2E1 microsomes (i.e. measurement of activities) were performed using Vivid® fluorogenic substrate EOMCC (3-cyano-7-(ethoxymethoxy)

coumarin) as per the standard Invitrogen Screening Kit protocol (Marks et al; 2002, 2003). EOMCC is demethylated by human CYP2E1 as well as CYP2D6 to the fluorescent product 3-cyano-7-hydroxycoumarin (CHC). The reactions were carried out in a reaction volume of 100 µl/ well in 96-well black plates (Fisher Scientific, Catalogue No FB85083) at 37ºC in 100mM potassium phosphate buffer pH 8.0, containing 10 µM EOMCC, 2.5 pmole CYP2E1 and the NADPH regenerating system (1.3 mM NADP+, 3.3 mM glucose-6-phosphate, 3.3 mM $MgCl_2$, 0.4U/ml glucose-6-phosphate dehydrogenase). The fluorescent values were recorded on the Biotek Synegy HT plate reader using an excitation wavelength of 400 nm (20 nm) and emission wavelength of 460 nm (40 nm). Changes in fluorescence were measured as relative fluorescence units (RFU). Kinetic progression of reactions was measured for 30 min (Figure 5.17 (B) and Table 5.10). Concentrations of product formed were determined using CHC as a standard.

The standard curve of CHC was prepared using a range of concentrations of CHC (0, 39.1, 78.1, 156.3, 312.5, 625, 1250 pmole/ ml). The assay for the standard was performed in 96-well black plates. The fluorescent values (RFU) were recorded on the Biotek Synegy HT plate reader using an excitation wavelength of 400 nm (20 nm) and emission wavelength of 460 nm (40 nm). Standard curve was plotted and CHC concentrations in test samples were measured using the equation from the standard curve. The standard curve is shown in Figure 5.17 (A).

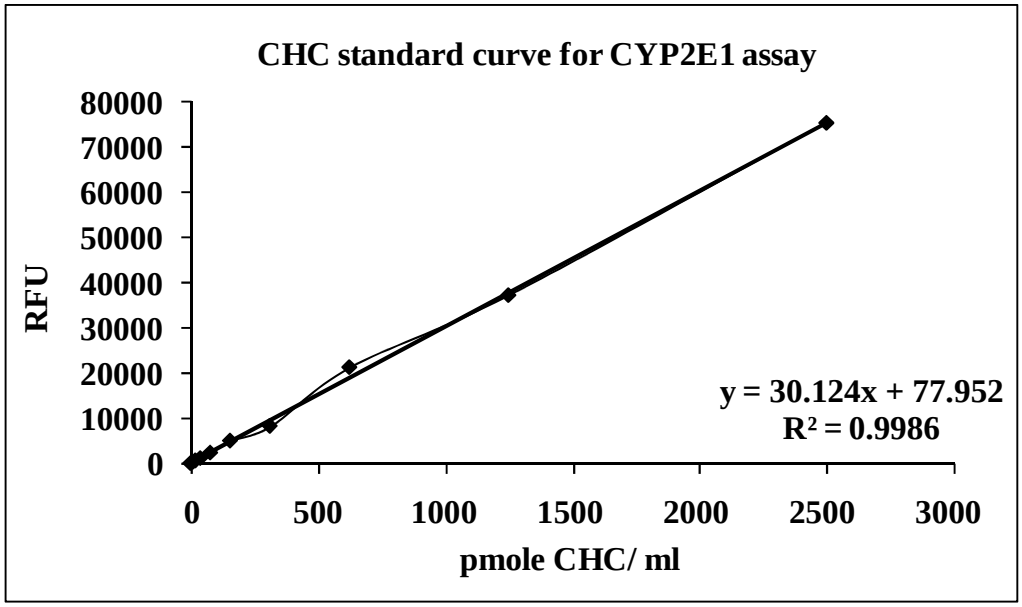

Figure 5.17 (A). CHC standard curve. The curve was prepared as described in Section 5.7.3

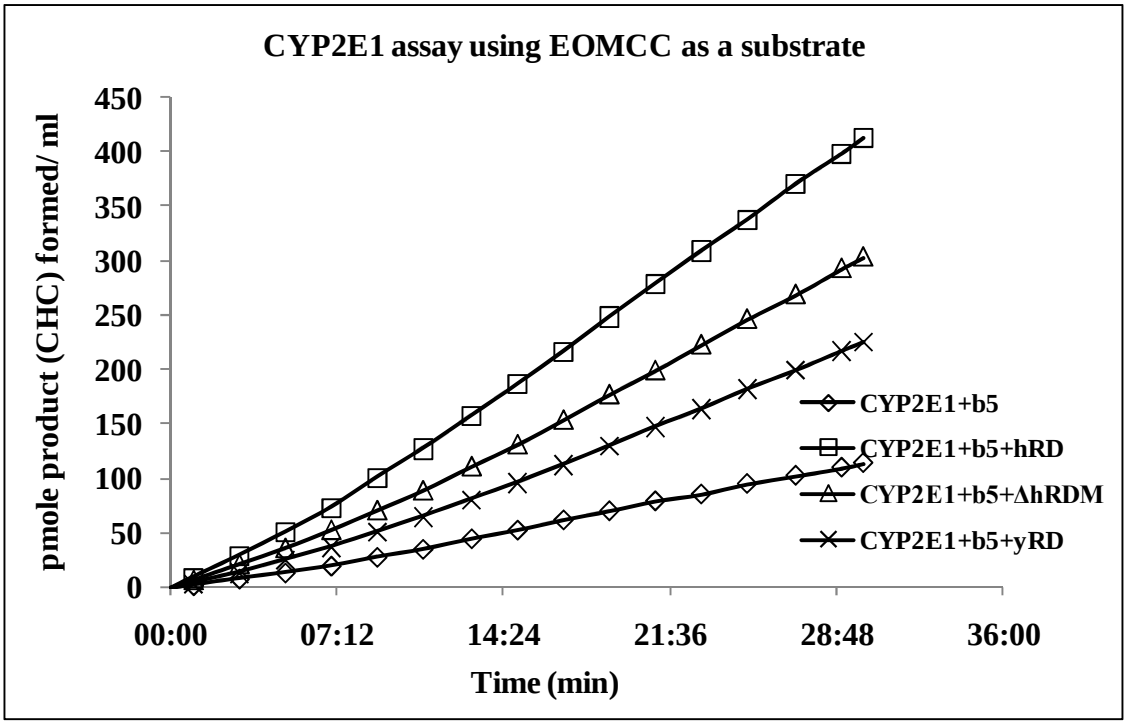

Figure 5.17 (B). Kinetic analysis of CYP2E1 catalytic activities using EOMCC as a substrate. Sf9 cells were co-infected with CYP2E1, CPR and cytochrome b_5

baculoviruses at an MOI of 1, 0.1 and 0.1 pfu/ cell, respectively. The catalytic activities of CYP2E1 were measured in microsomes prepared at 63h post-infection. The enzyme assay was performed as described in Section 5.7.3.

Table 5.10. CYP2E1 enzyme reaction rates in co-expressed microsomes. Sf9 cells were co-infected with CYP2E1, the CPR and b_5 baculoviruses at an MOI of 1, 0.1 and 0.1 pfu/ cell, respectively. The reaction rates were measured in microsomes prepared at 63h post-infection. EOMCC assay was performed as described in Section 5.7.3.

Microsomes	CYP2E1 reaction rates (pmole CHC formed/ min/ pmole of CYP2E1)
CYP2E1+ b_5	0.1581
CYP2E1+ b_5 + hRD	0.5671
CYP2E1+ b_5 + ΔhRDM	0.4149
CYP2E1+ b_5 + yRD	0.3077

Reductase activities of CPRs in CYP2E1 co-expressed microsomes were analysed using reductase assay as described in 'Materials and Methods' (Section Number 2.4.7) using MTT as a substrate. Reductase activity of hRD and yRD was comparable and reductase activity of ΔhRDM was lower than that of hRD and yRD (Table 5.11).

Table 5.11. NADPH cytochrome P450 reductase activities exhibited by hRD, ΔhRDM and yRD in CYP2E1 co-expressed microsomes. Sf9 cells were co-infected with CYP2E1 baculoviruses (MOI 1.0 pfu/cell), CPR baculoviruses (MOI 0.1 pfu/cell) and b_5 baculoviruses (MOI 0.1 pfu/cell), and microsomes were prepared 63 h post-infection. Reductase activity was measured by using MTT as described in 'Materials and Methods' (Section Number 2.4.7). The moles of MTT reduced per minute per mg of protein were calculated.

CPR Species	Reductase activity (nmole MTT reduced/min/mg protein)
CYP2E1+ b5	26.5 ± 3.8
CYP2E1+ b5+ hRD	217.7 ± 19.3
CYP2E1+ b5+ ΔhRDM	169.9 ± 17.1
CYP2E1+ b5+ yRD	276.1 ± 45.5

The coupling efficiency was calculated. The percent relative coupling efficiency of CPRs with CYP2E1 was calculated in comparison with ΔhRDM (Table 5.12). Surprisingly hRD and ΔhRDM couple equally well with CYP2E1 and coupling efficiency of yRD with CYP2E1 seems to be better than that with CYP1B1 and CYP1A2. The findings show that interaction of any particular CPR with CYP is dependent on the CYP isoform.

Table 5.12. Percent relative coupling efficiency of hRD, ΔhRDM and yRD with CYP2E1. CYP2E1 activity in the EOMCC assay and CPR activity measured in the MTT assay were used for the calculations. CYP2E1 activity was divided by CPR activity and percent relative coupling efficiency was measured.

Microsome samples	% Relative coupling efficiency
CYP2E1+ b_5+ ΔhRDM	100
CYP2E1+ b_5+ hRD	106.65
CYP2E1+ b_5+ yRD	45.64

5.7.4 CYP1A1 co-expression with ΔhRDM

CYP1A1 and CYP2C8 were co-expressed only with ΔhRDM as described in Section 5.7. The catalytic activity of CYP1A1 was measured using ethoxyresorufin-O-deethylase (EROD) assay (Klotz et al. 1984). The amount of resorufin produced was measured fluorometrically which reflects the level of 7-ethoxyresorufin o-deethylase activities.

The assay was performed as described before (Klotz et al. 1984). The reaction kinetics was carried out at 37ºC in a reaction volume of 100 µl/well in 96-well black plates with transparent flat bottom (Fisher, Cat. No. FB86083). The assay mixture contained 100 mM Potassium phosphate buffer pH 7.4, containing 5µM 7-ethoxyresorufin , 1.5 pmole CYP1A1 and the NADPH regenerating system (1.3 mM

NADP+, 3.3 mM G6P, 3.3 mM $MgCl_2$, 0.4U/ml G6PDH). Resorufin formation was measured fluorometrically on the Biotek Synegy HT plate reader (excitation wavelength of 528/20 nm and emission wavelength of 590/20 nm). Changes in fluorescence were recorded for 30 min as relative fluorescence units (RFU). Standard curve shown in Figure 5.15 (A) was used to calculate resorufin concentrations in test samples. CYP1A1 was successfully co-expressed with ΔhRDM as a catalytically active enzyme.

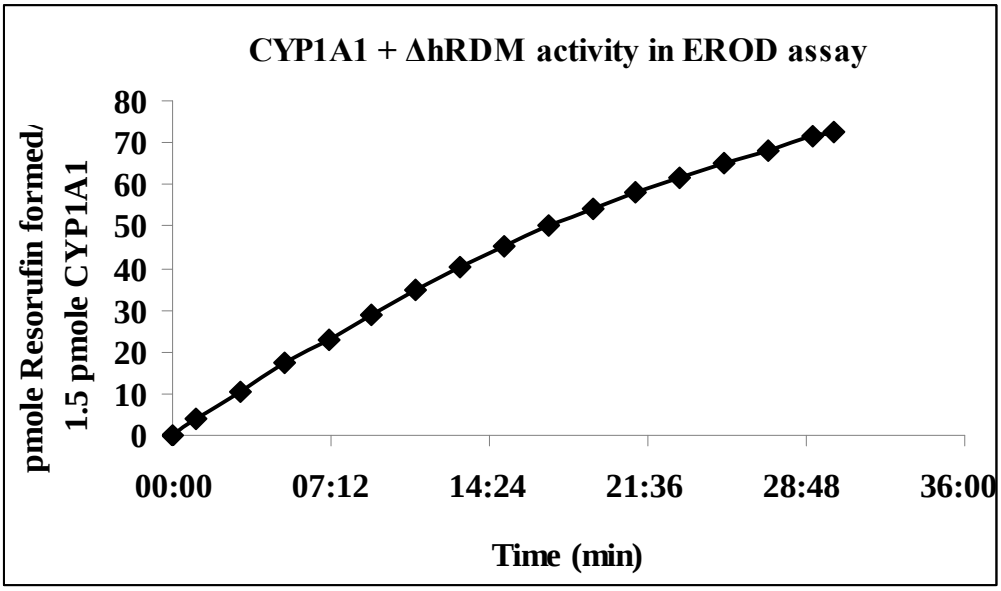

Figure 5.18. Kinetic analysis of CYP1A1 catalytic activity in EROD assay. Sf9 cells were co-infected with CYP1A1 and CPR baculoviruses at an MOI of 1 and 0.1 pfu/ cell, respectively. The catalytic activity of CYP1A1 was measured in microsomes prepared at 63h post-infection. The enzyme assay was performed as described above. The reaction rate observed was 1.608 pmole resorufin formed/ min/ pmole of CYP1A1.

5.7.5 CYP2C8 co-expression with ΔhRDM

Dibenzylfluorescein (DBF) dealkylation activities in the microsomal fractions prepared from the Sf9 cells co-infected with CYP2C8+b_5+ΔhRDM baculoviruses at an MOI of 1, 0.1 and 0.1 pfu/cell respectively for 63 h were determined. DBF is dealkylated by CYP2C and CYP3A to form the product, fluorescein. The production of the metabolite, fluorescein from the substrate DBF (BD-Gentest, Catalogue No 451755) was measured for 30 min at 37ºC. The reactions were carried out at 37ºC in a reaction volume of 0.1ml/well in 96-well black plates. The assay mixture contained 100mM Potassium phosphate buffer pH 8.0, containing 1 µM DBOMF , 4.0 pmole CYP2C8 and the NADPH regenerating system (1.3 mM NADP+, 3.3 mM G6P, 3.3 mM $MgCl_2$, 0.4U/ml G6PDH). Fluorescein formation was measured fluorometrically on the Biotek Synegy HT plate reader (excitation wavelength of 485/20 nm and emission wavelength of 528/20 nm). Changes in fluorescence were recorded for 30 min as relative fluorescence units (RFU). Metabolite of DBF, fluorescein was used to generate a standard curve (Chapter 4, Figure 4.10 (B)). Fluorescein formed per ml of the reaction over a period of 30 min in test samples (Figure 5.19) was calculated using the standard curve. CYP2C8 was successfully co-expressed with ΔhRDM as a catalytically active enzyme.

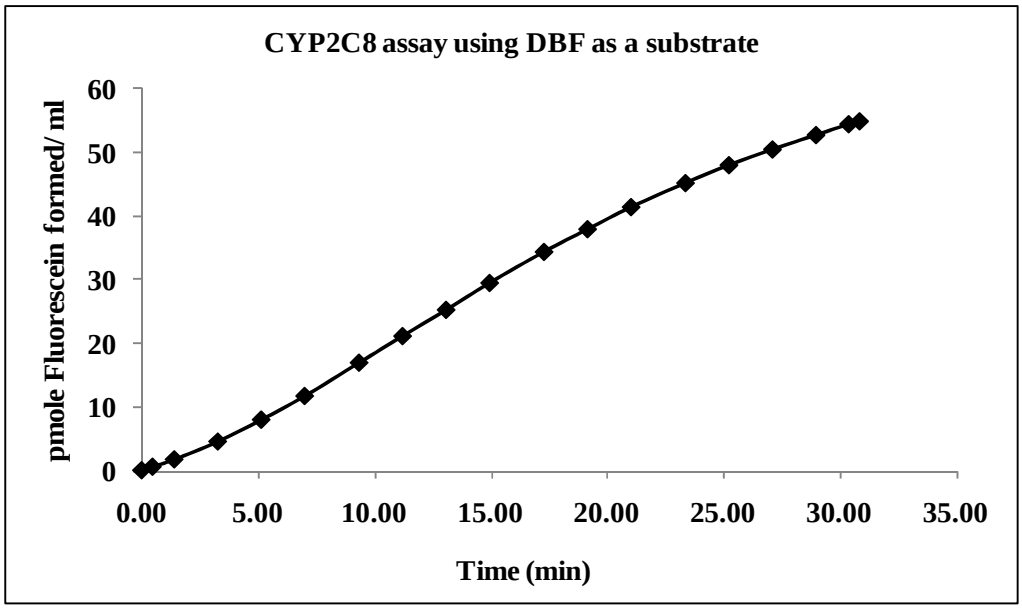

Figure 5.19. Kinetic analysis of CYP2C8 catalytic activity using DBF as a substrate. Sf9 cells were co-infected with CYP2C8, ΔhRDM and b_5 baculoviruses at an MOI of 1. 0.1 and 0.1 pfu/ cell, respectively. The catalytic activities of CYP2C8 were measured in microsomes prepared at 63h post-infection. The enzyme assay was performed as described above. The reaction rate observed was 0.047 pmole fluorescein formed/ min/ pmole of CYP2C8.

5.8 Conclusion

It has been reported that P450 enzymes and the accessory proteins (NADPH-P450 reductase and cytochrome b_5) interact with each other with different affinities (Shimada et. al, 2005). The objective of studying individual CYPs for their interactions with the CPRs was to elucidate whether we observe any differences in the affinities. However in our project, in order to study these affinities, we have taken an approach of studying coupling between CYP and CPR, where the enzyme catalytic activities are taken into account. We studied the CPRs, viz. hRD, ΔhRDM and yRD, in context of three more CYPs – CYP1B1, CYP1A2 and CYP2E1. We also studied CYP1A1 and CYP2C8, though only in the context of ΔhRDM. In the case of CYP2C8 and CYP2E1, apart from a CPR, a third protein cytochrome b_5 was also co-expressed. Cytochrome b_5 is known to augment CYP2C8 and CYP2E1 mediated monooxygenase reactions (Porter, 2002). In conclusion, we summarise the findings of Chapter 5 as follows,

- The five human cytochrome P450 enzymes CYP1A1, CYP1A2, CYP1B1, CYP2C8 and CYP2E1 were cloned into the transfer vector pFastBac1, recombinant bacmids were made and baculoviruses for the CYPs were generated successfully.

- The five CYPs were expressed alone and also co-expressed with the CPRs and where necessary with a third protein cytochrome b_5. The CYPs were expressed as catalytically active enzymes by means of co-infection with multiple recombinant baculoviruses. Multiple baculoviruses can be used to express a productive monooxygenase system in insect cells.

- It was observed through Western blot densitometry and CO-binding difference spectra that CPRs destroy the CYP holoproteins without altering CYP apoprotein levels. This would indicate that CPRs do not modulate CYP expression at the transcriptional level but are responsible for destruction of CYP holoprotein which is a result of ROS induction by CPRs. The experimental evidence for ROS generation by CPRs has been presented in Chapters 3 and 4.

- The enzyme assays for CYPs and CPRs were set up and used for studying the CYP-CPR interactions. ΔhRDM was identified as the most efficient CPR, amongst hRD, ΔhRDM and yRD, in terms of its ability to cause less damage to CYP holoprotein and to support CYP catalytic activities more efficiently with the exception of CYP2E1 where hRD was found to be the best in terms of supporting the enzyme activity.

- In co-expressed microsomes, reduction potential of yRD in MTT assay is similar to hRD or sometimes better, but yRD does not support CYP activity very well, which indicates that its reduction potential towards MTT is not directly proportional to its ability to support CYP catalytic activities.

- The coupling efficiency of yRD with the CYPs was found to be inferior to ΔhRDM and hRD which indicates that use of yRD for human CYP expressions particularly in the 'insect cell expression system' may not be physiologically feasible. As coupling efficiency of the genetically engineered molecule ΔhRDM

was higher than hRD and yRD, relative coupling efficiencies for hRD and yRD were calculated assuming ΔhRDM coupling efficiency as 100%. The coupling efficiencies of CYP1B1, CYP1A2 and CYP2E1 with hRD, ΔhRDM and yRD are summarised below in the Table 5.13.

Table 5.13. Percent relative coupling efficiencies of hRD, ΔhRDM and yRD with CYP1B1, CYP1A2 and CYP2E1.

		coupling efficiency	
CYP/ CPR	ΔhRDM	hRD	yRD
CYP1B1	100%	63.49	24.78
CYP1A2	100%	33.73	24.9
CYP2E1	100%	106.65	45.64

- The full length NADPH cytochrome P450 reductase, hRD, coupled as efficiently as ΔhRDM with CYP2E1; hRD and yRD were specifically very destructive to CYP1A2 as compare to other CYPs, which proves that different CPRs have different affinities towards the CYP isoforms.

Chapter 6 Cytochrome P450 inhibition – using known selective inhibitors to profiling of the natural product Plumbagin, a naphthoquinone

6.1 Introduction

Evaluation of specific cytochrome P450 enzyme inhibition by a drug candidate is crucially important as co-administration of drugs may result in one or both inhibiting the other's metabolism, a concept known as 'pharmacokinetic drug–drug interactions'(Li, 1997). This may alter plasma levels and potentially cause adverse drug reactions or toxicity; therefore, cytochrome P450 inhibition studies are vital for predicting drug-drug interactions (DDI).

DDI remains an important aspect of clinical practice and new drug discovery process. The antifungal agent ketoconazole, a potent inhibitor of CYP3A4, can interact with drugs that are potential substrates of CYP3A4. One example of this is the interaction between the inhibitor ketoconazole and the substrate terfenadine. Co-administration of ketoconazole and terfenadine leads to increased plasma levels of terfenadine, resulting in cardiotoxicity. The interaction between terfenadine and ketoconazole is known as an inhibitory drug–drug interaction, where one drug (ketoconazole) inhibits the metabolism of another drug (terfenadine), leading to a higher than intended plasma level (Li, 2005). The major clinical consequence of inhibitory DDI is undesired drug toxicity (Miller et al. 2000).

In drug metabolism or CYP inhibition studies, usually cDNA-expressed microsomes that contain only one specific human CYP isoform are used as an *in vitro* system. Of the human P450 enzymes, a relatively small subset of the CYPs (CYP1A2, CYP2D6, CYP2C9, CYP2C19, CYP3A4 and CYP2E1) appears to be the most commonly responsible for metabolism of drugs and associated drug-drug interactions (Spatzenegger and Jaeger 1995). More recently, some other human P450 enzymes, such as CYP3A5, CYP2B6, and CYP2C8, have come to the fore because they have been implicated in the metabolism of a number of marketed drugs and physiologically important endogenous molecules **(**O'Donnell et al. 2006).

There is some degree of similarity among the CYP enzyme structures. However, that structural similarity of enzymes cannot be used to predict which isoforms will be responsible for a drug's metabolism. In view of that, the pharmaceutical industry has found it highly desirable to develop high-throughput screening assays on the basis of cDNA-expressed microsomes that contain only one specific human P450 isoform.

Cytochrome P450 inhibition is measured via CYP enzyme assays in the presence of a range of concentrations of a test compound and enzyme activity is compared to the vehicle control. A compound concentration responsible for 50% inhibition of the enzyme activity (IC_{50}) is then calculated. Wide-scale determination of IC_{50}s of potential drug candidates from mechanism-based data, using *in vitro* systems, allows dramatic reduction in the number of *in vivo* studies that were previously required.

In this chapter, we present results from inhibition studies with the CYP isozymes, CYP1A1, CYP1A2, CYP1B1, CYP2D6 and CYP3A4. The CYP inhibition experiments were performed using our own CYP enzymes so as to find out if there are any differences in the catalytic properties of the electron donor partner hRD and its variant ΔhRDM with respect to activation of the CYPs. The primary objective of our inhibition studies was to determine whether the genetically engineered variant of the full length NADPH cytochrome P450 reductase (ΔhRDM) results in any change in quantitative inhibition of the CYPs that are activated by the native human CPR (hRD) – in other words, whether inhibition data from these two systems (one supported by hRD and other by ΔhRDM) is different from each other. In order to do so, we compared different CYP–ΔhRDM complexes with CYPs whose activities were supported by hRD in inhibition studies.

Known selective inhibitors, α-naphthoflavone (for CYP1A1 and CYP1B1; Shimada et al. 1998), furafylline (for CYP1A2; Tassaneeyakul et al. 1994), quinidine (for CYP2D6; Von Bahr et al. 1980) and ketoconazole (for CYP3A4; Olkkola et al. 1994) have been used for the comparative inhibition studies.

Apart from the above mentioned reference standards, the natural naphthoquinone plumbagin, was analysed for its ability to inhibit CYP1A1, CYP1A2, CYP1B1, CYP2D6 and CYP3A4. Plumbagin is isolated from the roots of *plumbago zeylannica* (Chitrak) and has been used in Indian ayurvedic medicine for thousands of years (Iyengar and Pendse 1966). The compound has potential antiproliferative activity

against several tumour types (Acharya et al. 2008) and it also has anti-microbial activity (Farr et al. 1985). At De Montfort University, we have been involved in investigating anti-proliferative activity of different natural compounds. In our experiments, plumbagin proved to be quite efficacious and that was the reason why we chose to investigate its CYP inhibition profile. As described earlier, assessment of the *in vitro* CYP inhibition potential of plumbagin may have important implications for predicting the likelihood of plumbagin's interactions with other marketed anticancer agents.

6.2 IC_{50} Determination

The IC_{50} determination methodology was adapted from protocols obtained from BD Biosciences with some modifications. The assays were performed in 96-well black microtitre plates with transparent flat bottom (Fisher, Catalogue No FB86083). The template for plate set up is shown in Figure 6.1. The row designations are A through H and the column designations are 1 through 12. The assays were performed in duplicate rows of 12 wells. The test compound was added to the wells in column one and serially diluted 3-fold to the wells in column 8. Wells in columns 9 and 10 were control wells which contained no test compound (therefore no inhibition, that is full signal, was detected). The wells in columns 11 and 12 were blanks. To the blank wells stop solution was added prior to the addition of CYP enzymes and their respective substrates. The only signal detected in blanks was background noise. Rows A/B and C/D were replicates. The assay was conducted in a final volume of 200 µl per well.

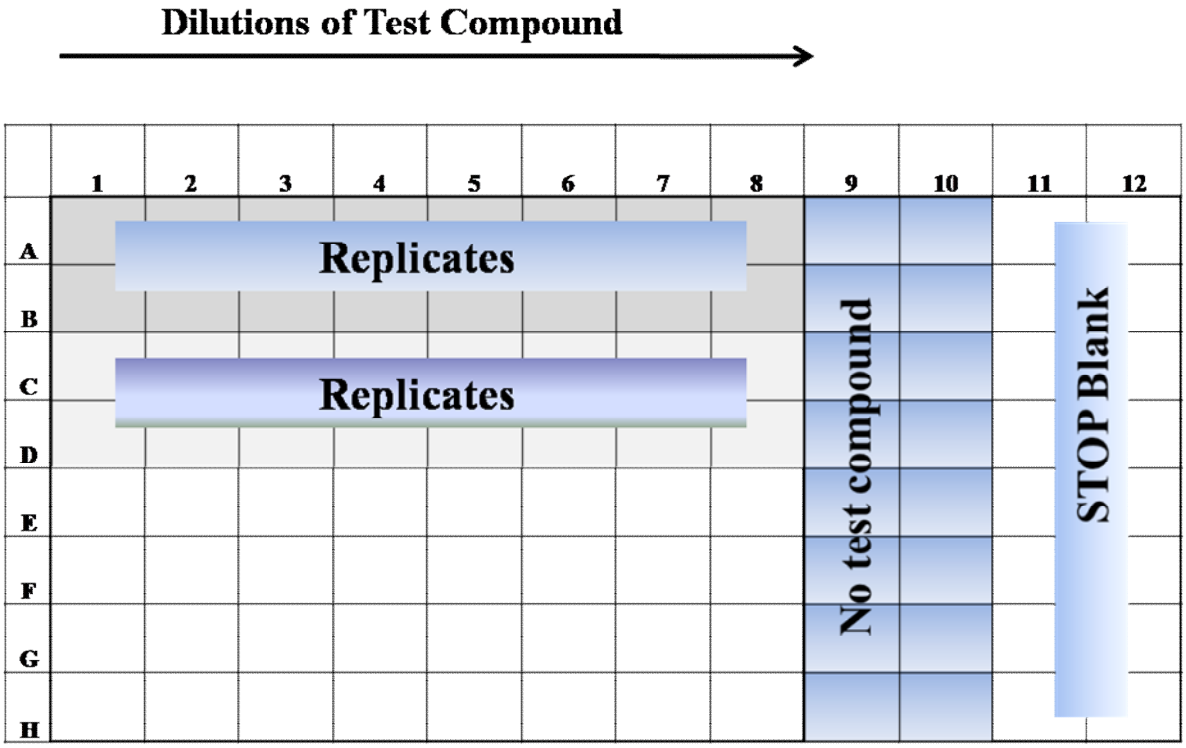

Figure 6.1. 96-well microtitre plate set up for IC_{50} determination in CYP inhibition assays.

6.3 CYP1A1 inhibition by α-naphthoflavone and plumbagin

The CYP1A1 microsomes co-expressed with hRD and ΔhRDM were subjected to inhibition studies. The protein expressions and microsome preparations were performed as described in Chapter 5. CYP1A1 inhibition by reference standard (i.e. the known inhibitor), α-naphthoflavone, and the test compound, plumbagin, was performed using the end point EROD assay. EROD assay is described in Chapter 5. In the assay plate, into the wells in column 1, 144 µl and into the wells in columns 2 to 12, 100 µl of the NADPH regenerating system was added (1.3 mM NADP+, 3.3 mM G6P, 3.3 mM $MgCl_2$, 0.4U/ml G6PDH). 6 µl of the α-naphthoflavone stock (50 µM prepared in

acetonitrile) was added to A1 and B1 wells. 6 µl of the plumbagin stock (500 µM prepared in acetonitrile) was added to C1 and D1 wells. 50 µl of the solutions from the wells in column 1 to the wells in columns 2 through 8 were serially diluted using a multichannel pipette. In order to minimize the potential carry over, pipette tips were changed during every step of the serial dilution. The extra 50 µl solution in the wells in column 8 was removed and discarded. The plate was covered with a lid and placed in a 37°C incubator for 10 min to pre-warm the solution and the plate. Then to the wells in columns 1 through 10, 100 µl of the enzyme/substrate mix was added to the final concentration of 5 µM 7-ethoxyresorufin and 1.5 pmole CYP1A1 in 100 mM potassium phosphate buffer pH 7.4. The lid of the plate was replaced and the plate was incubated at 37°C for 15 min. At the end of the incubation period, the reaction was stopped by dispensing 75 µl of the STOP solution to each well (80% acetonitrile and 20% 0.5 M Tris base). To the blank wells in column 11 and 12, STOP solution was added prior to initiation of the reaction. At the end, 100 µl of the enzyme/substrate mix was added to the wells in columns 11 and 12. The plate was then scanned on the Biotek Synegy HT plate reader for measuring relative fluorescence units (RFU) at excitation wavelength of 528/20 nm and emission wavelength of 590/20 nm. The averages of replicates were used for calculating the percentage (%) inhibition of CYP1A1 at every concentration of α-naphthoflavone and plumbagin that was tested. The % inhibition was calculated using the RFU values obtained in control wells with the help of the formula,

$$\% \text{ Inhibition} = 100 - \left(\frac{\text{Test - Blank}}{\text{Control - Blank}} \text{ X } 100 \right)$$

The percentage inhibition calculated for each concentration of the compounds was then used for calculating IC_{50} value using the formula,

$$IC_{50} = \left[\frac{50\ \% - \text{low percentage}}{\text{high percentage} - \text{low percentage}} \ X\ (\text{high concentration} - \text{low concentration}) \right] + \left[\text{low concentration} \right]$$

where, low percentage is percent inhibition less than 50% and high percentage is percent inhibition greater than 50%. High and low concentrations are respective concentrations of the compounds at which the high percentage and low percentage inhibition is observed.

Table 6.1 Alpha-naphthoflavone and plumbagin IC_{50} values in assays that monitor the inhibition of CYP1A1+hRD and CYP1A1+ΔhRDM. Data are presented as mean values ± STDEV of duplicates of single experiment.

Microsome samples	**α-Naphthoflavone IC_{50} (µM)**	**Plumbagin IC_{50} (µM)**
CYP1A1+hRD	0.0703 ± 0.008	5.88149 ± 0.683
CYP1A1+ΔhRDM	0.06 ± 0.005	5.3194 ± 0.81

Results depicted in Table 6.1 show that there are no significant differences in IC_{50} values of the two compounds when tested with CYP1A1+ hRD and CYP1A1+ ΔhRDM ($P > 0.05$). Moreover the dose-dependent responses to the inhibition of

CYP1A1, when separately co-expressed with hRD or with ΔhRDM, by α-naphthoflavone are very similar (Figure 6.2). This is true for plumbagin too (Figure 6.3). These comparative inhibition studies, using CYP1A1+hRD and CYP1A1+ΔhRDM, do not show any significant difference in IC_{50} values or dose-response profiles of the two compounds. The results indicate that the novel, genetically engineered ΔhRDM does not at all alter the nature of the active site of the CYP1A1 – if it did, IC_{50} values and the dose-response curves would have been noticeably different. Therefore, we would like to suggest that CYP microsomes that use ΔhRDM as the electron donor protein can be confidently used for drug metabolism studies

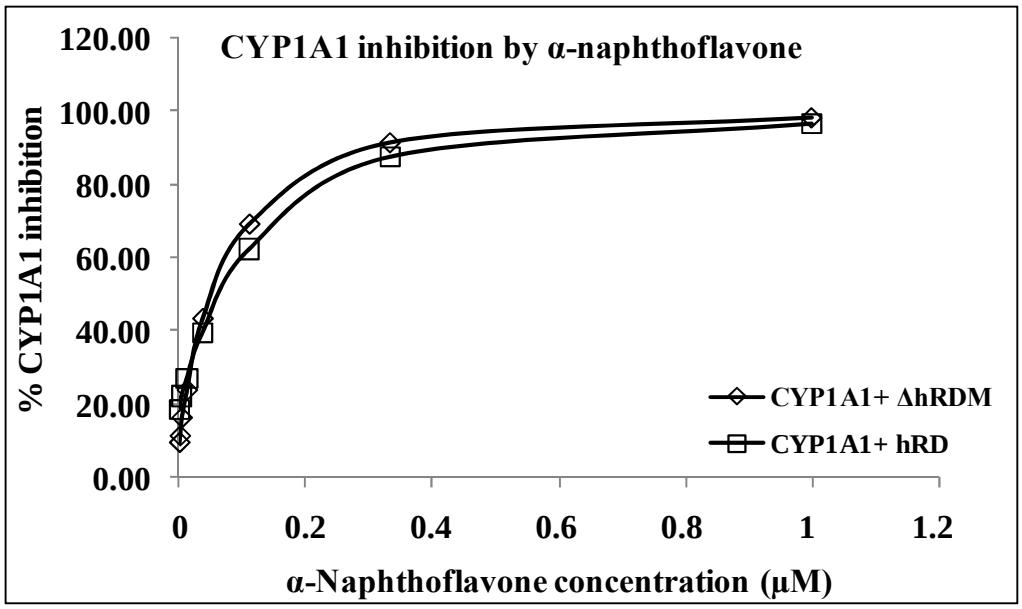

Figure 6.2. The CYP1A1 inhibition by α-naphthoflavone at various concentrations. Inhibition studies were performed as described in Section 6.3. Each value represents the mean of individual determinations.

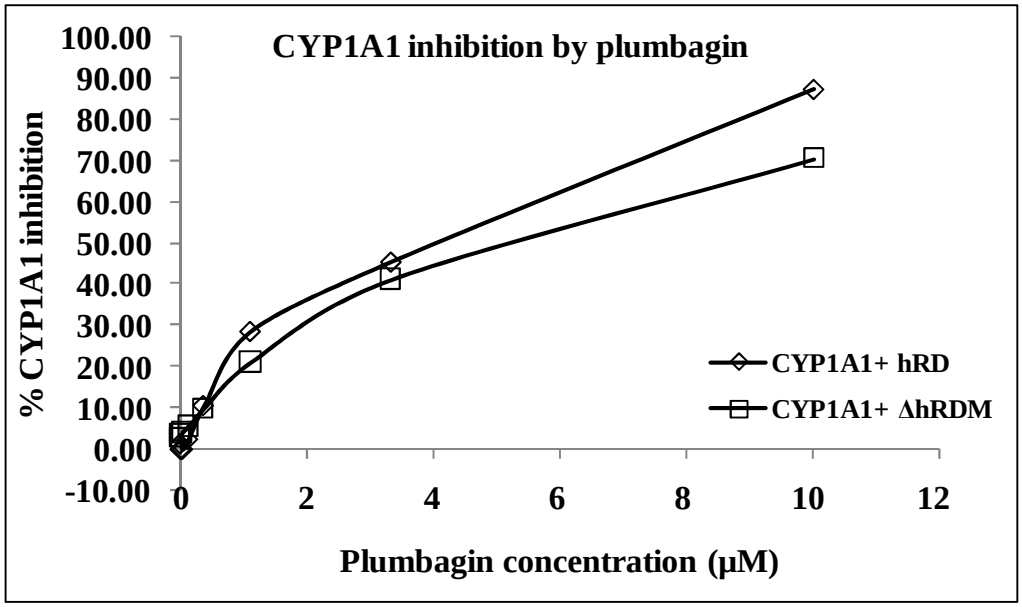

Figure 6.3. The CYP1A1 inhibition by plumbagin at various concentrations. Inhibition studies were performed as described in Section 6.3. Each value represents the mean of individual determinations.

6.4 CYP1B1 inhibition by α-naphthoflavone and plumbagin

The CYP1B1 microsomes that co-express hRD and ΔhRDM were subjected to inhibition studies. CYP1B1 inhibition by the reference standard, α-naphthoflavone, and test compound, plumbagin, was performed using the end point EROD assay. The inhibition assay was performed as described in Section 6.3 except that CYP1B1 microsomes were used in the place of CYP1A1.

Table 6.2. Alpha-naphthoflavone and plumbagin IC_{50} values in assays that monitor the inhibition of CYP1B1+hRD and CYP1B1+ΔhRDM. Data are presented as mean values ± STDEV of duplicates of single experiment.

Microsome samples	**α-Naphthoflavone IC_{50} (nM)**	**Plumbagin IC_{50} (μM)**
CYP1B1+hRD	0.780 ± 0.092	2.3543 ± 0.155
CYP1B1+ΔhRDM	0.811 ± 0.068	2.4038 ± 0.17

As shown in Table 6.2 there are no significant differences in the IC_{50} values for the CYP1B1+ hRD and CYP1B1+ ΔhRDM ($P > 0.05$). The CYP1B1 inhibition by α-naphthoflavone and plumbagin in CYP1B1+hRD and CYP1B1+ΔhRDM samples was dose dependent (Figure 6.4 and Figure 6.5). The comparative inhibition studies using CYP1B1+hRD and CYP1B1+ΔhRDM did not show any significant difference in the IC_{50} or dose-response values of the two compounds.

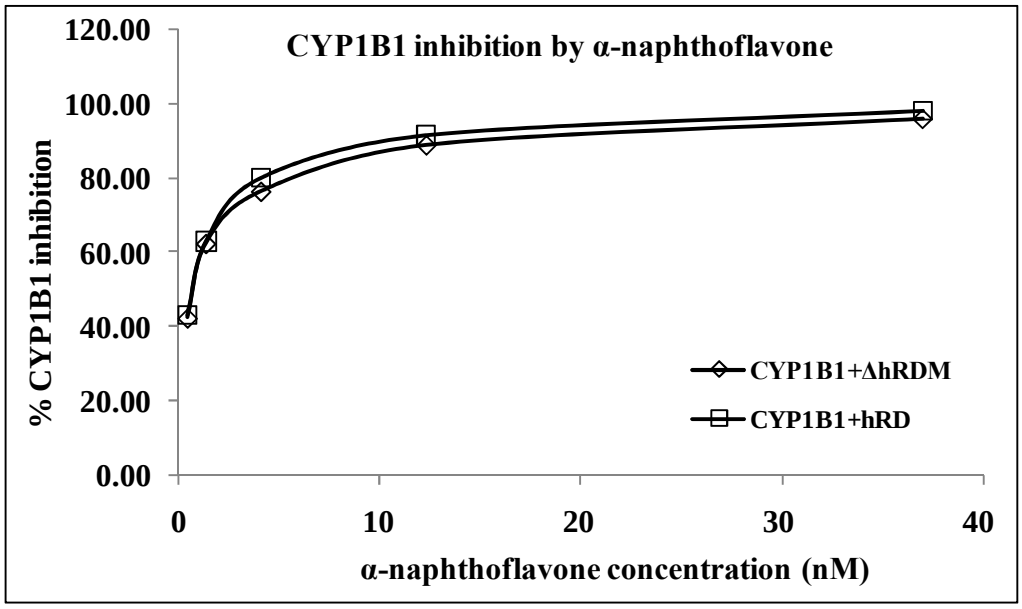

Figure 6.4. The CYP1B1 inhibition by α-Naphthoflavone at various concentrations. Inhibition studies were performed as described in Section 6.4. Each value represents the mean of individual determinations.

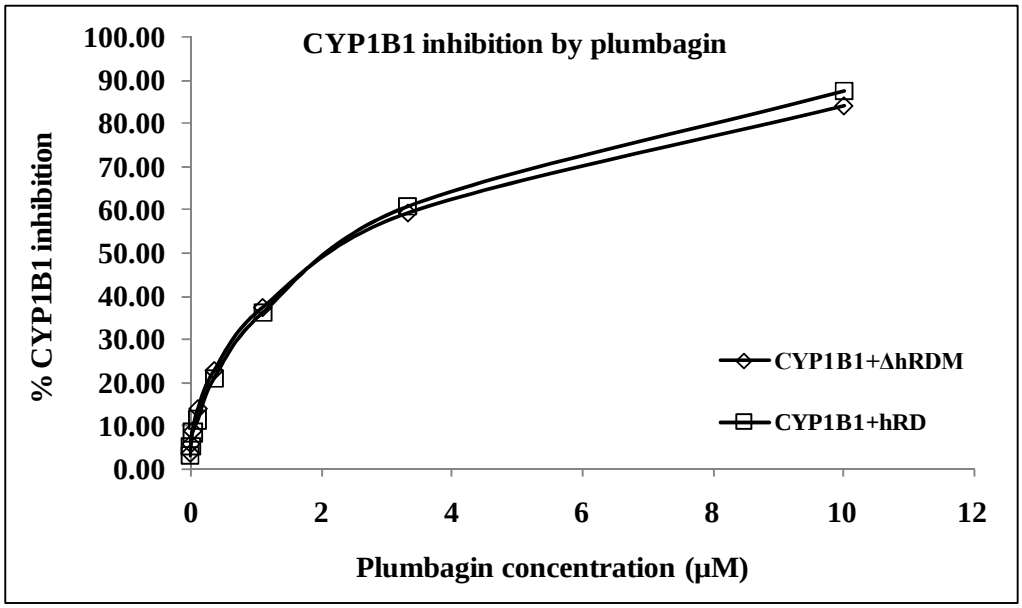

Figure 6.5. The CYP1B1 inhibition by plumbagin at various concentrations. Inhibition studies were performed as described in Section 6.4. Each value represents the mean of individual determinations.

6.5 CYP1A2 inhibition by furafylline and plumbagin

The CYP1A2 microsomes co-expressed with hRD and ΔhRDM were subjected to inhibition studies. CYP1A2 inhibition by the reference standard, furafylline, and test compound, plumbagin, was performed using CEC assay. CYP1A2 expression in Sf9 cells, microsome preparation and assay using CEC as a substrate is described in Chapter 5. In the assay plate, into the wells in column 1, 144 µl and into the wells in columns 2 to 12, 100 µl of the NADPH regenerating system was added (1.3 mM NADP+, 3.3 mM G6P, 3.3 mM $MgCl_2$, 0.4U/ml G6PDH). 6 µl of the furafylline stock (5 mM prepared in acetonitrile) was added to A1 and B1 wells. 6 µl of the plumbagin stock (500 µM prepared in acetonitrile) was added to C1 and D1 wells. 50 µl of the solutions from the wells in column 1 to the wells in columns 2 through 8 were serially diluted using a multichannel pipette. In order to minimize the potential carry over, pipette tips were changed during every step of the serial dilution. The extra 50 µl solution in the wells in column 8 was removed and discarded. The plate was covered with a lid and placed in a 37°C incubator for 10 min to pre-warm the solution and the plate. Then to the wells in columns 1 through 10, 100 µl of the enzyme/substrate mix was added to the final concentration of 50 µM CEC and 1.0 pmole CYP1A2 in 100 mM potassium phosphate buffer pH 7.4. The lid of the plate was replaced and the plate was incubated at 37°C for 15 min. At the end of the incubation period, the reaction was stopped by dispensing 75 µl of the STOP solution to each well (80% acetonitrile and 20% 0.5 M Tris base). To the blank wells in column 11 and 12, STOP solution was added prior to initiation of the reaction. At the end, 100 µl of the enzyme/substrate mix was added to the wells in columns 11 and 12. The plate was then scanned on the Biotek Synegy HT plate reader for measuring relative fluorescence units (RFU) at excitation wavelength of 409/20 nm

and emission wavelength of 460/20 nm. The averages of replicates were used for calculating the % inhibition of CYP1A2 at every concentration of furafylline and plumbagin. The percent inhibition was calculated in comparison with control using the formula,

$$\% \text{ Inhibition} = 100 - \left(\frac{\text{Test - Blank}}{\text{Control - Blank}} \text{ X } 100 \right)$$

The percent inhibition calculated for each concentration of the compounds was then used for calculating IC_{50} value using the formula,

$$IC_{50} = \left[\frac{50\ \% \text{ - low percentage}}{\text{high percentage - low percentage}} \text{ X } (\text{high concentration} - \text{low concentration}) \right] + \left[\text{low concentration} \right]$$

where low percentage is percent inhibition less than 50% and high percentage is percent inhibition greater than 50%. High and low concentrations are respective concentrations of the compounds at which the high percentage and low percentage inhibition is observed.

Table 6.3. Furafylline and plumbagin IC_{50} values in CYP1A2+hRD and CYP1A2+ΔhRDM inhibition assays. Data are presented as mean values ± STDEV of duplicates of single experiment.

Microsome samples	**Furafylline IC_{50} (µM)**	**Plumbagin IC_{50} (µM)**
CYP1A2+hRD	1.5217 ± 0.235	1.2975 ± 0.302
CYP1A2+ΔhRDM	1.6809 ± 0.269	1.4256 ± 0.277

As shown in Table 6.3, there are no significant differences in IC_{50} values for the CYP1A2+ hRD and CYP1A2+ ΔhRDM ($P > 0.05$). The CYP1A2 inhibition by furafylline and plumbagin in CYP1A2+hRD and CYP1A2+ΔhRDM samples was dose dependent (Figure 6.6 and Figure 6.7). The comparative inhibition studies using CYP1A2+hRD and CYP1A2+ΔhRDM did not show significant difference in IC_{50} or dose-response values of the compounds.

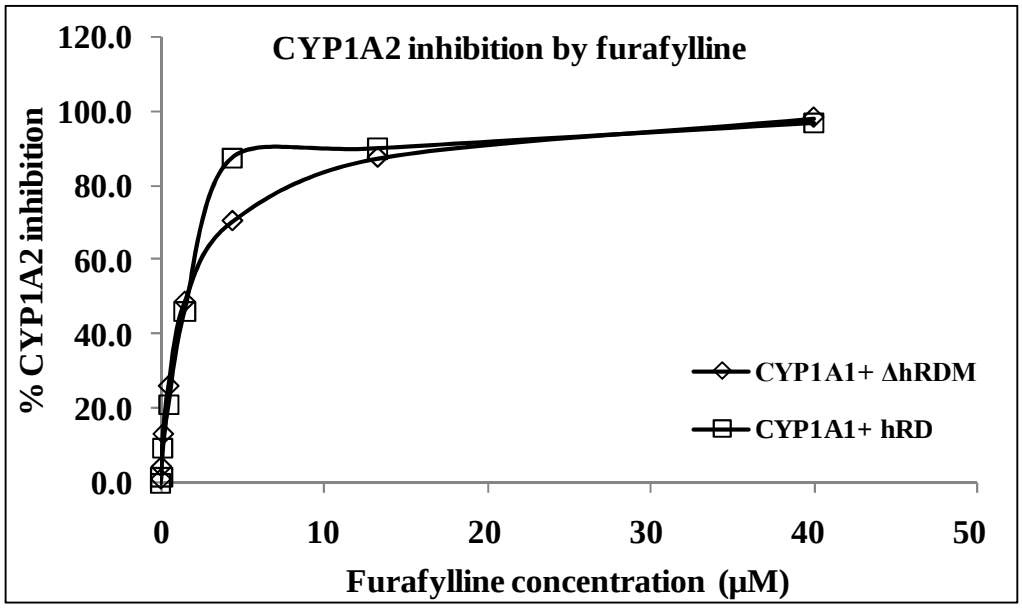

Figure 6.6. The CYP1A2 inhibition by furafylline at various concentrations. Inhibition studies were performed as described in Section 6.5. Each value represents the mean of individual determinations.

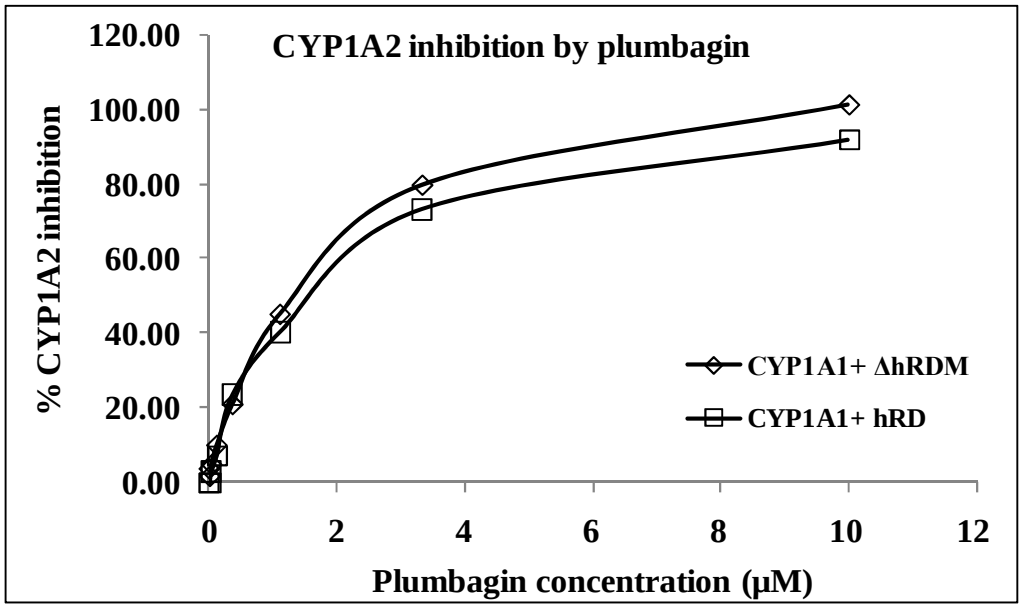

Figure 6.7. The CYP1A2 inhibition by plumbagin at various concentrations. Inhibition studies were performed as described in Section 6.5. Each value represents the mean of individual determinations.

6.6 CYP2D6 inhibition by quinidine and plumbagin

The CYP2D6 microsomes, co-expressed with hRD and ΔhRDM, were subjected to inhibition studies. CYP2D6 inhibition by the reference standard, quinidine, and test compound, plumbagin, was performed using AMMC assay. CYP2D6 expression, microsome preparation and assay using AMMC as a substrate are described in Chapter 3. In the assay plate, into the wells in column 1, 144 µl and into the wells in columns 2 to 12, 100 µl of the NADPH regenerating system was added (1.3 mM NADP+, 3.3 mM G6P, 3.3 mM $MgCl_2$, 0.4U/ml G6PDH). 6 µl of the quinidine stock (25 µM prepared in acetonitrile) was added to A1 and B1 wells. 6 µl of the plumbagin stock (500 µM prepared in acetonitrile) was added to C1 and D1 wells. 50 µl of the solutions from the wells in column 1 to the wells in columns 2 through 8 were serially diluted using a multichannel pipette. In order to minimize the potential carry over, pipette tips were changed during every step of the serial dilution. The extra 50 µl solution in the wells in column 8 was removed and discarded. The plate was covered with a lid and placed in 37°C incubator for 10 min to pre-warm the solution and the plate. Then to the wells in columns 1 through 10, 100 µl of the enzyme/substrate mix was added to the final concentration of 1.5 µM AMMC and 1.5 pmole CYP2D6 in 100 mM Potassium phosphate buffer pH 8. The lid of the plate was replaced and the plate was incubated at 37°C for 30 min. At the end of the incubation period, the reaction was stopped by dispensing 75 µl of the STOP solution to each well (80% acetonitrile and 20% 0.5 M Tris base). To the blank wells in column 11 and 12, STOP solution was added prior to initiation of the reaction. At the end 100 µl of the enzyme/substrate mix was added to the wells in columns 11 and 12. The plate was then scanned on the Biotek Synegy HT plate reader for measuring relative fluorescence units (RFU) at excitation wavelength of

390/20 nm and emission wavelength of 460/40 nm. The averages of replicates were used for calculating the % inhibition of CYP2D6 at every concentration of quinidine and plumbagin. The percent inhibition was calculated in comparison with control using the formula,

$$\% \text{ Inhibition} = 100 - \left(\frac{\text{Test - Blank}}{\text{Control - Blank}} \text{ X } 100 \right)$$

The percent inhibition calculated for each concentration of the compounds was then used for calculating IC_{50} value using the formula,

$$IC_{50} = \left[\frac{50\ \% \text{ - low percentage}}{\text{high percentage - low percentage}} \text{ X (high concentration – low concentration)} \right] + \left[\text{low concentration} \right]$$

where, low percentage is percent inhibition less than 50% and high percentage is percent inhibition greater than 50%. High and low concentrations are respective concentrations of the compounds at which the high percentage and low percentage inhibition is observed.

Table 6.4. Quinidine and plumbagin IC_{50} values in CYP2D6+hRD and CYP2D6+ΔhRDM inhibition assays. Data are presented as mean values ± STDEV of duplicates of single experiment.

Microsome samples	**Quinidine IC_{50} (µM)**	**Plumbagin IC_{50} (µM)**
CYP2D6+ hRD	0.0132 ± 0.002	2.4599 ± 0.241
CYP2D6+ ΔhRDM	0.0111 ± 0.002	2.2508 ± 0.305

As shown in Table 6.4, there are no significant differences in IC_{50} values for the CYP2D6+ hRD and CYP2D6+ ΔhRDM ($P > 0.05$). The CYP2D6 inhibition by Quinidine and plumbagin in CYP2D6+hRD and CYP2D6+ΔhRDM samples was dose dependent (Figure 6.8 and Figure 6.9). The comparative inhibition studies using CYP2D6+hRD and CYP2D6+ΔhRDM did not show significant difference in IC_{50} or dose-response values of the compounds.

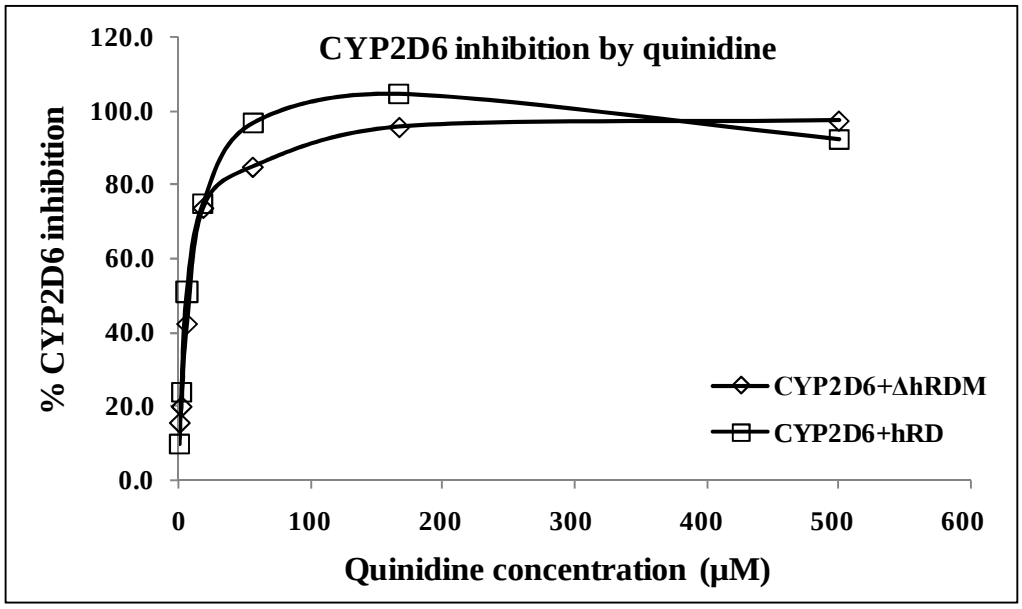

Figure 6.8. The CYP2D6 inhibition by quinidine at various concentrations. Inhibition studies were performed as described in Section 6.6. Each value represents the mean of individual determinations.

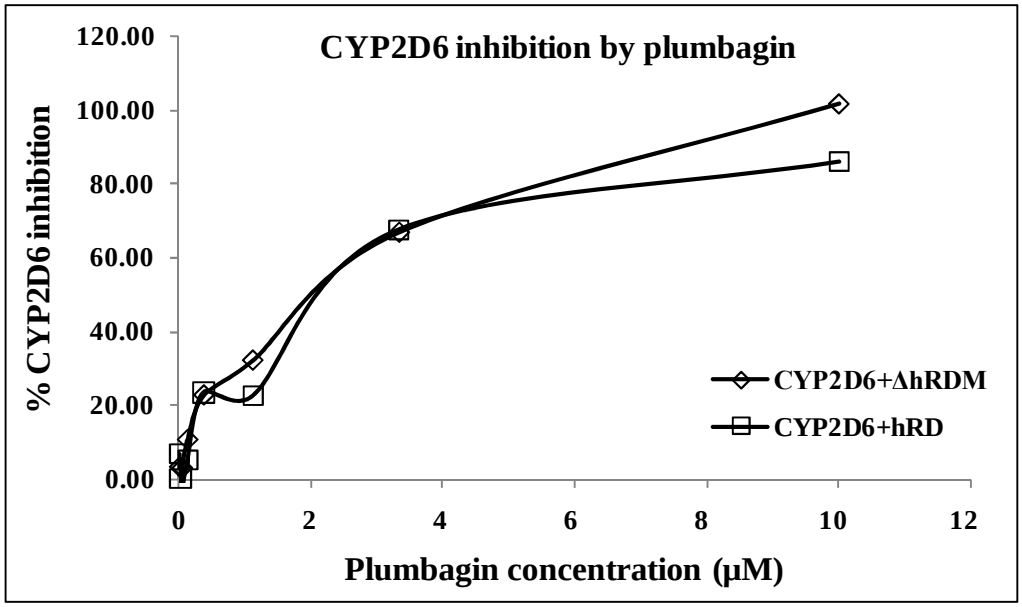

Figure 6.9. The CYP2D6 inhibition by plumbagin at various concentrations. Inhibition studies were performed as described in Section 6.6. Each value represents the mean of individual determinations.

6.7 CYP3A4 inhibition by ketoconazole and plumbagin

The CYP3A4 microsomes, co-expressed with hRD and ΔhRDM, were subjected to inhibition studies. CYP3A4 inhibition by the reference standard, ketoconazole, and test compound, plumbagin, was performed using DBOMF assay. CYP3A4 expression in Sf9 cells, microsome preparation and assay using DBOMF as a substrate are described in Chapter 4. In the assay plate, into the wells in column-1, 144 µl and into the wells in columns 2 to 12, 100 µl of the NADPH regenerating system was added (1.3 mM NADP+, 3.3 mM G6P, 3.3 mM $MgCl_2$, 0.4U/ml G6PDH). 6 µl of the ketoconazole stock (250 µM prepared in acetonitrile) was added to A1 and B1 wells. 6 µl of the plumbagin stock (500 µM prepared in acetonitrile) was added to C1 and D1 wells. 50 µl of the solutions from the wells in column 1 to the wells in columns 2 through 8 were serially diluted using a multichannel pipette. In order to minimize the potential carry over, pipette tips were changed during every step of the serial dilution. The extra 50 µl solution in the wells in column 8 was removed and discarded. The plate was covered with a lid and placed in 37°C incubator for 10 min to prewarm the solution and the plate. Then to the wells in columns 1 through 10, 100 µl of the enzyme/substrate mix was added to the final concentration of 10 µM DBOMF and 1.0 pmole CYP3A4 in 100 mM Potassium phosphate buffer pH 8.0. The lid of the plate was replaced and the plate was incubated at 37°C for 10 min. At the end of the incubation period, the reaction was stopped by dispensing 75 µl of the STOP solution to each well (80% acetonitrile and 20% 0.5 M Tris base). To the blank wells in column 11 and 12, STOP solution was added prior to initiation of the reaction. At the end 100 µl of the enzyme/substrate mix was added to the wells in columns 11 and 12. The plate was then scanned on the Biotek Synegy HT plate reader for measuring relative

fluorescence units (RFU) at excitation wavelength of 485/20 nm and emission wavelength of 528/20 nm. The averages of replicates were used for calculating the % inhibition of CYP3A4 at every concentration of ketoconazole and plumbagin. The percent inhibition was calculated in comparison with control using the formula,

$$\% \text{ Inhibition} = 100 - \left(\frac{\text{Test - Blank}}{\text{Control - Blank}} \text{ X } 100 \right)$$

The percent inhibition calculated for each concentration of the compounds was then used for calculating IC_{50} value using the formula,

$$IC_{50} = \left[\frac{50\ \% - \text{low percentage}}{\text{high percentage - low percentage}} \text{ X } (\text{high concentration} - \text{low concentration}) \right] + \left[\text{low concentration} \right]$$

where low percentage is percent inhibition less than 50% and high percentage is percent inhibition greater than 50%. High and low concentrations are respective concentrations of the compounds at which the high percentage and low percentage inhibition is observed.

Table 6.5. Ketoconazole and plumbagin IC_{50} values in CYP3A4+b_5+hRD and CYP3A4+b_5+ΔhRDM inhibition assays. Data are presented as mean values ± STDEV of duplicates of single experiment.

Microsome samples	**Ketoconazole IC_{50} (µM)**	**Plumbagin IC_{50} (µM)**
CYP3A4+b_5+ hRD	0.0017 ± 0.0002	5.8971 ± 0.711
CYP3A4+b_5+ ΔhRDM	0.0019 ± 0.0002	5.536 ± 0.403

As shown in Table 6.5 there are no significant differences in IC_{50} values for the CYP3A4+b_5+hRD and CYP3A4+b_5+ΔhRDM ($P > 0.05$). The CYP3A4 inhibition by ketoconazole and plumbagin in CYP3A4+b_5+hRD and CYP3A4+b_5+ΔhRDM samples was dose dependent (Figure 6.10 and Figure 6.11). The comparative inhibition studies using CYP3A4+b_5+hRD and CYP3A4+b_5+ΔhRDM did not show significant difference in IC_{50} or dose-response values of the compounds.

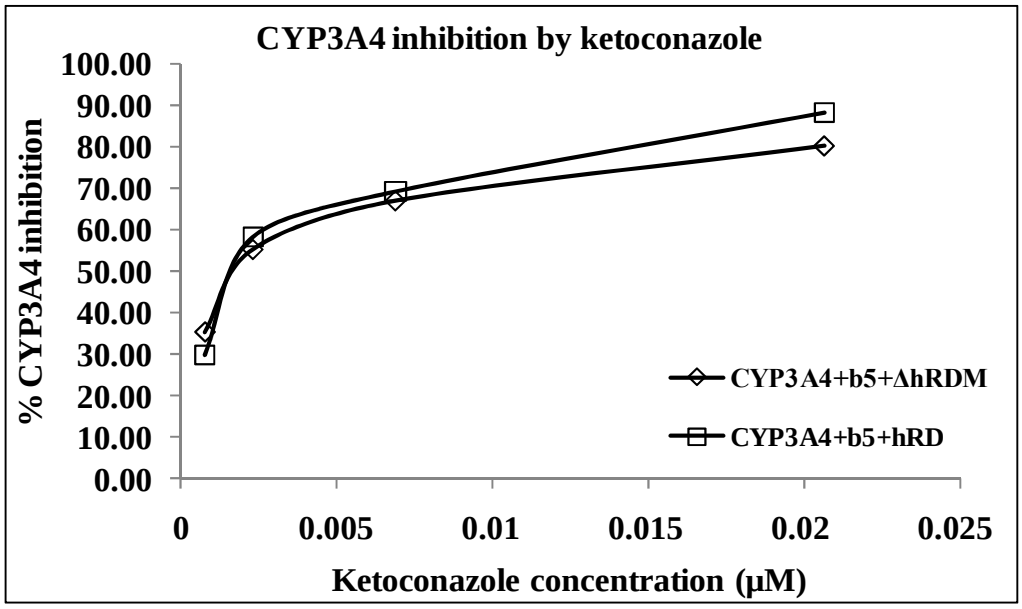

Figure 6.10. The CYP3A4 inhibition by ketoconazole at various concentrations. Inhibition studies were performed as described in Section 6.7. Each value represents the mean of individual determinations.

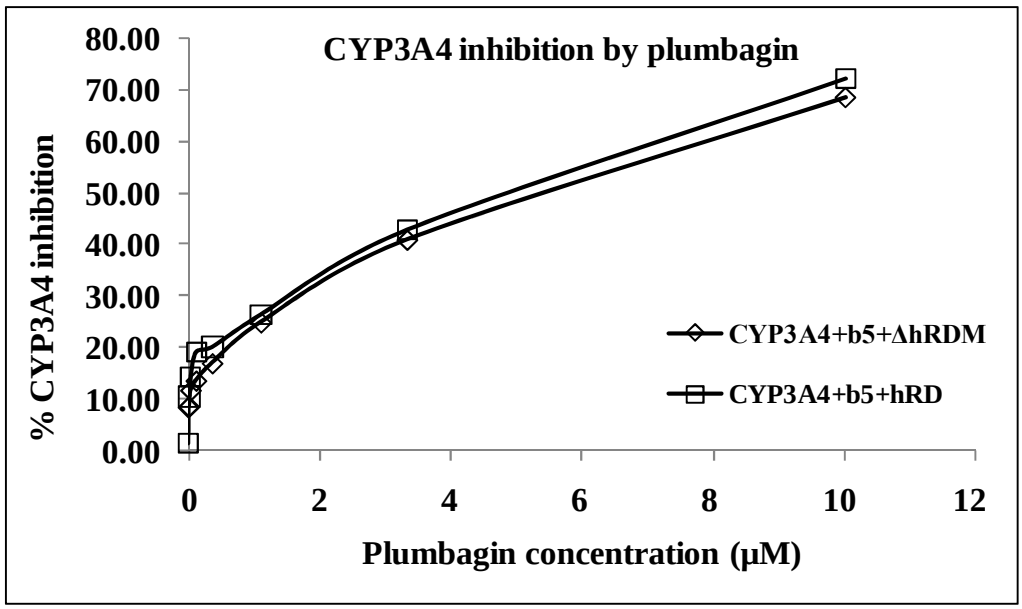

Figure 6.11. The CYP3A4 inhibition by plumbagin at various concentrations. Inhibition studies were performed as described in Section 6.7. Each value represents the mean of individual determinations.

6.8 Conclusion

The CYP inhibition assays were successfully set up and performed for CYP1A1, CYP1A2, CYP1B1, CYP2D6 and CYP3A4 enzymes. The mean IC_{50} values found for the known inhibitors, α-naphthoflavone, furafylline, quinidine and ketoconazole were consistent with that reported previously (Crespi et al. 1997).

As presented in previous Chapters, we have identified ΔhRDM as a relatively superior CPR with respect to its ability to cause less damage to the CYPs and its ability to couple with the CYPs. However, it was important to study its behaviour and directly compare it with the human native CPR in the most important aspect of drug metabolism, namely experiments related to CYP inhibition studies. From the results obtained from the comparative CYP inhibition experiments, we did not observe any significant differences in the IC_{50} values of the compounds for inhibition of CYPs activated by hRD and ΔhRDM. The CYP inhibition by reference standards in hRD as well as ΔhRDM co-expressed CYP samples was dose dependent. The inhibition studies demonstrated that even though ΔhRDM is a genetically engineered novel form of human CPR, it does not alter the quantification of CYP inhibition by the chemical compounds. This comprehensive *in vitro* assessment of ΔhRDM has provided evidence in support of its use as an effective electron donor protein.

Apart from the reference standards, we analysed the natural naphthoquinone plumbagin for its ability and specificity to inhibit the CYPs. Plumbagin also inhibited all the CYP reactions in a dose dependent manner. Plumbagin IC_{50} values in hRD and

ΔhRDM co-expressed CYP samples were not significantly different. Interestingly however, we found that plumbagin has higher affinity towards CYP1A2 over other CYPs that we studied (Table 6.6). It inhibits CYP1A2 as potently as does the reference standard, furafylline.

Table 6.6 Plumbagin IC_{50} values in hRD and ΔhRDM supported CYPs. Data are presented as mean values ± STDEV of duplicates of single experiment.

Microsome samples	**Plumbagin IC_{50} (μM)**
CYP1A1+hRD	5.88149 ± 0.683
CYP1A1+ΔhRDM	5.3194 ± 0.81
CYP1B1+hRD	2.3543 ± 0.155
CYP1B1+ΔhRDM	2.4038 ± 0.17
CYP1A2+hRD	1.2975 ± 0.302
CYP1A2+ΔhRDM	1.4256 ± 0.277
CYP2D6+hRD	2.4599 ± 0.241
CYP2D6+ΔhRDM	2.2508 ± 0.305
CYP3A4+b_5+ hRD	5.8971 ± 0.711
CYP3A4+b_5+ ΔhRDM	5.536 ± 0.403

CYP1A2 activates PAHs, nitrosamines, aflatoxin B_1, and especially aryl amines into forms that can bind to DNA, produce mutations and cause cancer (Aoyama et al. 1990; Shimada et al. 1996; Macé et al. 1997; Hammons et al. 1997; Hecht 1998). It has also been shown previously that CYP1A2 function is strongly induced by tobacco smoke (Tantcheva-Poor et al. 1999; Kalow and Tang 1991) and some herbal dietary supplements (Ryu and Chung 2003). The ability of plumbagin to inhibit CYP1A2 suggests that it may possess chemopreventive properties. These preliminary findings with plumbagin need further in-depth studies in the future.

Chapter 7 Discussion

The aim of this thesis was to devise an insect cell expression system that would allow improvement of the levels and activities of the drug metabolising cytochrome P450 enzymes (CYPs) and contribute to the understandings of CYP-CPR interactions.

Previously, it has been reported that the catalytic activity of a particular CYP is determined not only by the abundance of the CYP, but also by the amount of CPR (Crespi and Miller 1999). Although CPR's abundance is essential for CYP activity, paradoxically some results indicate that CPR is directly or indirectly involved in the degradation of CYP holoprotein (Pederson and Aust 1975; Guengerich 1978; Trakshel et al. 1986). It also appears that coupling of CYP to CPR is very crucial for CYP catalytic activity. However some CYPs, such as CYP2E1, have shown a high degree of uncoupling (Wang et al. 1996). Literature data have shown that CPR is absolutely essential for CYP catalytic activity, however at the same time CPR is detrimental for the expression of CYPs (Ding et al. 1997). My research addressed this paradox to some extent by designing a genetically engineered variant of the human CPR which is less toxic and couples well with CYPs than the human native CPR. In addition, use of a high-activity CPR from yeast in my studies allowed us to improve our understanding on CYP-CPR interactions.

In this study it was important to investigate the effect of various CPRs on the expression and enzyme activities of CYP holoenzymes in a well defined eukaryotic model system. Expression of CYPs in the baculovirus expression system provides the unique advantage of being able to co-infect with two or more recombinant baculoviruses. This would allow the CYP to CPR ratio to be changed by altering the MOI for each virus (Tamura 1992). In line with this, we thought that the baculovirus expression system would be ideal to study CYP-CPR interactions for my studies.

We aimed to find a set of experimental conditions that would be less destructive to CYPs and which would yield higher CYP activity. I have cloned, expressed and studied the seven CYPs, CYP3A4, CYP2E1, CYP2D6, CYP1A2, CYP1A1, CYP1B1 and CYP2C8 in conjunction with different CPR species (the native human CPR, variants of human CPR and the yeast CPR) and b_5 (where necessary). The findings of the experiments performed are discussed in the following sections.

7.1 Cloning, expression, localisation and enzymatic activities of the CPRs

With the exception of some plants, a single CPR of a particular eukaryotic species interacts with all other CYP enzymes of the same species (Benveniste 1991). Since improving the understanding by which CPR interacts with various CYPs was an important goal of this thesis, we initially cloned and expressed native human CPR (hRD), its variants (ΔhRD and ΔhRDM) and yeast CPR (yRD) in Sf9 insect cells.

Previously it has been found that the proteolytic cleavage of 56 N-terminal amino acids from human CPR results in loss of the ability of the CPR to interact and transfer electrons to CYPs (Bonina et al. 2005) which confirms the importance of the N-terminal sequence for catalysis. In this study we have demonstrated that the NH_2-terminal 24-amino acid truncated version of hRD, viz. ΔhRD does not anchor on the microsomal membranes. However interestingly, the other variant, ΔhRDM which also lacks the N-terminal 24-amino acids but contains an extra 17-amino acid sequence (SSEQKLISEEDLNGSRL) linked to ΔhRD's COOH (C)-terminus has the ability to adhere once again to microsomal membranes like the native CPR (Figure 3.16). This C-terminal 17-amino acid sequence includes a 12-amino acid motif (EQKLISEEDLN) which is often referred to as the *c*-myc tag and belongs to an exposed epitope in the oncogenic protein *c*-myc (Evan et al. 1985). We reasoned that by deleting an N-terminal domain and introducing an unusual peptide fragment at the C-terminus, we may have grossly altered the membrane-binding topology of the engineered molecule, ΔhRDM. It is possible that the C-terminal tag is the source of the ΔhRDM's ability to anchor on to the microsomal membranes. The *c*-myc tag is generally used as an epitope tag for immune-detection of novel proteins and can be added to either the N-terminus or C-terminus of a known protein coding sequence. Some previous studies have shown that an epitope tag may or may not affect a target protein activity or its folding and topology (Sells and Chernoff 1995; Jarvik and Telmer 1998; Chavand et al. 2001).

In the beginning of this study, apart from human CPRs, we also cloned and expressed yeast NADPH cytochrome P450 reductase in insect cells. As human CPR functions extremely poorly in yeast (unpublished results from our lab), it has rarely been used in the published literature for expression of human CYPs in yeast. However, although yeast CPR has been successfully used for heterologous expression of human CYPs in yeast, it has never been used for expression studies in any other eukaryotic cell system. We therefore decided to explore the interactions of yeast CPR with human CYPs in insect cell microsomes (ER membranes).

Reductase assays on hRD, ΔhRD, ΔhRDM and yRD using the artificial substrate, MTT, revealed that the CPRs when expressed alone have different reduction potentials towards MTT (Table 3.1). Reductase activity of yRD was highest amongst all the CPRs. ΔhRD reductase activity on microsomes was equal to the negative control (i.e. cells which do not contain any recombinant gene). This was expected as the ΔhRD product does not anchor to (at least not present in) the microsomal membranes as revealed by Coomassie staining and Western blotting (see Section 3.5). Our experiments have consistently failed to show any reductase activity of ΔhRD in the MTT assay even in the soluble cytosolic fraction of the cell lysate. It may be that ΔhRD is highly unstable in the cytosol of insect cells possibly where it is subjected to spontaneous digestion by intracellular proteases. However, interestingly the genetically engineered molecule, ΔhRDM, was found to be catalytically active towards reduction of the artificial substrate, MTT. Therefore, we were extremely keen to assess whether ΔhRDM was catalytically active towards its physiological substrate, CYP. The reduction potential of ΔhRDM was significantly lower than that of hRD and yRD.

Before we could study interactions of these CPRs via co-expression with various CYPs, we opted to optimise CYP expression in insect cells using CYP2D6 as a model – CYP2D6 being an important CYP isozyme in drug metabolism studies. The optimisation of CYP expression is discussed in the following section.

7.2 Optimisation of CYP expression

In order to find out the optimal multiplicity of infection of CYP and CPR baculoviruses (MOI) for producing spectrally active CYP, we infected Sf9 cells with BV-2D6 using a range of MOIs (from 1 x 10^{-1} pfu/cell to 4 pfu/cell). The spectral analysis of all the microsomes was typical of P450 proteins. However it was observed that infection with the lowest MOI of 0.1 pfu/cell resulted in a major peak at 450 nm and a very small peak at 420 nm (Figure 3.19). The peak at 420 nm is an indication of spectrally inactive CYP. A clear indication of the best MOI for CYP infection (i.e. the MOI which produces the highest level of CYPs) was obtained. Increasing the CYP MOI above this level was associated with an increase in the peak at 420 nm. These results suggest that using higher MOIs of BV-2D6 result in a gradual increase in the formation of inactive CYP2D6. This is possibly a result of misfolding of the over-expressed protein. It could be inferred that optimal expression of spectrally active CYP depends on accumulation of properly folded CYP2D6 protein in the microsomal membranes which can be achieved by infecting the insect cells with a lower MOI. It also implies that high levels of spectrally active CYP can not be simply produced by gradually increasing the initial MOI.

7.3 Co-expression of CYP2D6 with the CPRs and their interactions

In parallel to the results from MTT assays, in co-expressed microsomes the reductase activity of yRD was the highest amongst all the CPRs followed by hRD and ΔhRDM (Table 3.4). ΔhRD reductase activity was equal to negative control which was expected as it only corroborated the results obtained with MTT. This strongly suggested that the ΔhRD product may not anchor to microsomal membranes. Interestingly however, it was observed that the strongest CPR, yRD, resulted in the lowest yield of spectrally active CYP2D6 in microsomes which co-express CYP2D6 and yRD. The second strongest CPR, hRD, also resulted in a lower yield of spectrally active CYP2D6. Amongst all the CPRs studied, ΔhRDM which has the lowest reduction potential towards the artificial substrate MTT appeared to yield the highest content of spectrally active CYP2D6 (Table 3.2).

All the CPRs studied did decrease the spectrally active CYP holoenzyme produced in co-expression studies (Table 3.2 & Figure 3.21). Intriguingly though, the immunologically detectable apoprotein levels were found to be unaffected by co-expression of different CPRs (Table 3.3). The detrimental effect of the CPRs on CYP2D6 holoprotein was of dissimilar magnitude and it depended on the CPR that was co-expressed. We were then able to show the possible cause of CYP2D6 holoprotein destruction by CPRs. The reactive oxygen species (ROS) assays indicated that the

reason behind this destruction is likely to be oxidative damage triggered by CPRs (Figure 3.23 & 3.24). This data demonstrate that CPRs do not modulate CYP expression at the gene transcriptional or protein translational levels but reduce CYP holoenzyme levels by means of oxidative damage.

LC/MS analysis using dextromethorphan as a substrate showed that in comparison to hRD co-expressed CYP2D6, the ΔhRDM co-expressed CYP2D6 had increased enzyme activity as seen by increased Vmax and thereby overall efficiency of catalysis (Table 3.8). No significant changes were observed in the Km values stating that the affinity of the substrate towards CYP2D6 holoenzyme has not changed but the higher coupling efficiency of ΔhRDM has resulted in an increased Vmax thereby quadrupling of the efficiency of catalysis.

CYP2D6 enzyme activities supported by per unit of CPRs were calculated in terms of coupling efficiency. Based on the CYP2D6 fluorometric enzyme assays (Figure 3.25(B), 3.26(B) & 3.27), percentage relative coupling efficiency (Figure 3.28) and efficiency of catalysis (Table 3.8), it can be concluded that the ΔhRDM, which has the weakest reduction potential, surprisingly provides the best CYP2D6 reaction rates in comparison with the two wild-type CPRs – hRD and yRD. We found that ΔhRDM not only coupled far better to CYP2D6 than the native human CPR (hRD) but also yields higher levels of CYP2D6 with far less destruction of the CYP. Despite the strong reduction potential towards MTT, yRD does not couple equally effectively with CYP2D6. This means that the ability of a CPR to reduce an artificial substrate is not

directly proportional to its ability to reduce the physiological substrate. CYP2D6 activity measured in the CPR co-expressed microsomes indicated that the strength of the reductase does not determine CYP activity – it is the ability of CPR to couple with CYP which is crucial.

Since ΔhRDM shows clear superiority over the two reductases hRD and yRD (being less destructive to the CYP2D6 holoprotein and having better reaction rates), we thought of increasing the ΔhRDM amounts during co-expression with CYP2D6. By doubling the MOI of BV-ΔhRDM during co-expression, substantial increase in rates of reaction were observed (Figure 3.29). A similar experiment was performed with CYP2D6 and hRD and again an increase in the reaction rates were observed (Figure 3.30). However, even though doubling of MOIs of both BV-ΔhRDM and BV-hRD improved the enzyme reaction rates, this was traded off against a sharp decrease in the amount of spectrally active CYP2D6 (Table 3.9). This experiment allowed us to understand that controlling CPR expression levels is important for achieving a balance between amounts of spectrally active enzyme and its catalytic activity. It was also noted from this particular experiment that the spectrally active CYP2D6 at 5:1 ratio of CYP2D6 : ΔhRDM was more that 100% higher than the CYP2D6 obtained when the CYP2D6 : hRD ratio was 5:1 (Table 3.9). Thus, ΔhRDM clearly provides room for further improvement.

Based on the results obtained, Chapter 3 clearly illustrates that peak enzymatic activity cannot simply be obtained by increasing the MOI of a CPR baculovirus or by

using a CPR which has very strong reduction potential. Coupling efficiency of a CPR is extremely important to achieve the best enzymatic activity of the CYP. In conclusion ΔhRDM, a genetically engineered variant of human CPR, offers advantages of high-level expression of CYP2D6 with better reaction rates. ΔhRDM also offers an improvement in the ratio of spectrally active CYP2D6 to spectrally inactive CYP2D6.

7.4 Interaction of CYP3A4 with the CPRs

Our results in Chapter 3 indicated that the yeast CPR, yRD, can act as an alternative electron donor to the human CPR, hRD, for the general activation of human CYPs. We wanted to explore if the results obtained from the co-expression studies of yRD and CYP2D6, which express optimal activity in the absence of cytochrome b_5, are applicable in the context of another CYP where the presence of cytochrome b_5 is essential. We chose CYP3A4, which is also widely used for drug metabolism studies, for these studies.

We therefore co-expressed the yeast CPR and human CYP3A4 enzymes in insect cells along with cytochrome b_5 in Chapter 4. We have also co-expressed different human CPRs (hRD, ΔhRD and ΔhRDM) with human CYP3A4 at optimal MOIs and have compared our results with experiments that allow co-expression of the yeast CPR (yRD) and CYP3A4 using similar MOIs. All co-expression studies were performed in the presence of human cytochrome b_5.

Literature data have shown the reduction in human CYP levels when co-expressed with a CPR in baculovirus expression systems (Chen et. al. 1997; Wang et. al. 1996; Paine et. al. 1996). Our results are in agreement with these reports. We have linked this effect to the increased production of hydroxyl radicals in Chapter 3 (Figure 3.23 & 3.24). Like CYP2D6, CYP3A4 holoenzyme levels also changed with different magnitudes depending on which reductase species was used for co-expression with CYP3A4 (Table 4.1). Co-expression of yRD and hRD resulted in lower CYP3A4 holoenzyme content than when ΔhRDM was co-expressed.

In CYP3A4 co-expressed microsomes, yRD enzyme activity towards its artificial substrate MTT was higher than hRD and ΔhRDM (Table 4.4). However CYP3A4 catalytic activity towards de-alkylation of DBOMF in yRD co-expressed microsomes was extremely poor in comparison to hRD or ΔhRDM co-expressed microsomes (Figure 4.11). The CYP3A4 activity in the presence of cytochrome b_5 and yeast CPR was nearly as low as the activities observed in the microsomes that co-express only CYP3A4 and b_5. It should be noted that reaction rates of yRD supported CYP2D6 enzyme activities are much better, as presented in Chapter 3 (Figure 3.25(B), 3.26(B) & 3.27). This observation indicates that yRD does not support CYP3A4 activity as effectively as it supports CYP2D6 activity on insect cell microsomes.

To determine whether the oxidative damage to CYP3A4 by yRD is accelerated by co-expressing the third protein cytochrome b_5, reactive oxygen species (ROS) in cells infected with CPR and cytochrome b_5 baculoviruses were measured. Our results

from the H_2DCFDA assay showed that both yRD and hRD induce higher amounts of reactive oxygen species than ΔhRDM. However, co-expression of b_5 with CPRs did not noticeably alter the ROS levels induced by CPRs in insect cells (Table 4.6).

In spite of similar amounts of CYP3A4 holoprotein content in microsomes co-expressing yRD and hRD (Table 4.1), CYP3A4 catalytic activity in the presence of yRD is unusually poor as compared to CYP3A4 activity in the presence of hRD and ΔhRDM (Figure 4.11). We do not know the reason for this; however it is very likely that oxidative damage is not the complete reason for the poor CYP3A4 catalytic activity in the presence of yRD. It is possible that the specific intracellular environment in insect cells may not support the interaction of yRD with human CYP3A4 in the presence of human cytochrome b_5. This may suggest the importance for a CYP and the CPR to have correct spatial orientation of their redox centres for effective electron transfer. Recently, protein crystal structure of yeast CPR has been solved which reveals that it has a second FMN binding site at the interface of the two connecting FMN binding domains. The two FMN binding domains have different accessibilities to the bulk solvent and different amino acid environments (Lamb et al 2006). Electrostatic forces have been shown experimentally to limit accessibility of electron transfer sites on CPR for its charged redox partners (Voznesensky and Schenkman 1994). One could speculate that the human cytochrome b_5, bound to CYP3A4, plays a major role in hindering the transfer of electrons from the yeast CPR, yRD, to the CYP3A4 active site on insect cell microsomes.

In conclusion, our findings in Chapter 4 demonstrate that (1) yRD perceptibly lacks the ability to support human CYP3A4 catalytic activity on insect cell ER membranes, in the presence of cytochrome b_5, (2) Co-expression of cytochrome b5 did not seem to play any role in increasing or decreasing the ROS induced by CPRs, (3) in comparison with yRD, human reductases hRD and ΔhRDM are probably the better redox partners for a human CYP which demands cytochrome b_5 for manifestation of optimal activity – this could be due to the inability of CYP3A4 and yRD to form a mutually correct spatial orientation in the intracellular endoplasmic reticular environment afforded by insect cells and (4) once again the variant of hRD enzyme, ΔhRDM, appears to be far superior to the wild-type hRD in terms of its ability to couple with CYP3A4 and to produce higher amounts of a spectrally-active, catalytically-useful CYP enzyme.

7.5 Interaction of CYP1A1, CYP1B1, CYP1A2, CYP2C8 and CYP2E1 with the CPRs

Previously it was found that electrostatic forces play an important role in the interactions between electron transfer proteins and in many cases these pairing interactions are responsible for the complex formation; in contrast, repulsion between the charged residues of two proteins may interfere with protein-protein complex formation (Voznesensky and Schenkman 1992). The different distribution of charges on CPR binding sites may cause different CYPs to have different affinities for CPR (Voznesensky and Schenkman 1994). Recently it has been shown in protein binding

assays that CYPs and the accessory proteins (CPR and cytochrome b_5) interact with each other with different affinities (Shimada et. al. 2005).

In Chapter 5, we have examined the interactions of the CPRs with several other CYP isoforms from different sub-families. In order to study these affinities, we have taken an approach of studying coupling between CYP and CPR, where the enzyme catalytic activities are taken into account. We studied the CPRs, viz. hRD, ΔhRDM and yRD, in the context of three more CYPs – CYP1B1, CYP1A2 and CYP2E1. We also studied CYP1A1 and CYP2C8, though only in the context of ΔhRDM. In the case of CYP2C8 and CYP2E1, apart from a CPR, a third protein cytochrome b_5 was also co-expressed. Cytochrome b_5 is known to augment CYP2C8 and CYP2E1 mediated monooxygenase reactions (Porter, 2002).

Based on Western blot densitometry (Figure 5.13 (A) & (B)) and CYP holoenzyme content (Table 5.5 & 5.9), it was again observed that CPRs destroy CYP1A2 and CYP2E1 holoproteins without altering the CYP apoprotein levels. This would indicate that CPRs generically do not modulate CYP expression at the transcriptional or translational level but are responsible for the destruction of CYP holoprotein which is a result of ROS induction by CPRs.

In the co-expressed microsomes, reduction potential of yRD in the MTT assay was higher than hRD or sometimes similar, but yRD did not support CYP activity as

efficiently as the human CPR. ΔhRDM was identified as the most effective CPR, amongst hRD, ΔhRDM and yRD, as it caused less damage to CYP holoprotein and supported CYP catalytic activities more efficiently.

The coupling efficiency of yRD with the CYPs was found to be inferior to ΔhRDM and hRD which indicates that use of yRD for human CYP expressions, particularly in the 'insect cell expression system', may not be physiologically feasible. While comparing coupling efficiency of yRD with various CYPs, it was observed that it couples relatively better with CYP2E1 and CYP2D6 in comparison to other CYPs that we studied (Table 7.1). The genetically engineered molecule ΔhRDM coupled more efficiently with the CYPs than hRD and yRD. As coupling efficiency of ΔhRDM was higher than hRD and yRD, relative coupling efficiencies for hRD and yRD were calculated assuming ΔhRDM coupling efficiency as 100%. The coupling efficiencies of CYP2D6, CYP3A4, CYP1B1, CYP1A2 and CYP2E1 with hRD, ΔhRDM and yRD are summarised in the table below.

Table 7.1 Percent relative coupling efficiencies of hRD, ΔhRDM and yRD with CYP2D6, CYP3A4, CYP1B1, CYP1A2 and CYP2E1.

		coupling efficiency	
CYP/ CPR	ΔhRDM	hRD	yRD
CYP2D6	100	55.6	44.89
CYP3A4	100	65.31	29.17
CYP1B1	100	63.49	24.78
CYP1A2	100	33.73	24.9
CYP2E1	100	106.65	45.64

The above results suggest that different CPRs have different affinities towards the different CYP isoforms which could account for the variations on the charges on CYP and CPR binding sites and spatial orientation of their redox centres.

7.6 Cytochrome P450 inhibition

We identified ΔhRDM as a relatively superior CPR with respect to its abilities to (1) cause less damage to the CYPs and (2) overall couple better with the CYPs. However, it was important to study its allosteric behaviour and directly compare it with the human native CPR in the most important aspect of drug metabolism, namely experiments related to CYP inhibition studies. The CYP inhibition assays were successfully set up and performed for CYP1A1, CYP1A2, CYP1B1, CYP2D6 and

CYP3A4 enzymes in order to determine whether there are any differences in the catalytic properties of the electron donor partner hRD and its variant ΔhRDM with respect to activation of the CYPs. The mean IC_{50} values found for the known inhibitors, α-naphthoflavone, furafylline, quinidine and ketoconazole were consistent with that reported previously (Crespi et al. 1997).

From the results obtained from the comparative CYP inhibition experiments, we did not observe any significant differences in the IC_{50} values of the compounds for inhibition of CYPs activated by hRD and ΔhRDM. The CYP inhibition by reference standards in hRD as well as ΔhRDM co-expressed CYP samples was dose dependent. The inhibition studies demonstrated that even though ΔhRDM is a genetically engineered novel form of human CPR, it does not alter the quantification of CYP inhibition by the chemical compounds. This comprehensive *in vitro* assessment of ΔhRDM has provided evidence in support of its use as an effective electron donor protein for CYPs.

Apart from the reference standards, we analysed the natural naphthoquinone, plumbagin, for its ability and specificity to inhibit the CYPs. Plumbagin also inhibited all the CYP reactions in dose dependent manner. Plumbagin IC_{50} values in hRD and ΔhRDM co-expressed CYP samples were not significantly different. Interestingly however, we found that plumbagin has higher affinity towards CYP1A2 inhibition over other CYPs that we studied (Table 6.6). It inhibits CYP1A2 as potently as does the reference standard, furafylline.

Previously, it has been shown that CYP1A2 function is strongly induced by tobacco smoke (Tantcheva-Poor et al. 1999; Kalow and Tang 1991) and some herbal dietary supplements (Ryu and Chung 2003). Furthermore CYP1A2 has been implicated in activation of PAHs, nitrosamines, aflatoxin B_1, and especially aryl amines into forms that can bind to DNA, produce mutations and cause cancer (Aoyama et. al. 1990; Shimada et. al. 1996; Macé et. al. 1997; Hammons et. al. 1997; Hecht 1998). In line with this, the ability of plumbagin to inhibit CYP1A2 suggests that it may possess anticancer chemopreventive properties. These preliminary findings with plumbagin warrant further studies to elucidate its *in vivo* role in CYP1A2 inhibition.

7.7 Summary

In summary, we have devised a functionally active CYP expression system which uses a genetically engineered human CPR, ΔhRDM. The system provides some unique advantages over the CYP expression system that uses human native CPR, hRD, as the electron donor protein. Use of ΔhRDM as electron donor to CYPs allowed us to achieve our goal of improving CYP expression levels and in the coupling of CYPs with a CPR. The key findings of the thesis are summarised below.

- Truncation of a 24-amino acid charged region at NH_2-terminal end of hRD, prevents association of the resultant molecule, ΔhRD, to microsomal membranes. ΔhRDM which also lacks the N-terminal 24-amino acids but contains an extra 17-amino acid sequence

(SSEQKLISEEDLNGSRL) linked to ΔhRD's C-terminus has the ability to adhere once again to microsomal membranes.

- Co-expression of all the CPRs with the CYPs resulted in reduction of CYP holoprotein without altering the apoprotein levels. The detrimental effect of the CPRs on CYP holoprotein was of different magnitudes depending on the CPR that was co-expressed.

- CPRs do not modulate the CYP expression at the gene transcriptional or protein translational levels but are responsible for reduction in CYP holoenzyme levels by means of oxidative damage. Co-expression of cytochrome b_5 does not seem to play any role in increasing or decreasing the oxidative damage caused by CPRs.

- The ability of a CPR to reduce an artificial substrate is not directly proportional to its ability to reduce the physiological substrate. The strength of the reductase does not determine CYP activity – it is the ability of CPR to couple with CYP which is crucial.

- Different CPRs have different affinities towards the different CYP isoforms which could account for the variations on the charges on CYP and CPR binding sites and spatial orientation of their redox centres.

- ΔhRDM, a genetically engineered variant of human CPR offers advantages of high-level expression of CYP with better reaction rates. ΔhRDM also offers an improvement in the ratio of spectrally active CYP2D6 to spectrally inactive CYP2D6.

- The inhibition studies demonstrate that even though ΔhRDM is a genetically engineered form of human CPR, it does not alter the quantification of CYP inhibition by chemical compounds. It implies that the allosteric interactions, which modulate enzyme active site conformations, of ΔhRDM and hRD with a particular CYP are similar.

- This comprehensive *in vitro* assessment of ΔhRDM has provided evidence in support of its use as an effective electron donor protein for CYPs.

7.8 Prospects for the future

In this project we have identified ΔhRDM as a relatively superior electron donor protein to the CYPs. However for reasons that are poorly understood any particular CPR has different affinities to different CYPs. Crystal structure of the FMN binding domain of human CPR has been solved which indicates that the FMN domain has an unusual surface charge distribution, leading to a very strong dipole, which may be involved in docking a CYP into place for electron transfer (Zhao et al. 1999). This surface is thought to be the most suitable for electron transfer from CPR. Site-directed mutagenesis studies have revealed that different parts of the FMN domain are involved in CYP and cytochrome *c* binding (Shen and Kasper 1995) – besides MTT, cytochrome *c* is another artificial electron transfer substrate for CPRs. Studies with cytochrome b_5 also indicate that its binding site on CPR is distinct from that of CYP (Nadler and Strobel 1991). It may be that every individual CYP isozyme has a slightly different

interaction with CPR. Extensive site-directed mutagenesis studies in FMN domain of CPR might throw more light on whether different amino acid residues of this domain are involved in interaction with individual CYPs. In addition site-directed mutagenesis studies are also needed on ΔhRDM to understand which amino acid residues are exactly responsible for giving this molecule the ability to anchor on to the ER membranes. These further studies may help us to define a human CPR with even better properties than ΔhRDM.

Chapter 8 References

Acharya, B.R., Bhattacharyya, B. and Chakrabarti, G. (2008) The natural naphthoquinone plumbagin exhibits antiproliferative activity and disrupts the microtubule network through tubulin binding. ***Biochemistry***, 47(30), pp. 7838-7845.

Anderson, D., Harris, R., Polayes, D., Ciccarone, V., Donahue, R., Gerard, G., and Jessee, J. (1996) Rapid generation of recombinant baculoviruses and expression of foreign genes using the Bac-To-Bac® baculovirus expression system. ***Focus***, 17, pp. 53-58.

Anttila, S., Hietanen, E., Vainio, H., Camus, A.M., Gelboin, H.V., Park, S.S., Heikkilä, L., Karjalainen, A. and Bartsch, H. (1991) Smoking and peripheral type of cancer are related to high levels of pulmonary cytochrome P450IA in lung cancer patients. ***Int J Cancer***, 47(5), pp. 681-685.

Aoyama, T., Yamano, S., Guzelian, P.S., Gelboin, H.V. and Gonzalez, F.J. (1990) Five of 12 forms of vaccinia virus-expressed human hepatic cytochrome P450 metabolically activate aflatoxin B1. ***Proc Natl Acad Sci***, 87 (12), pp. 4790-4793.

Atkins, A.L. (1999) Preparation of yeast cells for confocal microscopy, In Paddock, S.W (ed) Confocal Microscopy: methods and protocols. ***Methods in Mol Biol***, 122, pp. 131-140.

Ayres, M.D., Howard, S. C., Kuzio, J., Lopez Ferber, M. and Possee, R. D. (1994) The complete DNA sequence of *Autographa californica* nuclear polyhedrosis virus. ***Virology***, 202 (2), pp. 586–605.

Backes, W.L. and Kelley, R.W. (2003) Organization of multiple cytochrome P450s with NADPH-cytochrome P450 reductase in membranes. ***Pharmacol Ther***, 98(2), pp. 221-33.

Bardsley, J.S. (1994) Establishment of human tissue banks. ***Hum Exp Toxicol***, 13 (6), pp. 435-437.

Barnes, H.J., Arlotto, M. P. and Waterman, M. R. (1991) Expression and enzymatic activity of recombinant cytochrome P450 17α-hydroxylase in *Escherichia coli*. ***Proc Natl Acad Sci***, 88, pp. 5597-5601.

Battula, N., Sagara, J. and Gelboin, H.V. (1987) Expression of P1-450 and P3-450 DNA Coding Sequences as Enzymatically Active Cytochromes P-450 in Mammalian Cells. ***Proc. Natl. Acad. Sci***. 84(12), pp. 4073-4077.

Beaune, P. (1993) [Human cytochromes P450. Applications in pharmacology]. ***Therapie***, 48 (6), pp. 521-526.

Benveniste, I., Lesot, A., Hasenfratz, M.P., Kochs, G. and Durst, F. (1991) Multiple forms of NADPH-cytochrome P450 reductase in higher plants. ***Biochem Biophys Res Commun***, 177 (1), pp. 105-112.

Bertz, R.J. and Granneman, G.R. (1997) Use of in vitro and in vivo data to estimate the likelihood of metabolic pharmacokinetic interactions. ***Clin Pharmacokinet***, 32(3), pp. 210-258.

Blanck, J., Smettan, G., Ristau, O., Ingelman-Sundberg, M. and Ruckpaul, K. (1984) Mechanism of rate control of the NADPH dependent reduction of cytochrome P-450 by lipids in reconstituted phospholipid vesicles. ***Eur J Biochem***, 144 (3), pp. 509-513.

Bondza-Kibangou, P., Millot, C., Dufer, J. and Millot, J.M. (2004) Modifications of cellular autofluorescence emission spectra under oxidative stress induced by 1 alpha,25dihydroxyvitamin D(3) and its analog EB1089. ***Technol Cancer Res Treat***, 3 (4), pp. 383-391.

Bonina, T.A., Gilep, A.A., Estabrook, R.W. and Usanov, S.A. (2005) Engineering of proteolytically stable NADPH-cytochrome P450 reductase. Biochemistry, 70 (3), pp. 357-365.

Bowen, W.P., Carey, J.E., Miah, A., McMurray, H.F., Munday, P.W., James, R.S., Coleman, R.A. and Brown, A.M. (2000) Measurement of cytochrome P450 gene

induction in human hepatocytes using quantitative real-time reverse transcriptase-polymerase chain reaction. ***Drug Metab Dispos***, 28(7), pp. 781-8.

Bradford, M.M. (1976) A rapid and sensitive method for the quantitation of microgram quantities of protein utilizing the principle of protein-dye binding. ***Anal Biochem***, 72, pp. 248-254.

Brian, W.R., Sari, M.A., Iwasaki, M., Shimada, T., Kaminsky, L.S. and Guengerich, F,P. (1990) Catalytic activities of human liver cytochrome P-450 IIIA4 expressed in Saccharomyces cerevisiae. ***Biochemistry***, 29(51), pp. 11280-11292.

Capdevila, J.H., Falck, J.R. and Harris, R.C. (2000) Cytochrome P450 and arachidonic acid bioactivation. Molecular and functional properties of the arachidonate monooxygenase. ***J Lipid Res***, 41(2), pp. 163-81.

Chang, T.K., Yu, L., Maurel, P. and Waxman, D.J. (1997) Enhanced cyclophosphamide and ifosfamide activation in primary human hepatocyte cultures: response to cytochrome P-450 inducers and autoinduction by oxazaphosphorines. ***Cancer Res***, 57(10), pp. 1946-54.

Chauret, N., Dobbs, B., Lackman, R.L., Bateman, K., Nicoll-Griffith, D.A., Stresser, D.M., Ackermann, J.M., Turner, S.D., Miller, V.P. and Crespi, C.L. (2001) The use of 3-[2-(N,N-diethyl-N-methylammonium)ethyl]-7-methoxy-4-methylcoumarin (AMMC) as a specific CYP2D6 probe in human liver microsomes. ***Drug Metab Dispos***, 29 (9), pp. 1196-1200.

Chavand, O., Spilsbury, K. and Rakoczy, P.E. (2001) Addition of a c-myc epitope tag within the VEGF protein does not affect in vitro biological activity. ***Biochem Cell Biol***, 79(1), pp. 107-112.

Chen, L., Buters, J.T., Hardwick, J.P., Tamura, S., Penman, B.W., Gonzalez, F.J. and Crespi, C.L. (1997) Coexpression of Cytochrome P4502A6 and Human NADPH-P450 Oxidoreductase in the Baculovirus System. ***Drug Metab Dispos***, 25 (4), pp. 399-405.

Chen, Z. and Banerjee, R. (1998) Purification of Soluble Cytochrome b5 as a Component of the Reductive Activation of Porcine Methionine Synthase. ***J Biol Chem***, 273 (40), 26248-26255.

Crespi, C.L. and Miller, V.P. (1999) The use of heterologously expressed drug metabolizing enzymes-state of the art and prospects for the future. ***Pharmacol Ther***, 84 (2), pp. 121-131.

Crespi, C.L., Miller, V.P. and Penman, B.W. (1997) Microtiter plate assays for inhibition of human, drug-metabolizing cytochromes P450. ***Anal Biochem***, 248(1), pp. 188-90.

Crespi, C.L., Penman, B.W., Leakey, J.A., Arlotto, M.P., Stark, A., Parkinson, A., Turner, T., Steimel, D.T., Rudo, K., Davies, R.L. et al. (1990) Human cytochrome P450IIA3: cDNA sequence role of the enzyme in the metabolic of promutagens comparison to nitrosamine activation by human cytochrome P450IIE1. ***Carcinogenesis***, 11 (8), pp. 1293-1300.

Dai, Y., Rashba-Step, J. and Cederbaum, A.L. (1993) Stable expression of human cytochrome P4502E1 in HepG2 cells: characterization of catalytic activities and production of reactive oxygen intermediates. ***Biochemistry***, 32 (27), pp. 6928-6937.

Danielson, P.B. (2002) The cytochrome P450 superfamily: biochemistry, evolution and drug metabolism in humans. ***Curr Drug Metab***, 3 (6), pp. 561-597.

Deeni, Y.Y., Paine, M.J., Ayrton, A.D., Clarke, S.E., Chenery, R. and Wof, C.R. (2001) Expression, purification, and biochemical characterization of a human cytochrome P450 CYP2D6-NADPH cytochrome P450 reductase fusion protein. ***Arch Biochem biophys***, 396 (1), pp. 16-24.

Ding, S., Yao, D., Burchell, B., Wolf, C.R. and Friedberg, T. (1997) High Levels of Recombinant CYP3A4 Expression in Chinese Hamster Ovary Cells Are Modulated by Coexpressed Human P450 Reductase and Hemin Supplementation. ***Arch of Biochem and Biophys***, 348(2), pp. 403-410(8).

Doehmer, J., Dogra, S., Friedberg, T., Monier, S., Adesnik, M., Glatt, H. and Oesch, F. (1988) Stable Expression of Rat Cytochrome P-450IIB1 cDNA in Chinese Hamster Cells (V79) and Metabolic Activation of Aflatoxin B1. ***Proc Natl Acad Sci***, 85(16), pp. 5769-5773.

Dong, J. and Porter, T.D. (1996) Coexpression of Mammalian Cytochrome P450 and Reductase in *Escherichia coli*. ***Arch Biochem Biophys***, 327 (2), pp. 254-259.

Edwards, R.J., Adams, D.A., Watts, P.S., Davies, D.S. and Boobis, A.R. (1998) Development of a comprehensive panel of antibodies against the major xenobiotic metabolising forms of cytochrome P450 in humans. ***Biochem Pharmacol***, 56(3), pp. 377-87.

Ellis, S.W., Ching, M.S., Watson, P.F., Henderson, C.J., Simula, A.P., Lennard, M.S., Tucker, G.T. and Woods, H.F. (1992) Catalytic activities of human debrisoquine 4-hydroxylase cytochrome P450 (CYP2D6) expressed in yeast. ***Biochem Pharmacol***, 44 (4), pp. 617-620.

Enoch, H.G. and Strittmatter, P. (1979) Cytochrome b5 reduction by NADPH-cytochrome P-450 reductase. ***J Biol Chem***, 254, pp. 8976-8981.

Estabrook, R.W. (2003) A passion for P450s (rememberances of the early history of research on cytochrome P450). ***Drug Metab Dispos***, 31 (12), pp. 1461-1473.

Estabrook, R.W., Franklin, M.R., Cohen, B., Shigamatzu, A. and Hildebrandt, A.G. (1971) Biochemical and genetic factors influencing drug metabolism. Influence of hepatic microsomal mixed function oxidation reactions on cellular metabolic control. ***Metabolism***, 20(2), pp. 187-199.

Eugster, H.P. and Sengstag, C. (1993) Saccharomyces cerevisiae: an alternative source for human microsomal liver enzymes and its use in drug interaction studies. ***Toxicology***, 82 (1-3), pp. 61-73.

Evan, G.I., Lewis, G.K., ramsay, G. and Bishop, J.M. (1985) Isolation of monoclonal antibodies specific for human c-myc proto-oncogene product. ***Mol Cell Biol***, 5 (12), pp.3610-3616.

Farr, S.B., Natvig, D.O. and Kogoma, T. (1985) Toxicity and mutagenicity of plumbagin and the induction of a possible new DNA repair pathway in Escherichia coli. ***J Bacteriol***, 164(3), pp. 1309-1316.

French, J.S., Guengerich, F.P. and Coon, M.J. (1980) Interactions of cytochrome P450, NADPH-cytochrome P-450 reductase, phospholipid, and substrate in the reconstituted liver microsomal enzyme system. ***J Biol Chem***, 255 (9), pp. 4112-4119.

Fukushima, H., Takeda, T., Sasaki, N., Watanabe, T. and Nozawa, Y. (1984) Isolation of detergent-solubilized NADPH-cytochrome *c* reductase from *Tetrahymena* microsomes, with regard to thermoadaptive regulation of fatty acyl-CoA desaturase activity. ***Comparative Biochemistry and Physiology Part B: Biochemistry and Molecular Biology,*** 78 (4), pp. 855-858.

Ged, C., Rouillon, J.M., Pichard, L., Combalbert, J., Bressot, N., Bories, P., Michel, H., Beaune, P. and Maurel, P. (1989) The increase in urinary excretion of 6 beta-hydroxycortisol as a marker of human hepatic cytochrome P450IIIA induction. ***Br J Clin Pharmacol***, 28(4), pp. 373-387.

Gonzalez, F.J. (1992) Human cytochromes P450: problems and prospects. ***Trends Pharmacol Sci***, 13 (9), pp. 346-352.

Gonzalez, F.J. and Korzekwa, K.R. (1995) Cytochromes P450 expression systems. ***Annu Rev Pharmacol Toxicol***, 35, pp. 369-390.

Gonzalez, F.J., Kimura, S., Tamura, S. and Gelboin, H.V. (1991) Expression of mammalian cytochrome P450 using baculovirus Methods. ***Enzymol***, 206, pp. 93-99.

Graham, S.E. and Peterson, J.A. (1999) How similar are P450s and what can their differences teach us? ***Arch Biochem Biophys***, 369 (1), pp. 24-29.

Groves, J. (1995) Models and Mechanism of Cytochrome P450 Action. ***Cytochrome P450: Structure, Mechanism, and Biochemistry***, 3rd ed., pp. 1-48.

Guengerich, F.P. (1978) Destruction of heme and hemoproteins mediated by liver microsomal reduced nicotinamide adenine dinucleotide phosphate-cytochrome P-450 reductase. ***Biochemistry***, 17(17), pp. 3633-3639.

Guengerich, F.P. (1995) Influence of nutrients and other dietary materials on cytochrome P-450 enzymes. ***Am J Clin Nutr***, 61(3 Suppl), pp. 651S-658S.

Guengerich, F.P. (1999) Cytochrome P-450 3A4: regulation and role in drug metabolism. ***Annu Rev Pharmacol Toxicol***, 39, pp. 1-17.

Guengerich, F.P. and Shimada, T. (1991) Oxidation of toxic and carcinogenic chemicals by human cytochrome P-450 enzymes. ***Chem Res Toxicol***, 4(4), pp. 391-407.

Hakkola, J., Pasanen, M., Pelkonen, O., Hukkanen, J., Evisalmi, S., Anttila, S., Rane, A., Mäntylä, M., Purkunen, R., Saarikoski, S., Tooming, M. and Raunio, H. (1997) Expression of CYP1B1 in human adult and fetal tissues and differential inducibility of CYP1B1 and CYP1A1 by Ah receptor ligands in human placenta and cultured cells. ***Carcinogenesis***, 18(2), pp. 391-397.

Hammons, G.J., Milton, D., Stepps, K., Guengerich, F.P., Tukey, R.H. and Kadlubar, F.F. Metabolism of carcinogenic heterocyclic and aromatic amines by recombinant human cytochrome P450 enzymes. ***Carcinogenesis***, 18(4), pp. 851-854.

Hanahan, D. (1983) Studies on transformation of Escherichia coli with plasmids. *J Mol Biol*, 166 (4), pp. 557-580.

Hannermann, F., Bichet, A., Ewen, K. M. and Bernhardt, R. (2007) Cytochrome P450 systems--biological variations of electron transport chains. ***Biochim Biophys Acta***, 1770 (3), pp. 330-344.

Harris, R. and Polayes, D. (1997) A new baculovirus expression vector for the simultaneous expression of two heterologous proteins in the same insect cell. ***Focus***, 19. pp. 6-8.

Haugen, D.A., Armes, L.G., Yasunobu, K.T. and Coon, M.J. (1997) Amino-terminal sequence of phenobarbital-inducible cytochrome P-450 from rabbit liver

microsomes: similarity to hydrophobic amino-terminal segments of preproteins. ***Biochem Biophys Res Commun***, 77(3), pp. 967-973.

Hayashi, K., Sakaki, T., Kominami, S., Inouye, K. and Yabusaki, Y. (2000) Coexpression of genetically engineered fused enzyme between yeast NADPH-P450 reductase and human cytochrome P450 3A4 and human cytochrome b5 in yeast. ***Arch Biochem Biophys***, 381 (1), pp. 164-170.

Hecht, S.S. (1997) Approaches to cancer prevention based on an understanding of N-nitrosamine carcinogenesis. ***Proc Soc Exp Biol Med***, 216(2), pp. 181-191.

Hecht, S.S. (1999) DNA adduct formation from tobacco-specific N-nitrosamines. ***Mutat Res***, 424(1-2), pp. 127-142.

Hildebrandt, A. and Estabrook, R.W. (1971) Evidence for the participation of cytochrome b 5 in hepatic microsomal mixed-function oxidation reactions. ***Arch Biochem Biophys***, 143 (1), pp. 66-79.

Holloway, P.W. and Katz, J.T. (1975) Effect of cytochrome b5 on the size, density, and permeability of phosphatidylcholine vesicles. ***J Biol Chem***, 250 (23), pp. 9002-9007.

Holmans, P.L., Shet, M.S., Martin-Wixtrom, C.A., Fisher, C.W. and Estabrook, R.W. (1994) The high-level expression in Escherichia coli of the membrane-bound form of human and rat cytochrome b5 and studies on their mechanism of function. ***Arch Biochem Biophys***, 312(2), pp. 554-65.

Horecker, B.L. (1950) Triphosphopyridine nucleotide-cytochrome c reductase in liver. ***J Biol Chem***, 183, pp. 593-605.

Imaoka, S., Yamada, T., Hiroi, T., Hayashi, K., Sakaki, T., Yabusaki, Y. and Funae, Y. (1996) Multiple forms of human P450 expressed in Saccharomyces cerevisiae. Systematic characterization and comparison with those of the rat. ***Biochem Pharmacol***, 51(8), pp. 1041-1050.

Iwata, H., Fujita, K., Kushida, H., Suzuki, A., Konno, Y., Nakamura, K., Fujino, A. and Kamataki, T. (1998) High Catalytic Activity of Human Cytochrome P450 Co-

expressed with Human NADPH-Cytochrome P450 Reductase in *Escherichia coli*. ***Biochem Pharmacol***, 55 (8), pp. 1315-1325.

Iyanagi, T. and Mason, H.S. (1973) Some properties of hepatic reduced nicotinamide adenine dinucleotide phosphate-cytochrome c reductase. ***Biochemistry***, 12 (12), pp. 2297-2308.

Iyanagi, T., Anan, F.K., Imai, Y. and Mason, H.S. (1978) Studies on the microsomal mixed function oxidase system: redox properties of detergent-solubilized NADPH-cytochrome P-450 reductase. ***Biochemistry***, 17 (11), pp. 2224-2230.

Iyengar, M.A. and Pendse, G.S. (1966) Plumbago zeylanica L. (Chitrak). A gastrointestinal flora normaliser. ***Planta Med***, 14(3), pp. 337-351.

Jarvik, J.W. and Telmer, C.A. (1998) Epitope tagging. ***Ann Rev Genet,*** 32, pp. 601-618.

Kalow, W. and Tang, B.K. (1991) Caffeine as a metabolic probe: exploration of the enzyme-inducing effect of cigarette smoking. ***Clin Pharmacol Ther***, 49(1), pp. 44-48.

Kaminsky, L.S., Dunbar, D.A., Wang, P.P., Beaune, P., Larrey, D., Guengerich, F.P., Schnellmann, R.G. and Sipes, I.G. (1984) Human hepatic cytochrome P-450 composition as probed by in vitro microsomal metabolism of warfarin. ***Drug Metab Dispos***, 12 (4), 470-477.

Kapucuoglu, N., Coban, T., Raunio, H., Pelkonen, O., Edwards, R.J., Boobis, A.R. and Iscan, M. (2003) Expression of CYP3A4 in human breast tumour and non-tumour tissues. ***Cancer Lett***, 202(1), pp. 17-23.

Klingenberg, M. (1958) Pigments of rat liver microsomes. ***Arch Biochem Biophys***, 75 (2), pp. 376-386.

Klotz, A.V., Stegeman, J.J. and Walsh, C. (1984) An alternative 7-ethoxyresorufin O-deethylase activity assay: a continuous visible spectrophotometric method for measurement of cytochrome P-450 monooxygenase activity. ***Anal Biochem***, 140(1), pp. 138-145.

Kocarek, T.A., Schuetz, E.G., Strom, S.C., Fisher, R.A. and Guzelian PS. (1995) Comparative analysis of cytochrome P4503A induction in primary cultures of rat, rabbit, and human hepatocytes. ***Drug Metab Dispos***, 23(3), pp. 415-421.

Kolars, J.C., Schmiedlin-Ren, P., Schuetz, J.D., Fang, C. and Watkins, P.B. (1992) Identification of rifampin-inducible P450IIIA4 (CYP3A4) in human small bowel enterocytes. ***J Clin Invest***, 90(5), pp. 1871-1878.

Lamb, D.C., Kim, Y., Yermalitskaya, L.V., Yermalitsky, V.N., Lepesheva, G.I., Kelly, S.L., Waterman, M.R. and Podust, L.M. (2006) A second FMN binding site in yeast NADPH-cytochrome P450 reductase suggests a mechanism of electron transfer by diflavin reductases. ***Structure***, 14(1), pp. 51-61.

Landi, M.T., Sinha, R., Lang, N.P. and Kadlubar, F.F. (1999) Human cytochrome P4501A2. ***IARC Sci Publ***, 148, pp. 173-95.

Lee, C.A., Kadwell, S. H., Kost, T. A. and Serabjitsingh, C. J. (1995) CYP3A4 expressed by insect cells infected with a recombinant baculovirus containing both CYP3A4 and human NADPH-cytochrome P450 reductase is catalytically similar to human liver microsomal CYP3A4. ***Arch Biochem Biophys***, 319 (1), pp. 157-167.

Li, A.P. (2001) Screening for human ADME/Tox drug properties in drug discovery. ***Drug Discov Today***, 6(7), pp. 357-366.

Li, A.P., ed. (1997) Advances in Pharmacology: Pharmacokinetic Drug–Drug Interactions (Vol. 43), Academic Press.

Lieber, C.S. (1997) Cytochrome P-4502E1: its physiological and pathological role. ***Physiol Rev***, 77(2), pp. 517-544.

Lu, A.Y. and Coon, M.J. (1968) Role of hemoprotein P-450 in fatty acid omega-hydroxylation in a soluble enzyme system from liver microsomes. ***J Biol Chem***, 243 (6), pp. 1331-1332.

Lu, A.Y., Junk, K.W. and Coon, M.J. (1969) Resolution of the cytochrome P-450-containing omega-hydroxylation system of liver microsomes into three components. ***J Biol Chem***, 244 (13), pp. 3714-3721.

Luckow, V. (1991) Cloning and expression of heterologous genes in insect cells with baculovirus vectors. Prokop, A., Bajpai, R. K. and Ho, C. S. (Eds.). In: ***Recombinant DNA technology and applications***, McGraw-Hill, Inc., pp. 97−104.

Luckow, V.A., Lee, S. C., Barry, G. F. and Olins, P. O. (1993) Efficient generation of infectious recombinant baculoviruses by site-specific transposon-mediated insertion of foreign genes into a baculovirus genome propagated in *Escherichia coli*. ***J Virol***, 67 98), pp. 4566-4579.

Macé, K., Aguilar, F., Wang, J.S., Vautravers, P., Gómez-Lechón, M., Gonzalez, F.J., Groopman, J., Harris, C.C. and Pfeifer, A.M. (1997) Aflatoxin B1-induced DNA adduct formation and p53 mutations in CYP450-expressing human liver cell lines. ***Carcinogenesis***, 18(7), 1291-1297.

Marks, B.D,, Goossens, T.A,, Braun, H.A,, Ozers, M.S,, Smith, R.W., Lebakken, C. and Trubetskoy, O.V. (2003) High-throughput screening assays for CYP2B6 metabolism and inhibition using fluorogenic Vivid® substrates. ***AAPS PharmSci***, 5, pp. E18.

Marks, B.D., Smith, R.W., Braun, H.A., Goossens, H.A., Christenson, M., Ozers, M.S., Lebakken, C.S. and Trubetskoy, O.V., (2002) A high throughput screening assay to screen for CYP2E1metabolism and inhibition using a fluorogenic Vivid® P450 substrate. ***Assay Drug Dev Technol***, 1, pp. 73-81.

Masters, C. J. (1998) On the role of the peroxisome in the metabolism of drugs and xenobiotics. ***Biochemical Pharmacology***, 56 (6), pp. 667-673.

Mauk, M.R. and Mauk, A.G. (1982) Interaction between cytochrome b5 and human methemoglobin. ***Biochemistry***, 21 (19), 4730-4734.

Miller, V.P., Stresser, D.M., Blanchard, A.P., Turner, S. and Crespi, C.L. (2000) Fluorometric high-throughput screening for inhibitors of cytochrome P450. ***Ann N Y Acad Sci***, 919, pp. 26-32.

Mokashi, V., Li, L. and Porter, T.D. (2003) Cytochrome b5 reductase and cytochrome b5 support the CYP2E1-mediated activation of nitrosamines in a recombinant Ames test. ***Arch Biochem Biophys***, 412 (1), pp. 147-152.

Morel, F., Beaune, P.H., Ratanasavanh, D., Flinois, J.P., Yang, C.S., Guengerich, F.P, and Guillouzo A. (1990) Expression of cytochrome P-450 enzymes in cultured human hepatocytes. ***Eur J Biochem***, 191(2), pp. 437-444.

Mullis, K., Faloona, F., Scharf, S., Saiki, R., Horn, G. and Erlich, H. (1986) Specific enzymatic amplification of DNA in vitro: the polymerase chain reaction. ***Cold Spring Harb Symp Quant Biol***, 51 (1), pp. 263-273.

Murray, G.I., Taylor, M.C., McFadyen, M.C., McKay, J.A., Greenlee, W.F., Burke, M.D. and Melvin, W.T. (1997) Tumor-specific expression of cytochrome P450 CYP1B1. ***Cancer Res***, 57(14), pp. 3026-3031.

Nadler, S.G. and Strobel, H.W. (1991) Identification and characterization of an NADPH-cytochrome P450 reductase derived peptide involved in binding to cytochrome P450. ***Arch Biochem Biophys***, 290(2), pp. 277-284.

Nakajima, M., Fujiki, Y., Kyo, S., Kanaya, T., Nakamura, M., Maida, Y., Tanaka, M., Inoue, M. And Yokoi, T. (2005) Pharmacokinetics of paclitaxel in ovarian cancer patients and genetic polymorphisms of CYP2C8, CYP3A4, and MDR1. ***J Clin Pharmacol***, 45 (6), pp. 674-682.

Narimatsu, S., Takatsu, N., Yamano, S., Inoue, Y., Hanioka, N., Kiryu, K., Naito, S., Gonzalez, F.J. and Yamamoto, S. (2006) The effect of dimethyl sulfoxide on the function of cytochrome P450 2D6 in HepG2 cells upon the co-expression with NADPH-cytochrome P450 reductase. ***Chem Biol Interact***, 159 (1), pp. 47-57.

Nebert, D.W. and McKinnon, R.A. (1994) Cytochrome P450: evolution and functional diversity. ***Prog Liver Dis***, 12, pp. 63-97.

Nebert, D.W., Adesnik, M., Coon, M.J., Estabrook R.W., Gonzalez, F.J., Guengerich, F.P., Gunsalus, I.C., Johnson, E.F., Kemper, B. and Levin, W. et al. (1987) The P450 gene superfamily: recommended nomenclature. ***DNA***, 6 (1), pp. 1-11.

Nebert, D.W., McKinnon, R.A. and Puga, A. (1996) Human drug-metabolizing enzyme polymorphisms: effects on risk of toxicity and cancer. ***DNA Cell Biol***, 15(4), 273-280.

Nebert, D.W., Nelson, D.R., Adesnik, M., Coon, M.J., Estabrook R.W., Gonzalez, F.J., Guengerich, F.P., Gunsalus, I.C., Johnson, E.F. and Kemper, B. et al. (1989) The P450 superfamily: updated listing of all genes and recommended nomenclature for the chromosomal loci. ***DNA***, 8 (1), pp. 1-13.

Nebert, D.W., Nelson, D.R., Coon, M.J., Estabrook R.W., Feyereisen, R., Fujii-Kuriyama, Y., Gonzalez, F.J., Guengerich, F.P., Gunsalus, I.C., Johnson, E.F. et al. (1991) The P450 superfamily: update on new sequences, gene mapping, and recommended nomenclature. ***DNA Cell Biol***, 10 (1), pp. 1-14.

Nelson, D.R. (1999) Cytochrome P450 and the individuality of species. ***Arch Biochem Biophys***, 369(1), pp. 1-10.

Nelson, D.R., Kamataki, T., Waxman, D.J., Guengerich, F.P., Estabrook, R.W., Feyereisen, R., Gonzalez, F.J., Coon, M.J., Gunsalus, I.C., Gotoh O. et al. (1993) The P450 superfamily: update on new sequences, gene mapping, accession numbers, early trivial names of enzymes, and nomenclature. ***DNA Cell Biol***, 12 (1), pp. 1-51.

Nelson, D.R., Koymans, L., Kamataki, T., Stegeman, J.J., Feyereisen, R., Waxman, D.J., Waterman, M.R., Gotoh, O., Coon, M.J., Estabrook, R.W., Gunsalus, I.C. and Nebert, D.W. (1996) P450 superfamily: update on new sequences, gene mapping, accession numbers and nomenclature. ***Pharmacogenetics***, 6 (1), pp. 1-42.

Noshiro, M., Harada, N. and Omura, T. (1979) Immunochemical study on the participation of cytochrome b5 in drug oxidation reactions of mouse liver microsomes. ***Biochem Biophys Res Commun***, 91 (1), pp. 207-213.

O'Donnell, C.J., Grime, K., Courtney, P., Slee, D. and Riley, R.J. (2007) The development of a cocktail CYP2B6, CYP2C8, and CYP3A5 inhibition assay and a preliminary assessment of utility in a drug discovery setting. ***Drug Metab Dispos***, 35(3), pp. 381-385.

Olkkola, K.T., Backman, J.T. and Neuvonen, P.J. (1994) Midazolam should be avoided in patients receiving the systemic antimycotics ketoconazole or itraconazole. ***Clin Pharmacol Ther***, 55(5), pp. 481-485.

Omiecinski, C.J., Remmel, R.P. and Hosagrahara, V.P. (1999) Concise review of the cytochrome P450s and their roles in toxicology. ***Toxicol Sci***, 48 (2), pp. 151-156.

Omura, T. and Sato, R. (1964) The carbon monoxide-binding pigment of liver microsomes. I. Evidence for its hemoprotein nature. ***J Biol Chem***, 239, pp. 2370-2378.

Paine, M.J., Gilham, D., Roberts, G.C. and Wolf, C.R. (1996) Functional high level expression of cytochrome P450 CYP2D6 using baculoviral expression systems. ***Arch Biochem Biophys***, 328(1), pp. 143-150.

Parkinson, A. (1996) Biotransformation of Xenobiotics. ***Casarette and Daull's Toxicology: the basic science of poisons***, 5th ed., pp. 113-186.

Pederson, T.C. and Aust, S.D. (1975) The mechanism of liver microsomal lipid peroxidation. ***Biochim Biophys Acta***, 385(2), pp. 232-241.

Pelkonen, O., Mäenpää, J., Taavitsainen, P., Rautio, A. and Raunio, H. (1998) Inhibition and induction of human cytochrome P450 (CYP) enzymes. ***Xenobiotica***, 28(12), pp. 1203-1253.

Perrot, N., Nalpas, B., Yang, C.S. and Beaune, P.H. (1989) Modulation of cytochrome P450 isozymes in human liver, by ethanol and drug intake. ***Eur J Clin Invest***, 19(6), pp. 549-555.

Peyronneau, M.A., Renaud, J.P., Truan, G., Urban, P., Pompon, D. and Mansuy, D. (1992) Optimization of yeast-expressed human liver cytochrome P-450 3A4 catalytic activities by coexpressing NADPH-cytochrome P-450 and cytochrome b5. ***Eur J Biochem***, 207 (1), pp. 109-116.

Phillips, A.H. and Langdon, R.G. (1962) Hepatic triphosphopyridine nucleotide cytochrome c reductase: isolation, characterization, and kinetic studies. ***J Biol Chem***, 237, pp. 2652-2660.

Pichard, L., Fabre, I., Daujat, M., Domergue, J., Joyeux, H. and Maurel, P. (1992) Effect of corticosteroids on the expression of cytochromes P450 and on cyclosporin A oxidase activity in primary cultures of human hepatocytes. ***Mol Pharmacol***, 41(6), pp. 1047-1055.

Polayes, D., Harris, R., Anderson, D. and Ciccarone, V. (1996) New naculovirus expression vectors for the purification of recombinant proteins from insect cells. ***Focus***, 18, pp. 10-13.

Porter, T.D. (2002) The roles of cytochrome b5 in cytochrome P450 reactions. ***J Biochem Mol Toxicol***, 16 (6), pp. 311-316.

Poulos, T.L., Finzel, B.C. and Howard, A.J. (1986) Crystal structure of substrate-free Pseudomonas putida cytochrome P-450. ***Biochemistry***, 25 (18), pp. 5314-5322.

Pritchard, M.P., Glancey, M.J., Blake, J.A., Gilham, D.E., Burchell, B., Wolf, C.R. and Friedberg, T. (1998) Functional co-expression of CYP2D6 and human NADPH-cytochrome P450 reductase in *Escherichia coli*. ***Pharmacogenetics***, 8 (1), 33-42.

Raunio, H., Husgafvel-Pursiainen, K., Anttila, S., Hietanen, E., Hirvonen, A. and Pelkonen, O. (1995) Diagnosis of polymorphisms in carcinogen-activating and inactivating enzymes and cancer susceptibility--a review. ***Gene***, 159(1), pp. 113-121.

Renaud, J.P., Cullin, C., Pompon, D., Beaune, P. and Mansuy, D. (1990) Expression of human liver cytochrome P450 IIIA4 in yeast. A functional model for the hepatic enzyme. ***Eur J Biochem***, 194(3), pp. 889-896.

Rendic, S. and DiCarlo, F.J. (1997) Human cytochrome P450 enzymes: a status report summarizing their reactions, substrates, inducers, and inhibitors. ***Drug Metab Rev***, 29 (1-2), pp. 413-580.

Richardson, T.H., Griffin, K.J., Jung, F., Raucy, J.L. and Johnson, E.F. (1997) Targeted antipeptide antibodies to cytochrome P450 2C18 based on epitope mapping of an inhibitory monoclonal antibody to P450 2C51. ***Arch Biochem Biophys***, 338(2), pp. 157-64.

Rodríguez-Antona, C., Jover, R., Gómez-Lechón, M.J. and Castell, J.V. (2000) Quantitative RT-PCR measurement of human cytochrome P-450s: application to drug induction studies. ***Arch Biochem Biophys***, 376(1), pp. 109-116.

Ronis, M.J., Badger, T.M., Shema, S.J., Roberson, P.K. and Shaikh, F. (1996) Reproductive toxicity and growth effects in rats exposed to lead at different periods during development. ***Toxicol Appl Pharmacol***, 136(2), pp. 361-371.

Ryu, S.D. and Chung, W.G. (2003) Induction of the procarcinogen-activating CYP1A2 by a herbal dietary supplement in rats and humans. ***Food Chem Toxicol***, 41(6), pp. 861-866.

Savas, U. and Jefcoate, C.R. (1994) Dual regulation of cytochrome P450EF expression via the aryl hydrocarbon receptor and protein stabilization in C3H/10T1/2 cells. ***Mol Pharmacol***, 45(6), pp. 1153-1159.

Schägger, H. and von Jagow, G. (1987) Tricine-sodium dodecyl sulfate-polyacrylamide gel electrophoresis for the separation of proteins in the range from 1 to 100 kDa. ***Anal Biochem***, 166 (2), pp. 368-379.

Schenkman, J.B. and Jansson, I. (2003) The many roles of cytochrome b5. ***Pharmacol Ther***, 97 (2), pp. 139-152.

Schmidt, J.V. and Bradfield, C.A. (1996) Ah receptor signaling pathways. ***Annu Rev Cell Dev Biol***, 12, pp. 55-89.

Schuetz, E.G., Schuetz, J.D., Strom, S.C., Thompson, M.T., Fisher, R.A., Molowa, D.T., Li, D. and Guzelian, P.S. (1993) Regulation of human liver cytochromes P-

450 in family 3A in primary and continuous culture of human hepatocytes. ***Hepatology***, 18(5), pp. 1254-1262.

Schwarz, D., Kisselev, P., Honeck, H., Cascorbi, I., Schunck, W.H. and Roots, I. (2001) Co-expression of human cytochrome P4501A1 (CYP1A1) variants and human NADPH-cytochrome P450 reductase in the baculovirus/insect cell system. ***Xenobiotica***, 31(6), pp. 345-356.

Sells, M.A. and Chernoff, J. (1995) Epitope-tag vectors for eukaryotic protein production. ***Gene***, 152, pp. 187-189.

Shen, A.L. and Kasper, C.B. (1995) Role of acidic residues in the interaction of NADPH-cytochrome P450 oxidoreductase with cytochrome P450 and cytochrome c. ***J Biol Chem***, 270 946), pp. 27475- 27480.

Shephard, E.A., Phillips, I.R. Santisteban, I., West, L.F., Palmer, C.N., Ashworth, A. and Povey, S. (1989) Isolation of a cytochrome P-450 reductase cDNA clone and localization of the corresponding gene to chromosome 7q11.2. ***Ann Hum Genet***, 53 (4), pp. 291-301.

Shet, M.S., Fisher, C.W., Arlotto, M.P., Shackleton, C.H., Holmans, P.L., Martin-Wixtrom, C.A., Saeki, Y. and Estabrook, R.W. (1994) Purification and enzymatic properties of a recombinant fusion protein expressed in Escherichia coli containing the domains of bovine P450 17A and rat NADPH-P450 reductase. ***Arch Biochem Biophys***, 311(2), pp. 402-417.

Shimada, T. and Guengerich, F.P. (1985) Participation of a rat liver cytochrome P-450 induced by pregnenolone 16 alpha-carbonitrile and other compounds in the 4-hydroxylation of mephenytoin. ***Mol Pharmacol***, 28 (2), pp. 215-219.

Shimada, T., Hayes, C.L., Yamazaki, H., Amin, S., Hecht, S.S., Guengerich, F.P. and Sutter, T.R. (1996) Activation of chemically diverse procarcinogens by human cytochrome P-450 1B1. ***Cancer Res***, 56(13), pp. 2979-2984.

Shimada, T., Mernaugh, R.L. and Guengerich, F.P. (2005) Interactions of mammalian cytochrome P450, NADPH-cytochrome P450 reductase, and cytochrome b(5) enzymes. ***Arch Biochem Biophys***, 435 (1), pp. 207-216.

Shimada, T., Misono, K.S. and Guengerich, F.P. (1986) Human liver microsomal cytochrome P-450 mephenytoin 4-hydroxylase, a prototype of genetic polymorphism in oxidative drug metabolism. Purification and characterization of two similar forms involved in the reaction. ***J Biol Chem***, 261 (2), pp. 909-921.

Shimada, T., Yamazaki, H., Foroozesh, M., Hopkins, N.E., Alworth, W.L. and Guengerich, F.P. (1998) Selectivity of polycyclic inhibitors for human cytochrome P450s 1A1, 1A2, and 1B1. ***Chem Res Toxicol***, 11(9), pp. 1048-1056.

Shimada, T., Yamazaki, H., Mimura, M., Inui, Y. And Guengerich, F.P. (1994) Interindividual variations in human liver cytochrome P-450 enzymes involved in the oxidation of drugs, carcinogens and toxic chemicals: studies with liver microsomes of 30 Japanese and 30 Caucasians. ***J Pharmacol Exp Ther***, 270 (1), pp. 414-423.

Shou, M., Lin, Y., Lu, P., Tang, C., Mei, Q., Cui, D., Tang, W., Ngui, J.S., Lin, C.C., Singh, R., Wong, B.K., Yergey, J.A., Lin, J.H., Pearson, P.G., Baillie, T.A., Rodrigues, A.D. and Rushmore, T.H. (2001) Enzyme kinetics of cytochrome P450- mediated reactions. ***Curr Drug Metab***, 2 (1), pp. 17-36.

Simmons, D.L., Lalley, P.A. and Kasper, C.B. (1985) Chromosomal assignments of genes coding for components of the mixed-function oxidase system in mice. Genetic localization of the cytochrome P-450PCN and P-450PB gene families and the nadph-cytochrome P-450 oxidoreductase and epoxide hydratase genes. ***J Biol Chem***, 260 (1), pp. 515-521.

Song, B.J., Veech, R.L. and Saenger, P. (1990) Cytochrome P450IIE1 is elevated in lymphocytes from poorly controlled insulin-dependent diabetics. ***J Clin Endocrinol Metab***, 71(4), pp. 1036-1040.

Spatzenegger, M. and Jaeger, W. (1995) Clinical importance of hepatic cytochrome P450 in drug metabolism. ***Drug Metab Rev***, 27 (3), pp. 397-417.

Strittmatter, P. (1967) ***Methods Enzymol***, 10, pp. 561-565.

Strittmatter, P. and Velick, S.F. (1956) The isolation and properties of microsomal cytochrome. ***J Biol Chem***, 221(1), pp. 253-264.

Summers, M.D. and Smith, G.E. (1987) A Manual of Methods for Baculovirus Vectors and Insect Cell Culture Procedures. ***Texas Agricultural Experiment Station***, Bulletin No. 1555.

Sutter, T.R. and Loper, J.C. (1989) Disruption of the Saccharomyces cerevisiae gene for NADPH cytochrome P450 reductase causes increased sensitivity to ketoconazole. ***Biochem Biophys Res Commun***, 160 (3), pp. 1257-1266.

Sutter, T.R., Tang, Y.M., Hayes, C.L., Wo, Y.Y., Jabs, E.W., Li, X., Yin, H., Cody, C.W. and Greenlee, W.F. (1994) Complete cDNA sequence of a human dioxin-inducible mRNA identifies a new gene subfamily of cytochrome P450 that maps to chromosome 2. ***J Biol Chem***, 269(18), pp. 13092-13099.

Szczesna-skorupa, E., Chen, C.D., Liu, H. and Kemper, B. (2004) Gene expression changes associated with the endoplasmic reticulum stress response induced by microsomal cytochrome p450 overproduction. ***J Biol Chem***, 279 (14), pp. 13953-13961.

Takesue, S. and Omura T. (1970) Purification and Properties of NADH-cytochrome b5 Reductase Solubilized by Lysosomes from Rat Liver Microsomes. ***J Biochem***, 67, pp. 267-276.

Tamura, S., Korzekwa, K.R., Kimura, S., Gelboin, H.V. and Gonzalez, F.J. (1992) Baculovirus-mediated expression and functional characterization of human NADPH-P450 oxidoreductase. ***Arch Biochem Biophys***, 293 (2), pp. 219-223.

Tang, Y.M., Chen, G.F., Thompson, P.A., Lin, D.X., Lang, N.P. and Kadlubar, F.F. (1999) Development of an antipeptide antibody that binds to the C-terminal region of human CYP1B1. ***Drug Metab Dispos***, 27(2), pp. 274-280.

Tantcheva-Poór, I., Zaigler, M., Rietbrock, S. and Fuhr, U. (1999) Estimation of cytochrome P-450 CYP1A2 activity in 863 healthy Caucasians using a saliva-based caffeine test. ***Pharmacogenetics***, 9(2), pp. 131-144.

Tassaneeyakul, W., Birkett, D.J., Veronese, M.E., McManus, M.E., Tukey, R.H. and Miners, J.O. (1994) Direct characterization of the selectivity of furafylline as an inhibitor of human cytochromes P450 1A1 and 1A2. ***Pharmacogenetics***, 4(5), pp. 281-284.

Trakshel, G.M., Kutty, R.K. and Maines, M.D. (1986) Cadmium-mediated inhibition of testicular heme oxygenase activity: the role of NADPH-cytochrome c (P-450) reductase. ***Arch Biochem Biophys***, 251(1), pp. 175-187.

Truan, G., Cullin, C., Reisdorf, P., Urban, P. and Pompon, D. (1993) Enhanced in vivo monooxygenase activities of mammalian P450s in engineered yeast cells producing high levels of NADPH-P450 reductase and human cytochrome b5. ***Gene***, 125 (1), pp. 49-55.

Vergeres, G. and Waskell, L. (1995) Cytochrome b5, its functions, structure and membrane topology. ***Biochimie***, 77 (7-8), pp. 604-20.

Vermillion, J.L., Ballou, D.P., Massey, V. and Coon, M.J. (1981) Separate roles for FMN and FAD in catalysis by liver microsomal NADPH-cytochrome P-450 reductase. ***J Biol Chem***, 256 (1), pp. 266-277.

Voice, M.W., Zhang, Y., Wof, C.R., Burchell, B. and Friedberg, T. (1999) Effects of human cytochrome b5 on CYP3A4 activity and stability in vivo. ***Arch Biochem Biophys***, 366 (1), pp. 116-124.

Von Bahr, C., Glaumann, H., Gudas, J. and Kaplowitz, N. (1980) Inhibition of hepatic metabolism of azathioprine by furosemide in human liver in vitro. ***Biochem Pharmacol***, 29(10), pp. 1439-1441.

Voznesensky, A.I. and Schenkman, J.B. (1994) Quantitative analyses of electrostatic interactions between NADPH-cytochrome P450 reductase and cytochrome P450 enzymes. ***J Biol Chem***, 269 (22), pp. 15724-15731.

Voznesensky, A.I. and Schenkman, J.B. (1992) The cytochrome P450 2B4-NADPH cytochrome P450 reductase electron transfer complex is not formed by charge-pairing. ***J Biol Chem***, 267(21), pp. 14669-14676.

Walsky, R.L. and Obach, R.S. (2004) Validated assay for human cytochrome_P450 activities. ***Drug Metab Dispos***, 32, pp. 647-660.

Wang, M.H., Patten, C.J., Yang, G.Y., Paranawithana, S.R., Tan, Y. and yang, C.S. (1996) Expression and coupling of human cytochrome P450 2E1 and NADPH-cytochrome P450 oxidoreductase in dual expression and co-infection systems with baculovirus in insect cells. ***Arch Biochem Biophys***, 334 (2), pp. 380-388.

Watanabe, M. (1998) Polymorphic CYP genes and disease predisposition--what have the studies shown so far? ***Toxicol Lett***, 102-103, pp. 167-171.

Werck-Reichhart, D. and Feyereisen, R. (2000) Cytochrome P450: a success story. ***Genome Biol***, 1 (6), pp. 3000.1- 3000.9.

Weyer, U. and Possee, R.D. (1991) A baculovirus dual expression vector derived from the *Autographa californica* nuclear polyhedrosis virus polyhedrin and p10 promoters: co-expression of two influenza virus genes in insect cells. ***J Gen Virol***, 72(12), pp. 2967–2974.

White, R.E., Sligar, S.G. and Coon, M.J. (1980) Evidence for a homolytic mechanism of peroxide oxygen-oxygen bond cleavage during substrate hydroxylation by cytochrome P-450. ***J Biol Chem***, 255 (23), pp. 11108-11111.

Wiliams, C.H. and Kamin, H. (1962) Microsomal triphosphopyridine nucleotide-cytochrome c reductase of liver. ***J Biol Chem***, 237, pp 587-595.

Willey, J.C., Coy, E.L., Frampton, M.W., Torres, A., Apostolakos, M.J., Hoehn, G., Schuermann, W.H., Thilly, W.G., Olson, D.E., Hammersley, J.R., Crespi, C.L. and Utell, M.J. (1997) Quantitative RT-PCR measurement of cytochromes p450 1A1, 1B1, and 2B7, microsomal epoxide hydrolase, and NADPH oxidoreductase expression in lung cells of smokers and nonsmokers. ***Am J Respir Cell Mol Biol***, 17(1), pp. 114-124.

Wolf, C.R., Seilman, S., Oesch, F., Mayer, R.T. and Burke, M.D. (1986) Multiple forms of cytochrome P-450 related to forms induced marginally by phenobarbital. Differences in structure and in the metabolism of alkoxyresorufins. *Biochem J*, 240 (1), pp. 27-33

Yabusaki, Y. (1995) Artificial P450/reductase fusion enzymes: what can we learn from their structures? ***Biochimie***, 77 (7-8), pp. 594-603.

Yamamoto, T., Suzuki, A. and Kohno, Y. (2003) High-throughput screening to estimate single or multiple enzymes involved in drug metabolism: microtitre plate assay using a combination of recombinant CYP2D6 and human liver microsomes. ***Xenobiotica***, 33 (8), pp. 823-839.

Yamano, S., Aoyama, T., McBride, O.W., Hardwick, J.P., Gelboin, H.V. and Gonzalez, F.J. (1989) Human NADPH-P450 oxidoreductase: complementary DNA cloning, sequence and vaccinia virus-mediated expression and localization of the CYPOR gene to chromosome 7. ***Mol Pharmacol***, 36 (1), pp. 83-88.

Yamazaki, H., Inui, Y., Wrighton, S.A., Guengerich, F.P, and Shimada T. (1995) Procarcinogen activation by cytochrome P450 3A4 and 3A5 expressed in Escherichia coli and by human liver microsomes. ***Carcinogenesis***, 16(9), pp. 2167-2170.

Yamazaki, H., Nakamura, M., Komatsu, T., Ohyama, K., Hatanaka, N., Asahi, S., Shimada, N., Guengerich, F.P., Shimada, T., Nakajima, M. and Yokoi, T. (2002) Roles of NADPH-P450 reductase and Apo- and Holo-cytochrome b5 on xenobiotic oxidations catalyzed by 12 recombinant human cytochrome P450s expressed in mambranes of *Escherichia coli*. ***Protein Expr Purif***, 24 (3), pp. 329-337.

Yasukochi, Y. and Masters B.S.S. (1976) Some properties of a detergent solubilized NADPH-cytochrome c (cytochrome P450) reductase purified by bispecific affinity chromatography. ***J Biol Chem***, 251,pp. 5337-5344.

Yim, S.K., Yun, C.H., Ahn, T., Jung, H.C. and Pan, J.G. (2005) A continuous spectrophotometric assay for NADPH-cytochrome P450 reductase activity using

3-(4,5-dimethylthiazol-2-yl)-2,5-diphenyltetrazolium bromide. ***J Biochem Mol Biol***, 38 (3), pp. 366-369.

Yin, O.Q., Tomlinson, B., Chow, A.H., Waye, M.M. and Chow, M.S. (2004) Omeprazole as a CYP2C19 marker in Chinese subjects: assessment of its gene-dose effect and intrasubject variability. ***J Clin Pharmacol***, 44 (6), pp. 582-589.

Zevin, S. and Benowitz, N.L. (1999) Drug interactions with tobacco smoking. An update. ***Clin Pharmacokinet***, 36(6), pp. 425-438.

Zhao, Q., Modi, S., Smith, G., Paine, M., McDonagh, P.D., Wolf, C.R., Tew, D., Lian, L.Y., Roberts, G.C. and Driessen, H.P. (1999) Crystal structure of the FMN-binding domain of human cytochrome P450 reductase at 1.93 A resolution. ***Protein Sci***, 8(2), pp. 298-306.

Zhou, S.F., Di, Y.M., Chanm E., Du, Y.M., Chow, V.D., Xue, C.C., Lai, X., Wang, J.C., Li, C.G., Tian, M, and Duan, W. (2008) Clinical pharmacogenetics and potential application in personalized medicine. ***Curr Drug Metab***, 9(8), pp. 738-784.